Development of a novel nitriding plant for the pressure vessel of the PBMR core unloading device

Ryno Willem Nell

B Eng (Mechanical) Honours

Dissertation submitted in fulfilment of the requirements for the degree Master of Engineering (Mechanical) at the Department of Mechanical Engineering of the North-West University

Supervisor: Prof. M Kleingeld

May 2010

Development of a novel nitriding plant for the pressure vessel of the PBMR Core Unloading Device

Author	:	Ryno Willem Nell
Student number	:	22065873
Supervisor	:	Prof. Marius Kleingeld
This degree	:	Master of Engineering (Mechanical)
Last degree received	:	B Eng (Hons) (Mechanical) with distinction at the University of Pretoria in 2007

ABSTRACT

The Pebble Bed Modular Reactor (PBMR) is one of the most technologically advanced developments in South Africa. In order to build a commercially viable demonstration power plant, all the specifically and uniquely designed equipment must first be qualified. All the prototype equipment is tested at the Helium Test Facility (HTF) at Pelindaba. One of the largest components that are tested is the Core Unloading Device (CUD).

The main function of the CUD is to unload fuel from the bottom of the reactor core to enable circulation of the fuel core. The CUD housing vessel forms part of the reactor pressure boundary. Pebble-directing valves and other moving machinery are installed inside its machined inner surface. It is essential that the interior surfaces of the CUD are case hardened to provide a corrosion- and wear-resistant layer. Cold welding between the moving metal parts and the machined surface must also be prevented. Nitriding is a case hardening process that adds a hardened wear- and corrosion-resistant layer that will also prevent cold welding of the moving parts in the helium atmosphere.

Only a few nitriding furnaces exist that can house a forging as large as the CUD of the PBMR. Commercial nitriding furnaces in South Africa are all too small and have limited flexibility in terms of the nitriding process. The nitriding of a vessel as large as the CUD has not yet been carried out commercially. The aim of this work was to design and develop a custom-made nitriding plant to perform the nitriding of the first PBMR/HTF CUD.

Proper process control is essential to ensure that the required nitrided case has been obtained. A new concept for a gas nitriding plant was developed using the nitrided vessel interior as the nitriding process chamber. Before the commencement of detail design, a laboratory test was performed on a scale model vessel to confirm concept feasibility. The design of the plant included the mechanical design of various components essential to the nitriding process.

SUMMARY

A special stirring fan with an extended length shaft was designed, taking whirling speed into account. Considerable research was performed on the high temperature use of the various components to ensure the safe operation of the plant at temperatures of up to 600°C. Nitriding requires the use of hazardous gases such as ammonia, oxygen and nitrogen. Hydrogen is produced as a by-product and therefore safety was the most important design parameter. Thermohydraulic analyses, i.e. heat transfer and pressure drop calculations in pipes, were also performed to ensure the successful process design of the nitriding plant.

The nitriding plant was subsequently constructed and operated to verify the correct design. A large amount of experimental and operating data was captured during the actual operation of the plant. This data was analysed and the thermohydraulic analyses were verified. Nitrided specimens were subjected to hardness and layer thickness tests.

The measured temperature of the protruding fan shaft was within the limits predicted by Finite Element Analysis (FEA) models. Graphs of gas flow rates and other operation data confirmed the inverse proportionality between ammonia supply flow rate and measured dissociation rate. The design and operation of the nitriding plant were successful as a nitride layer thickness of 400 µm and hardness of 1 200 Vickers hardness (VHN) was achieved.

This research proves that a large pressure vessel can successfully be nitrided using the vessel interior as a process chamber.

Keywords: Core Unloading Device (CUD), nitriding, Pebble Bed Modular Reactor (PBMR), Vickers hardness (VHN), Helium Test Facility (HTF), thermohydraulic, Finite Element Analysis (FEA), cold welding – metal parts weld instantly due to the helium atmosphere

Ontwikkeling van ‘n nuwe gasnitreringsaanleg vir die drukvat van die PBMR se Kernontlaaimasjien

Outeur	:	Ryno Willem Nell
Studentenommer	:	22065873
Studieleier	:	Prof. Marius Kleingeld
Vir die graad	:	Magister in Ingenieurswese (Meganies)
Laaste graad ontvang	:	B Ing Honneurs (Meganies) met lof aan die Universiteit van Pretoria in 2007

SAMEVATTING

Die korrelbed - modulêre reaktor (PBMR) is een van die mees tegnologies gevorderde ontwikkelingsprojekte in Suid-Afrika. Om ’n suksesvolle demonstrasiekragstasie te bou, moet al die spesiaal ontwerpte toerusting eers gekwalifiseer word. Al die prototipe-toerusting word by die Heliumtoetsfasiliteit (HTF) by Pelindaba getoets. Een van die grootste komponente wat getoets word, is die Kernontlaaitoestel (CUD).

Die hooffunksie van die CUD is om brandstof te ontlaai by die onderkant van die reaktorkern om sirkulasie van die brandstofkern te bewerkstellig. Die CUD-omhulsel maak deel uit van die reaktordrukgrens. Kleppe wat sfere rondbeweeg, asook ander bewegende masjinerie, word binne-in die gemasjineerde binnekant geïnstalleer. Dit is noodsaaklik dat die binneste oppervlakke van die CUD genitreer moet word om ’n roes- en slytasieweerstandige laag te voorsien. Nitrering voorkom ook die koue vassweising van bewegende dele in die heliumatmosfeer.

Slegs ’n paar nitreringsoonde wat ’n drukvat so groot soos die PBMR CUD kan huisves, bestaan wêreldwyd. Die kommersiële nitreeraanlegte in Suid-Afrika is te klein en laat ook nie genoeg ruimte met die prosesbeheer toe nie. Tot op datum is die nitrering van ’n drukvat so groot soos die CUD nog nie kommersieël aangepak nie. Die doel van hierdie werkstuk was om ’n doelgerigte nitreringsaanleg te ontwerp om die nitrering van die eerste PBMR/HTF CUD uit te voer.

Behoorlike prosesbeheer is belangrik om die regte nitreerlaag te verseker. ’n Nuwe konsep is ontwikkel vir ’n gasnitreringsaanleg, naamlik om die drukvat-binneruim te gebruik vir ’n nitreringsreaksiekamer. Voordat daar met die gedetailleerde ontwerp begin is, is ’n laboratoriumtoets gedoen op ’n kleiner drukvat om die haalbaarheid van die konsep te bevestig.

OPSOMMING

Die ontwerp van die aanleg het die meganiese masjienontwerp van verskeie komponente ingesluit wat noodsaaklik was vir die nitreringsproses.

’n Spesiale gasmengwaaier met ’n lang as is ontwerp met inagneming van die natuurlike frekwensie van die as. Baie navorsing is gedoen oor die gebruik van verskillende komponente by hoë temperature om die veilige bedryf van die aanleg te verseker by temperature so hoog soos 600°C. Nitrering vereis die gebruik van gevaarlike gasse soos ammoniak, suurstof en stikstof. Waterstof word as ’n neweproduk vrygestel en daarom is veiligheid baie belangrik. Daar is verskeie termohidrouliese analises, soos hitteoordrag- en drukvalberekeninge in pype, gedoen om die suksesvolle prosesontwerp van die aanleg te verseker.

Die nitreringsaanleg is daarna gebou en bedryf om die ontwerp te verifieer. Gedurende die bedryf van die aanleg is ’n groot hoeveelheid eksperimentele en bedryfsdata ingesamel. Die data is ontleed en die termohidrouliese analises is geverifieer. Daarna is die genitreerde monsters vir hardheid- en nitreerlaagdiktetoetse gestuur.

Die gemete temperatuur van die deel van die waaieras wat uit die oond steek was tussen die limiete wat deur eindige-elementanalise-modelle (FEA-modelle) voorspel is. Grafieke van die gas vloeitempo’s en ander bedryfsdata het die indirek eweredige verwantskap tussen ammoniak-vloeitempo en die gemete reaksie-kraaktempo bevestig. Die ontwerp en bedryf van die nitreringsaanleg was ’n sukses aangesien ’n nitreerlaagdikte van 400 µm en hardheid van 1 200 Vicker’s hardheid (VHN) verkry is. As gevolg van die hoë aanvanklike kraaktempo, was daar ’n moontlikheid dat ’n wit laag gevorm het en die bestaan daarvan kan bevestig word met verdere werk.

Hierdie navorsing bewys dat ’n groot drukvat wel suksesvol genitreer kan word deur die binneruim as nitreringsreaksiekamer te gebruik. ’n Suksesvolle oplossing is dus gevind vir die probleem en die eindresultaat is ’n semi-draagbare ontwerp wat met kommersiële aanlegte kan kompeteer teen ’n veel laer koste.

Sleutelwoorde: kernontlaaitoestel (CUD), nitrering, korrelbed- modulêre reaktor (PBMR), Vicker’s hardhead (VHN), heliumtoetsfasiliteit (HTF), termo-hidrolies, eindige-elementanalise (FEA), koue vassweising – metaalonderdele sweis onmiddelik vas as gevolg van die heliumatmosfeer

ACKNOWLEDGEMENTS

This research could not have been completed successfully without the help of the following people:

- Mike Nieuwoudt (CUD design engineer) for awarding me the project and guiding me with the design and calculations
- Chris Koch of SAMS (Pty) Ltd (the metallurgist on the project) for his expert knowledge on nitriding, his laboratory experiments and the nitriding sample hardness and layer thickness tests
- Eric Van Eeden (CUD CAD designer) for making the detail drawings of the nitriding fan shaft, etc. and for helping with suppliers
- Gideon De Wet for his advice on the fan diameter sizing and flow calculations
- Joggie Wilcocks for managing the communication with DCD Dorbyl and setting up HAZOP meetings
- Attie Ferreira (project manager) for his help with the process design and being flexible with the budget
- Marius Knoetze for his help with writing a functional specification and operating description and successfully completing the HAZOP
- Zohn Genade for helping with the construction and operation of the plant and inputs at meetings and reviews
- Dash Chana for helping with the construction of the plant and inputs at meetings
- Opsie Ndlovu for helping with the construction of the plant and inputs at meetings
- Westinghouse Electric South Africa (Pty) Ltd and PBMR (Pty) Ltd for funding this research
- DCD Dorbyl Heavy Engineering, Vereeniging
- SM Projects for shaft and flange machining
- Morgan Carbon South Africa
- Johannesburg Valve and Fitting Company

TABLE OF CONTENTS

Heading *Page*

LIST OF FIGURES

LIST OF TABLES

ABBREVIATIONS AND ACRONYMS

Abbreviation or Acronym	Explanation / Definition
2D	two dimensional
3D	three dimensional
Al	aluminium
ALARA	As low as reasonably achievable
ASME	American Society of Mechanical Engineers
CAD	Computer Aided Design
CUD	Core Unloading Device
CFD	Computational Fluid Dynamics
Cr	chromium
DC	Direct Current
DPP	Demonstration Power Plant
FEA	Finite Element Analysis
FEM	Finite Element Method
FHSS	Fuel Handling and Storage System
HAZOP	Hazard and Operability Study
HTF	Helium Test Facility
HTGN	High Temperature Gas Nitriding
HV	Vickers hardness, also given as VHN
HRC	Rockwell C hardness scale
ID	inner diameter
ISO	International Standards Organization
N	nitrogen
NP	Nitriding Plant
OD	outer diameter
OHS	Occupational Health and Safety
PBMR	Pebble Bed Modular Reactor
PCD	pitch circle diameter
PFD	Process Flow Diagram
PFM	Process/Plant Functional Module
P&ID	Piping and Instrumentation Diagram
PTFE	Polytetrafluoroethylene (Teflon)
SEM	Scanning Electron Microscope
TBD	to be determined
TBV	to be verified
VSD	Variable Speed Drive

DEFINITIONS

Description	Explanation
Austenite	The phase in which the crystal structure of steel is cubic face centred at a temperature of above ±720 °C.
Axisymmetric model	A three-dimensional object can be modelled as axisymmetric, in CFD or FEA, when it is symmetrical about a central axis in all aspects. A cylinder is an example of an axisymmetric object.
'Bunte Burette'	An instrument to measure the crack ratio.
Coasting	The term used by furnace operators when the furnace burners are set to keep the temperature constant for a long period.
Cold welding	Mechanism by which clean metal surfaces weld together due to the absence of an oxide layer [1], [2]. When viewed under an electron microscope one will see peaks of the uneven surface finish welded together (metal atoms touching to form a metal chemical bond). Bearings seize at high temperatures due to cold welding and destruction of the oxide layer. Adhesion wear is a wear mechanism by which the peaks of a bearing/shaft are continuously broken off (pitting) as the peaks are cold welded to each other. Cold welding is a big problem in high vacuum conditions such as space [3]. It is also a problem in the helium atmosphere inside the PBMR pressure boundary.
Crack ratio	An indication of the cracking (dissociation) of ammonia gas into nascent nitrogen and hydrogen gas under high temperatures. A large crack ratio indicates a large amount of cracking (100% = full ammonia dissociation).
Ferrite	The phase in which the crystal structure of steel is cubic space centred at a temperature of below 720 °C.
Hold (furnace on hold)	The term used by furnace operators when the gas-fired burners are set for a low heating rate in order to allow conduction through the workpiece. This will enable the thick metal parts' temperature to catch up with the thin metal parts' temperature.
Inserts	Specially designed valves, speed sensors etc. are installed into the CUD and other valve blocks to direct fuel pebbles in the PBMR to the right sphere pipes etc.
Nascent nitrogen	The nitrogen that diffuses in the steel surface formed by cracking ammonia at high temperature. It is a nitrogen atom (a single unstable atom, not an N_2 molecule).
Nitriding	A surface hardening process by which nitrogen is introduced into the surface of a metal. Nitriding adds wear and corrosion resistance. The nitride layer prevents an oxide layer from forming on the metal surface.
Process chamber	A sealed container, containing gases at high temperature, in which the nitriding process takes place. In this case, the entire interior volume of the CUD housing is used as the nitriding process chamber.
Thermohydraulic calculation	Any calculation that includes heat transfer and pressure drop calculations in a conduit system or component.
White layer	The initial layer of diffused nitrogen on the metal surface (iron nitride; FeN layer). This is a highly soluble layer in the metal necessary to start the nitrogen diffusion process. It is formed at the start of the nitriding cycle if the crack ratio is 15 – 35%.

NOMENCLATURE

Symbol	Quantity	Unit
$A_{annulus}$	area of annulus cross section in CUD barrel	m^2
$A_{central}$	cross sectional area of fan air column	m^2
Cp	fan power coefficient	
C_p	specific heat capacity	J/kgK
D	diameter	m
D_h	hydraulic diameter	m
E	modulus of elasticity	Pa
F	volume flow	ℓ/hr
G	shear modulus of elasticity	Pa
h	heat transfer coefficient	W/m^2K
h_c	convective heat transfer coefficient	W/m^2K
I	shaft 2nd moment of inertia	m^4
I_G	shaft mass moment of inertia	kgm^2
I_p	shaft polar moment of inertia	m^4
k	heat conduction coefficient	W/mK
L	shaft length/column length	m
$\dot{m}$	mass flow	kg/s
Mfe	exiting mass flow at gas exit tubes	kg/s
n	whirling speed of shaft	Hz
Nu_D	Nusselt number, indication of heat transfer in pipe	
p	pressure	Pa
P	power	W
Pr	Prandtl number	
Re	Reynolds number	
Ra_D	Rayleigh number based on diameter	
SR	speed ratio (ratio of fan tip speed to air speed)	
t	time	s
T	torque due to torsion in a shaft	N.m
T_b	bulk temperature	K
T_{atm}	atmospheric temperature	K
T_{oper}	operating temperature	K
V	volume	m^3
v	air flow speed	m/s
V_1	air flow speed before fan	m/s
w	distributed load (shaft weight)	N/m
y	deflection	m
α	thermal expansion coefficient	1/°C
δ	deflection (shaft/beam end)	m
Δ	static deflection due to shaft's own weight	m
ρ	density	kg/m^3
σ	stress	Pa
τ	shear stress	Pa
μ	dynamic viscosity	Pa.s
υ	Poisson's ratio	
ν	kinematic viscosity	m^2/s
ω	whirling speed of shaft	rad/s
π	3.141592654…	

Note: Only the most important and frequently used symbols are defined here, other symbols and subscripts are defined in the main body of the report.

Chapter 1: Introduction

1.1. BACKGROUND TO THE PBMR AND THE CORE UNLOADING DEVICE

The Pebble Bed Modular Reactor (PBMR) is one of the most complex technological developments in the world. It involves a new generation nuclear power plant using high temperature gas reactor technology and is presently being developed in South Africa. The reactor core, for the 400 MW design, contains approximately 500 000 graphite fuel pebbles/spheres and uses graphite reflectors as a moderator[1]. The inner graphite matrix of each pebble contains hundreds of silicon-coated particles of enriched Uranium oxide.

The PBMR project includes the design and supply of three major support systems. These are the Fuel Handling and Storage System (FHSS), the Reactivity Control and Shutdown System (RCSS) and the Helium Inventory Control System (HICS)[2]. The Helium Test Facility (HTF), built at Pelindaba, serves as a test bed for most of the specifically designed first-of-a-kind equipment before it is used on the actual PBMR Demonstration Power Plant (DPP).

One of these uniquely designed components is the Core Unloading Device (CUD), a component of the FHSS. The CUD unloads the fuel pebbles at the bottom of the core. The position of the CUD in the plant is shown in Figure 1.1. After being unloaded the fuel pebble is measured for burn-up and then either reloaded at the top of the Reactor or transported to the spent fuel tanks. The CUD continuously circulates fuel through the reactor core during normal operation.

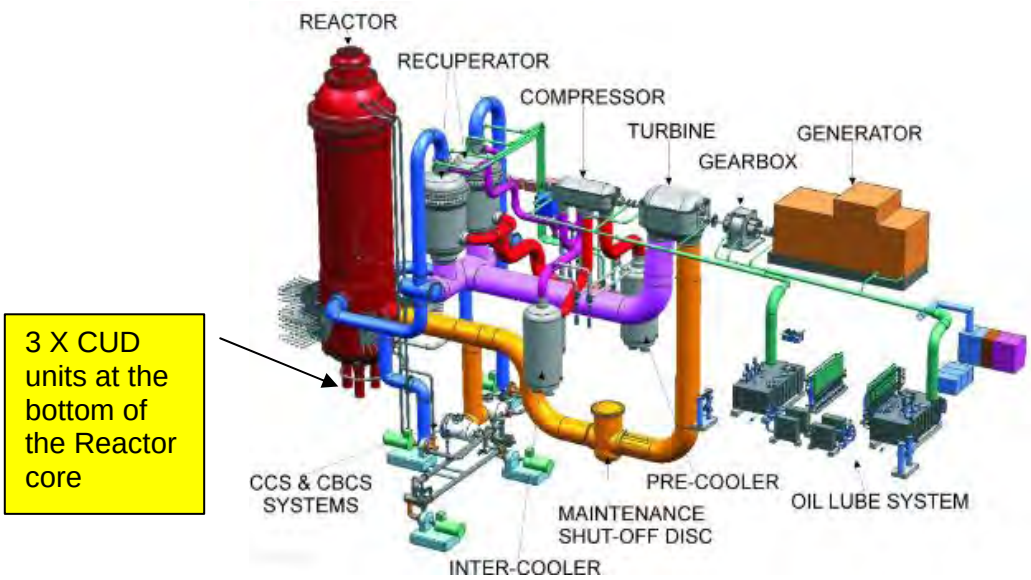

Figure 1.1: An illustration of one of the proposed PBMR plant layouts, courtesy of PBMR (Pty) Ltd. (picture from the PBMR website of 2006).

[1] This information is from the website of the PBMR company, www.pbmr.co.za, May 2008

[2] Westinghouse Electric South Africa (Pty) Ltd holds the contract for the design and supply of these systems.

1.2. BACKGROUND ON THE HTF CORE UNLOADING DEVICE

The HTF CUD is a large assembly consisting of various moving parts. A transparent CAD model of the whole CUD assembly is shown in Figure 1.2.a). The fuel unloading machinery inside the CUD is shown by a section view of the CUD in Figure 1.2.b).

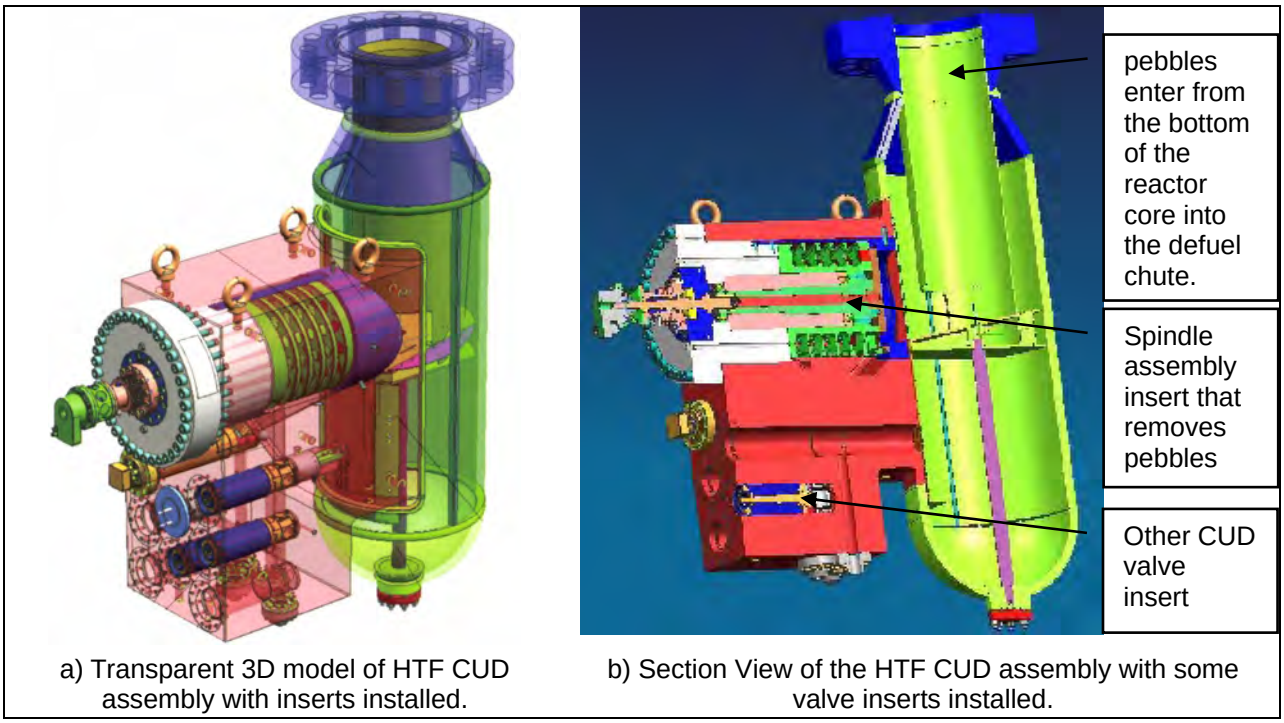

a) Transparent 3D model of HTF CUD assembly with inserts installed.

b) Section View of the HTF CUD assembly with some valve inserts installed.

Figure 1.2: Pictures of the HTF CUD CAD model to explain its purpose and operation.[3]

The largest part of the CUD assembly is the CUD housing which is shown in Figure 1.3. It measures 3 m x 2 m x 1.5 m and it consists mainly of a barrel and a block section.

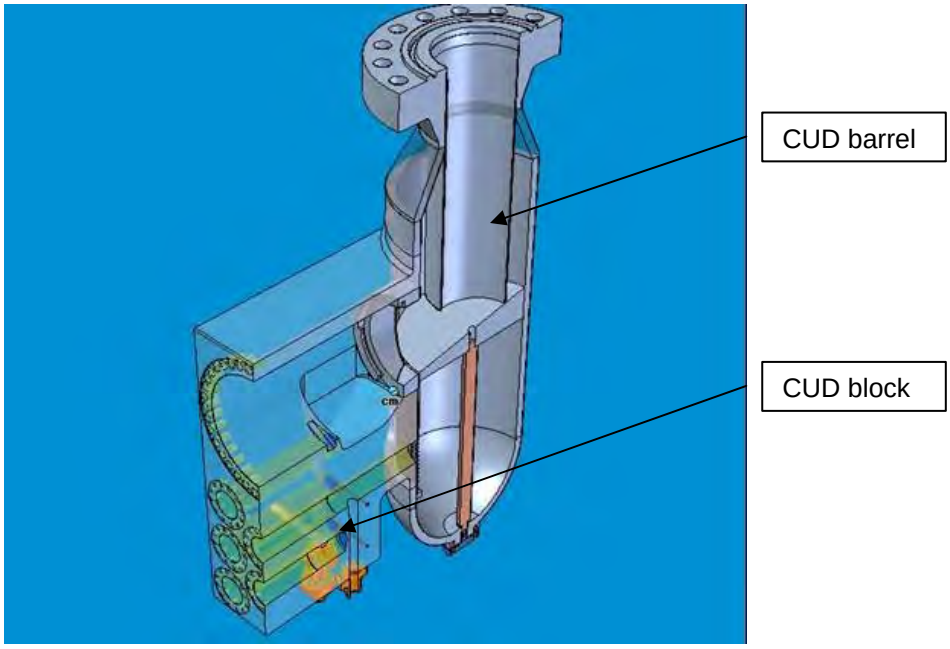

Figure 1.3: Section View of a CAD model of the CUD housing (this part will be nitrided).

[3] CUD CAD model courtesy of Westinghouse Electric South Africa (Pty) Ltd.

The spindle assembly insert (shown in Figure 1.4), sphere directing valve and indexer inserts, speed sensors and other moving mechanical equipment are installed into the insert holes machined into the CUD block.

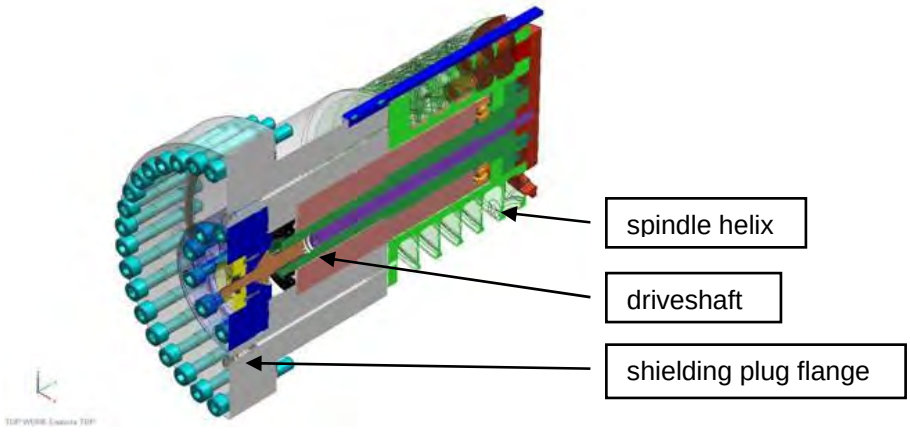

Figure 1.4: Spindle assembly insert CAD model.

During operation the inside of the CUD is filled with helium under a pressure of 9 MPa. The pressure boundary is formed by the CUD housing and the seals of the different valve inserts. The CUD operates by constantly turning the spindle helix shown in Figure 1.5. Pebbles are picked up by the rotating helix. In this way pebbles are removed one by one from the reactor core. At the other end of the helix the pebbles are sent to a sphere-directing valve or indexer and transported in a sphere pipe.

Figure 1.5: Photo of the actual plasma-nitrided CUD spindle helix.[4]

Valve inserts are also installed on other HTF equipment i.e. the sphere conveying block, measurement block and other valve block forgings[5]. All these valve blocks were nitrided to improve wear and corrosion resistance. Nitriding is a case-hardening process whereby nitrogen is introduced into the surface of a solid ferrous alloy by diffusion [4].

[4] Photo courtesy of Westinghouse Electric South Africa (Pty) Ltd. taken at MTP (Machine Tool Promotions) (Pty) Ltd.
[5] This information is from Westinghouse Electric South Africa (Pty) Ltd. the main supplier of components for the HTF.

The most important reason for nitriding the HTF equipment is to prevent cold welding between clean metal surfaces inside the helium gas pressure boundary of the HTF. Cold welding is an important concept for this research and it is therefore properly defined on p. xiii of this report. It is usually a problem in space and high vacuum applications [1], [2] and [3]. In the context of the HTF cold welding can occur between the links of a steel chain (chains are used to lower and raise the control rods of the Reactivity Control System). Cold welding can make the chain unflexible and unusable. The chains can be nitrided to prevent this coldwelding.

The inner surface of the CUD housing (see Figure 1.3) must also be nitrided. Nitriding will prevent cold welding between the nine inserts (including the spindle assembly) and the lining surfaces of the CUD housing's nine insert holes. The valve inserts will rotate to index and direct fuel pebbles resulting in friction between the moving parts of the inserts and the inner surface of the CUD insert hole. Friction in the helium environment will cause cold welding (there is no oxygen to replenish the rust or oxide layer, similar to space applications [1]). Cold welding will prevent the removal of the insert from the CUD hole for maintenance, rendering the CUD inoperable. The CUD housing differs from the other valve block forgings since it is much larger and weighs 14 tonnes. Nitriding the CUD can present a problem due to its size.

1.3. THE NITRIDING PROCESS

Nitriding is a case-hardening process whereby nascent nitrogen is introduced into the surface of a solid ferrous alloy by thermochemical diffusion, to form nitrides typically of iron, chromium and aluminium ([4] p.1 and [5] p. 68). The nitriding temperature for all steels is between 495°C and 565°C which is much lower than that of carburizing and other case-hardening techniques. The steel also remains in the ferrite phase as opposed to the austenite phase with carburizing. This means that very small dimensional changes occur and that nitriding can take place after final machining. Nitriding is a common industrial process used widely in the aircraft and automotive industry on engine parts (crankshafts), bearings, textile machinery and turbine generator systems.

The advantages of a nitrided surface layer include improved wear; corrosion [4] and fatigue resistance [6], [7]. Nitriding is also one of the most economic surface treatment solutions as shown in Figure 1.6.

Nitriding was chosen above other surface treatment options because it is economical, requires no machining afterwards and prevents cold welding to a greater extent than carburizing and other surface treatment options. When a steel surface is nitrided, it is chemically altered (nitrides formed), which makes the formation of an iron oxide layer unlikely. The absence of an iron oxide layer, that can break off under friction and expose clean metal surfaces, prevents

cold welding. A contaminated layer has an effect on the adhesion of metal surfaces [1]. Due to the fine fits and tolerances of the CUD machined surfaces, nitriding is preferred as it can be done after final machining. In contrast carburizing requires machining afterwards as the quenching distorts the workpiece. The CUD fabrication costs approximately R8 million and therefore mistakes during final machining cannot be tolerated.

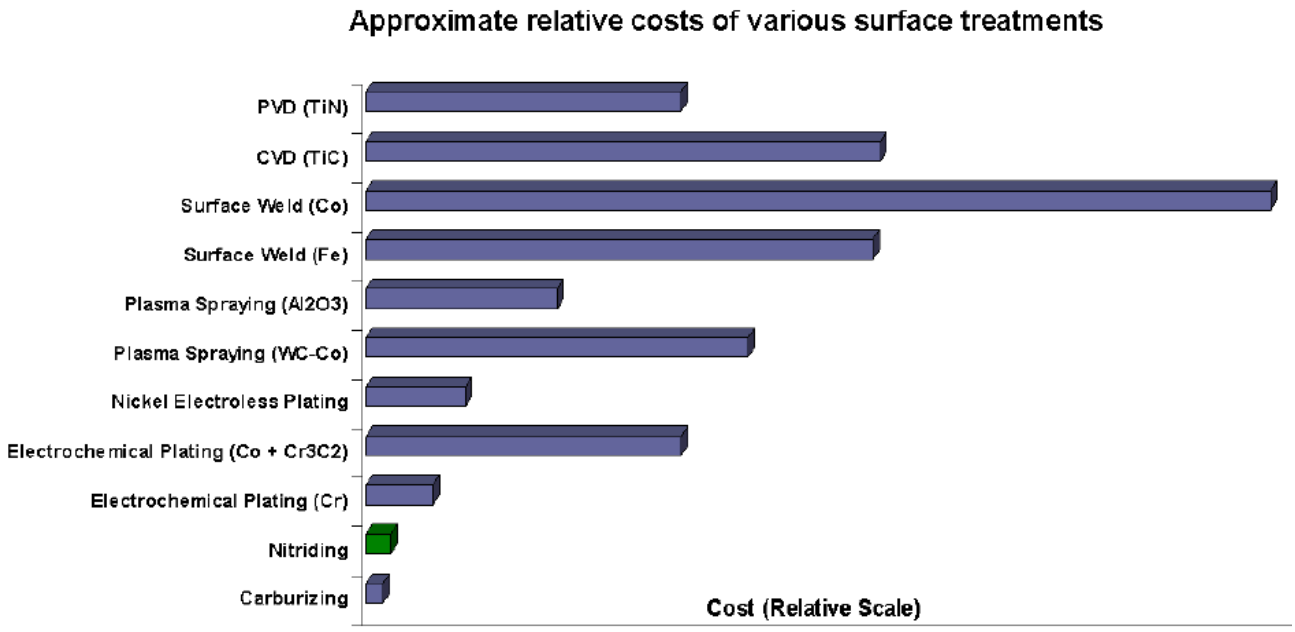

Figure 1.6: Relative costs of nitriding, from [12] (After J.R. Davis, Surface Engineering for Corrosion and Wear Resistance, ASM International, 2001).

1.4. PROBLEM DEFINITION

As previously mentioned, the CUD housing inner surface must be nitrided to provide a hardened wear-resistant layer, decrease corrosion and to prevent cold welding in helium. It is a large vessel measuring 3 m X 2.2 m X 1.5 m and it weighs 14 tonnes. A literature survey could not identify any existing nitriding facilities in South Africa, able to house such a large vessel. Furthermore, no records could be found that such a large workpiece had ever been nitrided before (see section 2.5). Smaller parts of the CUD were nitrided at existing plasma nitriding facilities (in Figure 1.5, the nitrided CUD spindle is shown).

Because no nitriding facilities in South Africa are capable of nitriding the CUD housing, an alternative route had to be followed. The literature survey further confirmed that a suitable nitriding plant would need to be purposefully designed and built for the HTF CUD. In addition the CUD housing is designed as an ASME VIII (Division 1) pressure vessel [9] and is constructed from ASME pressure vessel code steel. All the quality control requirements for heat treatment and other aspects of such a pressure vessel still apply.

The nitriding plant design will introduce other problems such as the development of a method to provide the necessary heating and nitriding process reactants for such a large vessel. This will require a process design of the plant, functional specification, thermohydraulic analysis, system operating description and mechanical design of components. Various components must be designed for high temperature use. The nitriding process must also be qualified by means of hardness tests and nitride layer thickness measurement.

1.5. OBJECTIVES OF THIS RESEARCH

The main objective of this research is the design of a nitriding plant to nitride the inner surface of the CUD housing pressure vessel.

As explained in section 1.4 it was concluded from the formal literature survey, that a new gas nitriding plant would need to be purposefully designed and built to nitride the CUD. The design will require the use of techniques from various engineering disciplines including metallurgical, mechanical and chemical or process engineering. The design and construction of the CUD Nitriding Plant (NP) can thus be seen as a multidisciplinary engineering project. The CUD housing was manufactured at DCD Dorbyl Heavy Engineering in Vereeniging and the heat treatment furnaces of DCD Dorbyl were available for use if the designed process required it.

The objectives are:

1. Perform the entire engineering project cycle from a literature survey of nitriding processes and facilities to concept design, detail design, construction, testing and finally verification and validation of the plant.
2. To successfully combine the different engineering disciplines to design a safe and effective nitriding plant that enables testing/qualifying the nitrided surface afterwards.
3. If successful the plant and process design will be used for nitriding future CUD vessels for the PBMR DPP.

1.6. CONTRIBUTIONS OF THIS RESEARCH

The design of the CUD NP resulted in the following contributions:

1. New method of creating a nitriding process chamber using the actual nitrided workpiece to form the process chamber (see Figure 1.7 for an explanation). Conventional all-round gas nitriding is therefore no longer the only method of performing gas nitriding.
2. Design of an extended length shaft assembly (2.5 m) to penetrate a pressure boundary at a temperature of 600 °C to stir the nitriding gas. This required the design of a new high temperature bearing to seal off the gas.

3. Design of various high temperature gas-sealing penetrations for gas piping etc. entering the nitriding process chamber.
4. The design of a method to temporarily modify an existing heat treatment furnace for use as a gas nitriding furnace. The furnace can then once again be used as a normal heat treatment furnace afterwards.
5. Thermohydraulic and process design of a gas nitriding plant using a modified existing heat treatment furnace.
6. Capturing of all the relevant process data (gas flows, workpiece surface temperatures etc.) to demonstrate the success of the nitriding process.
7. Design and implementation of a method to use nitride layer specimens to test the hardness and thickness of the nitrided surface layer of the workpiece, without damage to the workpiece surface.
8. A successful first attempt at producing the largest single nitrided forging.

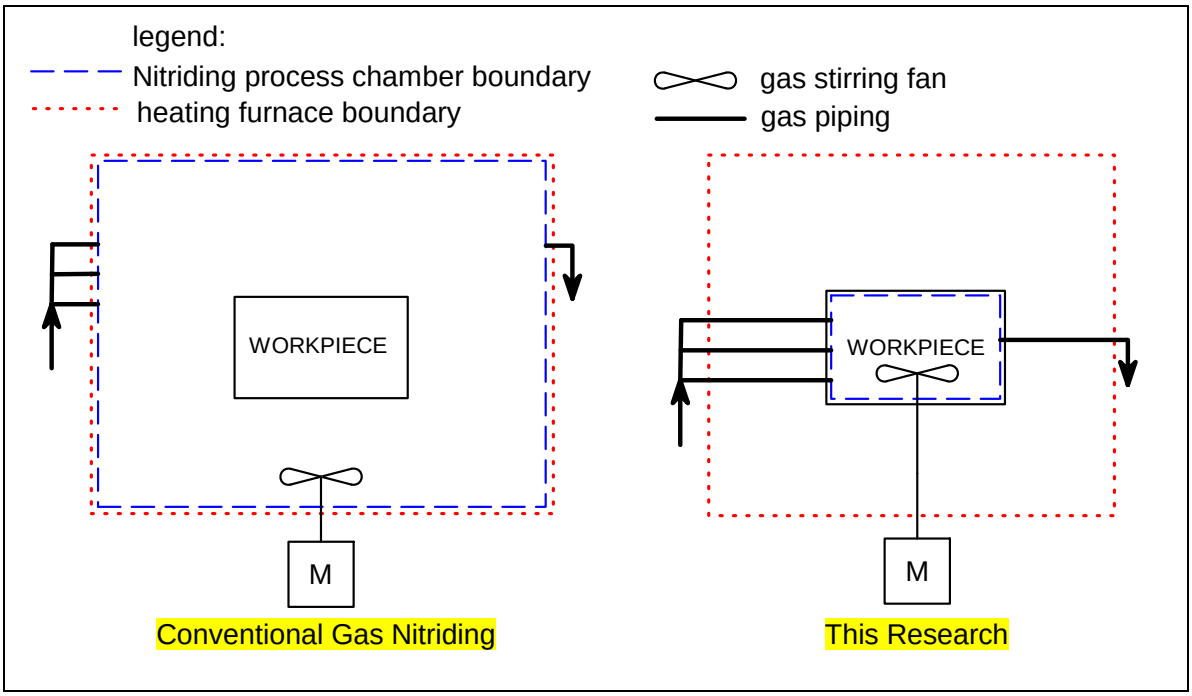

Figure 1.7: An illustration to explain the new method using the nitrided workpiece to form the process chamber.

1.7. STRUCTURE OF THE REPORT

1.7.1 LITERATURE SURVEY

The history of nitriding was investigated to determine when the process was invented and how it was commercialized.

A literature study was done to investigate metallurgical aspects and how to control the outcome of the nitriding process, i.e. the nitrided case. Existing facilities were investigated and no

recorded use of a pressure vessel as a nitriding process chamber was found and few pressure vessels were nitrided. Laboratory tests were performed and used as a guideline to the design of the CUD Nitriding Plant (NP).

The literature was also studied to find methods that could aid in the design of the high temperature gas seal for the rotating shaft penetration of the CUD NP.

1.7.2 CONCEPT DESIGN

Before the detail design of components can be started a feasible concept for the entire CUD NP must first be defined. The entire product development concept design process from functional analysis to concept screening and concept evaluation is followed until final concept selection.

1.7.3 DETAIL DESIGN

All the calculations and decisions made for the detail design of the various plant components are explained in detail. It involved mechanical machine design and process design including flowmeter sizing, thermohydraulic analysis etc. The fan shaft assembly, part of the Nitriding Furnace PFM, was one of the most challenging components to design.

1.7.4 EXPERIMENTAL STUDY/PLANT OPERATION

The developed design was constructed as a prototype and used as an experiment to validate the design and the physics modelling assumptions that were made.

The entire plant was built and operated to nitride the CUD pressure vessel with the newly developed method of gas nitriding.

1.7.5 VERIFICATION AND VALIDATION

The plant design was verified and validated with the experimental results. Validation required proving that relevant physics were modelled and that the plant design concept was feasible. Succesful nitriding proved that the design is valid. To verify the design the effectiveness of the design is evaluated by studying operation data and nitriding specimen tests.

Chapter 2: Literature Survey

2.1. HISTORY OF NITRIDING

2.1.1 DEVELOPMENT OF THE NITRIDING PROCESS

The Nitriding process was developed in the early 20th century [4] and plays an important role in present-day industrial applications. Nitriding and the derivative nitrocarburizing process are often used in the manufacturing of aircraft, bearings, automotive components, textile machinery, and turbine generation systems. Even though its chemistry is not fully understood, it remains one of the simplest case hardening techniques [4]. According to [4] and [10] the secret of the nitriding process is that it does not require a phase change from ferrite to austenite, like other case hardening techniques such as carburizing (carburizing also requires a further phase change from austenite to martensite by quenching and this causes large dimensional changes). The history of the development of the process and various discoveries will now be discussed.

Machlet: The process was first discovered by an American named Adolph Machlet, in the early 20th century [4]. He worked as a metallurgical engineer for the American Gas Company in Elizabeth, New Jersey. He knew that carburizing led to distortion due to long periods at austenitic temperatures and severe quenching. By experimenting he discovered nitrogen's high solubility in iron and discovered a process that overcame the distortion problem of carburizing. Nitrogen diffusion hardens the surface of plain irons and low-alloy steels and improves corrosion resistance. However, it is achieved without heating to elevated temperatures followed by rapid cooling. Cooling takes place freely within the nitrogen-filled process chamber. Thus there is a smaller risk of distortion. Initially, ammonia was decomposed, or 'cracked' by heat to introduce nascent nitrogen. Machlet soon realised that he needed to control the decomposition accurately. Hydrogen gas was used as a dilutant gas to reduce the amount of available nascent nitrogen to control the formed case metallurgy [4]. Case metallurgy needed to be controlled to prevent formation of a 'white layer' or 'compound zone', shown in Figure 2.1.

Machlet applied for his first patent on the nitriding process in March 1908 in Elizabeth, NJ, and it was approved five years later in June 1913. Furthermore, he continued to develop and expand the new process for many years and improved his understanding of its process metallurgy. The patent was named 'The Nitrogenization of Iron and Steel in an Ammonia Gas Atmosphere into which an Excess of Hydrogen has been introduced' [4]. Although Machlet's work was important it remained unrecognised and few modern nitriding practitioners know who he was. Most metallurgists are familiar with the German researcher Adolph Fry, who is

recognised as the ‘father of nitriding’. However, Machlet actually pioneered the nitriding process.

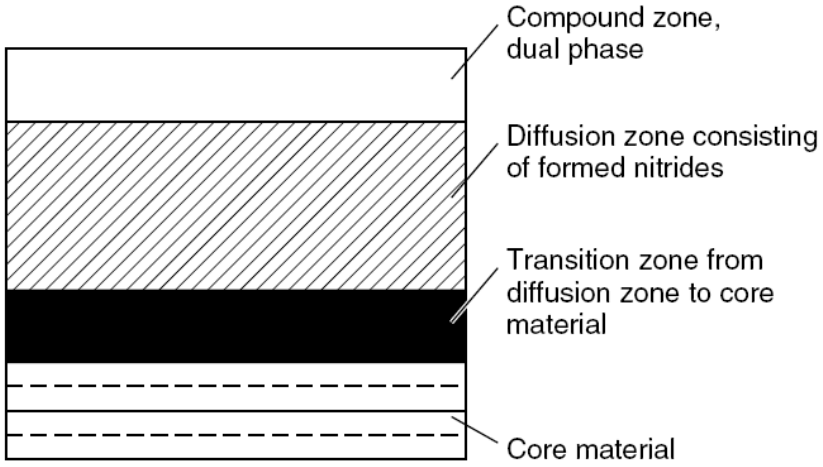

Figure 2.1: Cross section to show the layers of a typical nitrided case (not to scale), from [4].

Adolph Fry: In Germany, parallel research was conducted at Krupp Steel Works in Essen. The program was headed by Dr. Adolph Fry in 1906. He also recognised that nitrogen was very soluble in iron at high temperatures. However, early on in his research, Fry recognised that alloying elements strongly influenced metallurgical results. He applied for his patent in 1921, three years after World War I. It was granted in March 1924 [4]. Fry also used a technique to crack a nitrogen source with heat to liberate nitrogen for diffusion. Like Machlet, he used ammonia as a source gas, but he did not use hydrogen as a dilutant gas. Instead he developed the single-stage gas nitriding process as it is known today.

Fry investigated the effects of alloying elements on surface hardness and found that a high surface hardness was only achieved on steels with chromium, molybdenum, aluminium, vanadium and tungsten, all of which form ‘stable nitrides’. Fry also discovered the effects of process temperature on the case depth and surface metallurgy. Higher process temperatures could produce ‘nitride networks’ or a saturated solution of nitrogen in the immediate surface of the formed case. Since higher alloy steels were not available, Fry was responsible for developing a group of steels for Krupp known as the ‘Nitralloy’ group. These nitriding steels became internationally recognised as the Nitralloy steels that are still specified today.

In the late 1920s Thomas Firth and John Brown Steelworks (Firth Brown Steelworks), in Sheffield, England, began work on developing nitriding steels under the licensed guidance of Krupp Steels [4]. The Firth Brown steels were known as the ‘LK’ group, British Standard 970 as En 40A, En 40B, En 40C, En 41A and En 41B. The En 40 steels were chromium-molybdenum steels and the En 41 series contained aluminium, which produced a harder surface hardness after nitriding. Further effects of alloying elements will be discussed in section 2.3.

The main differences between nitriding processes developed in the US and in Germany are: The US process of Machlet used hydrogen as a dilutant gas to control nitriding potential and surface metallurgy, whereas the Germans controlled alloying and improved core hardness and tensile strength. Machlet's process was not commonly used in the US while the Germans exploited Fry's process. In the mid- to late 1920s information of Fry's process reached American industrialists and caused the Society of Manufacturing Engineers (SME) to take a strong interest. The SME sent Dr. Zay Jeffries to visit Dr. Fry in 1926 and after being invited to the annual SME conference in Chicago to present a paper, Fry sent his colleague Pierre Aubert to make a presentation. This started the commercialization of the process in the US.

After the presentation of Fry's work on the SME conference, American metallurgists started exploring nitriding process parameters and the effects of alloying on nitriding results.

McQuaid and Ketcham of the Timken Detroit Axle Company: They used typical equipment, as shown in Figure 2.2, to make the following findings that were presented in 1928 [4].

- Process temperature – higher nitriding temperatures had an effect on core hardness of alloy steels but little effect on nitride ability, higher temperatures also increased the risk of developing nitride networks, particularly at corners.
- Nitriding was much easier to control than carburizing.
- Corrosion properties of low-alloy and alloy steels were much improved.
- The first to study the white layer. It is composed of iron and other alloying element nitrides. The white layer or compound zone is very hard but brittle and should be avoided.
- The study of decarburization showed that the steel to be nitrided should clearly be free of surface decarburization; otherwise, the nitrided surface will exfoliate and peel away.

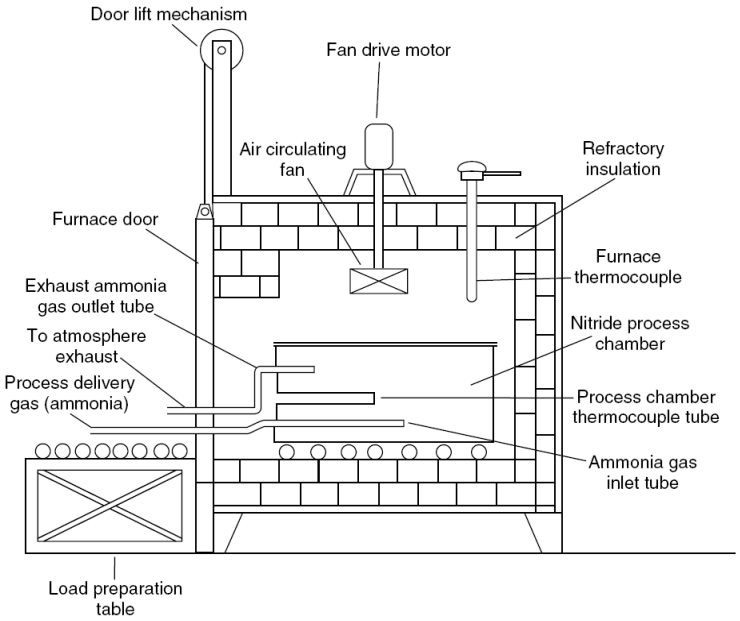

Figure 2.2: Schematic of a gas nitriding furnace used by McQuaid and Ketcham, picture from [4].

Robert Sergeson: He was associated with the Central Alloy Steel Corporation in Canton, Ohio and made the following discoveries that were presented in 1929 [4].

- Sergeson also found that nitriding was much easier to control than carburizing.
- Effect of reheating after nitriding – with increasing temperature; the core and surface hardness stability was much better than that for carburized and quenched alloy steel.
- Increased ammonia gas flow rate had little effect on immediate surface hardness and case depth. Increased process temperature increases case depth, but decreases surface hardness.
- He used alloy steels with chromium and aluminium and investigated effects of aluminium and nickel contents. He found that nickel was not a nitride-forming element and that it tended to retard the nascent nitrogen diffusion, when present, in significant quantities.

V.O. Homerberg and J.P. Walsted [4]: Homerberg was an associate professor of metallurgy at MIT and consulted for the Ludlum Steel Company along with Walsted to study the following.

- They discovered an increase of temperature up to 750 °C resulted in increased case depth and decreased surface hardness.
- Effect of decarburization – Surfaces must not be decarburized prior to nitriding.

2.1.2 EVOLUTION OF DIFFERENT NITRIDING TECHNIQUES

Two principal methods of nitriding steel today are by means of gas nitriding and plasma/ion Nitriding. Essentially it remains the introduction of nascent nitrogen by diffusion into the steel surface and the formation of nitrides typically of iron, chromium and aluminium [5]. Induction hardening is done by austenitizing (heated above 720 °C), whereas nitriding is typically done in a furnace operating at 495/525 °C for single stage gas nitriding and 495/565 °C for the double stage gas nitriding process (Floe process) [5]. The development of the most refined technique, the Floe process, will now be discussed in more detail.

Floe process: During early nitriding days the phenomenon of a white layer on the nitrided steel surface was a regular occurrence [4]. It was identified as a multi-phase compound layer of ε and γ' phases (more than 5% nitrogen see Figure 2.3). Considerable research was performed by Dr. Carl Floe, of the Massachusetts Institute of Technology, to identify the layer and its characteristics and to develop a process technique to reduce the white layer thickness [11]. This technique is known as the Floe process, or two-stage nitriding process (described in [4], [5] and [10]). The Floe Process has two distinct nitriding cycles as opposed to traditional single-stage gas nitriding. The first cycle is performed as a normal nitriding cycle at 500 °C and 15% to 30% ammonia dissociation. This will produce the nitrogen-rich compound layer at the

surface. For the next cycle the furnace is heated to 560 °C with gas dissociation increased to 75% to 85%. This two-stage process reduces the thickness of the compound zone.

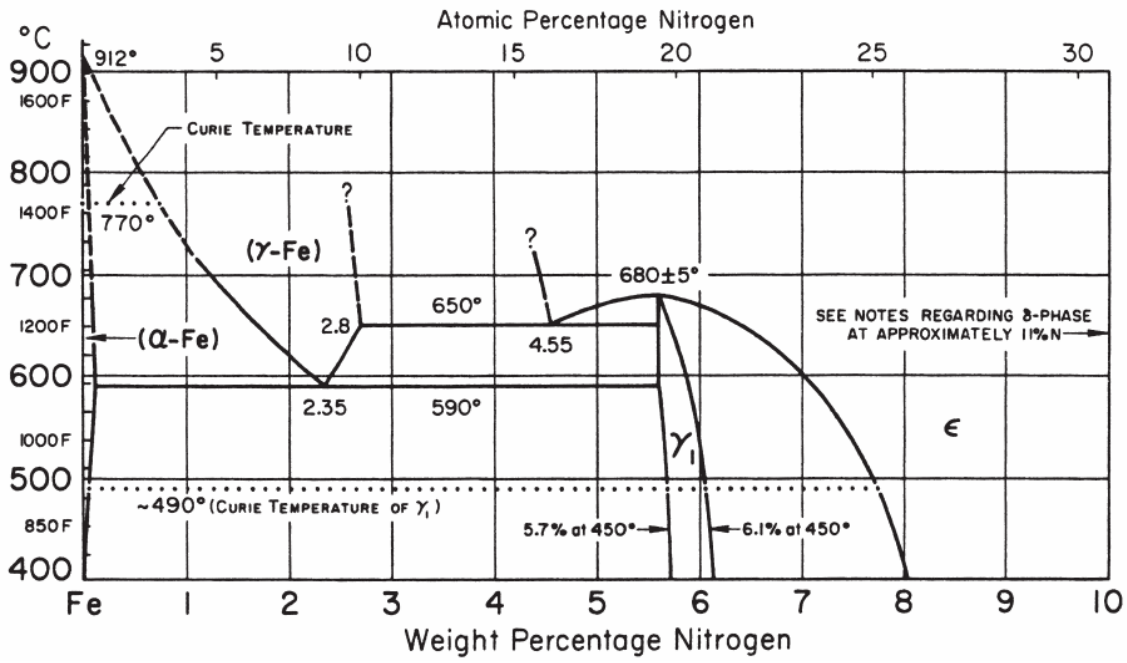

Figure 2.3: Iron-nitrogen equilibrium diagram. The δ-phase, not shown on this diagram, exists from 11.0 to 11.35% N at temperatures below approximately 500 °C (from [4]).

2.2. METALLURGICAL CONSIDERATIONS AND PROCESS REQUIREMENTS

2.2.1 BASIC IRON NITRIDE PHASES AND THE DIFFUSION PROCESS

As previously mentioned, nitriding is a thermochemical method of diffusing nascent nitrogen (see the definition on p.xiii) into the surface of mostly steels. The diffusion process can be explained by the solubility of nitrogen in iron [4] (see the iron-nitrogen equilibrium diagram in Figure 2.3). It is shown that the solubility limit of nitrogen in iron is temperature-dependent; at 450 °C the iron-base alloy will absorb up to 5.7% to 6.1% of N to form a γ' phase. Beyond this the surface phase formation on alloy steels will predominantly be an epsilon (ε) phase. This is strongly influenced by the carbon content of the steel i.e. the more carbon, the more potential for the ε phase to form (corrosion resistance increases from the γ'-phase to the ε- and carbo ε-phases [12]). If the temperature is further increased to the γ' phase temperature at 490 °C the 'window' or limit of solubility begins to decrease up to a temperature of ± 680 °C [4]. The crystal structures (bravais lattice) and phases are listed in Table 2.1.

Table 2.1: Phases in the Fe-N system, from [14] in [12].

Phases	Composition	Wt% (At%) N	N atoms per 100 Fe atoms	Bravais Lattice
Ferrite (α)	Fe	0.1 (0.4)	-	B.C.C.
Austenite (γ)	Fe	2.8 (11)	12.4	F.C.C.
Martensite (α')	Fe	2.6 (10)	11.1	B.C.Tetrag.
γ'	Fe_4N	5.9 (20)	25	Cubic
ε	Fe_2N_{1-x}	4.5-11.0 (18-32)	22 - 49.3	Hexagonal
ζ	Fe_2N	11.4 (33.3)	50	Orthorhombic

The crystal structure of a γ' phase is depicted in Figure 2.4.

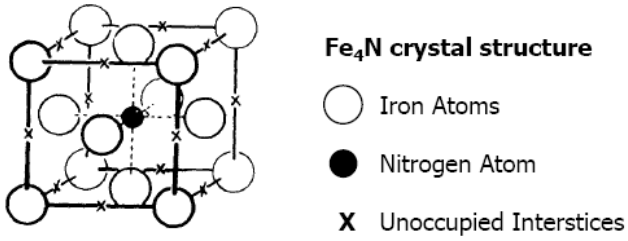

Figure 2.4: Fe_4N Crystal structure, from [14] in [12].

The equilibrium diagram in Figure 2.3 shows that control of the nitrogen diffusion will be critical to the process success (to ensure that the right phase is formed).

Some of the process parameters for gas nitriding according to [4] are:

• Furnace temperature

• Process control (see discussion below; control of the process parameters is necessary to ensure formation of an acceptable metallurgical case and repeatability of its requirements)

- Total surface area to be nitrided
- Process pressure inside the sealed process chamber
- Gas delivery pressure system into the sealed process chamber
- Exhaust gas system from the sealed process chamber
- Control of the preheat treatment procedure prior to nitriding, including stress relief and prehardening and tempering
- Quality and integrity of the steel surface precleaning prior to nitriding
- Consistent steel chemistry to maximize 'nitridability'

• Process time

• Gas flow

• Gas activity control

• Process chamber maintenance

All these factors help to reduce distortion during the process, while induced residual stresses still form due to nitriding. Nitriding also acts as a stabilizing process by providing an additional temper to the processed steel.

Mathematical description of the diffusion process:

As previously described case hardening results from diffusion of N into the substrate (solid solution) and precipitation of nitrides (FeN and nitride alloy elements) when holding the metal at suitable temperature (below 575°C). Ammonia (NH_3) is the nitrogenous gas typically used since it is metastable at nitriding temperature and decomposes on contact with iron [12].

The following chemical reaction takes place:

$2NH_3 \xrightarrow{\text{catalyst + heat}} 2N^{\bullet} + 3H_2$, where $N^{\bullet}$ is nascent nitrogen

To gain more insight into the mechanisms of the diffusion process it will now be described with an introduction to a mathematical model from Darbelly [12].

Mathematical model of Monolayer growth in a binary system (a pure Iron kinetic model):

Diffusion of solute N governs the growth kinetics. Flux balance equation at the γ'/α (α = ferrite) interface is given by equations from [12], [13] :

$$\frac{v^{\gamma'/\alpha}}{V_N^{\gamma'}}\left(u_N^{\gamma'/\alpha} - u_N^{\alpha/\gamma'}\right) = J_N^{\gamma'} - J_N^{\alpha}$$

where

$v^{\gamma'/\alpha}$ is migration rate of γ'/α interface
$V_N^{\gamma'}$ is partial volume/mole of N atom of γ' phase
$u_N^{\gamma'/\alpha}, u_N^{\alpha/\gamma'}$ contents of N on the γ' and α side of interface
$J_N^{\gamma'}, J_N^{\alpha}$ diffusion fluxes of N on the γ' and α side of interface

For more details and a description of the assumptions see [13].

The partial Gibbs free energy (or chemical potential) of N is the driving force for diffusion. The chemical diffusivity $\tilde{D}_N$ can be related to the selfdiffusion coefficient D_N^* using the thermodynamic factor ψ:

$$\tilde{D}_N = D_N^* \psi = \frac{U_N}{RT}\frac{\partial \mu_N}{\partial U_N}$$

U_N, μ_N N concentration and chemical potential

R gas constant

T absolute temperature

Using Fick's first law of diffusion for flux [13]:

$$J_N^{\gamma'} = \frac{\tilde{D}_N^{\gamma'}}{V_N^{\gamma'}}\frac{\partial u_N}{\partial z}$$

Integrating over the thickness of the layer and applying stationary diffusion assumption (constant flux over system) [13]:

$u_N^{\gamma'/s}$ N content at the surface $J_N^{\gamma'}\int_0^l dz = -\frac{1}{V_N^{\gamma'}}\int_{u_N^{\gamma'/s}}^{u_N^{\gamma'/\alpha}} \tilde{D}_N^{\gamma'} du_N$

Mathematical model of Multiphase growth in a binary system:

See Figure 2.5 for a graphical description of the symbols.

ε/γ': $\frac{v^{\varepsilon/\gamma'}}{V_N^{\varepsilon}}\left(u_N^{\varepsilon/\gamma'} - u_N^{\gamma'/\varepsilon}\right) = J_N^{\varepsilon} - J_N^{\gamma'}$

γ'/α: $\frac{v^{\gamma'/\alpha}}{V_N^{\gamma'}}\left(u_N^{\gamma'/\alpha} - u_N^{\alpha/\gamma'}\right) = J_N^{\gamma'} - J_N^{\alpha}$

Where $J_N^{\phi} = \frac{\tilde{D}_N^{\phi}}{V_N^{\phi}}\frac{\partial u_N}{\partial z}$ (Φ= ε, γ' or α)

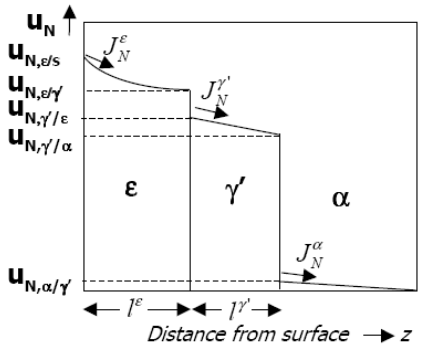

Figure 2.5: Diagram of metal phases to illustrate the mathematics of diffusion, from [12], [13].

Deviations occur from the pure Iron Kinetic model (binary model) due to:

- Nitride layer nucleation – In practice an equilibrium concentration of N in the atmosphere and the surface is prevented by the incubation time for formation of a compact nitride layer.
- The effect of C content – affects N activity (coefficient of diffusion) in α-Fe and ε, complex phases transformation (case of θ cementite ε carbonitride etc.)
- Alloying elements i.e. nitride (Cr, Mo, Al, V, Ti) and non-nitride (Ni) forming elements reduce the N diffusion coefficient in α-Fe.

To get more information on the above see references [12] and [13]. The mathematical model shows that the diffusion flux, chemical diffusivity and N content at the surface is a function of the N concentration (U_N) and chemical potential μ_N of the gas. The chemical potential influences the nitriding potential (amount of nascent nitrogen available). The method of nitriding process control, by controlling the nitriding potential to form a suitable case, is described next.

2.2.2 PROCESS CONTROL

According to [12] good process control improves:

- Process repeatability and economics
- Metallurgical requirements
- Operator interfacing, data trending and archiving

From [12] the key controls in nitriding are:

- Temperature must be constant (±15ºF or ±-9.5°C per AMS 2759/6 Gas Nitriding Specification) by means of Thermocouples and SPP
- Process gas monitored with a flow meter. Anhydrous ammonia and nitrogen shall be of the high purity grade (99.98%) with dew point -54ºF (-48ºC) or lower.
- The atmosphere is controlled by means of a dissociation pipette (burette) (±15% dissociation per AMS 2759/6) or gas analyzer
- Retort pressure must be slightly above atmosphere to prevent any O_2 from entering the vessel (risk of explosion) and still maintain flow through pipette or gas analyzer.

Control of Nitriding Potential [12]

Nitrogen solubility at the iron surface is determined by equilibrium of the reaction:

$NH_3 \Leftrightarrow \frac{3}{2}H_2 + [N]$, where $[N]$ is nascent nitrogen dissolved in Fe

hence for dilute solution of N in Fe, Henry's law states:

$$[a_N] = [\%N] = k\frac{pNH_3}{pH_2^{3/2}} \qquad [12], [15]$$

where k is an equilibrium constant at a given temperature and pNH_3 and pH_2 are the partial pressures in the gas.

Nitriding potential definition: $K_N = \frac{pNH_3}{pH_2^{3/2}}$

The nitriding potential must be kept low to ensure a thin compound layer [12], [15].

To determine nitriding potential the ammonia gas dissociation is measured. The exhaust gas of the process is a mixture of $2NH_3 + H_2 + N_2$ where ammonia is the only component soluble in water. A 'Burette' type instrument, shown in Figure 2.6, is used by capturing exhaust gas and letting water flow in it. The ammonia is dissolved creating a visual separation to measure the N_2 and H_2 volume.

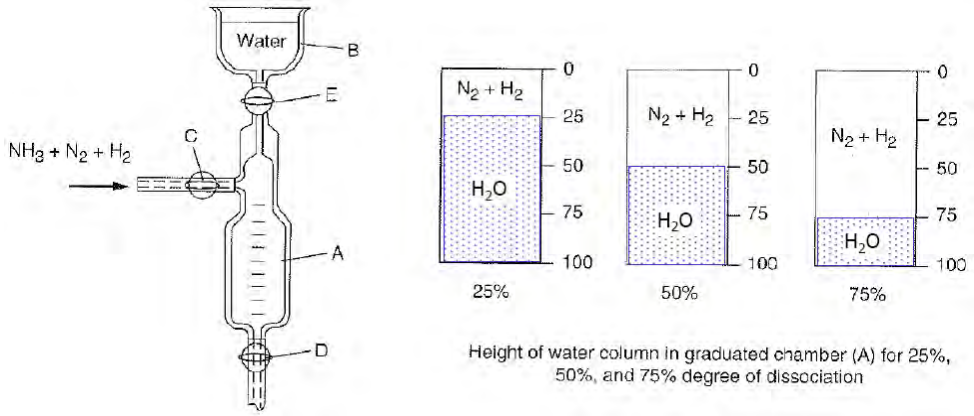

Figure 2.6: A 'Bunte Burette' instrument for measuring ammonia dissociation (from [12]).

The dissociation can also be measured with an electronic H_2 gas analyzer (see [12] and [17]). The measurement results are then interpreted as follows (see Figure 2.7).

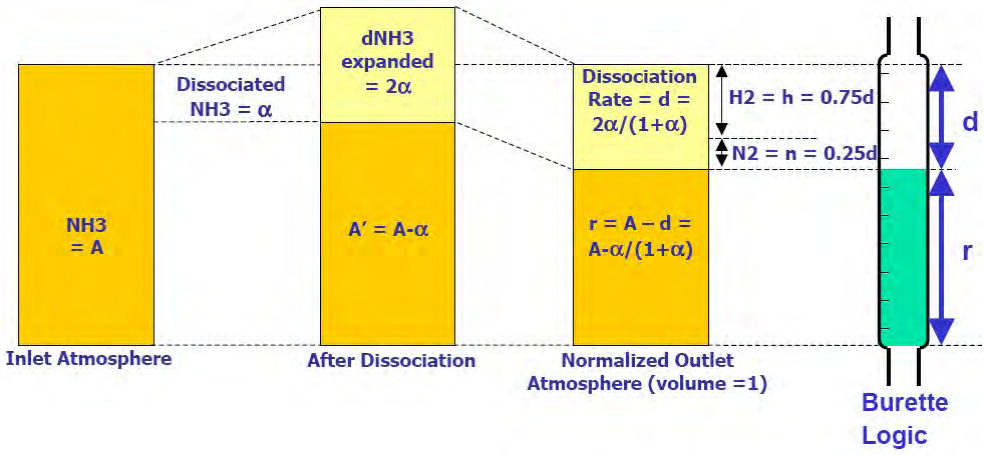

Figure 2.7: Illustration of interpreting a measurement on a Bunte Burette (from [12]).

The nitriding potential is now calculated as follows:

1. Measure $\%H_2$ using the analyzer: h
2. Calculate/read off Dissociation Rate d: $d = h/0.75$
3. Calculate α as a function of dissociation d: $\alpha = d/(2-d)$
4. Calculate Residual NH_3: $r = 1 - d$
5. Determine Nitriding Potential: $$K_N = \frac{r}{h^{3/2}} = \frac{1-d}{(0.75d)^{3/2}}$$

According to [12] the AMS standard 2759/10 for automatic control of gas nitriding by K_N requires a precision of ± 10% on the set point. An error of 2% in the analysis of the percentage H_2 translates into an error of about 20% for K_N at the low K_N set points that are required to achieve a very thin compound layer. The flow regulation and measurement will also need to be high precision to ensure that K_N is kept within limits.

2.3. NITRIDABLE STEELS

As first discovered by Adolph Fry in the early 1900s, the minimum surface hardness obtained with nitriding depends on the material being nitrided. Generally the maximum case hardness increases with increasing core hardness, but steel composition has a major influence [5]. Aluminium is a strong stable nitride former and the hardest cases are obtained with high aluminium steels such as Nitralloy steels (up to 1% Al, larger content has little effect [5]). High Al content can also result in alumina-type inclusions which are a disadvantage in some applications, but vacuum metallurgical considerations have helped to mitigate this. The chromium molybdenum 4100 series alloy steels (SAE designation) are most commonly used for nitriding (especially 4130 and 4140, for a 50 HRC case hardness). Higher chromium grade steels such as spec A983/A983M with 2.8-3.3% Cr obtain a 60 HRC case hardness [5].

Aluminium-containing steels produce a very hard, wear-resistant case but with low ductility. Chromium-containing low alloy steel provides considerably more ductility and lower case hardness ([10]). As discovered by Robert Sergeson, nickel in large quantities, tends to inhibit nitriding. Therefore grade 4340 does not respond as well as grade 4140 for the same nitriding cycle.

The other alloying elements (besides chromium and aluminium) used in commercial steels to form beneficial stable nitrides at nitriding temperatures are vanadium and tungsten. Molybdenum, in addition to being a nitride former, also reduces the risk of embrittlement at nitriding temperatures [10].

According to [10] the following steels can be gas nitrided for specific applications:

- Aluminium-containing low-alloy steels 7140 (Nitralloy G, 135M, N, EZ)
- Medium-carbon, chromium-containing low-alloy steels of the 4100, 4300, 5100, 6100, 8600, 8700, and 9800 series (SAE/AISI steel grade designation)
- Hot-work die steels containing 5% chromium such as H11, H12, and H13
- Low-carbon, chromium-containing low-alloy steels of the 3300, 8600 and 9300 series
- Air-hardening tool steels such as A-2, A-6, D-2, D-3 and S-7
- High-speed tool steels such as M-2 and M-4
- Nitronic stainless steels such as 30, 40, 50 and 60
- Ferritic and martensitic stainless steels of the 400 and 500 series
- Austenitic stainless steels of the 200 and 300 series
- Precipitation-hardening stainless steels such as 13-8 PH, 15-5 PH, 17-4 PH, 17-7 PH, A-286, AM350 and AM355.

The SAE/AISI steel grade designations are summarized as follows: 1000 series – carbon steels; 2000 – Nickel steels; 3000 – Nickel chromium steels; 4000- Molybdenum steels; 5000- Chromium steels etc. The British Nitriding steels developed by Thomas Firth and John Brown Steelworks in the late 1920s (see section 2.1.1) are given in Table 2.2.

Table 2.2: British Standard nitriding steels [4] (European EN standards).

	Composition, %								
Design ation	**C**	**Si**	**Mn**	**P**	**Cr**	**Mo**	**Ni**	**V**	**Al**
En 40 A	0.2-0.35	0.1-0.3	0.4-0.55	0.05max	2.9-4.0	0.6-0.8	0.4max	0	0
En 40 B	0.2-0.30	0.1-0.35	0.4-0.65	0.05max	2.9-3.5	0.4-0.7	0.4max	0.1-0.3	0
En 40 C	0.3-0.5	0.1-0.35	0.4-0.8	0.05max	2.9-3.5	0.7-1.2	0.4max	0.1-0.3	0
En 41 A	0.25-0.35	0.1-0.35	0.65max	0.05max	1.4-1.8	0.1-0.25	0.4max	0	0.9-1.3
En 41 B	0.25-0.45	0.1-0.35	0.65max	0.05max	1.4-1.8	0.1-0.25	0.4max	0	0.9-1.3

Note: The international designation for En 40 A, B, and C is 31 CrMoV 9. En 41 A and B are designated 34 CrAlMo 5. max, maximum

The steel that the CUD is manufactured from is an Italian forging of the ASME pressure vessel alloy steel of specification SA 336 and grade F22. The properties of this steel can be found

from [16]. It has a minimum tempering temperature of 675 °C. According to [5] the minimum tempering temperature must be at least 30 °C higher than the nitriding temperature to avoid loss in core strength and change in base material properties. The principal reason for the choice of F22 is its chemical composition which is very suitable for nitriding. Its composition is given in Table 2.3.

Table 2.3: Chemical composition of SA 336 F22 Class1/2 ([16] ASME II Subpart A).

Element	C	Mn	P	S	Si	Ni	Cr	Mo	V	Cu	N
%	0.05-0.15	0.3-0.6	0.025	0.025	0.5max	0	2.0-2.5	0.9-1.1	0	0	0

From Table 2.3 it is evident that the Cr and Mo contents are similar to that of the British Nitralloy steels and that they contain no Ni. SA 336 F22 has a yield strength of 310 Mpa and tensile strength of 515-690 Mpa at room temperature.

A final important nitriding materials comment is that nitriding usually does not improve the corrosion resistance for stainless steel. Although nitriding increases the surface hardness of stainless steels, the precipitation of chromium nitride causes significant decreases in corrosion resistance (austenitic stainless steel loses its corrosion resistance when nitrided above 480 °C; see [19] and [20]). Research shows that by lowering the nitriding temperature to 400 °C and reducing the chamber pressure combined with a technique called radio-frequency (r.f.) excitation plasma nitriding, the loss in corrosion resistance can be avoided (see [19]). Another new technique for nitriding austenitic and ferritic stainless steels, i.e. high temperature gas nitriding (HTGN), has recently been discovered (see section 2.4).

Other nitridable metals are alloys containing titanium and aluminium [21]. Research shows that nitriding increases the high temperature strength of Molybdenum Titanium Alloys by a factor of five [18]. These materials can be considered for use in future fusion reactors. Alloy steels remain the most commonly nitrided materials.

2.4. CURRENT RESEARCH IN THE NITRIDING FIELD

In order to improve the consistency of gas nitriding, research was done on intelligent computer control of the process (see [17]). Controlled gas nitriding has been successfully applied in the automotive industry [17]. Results show better wear resistance on nitrided surfaces than carburized ones, when the nitriding process is computer-controlled by the nitriding potential (see section 2.2.2). Other research focusing on modelling the nitriding process uses a magnetic sensor registering the growth of the nitrided layer to control the process [26].

Another new technique, i.e. High Temperature Gas Nitriding (HTGN) has recently been discovered for nitriding austenitic and ferritic stainless steels at high temperatures above 1050 °C, [22], [23] and [24]. This technique requires tempering afterwards below 450 °C. It is

performed in an N_2 atmosphere which is neither explosive nor toxic like the conventional gas nitriding techniques that use ammonia-hydrogen gas mixtures. This technique also improves cavitation erosion on impellers [22].

Laser nitriding, which is still in its early research phases, can be applied to tool and other steels [25]. It shows promise in selective nitriding of surfaces by using spot irradiation.

The literature presently does not include any research on new designs for gas nitriding plants or nitriding furnaces. The literature that will be discussed from this point onwards will be applicable to this study, i.e. the development of a new nitriding plant for the CUD.

2.5. EXISTING NITRIDING FACILITIES

2.5.1 AVAILABLE SUPPLIERS/EXISTING NITRIDING PLANTS

The purpose of the literature search in this section is to find existing nitriding facilities that can be used to nitride the CUD. This will obviate the requirement to design and construct a new nitriding plant especially for the CUD. It will also demonstrate whether a similar plant was previously constructed.

Most nitriding facilities in industry use either gas nitriding or plasma nitriding processes [5]. Gas nitriding facilities are frequently used in the automotive industry, but no large commercial gas nitriding furnaces (plants) could be found in South Africa[6]. Large gas nitriding furnaces do exist in countries outside South Africa. A picture of a nitriding furnace at the Ellwood National Crankshaft Company[7] where crankshafts for large engines (diesel locomotives, marine engines) are forged, machined and nitrided is shown in see Figure 2.8.

As can be seen from Figure 2.8 the particular furnace might just be large enough to house the CUD (see the man in the photo as a scale reference). Modifications will be required to handle and manoeuvre the 14 tonne CUD and ensure that it is kept in a stable position during nitriding. Even if a nitriding furnace in an overseas country could be modified to nitride the CUD the transport costs would entirely exceed the costs of modifying an existing heat treatment furnace in South Africa. Another possibility is using the plasma nitriding furnace of Bohler Uddeholm (Pty) Ltd in Kempton Park[8], the only commercial nitriding furnace in South Africa. However, from discussions between engineers of Bohler and Westinghouse Electric South Africa, this

[6] A company in Germiston, South Africa, called PH Heat Treatment did nitrocarburizing on small parts at the time of this study. However this process is not the same as pure gas nitriding (see www.phheat.co.za).

[7] The Ellwood National Crankshaft Company in Irvine, Pennsylvania, USA is now part of the Ellwood Group Incorporated. The website can be viewed on www.ellwoodgroup.com.

[8] The furnace is displayed on the website of Bohler Uddeholm (Pty) Ltd at www.bohler-uddeholm.co.za.

furnace would require extensive modifications to its top cover to make the CUD fit. It would also need extensive structural enhancements to enable it to accommodate the weight of the CUD. The other problem is that plasma nitriding is not the ideal process for nitriding the interior of the CUD, for the reasons given in section 2.5.2.

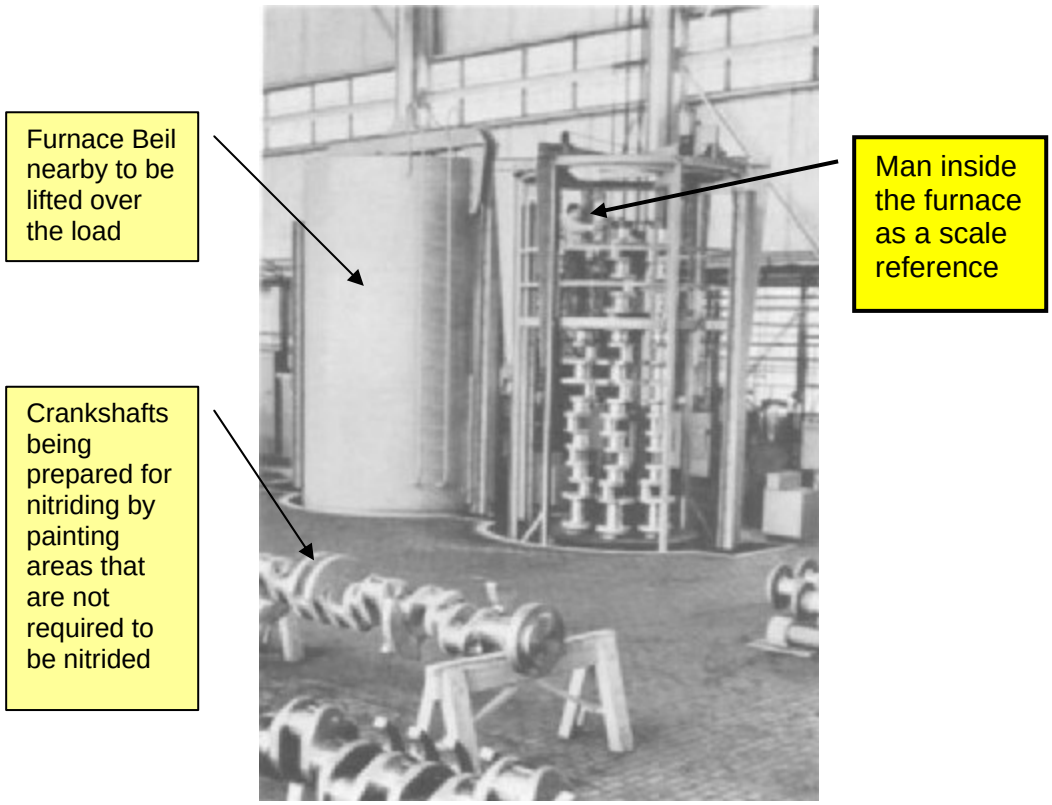

Figure 2.8: A large vertical gas nitriding furnace being loaded with crankshafts (courtesy Ellwood National Crankshaft Company, picture from [5]).

The most economical and effective solution would thus be to modify an existing heat treatment furnace at DCD Dorbyl Heavy Engineering in Vereeniging, where the CUD was also manufactured. A literature survey was performed on projects where existing heat treatment furnaces were modified for nitriding research purposes. One such example was research on low-pressure radio frequency (plasma) nitriding of austenitic stainless steel in an industrial-style heat-treatment furnace [19]. This study involved small nitriding specimens and r.f. nitriding (plasma nitriding derivative) was used. Another study where existing heat treatment furnaces were used is a patent, i.e *Method of nitriding work pieces of steel under pressure* [27]. Examples of the patented method show that a pressure vessel is filled with a predetermined amount of ammonia and nitrogen gas and then heated to the nitriding temperature in a pressure-resistant oven-type furnace. Constant pressures up to 8 Mpa are reached and the method produces 'pore-free' white layers consisting of a 100% γ phase (see Figure 2.3).

The literature shows that none of the studies performed involved using a large gas-fired top hat furnace similar to the one at DCD Dorbyl for gas nitriding, and it will thus be attempted for the first time in this research.

2.5.2 GAS NITRIDING VS. PLASMA NITRIDING

The next decision that needed to be made entailed the choice of the nitriding process that would be used for the CUD. Plasma nitriding will be explained first since most metallurgical considerations and historical background explained up to this point concerned gas nitriding. Plasma nitriding (also known as ion or glow discharge nitriding) is carried out in a chamber filled with nitrogen under partial vacuum conditions [5]. The workpiece is set up as a cathode and the vacuum vessel as the anode. Plasma is then formed under low pressure vacuum conditions by applying a high DC voltage. Inside the plasma nitrogen ions bombard the surface of the workpiece, heats it up, cleans it by sputtering and provides nitrogen ions (nascent nitrogen) for diffusion. A distinct lilac-coloured glow surrounds the workpiece (see Figure 2.9). The operating temperature for plasma nitriding is typically 350–580 °C with a bias towards the upper third of this range. The energy use is similar to that of gas nitriding, but the largest difference lies in the control of the nitrided case composition, as the white layer (compound layer) can be eliminated with this method (also see [28]).

The disadvantages of plasma nitriding are that it is not easy to perform selective nitriding (stop-off paints contaminate the vacuum chamber, [5] and [28]). In a gas nitriding furnace stop-off paints can easily be used. However, selective nitriding will not be necessary for the CUD. One major disadvantage of plasma nitriding is that it gives undesirable results in holes [5], due to hollow cathode/hole discharge and the CUD has many holes (or openings) of different diameters. Finally, plasma nitriding would be too expensive to implement on the existing furnace at DCD Dorbyl. Even modifying the plasma nitriding plant at Bohler would have cost millions of rands, since it would require an enormous mobile crane and the furnace would still not be able to carry the weight of the CUD[9].

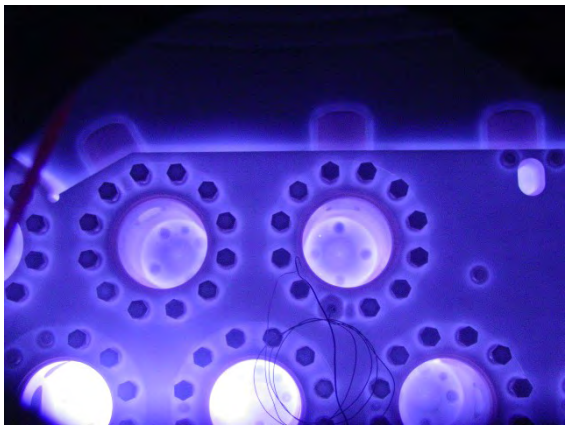

Figure 2.9: The FHSS valve blocks of the HTF being plasma nitrided at Bohler Uddeholm (Pty) Ltd. Photo courtesy of Westinghouse Electric South Africa (Pty) Ltd.

The nitriding process to be used for the CUD will thus be gas nitriding.

[9] This statement was made by Mike Nieuwoudt, the CUD designer at Westinghouse Electric SA (Pty) Ltd..

2.6. THE GAS NITRIDING PROCESS IN INDUSTRY

2.6.1 GAS NITRIDING PROCESS EQUIPMENT REQUIREMENTS

- First of all, a process chamber is prepared inside the furnace. It contains the gases at a slight overpressure to prevent the ingress of oxygen and other gases. Overpressure can be provided by letting gas exit through water to provide a downstream pressure to overcome.
- Furnace to provide the necessary heating, as shown in Figure 2.10.
- Nitrogen gas is usually used for purging before heating above 150 °C [10].
- A small amount of oxygen can be used for surface preparation (see [29] and [30] for the influence of surface pre-treatment on case formation), to oxidise the surface and act as a catalyst. Other surface preparation techniques such as 'sputtering' can also be used [29]. Stainless steel requires passivation with NH_4Cl pre-nitriding.
- Hydrogen gas can be used to dilute dissociated ammonia (Machlet section 2.1.1)
- Gas nitriding is mostly performed by cracking anhydrous ammonia to produce nascent nitrogen (HTGN uses N_2 gas at high temperature). Ammonia is metastable at nitriding temperature and decomposes on contact with iron [12].
- Stirring fan to ensure even distribution of the process gas and heat (see [31] for a typical Russian gas nitriding furnace design with a fan).
- A gas analyzer/Bunte Burette (see section 2.2.2)
- Flow meters, valves and other devices to control flow of the process gases.

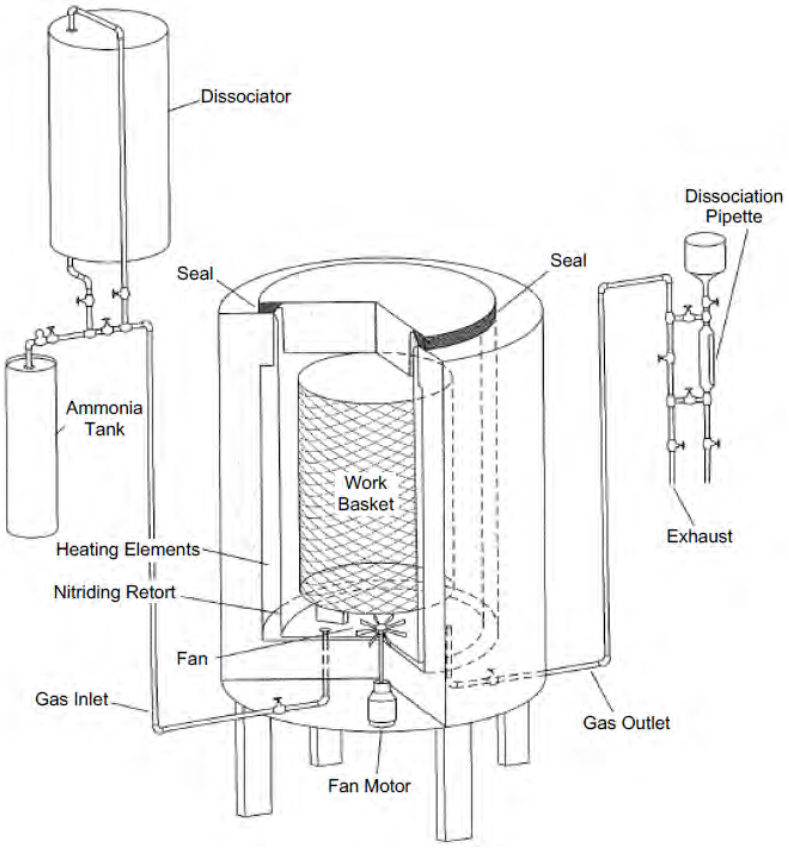

Figure 2.10: Schematic diagram to show components of a typical nitriding furnace, from [12].

2.6.2 CONTROL OF THE NITRIDING PROCESS AND CRACK RATIO

Control of the process parameters is necessary to ensure formation of an acceptable metallurgical case and repeatability of the metallurgical requirements. The most important process parameters for gas nitriding, according to [4] and [12], are repeated from sections 2.2.1 and 2.2.2:

- Furnace temperature must be constant (±15 °F/±9.5 °C per AMS 2759/6 Gas Nitriding Specification) by means of Thermocouples and SPP [12].
- Process gas monitored with a flow meter. Anhydrous ammonia and nitrogen shall be of the high purity grade (99.98%) with dew point -54 °F (-48 °C) or lower (increase NH_3 flow to reduce residence time and crack ratio [10]).
- Retort pressure slightly above atmosphere to prevent any O_2 from entering the vessel (risk of explosion) and still maintain flow through the Burette or gas analyzer
- Dissociation rate/crack ratio monitor and control – the atmosphere is controlled by means of a dissociation pipette (Burette) (±15% dissociation per AMS 2759/6) or gas analyzer.
- Process chamber maintenance.
- Process time.
- Fan speed.
- Process control (see section 2.2.1).

Computer control (control with the nitriding potential) was recently introduced in the automotive industry (see section 2.4 and [17]).

2.6.3 CONTROL OF NITRIDE LAYER PROPERTIES/QUALITY

The correct process control (as described above) needs to be performed in order to ensure the desired nitrided case. The required depth and hardness of the case must be determined beforehand and the importance of avoiding a compound white layer must also be taken into account. To reduce white layer (iron nitride network layer) thickness the double-stage gas nitriding cycle (Floe process) must be performed (see section 2.1.2). The Floe Process has two distinct nitriding cycles. The first cycle is performed as a normal nitriding cycle at 500 °C and 15% to 30% ammonia dissociation. This will produce the nitrogen-rich compound layer at the surface. For the next cycle the furnace is heated to 560 °C with gas dissociation increased to 75-85%. This two-stage process reduces the thickness of the white layer. The thin white layer that results (<0.025mm) can be polished off after nitriding [5]. According to [12] and [15], low K_N (low nitriding potential results in low dissociation rate) setpoints are required to achieve zero compound layer [12]. It is believed that the low dissociation rate of the first cycle of the Floe process forms a thin surface white layer and during the high dissociation rate of the second stage, the deeper interior of the case is nitrided [10].

To summarise the guidelines for the nitrided case are as follows:

- Increased furnace temperature results in increased case depth but decreased surface hardness (research by Robert Sergeson [4], [15]).
- Increased process time results in increased case depth.
- Increasing the gas supply rate will reduce residence or incubation time, to retard nucleation (reduce dissociation) for a compact nitride layer to form [12], [10].
- Increased furnace temperature results in increased dissociation rate [12], [15].
- Increased core material hardness and alloying element content result in increased case hardness.
- The correct surface pre-treatment and oxidation will also ensure a deeper case (see [29]). All oils must also be removed from the surface before nitriding.

After nitriding the Fe-N layer thickness can be evaluated by cutting through a nitrided sample and etching with an acid to view the nitrided layer under a Scanning Electron Microscope (SEM). The microhardness profile can be generated through the case depth with a Vickers indenter or any hardness test ([5] and [12]). Phase identification can be performed with Transmission Electron Microscopy (TEM) and X-ray diffraction [12], [6]. N concentration as a function of depth can be determined with a focused ion beam (FIB), TEM: electron energy-loss spectroscopy (EELS), electron probe X-ray micro-analysis (EPMA) and other metallurgical techniques explained in [12]. For the purpose of the CUD it is believed that a microscope photograph and a microhardness profile will be sufficient, see Figure 2.11.a) and b) respectively.

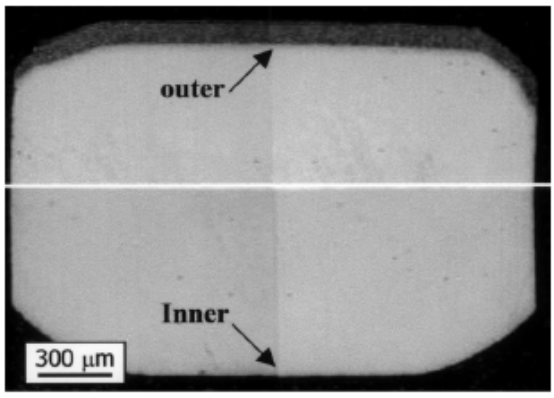

a) Photos of piston ring surface microstructure after nitriding, from [28].

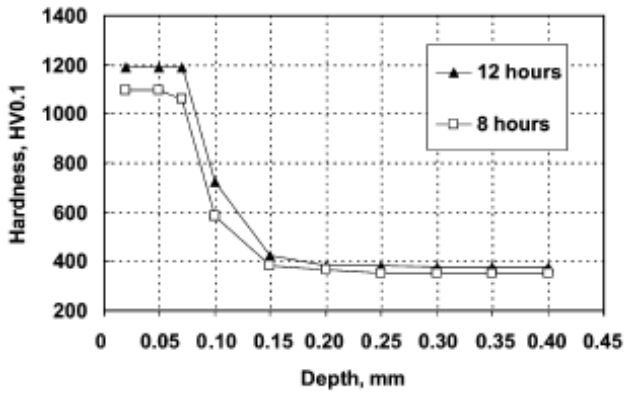

b) Microhardness profile of piston ring surface after nitriding, from [28].

Figure 2.11: Nitride layer evaluation techniques used for piston rings, from [28].

2.7. SMALL-SCALE LABORATORY TEST

2.7.1 PURPOSE OF THE LABORATORY TEST

Since gas nitriding is not performed commercially in South Africa there are various uncertainties regarding the practical application of the process. The expensive CUD housing, manufactured from ASME pressure vessel material, could not be used as a first-time experiment and therefore the process was tested on a small expendable forging by a metallurgical engineer, Chris Koch, of SAMS (Pty) Ltd. The process was tested by means of the vessel in Figure 2.12. It can be seen, in Figure 2.12, that the inside of the vessel is nitrided.

Figure 2.12: Experimental vessel that was nitrided on its inner surface (exterior is oxidised), picture taken at SAMS (Pty) Ltd.

The unique method of using the nitrided vessel interior as the process chamber was tested for the first time. The test setup included all the basic equipment that would be used in the nitriding of the actual CUD vessel. The expendable forging was also made of the same SA336 F22 steel as that of the CUD. The test was successful and a surface hardness of 600HV was achieved. The tests were performed with an electric furnace (see Figure 2.13). One of the lessons learned with the test is that the CUD inner surface temperature would be more important than furnace temperature, because of the large temperature gradient through the thick steel. Therefore, thermocouples would be required on the interior nitrided surface.

Figure 2.13: Small electric furnace used for the laboratory test, picture taken at SAMS (Pty) Ltd.

2.7.2 OUTPUT OF THE LABORATORY TESTS AND NP DESIGN GUIDE

The output of the tests was a set of instructions[10] from the metallurgist to guide the author with the design of the CUD NP.

Equipment requirements:

Heating Furnace

An electrical or gas heated furnace of suitable size, capable of reaching at least 800 °C , providing a heating rate of 50 °C – 100 °C/hr, while maintaining the temperature variance throughout the furnace within ± 5 °C.

CUD Vessel Preparation

Flanges for sealing all the ports on the vessel, must be manufactured. Only 20-30 kPa overpressure will be required in the vessel. Flange seals must be capable of at least 550 °C.

Flange - rotating shaft penetration and impeller

One flange on the vessel must be adapted to allow for a rotating shaft penetration with the necessary high-temperature seals. The shaft must penetrate deeply enough into the vessel to allow the fitment of an impeller to the front end. The impeller must be sized to create sufficient turbulence in the NH_3 gas ($N + H_2$) environment, during the gas Nitriding process.

Drainage Points

Water (steam at temperature) is generated during the gas nitriding process. Sufficient drainage points must be allowed for drainage at the lowest points of the vessel, as well as the off gas system, where the ‘used’ gas cools down, allowing water to condense.

Gas inlets

Flanges must be prepared with at least three gas inlet points for N_2; O_2 and NH_3 respectively. All should have gas valves and control Rotameters. All piping, valves, seals and flow meters that will come in direct contact with NH_3, must be made of stainless steel or glass (where applicable), to minimize corrosion and blockage due to reaction products. All piping must be of sufficient length to allow coupling of valves outside the furnace.

Gas outlet

[10] The output of the laboratory tests is part of a Westinghouse Electric SA internal document with number HTF-A-000417-152.

Provision must be made to allow gas to escape from the highest point in the vessel. The outlet pipe must allow for passing of H_2; undissociated NH_3 and unreacted N gas, which is developed in the process. The gas must be bubbled through a water trap to dissolve the NH_3 while the H_2 must be 'flared off' at a convenient point, far away from the furnace, to prevent unnecessary buildup of H_2 in the environment, reducing the possibility of an explosion. The gas outlet must also be equipped with a stainless steel valve to enable buildup and control of a slight overpressure in the vessel, and control of exit gas flow.

Temperature measurement

At least three thermocouples must be positioned inside the vessel at strategic points, allowing the temperature variance to be recorded during operation. Depending on the size and heating mechanism of the furnace, sufficient thermocouples should also be positioned outside the vessel. This will allow for monitoring and maintaining a constant external temperature gradient.

Nitriding step-by step procedure (similar to that used in industry; see [10])**:**

Vessel preparation

1. Prepare vessel as described above.
2. Place test samples of similar material at strategic points.

Preparation

1. Draw vacuum / or purge with N_2 to ensure removal of air.
2. Introduce raw NH_3 flow rate ±3000ℓ/hr to be verified (TBV), maintaining positive pressure in holder.
3. Raise the temperature to ± 200ºC.
4. Introduce O_2 @ 1,3 ℓ/min
5. Purge the mixture through while heating to 500ºC to the following procedure.

Heating to 500ºC

1. Room temperature to 450ºC @ 100ºC/hr
2. Soak at 450ºC for 1 hour
3. Close the O_2 - flow to the vessel
4. Heat to 500ºC @ 100ºC/hr
5. Hold at 500ºC for 2 hours

Start Nitriding Cycle

1. - NH_3 flow ± 50 ℓ/hr, to be determined (TBD), depending on vessel internal volume
   - Measure crack ratio, using "Bunte Burette"
2. - Heat to 555ºC from 500ºC @ 50ºC/hr
   - NH_3 flow ± 120 ℓ/hr (TBD)
   - Measure NH_3 dissociation on outlet gas, using "Bunte Burette"
3. - Soak @ 555ºC for 8 - 20 hours (TBV)
   - NH_3 flow ± 20 ℓ/hr (TBD), depending on vessel volume
   - Measure NH_3 dissociation on outlet gas regularly

Cycle Completion

1. Reduce temperature @ 20ºC/hr down to 450ºC
   - NH_3 gas flow 600 ℓ/hr (TBV) - depending on vessel volume
2. Switch off furnace and allow to cool to 80ºC while maintaining NH_3 flow
3. Switch off NH_3 and purge chamber with N_2 before opening.
4. Remove test samples and measure the Nitrided thickness optically and micro hardness by cross sectioning and polishing.

2.8. HIGH TEMPERATURE GAS SEALING BEARINGS

One of the major design challenges with the CUD NP would be the seal of the long rotating shaft that penetrates the process chamber. The leakage of high temperature ammonia gas would create an explosion hazard when present at a concentration of 15-25% in air [10]. To ensure industrial safety the NFPA 69 standards for Explosion Prevention Systems would be followed around the furnace. Hydrogen gas, a product of the nitriding cycle, is also explosive. The seal must minimise leakage of these gases. Little information for similar situations where a gas needs to be sealed on a high-temperature rotating shaft is available in the literature.

Gas turbine engines are an example where a high-temperature gas shaft seal is used to isolate the combustion chamber from the compressor chamber. These bearings are expensive and manufactured from ceramic materials, and also use other gases or pressurised liquid volumes as barriers (see [32] and [33]). One patent for a gas turbine used a complex carbon face seal as an alternative [34].

In South African industry a few solutions were found where graphite journal bearings were used for conveyors in drying furnaces for various manufacturing plants. These were installed by Carbone Lorraine (Le Carbone S.A (Pty) Ltd.) Synthetic diamond manufacturing machines also use high-temperature graphite bearings manufactured by Morgan Carbon SA (Pty) Ltd. However, gas sealing is not known to be a requirement for these applications. In some coal-fired boilers rotating shaft seals have been designed for gas sealing. However, these seals

do not have the same requirements as the CUD rotating shaft penetration. The applicability of these solutions will be evaluated during the design of the seal in chapter 4.

2.9. CONCLUSION

The history of nitriding shows that the process was discovered in the early 1900s (first patent applied for in 1908). The process was only accepted by industry in the late 1920's when the United States also started to show an interest.

The literature survey shows no recorded use of a pressure vessel as a nitriding process chamber and few pressure vessels were recorded to be nitrided. The design of a nitriding plant to accommodate a forging, as large as the CUD, and use its interior as the process chamber therefore appears to be novel.

Through extensive research of metallurgical aspects the process control parameters to ensure the desired nitrided case using gas nitriding were determined and summarised in par. 2.6.3. The output of the lab tests, see section 2.7.2, will be used as a guideline to design the CUD Nitriding Plant (NP).

The literature was also searched to aid in the design of the high temperature gas seal for the rotating shaft penetration for the CUD NP.

This concludes the literature survey and should place the dissertation topic, *Design of a novel nitriding plant for the pressure vessel of the PBMR Core Unloading Device*, into perspective for the reader.

Chapter 3: Concept Design

3.1. INTRODUCTION

Since this research is in essence a design project the full mechanical engineering design process was followed. The product development process described by [35] was followed to arrive at the final concept and final design specification for the HTF CUD NP. Although the design guidelines described in section 2.7.2 already lead to a gas nitriding plant type concept, the decision for the final concept must still be made in a scientific quantifiable manner. Since the entire NP consists of different systems, in strict terms the same concept design process should be followed for the design of each subsystem within the plant. Only the concept design of the system as a whole will be described in this chapter.

3.2. USERS' REQUIREMENTS

The users of the nitriding plant were interviewed to determine the customer needs for the plant. The interviews, together with various observations and the plant design instructions in section 2.7.2, led to the following interpreted user need statements.

The CUD Nitriding Plant:

1. is capable of nitriding large workpieces
2. nitrides the inner surface of a pressure vessel
3. is transportable
4. is easy to manufacture
5. is easy to operate
6. is safe to operate
7. provides a heating furnace capable of reaching a desired nitriding temperature
8. provides a heating furnace capable of maintaining a desired temperature
9. provides temperature measurement of the vessel interior surfaces
10. provides the necessary gases at the right flow rates
11. provides adequate control of the nitriding process
12. enables the user to nitride to a desired case depth and hardness
13. provides a means to measure the nitriding layer thickness and hardness
14. is economical to construct and operate
15. requires little maintenance

3.3. FUNCTIONAL ANALYSIS AND SIMULATION

The purpose of this step is to decompose the complex problem into simpler sub problems. This will clarify the problem in order to make the concept generation and design phases easier.

3.3.1 FUNCTIONAL DECOMPOSITION

Flow diagrams will be drawn up to define the processes of the gas nitriding plant and to identify the characteristics. An overview flow diagram is created along with its sub- flow diagrams.

3.3.1.1 SYSTEM LEVEL FUNCTION DIAGRAM

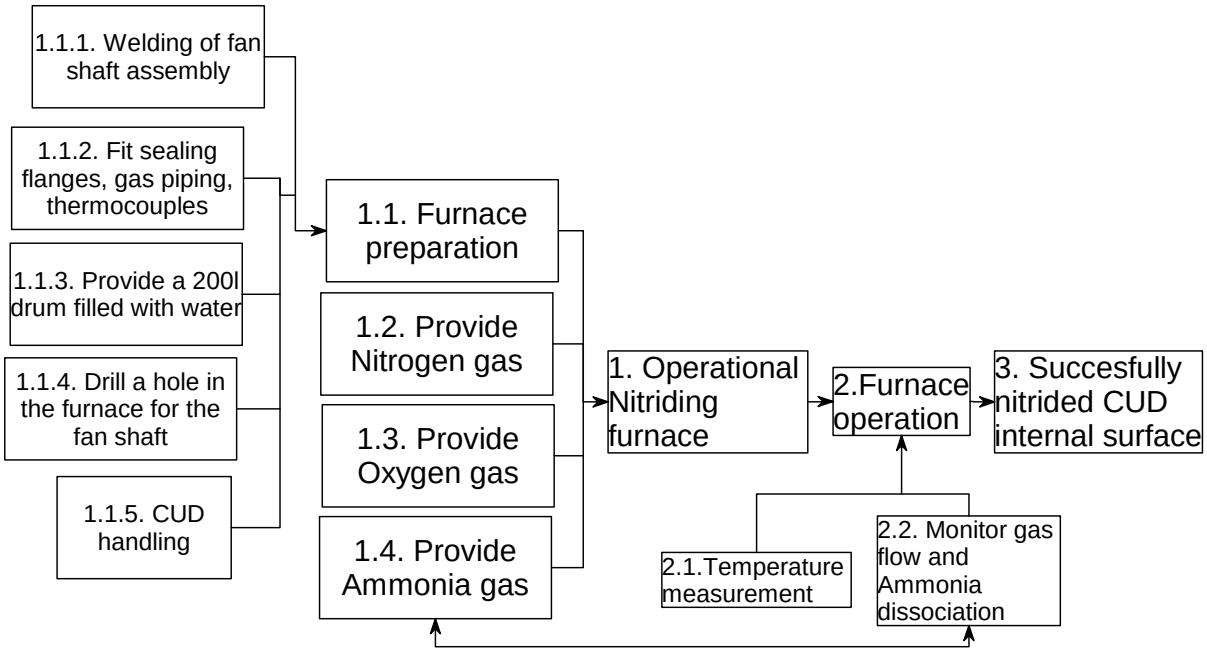

Figure 3.1: Overview System level Flow Diagram for functional decomposition.

3.3.2 MISSION LEVEL DIAGRAMS

The mission level diagrams to decompose functions 1.1 to 3. are given in Appendix A.

3.3.3 SYSTEM LEVEL FUNCTIONS

1. Supply gas for nitriding
2. Heat up the process chamber
3. Stir the gas to ensure turbulent mixing
4. Contain the gases inside the process chamber
5. Seal with gas pipe and other penetrations
6. Provide test samples to test for the quality of nitriding
7. Provide a means for the gas to exit

3.3.4 FIRST LEVEL FUNCTIONS

The main functions of the CUD nitriding plant are as follows:

1. **Supply Gas for Nitriding**
   - *1.1. Provide Gas flow (ammonia, oxygen and nitrogen)*
   - *1.2. Provide different gases for different stages/modes*

     ammonia for the nitriding cycle
     oxygen for the furnace preparation cycle (oxidising the CUD inner surface)
     nitrogen for purging and for safety purposes

   - *1.3. Provide Gas flow Control*
   - *1.4. Provide Gas flow measurement*
2. **Heat up the process chamber**
   - *2.1. Heat the Nitriding process chamber to the different required temperatures*
   - *2.2. Temperature control*
3. **Stir the gas to ensure turbulent mixing**
   - *3.1. Ensure turbulent gas flow inside the process chamber to ensure sufficient mixing*
   - *3.2. Penetrate the furnace wall and process chamber to insert mixer*
   - *3.3. Seal off the ammonia gas from the furnace*
4. **Contain the gases inside the process chamber**
   - *4.1. Contain and seal off the ammonia gas within the process chamber to prevent a possible explosion*
   - *4.2. Provide a contained volume and surface area for nitriding*
5. **Seal with gas pipe and other penetrations**
   - *5.1. Gas pipe penetrations prevent ammonia, oxygen and nitrogen gas from entering the furnace, flange seals also provide sealing*
   - *5.2. Thermocouple penetrations ensures thermocouples are placed inside the CUD housing without leakage into furnace*
6. **Provide test samples to test for the quality of nitriding**
   - *6.1. Samples for qualifying the nitriding process*
   - *6.2. Test for nitride layer thickness and hardness*
   - *6.3. Witness pieces to test for the heat treatment cycle effects*
7. **Provide a means for the Gas to Exit**
   - *7.1. Manage Pressure inside the process chamber*
   - *7.2. Direct the flow to either the ‘Bunte burette’ or the water drum*
   - *7.3. Control the flow through each exit flow gas pipe*
     - *i. Measure and balance the flowrate through each exit pipe*
   - *7.4. Measure the crack ratio*
   - *7.5. Capture the dissociated ammonia and other gases in water*

3.4. DESIGN REQUIREMENTS

3.4.1 DEVELOP A LIST OF METRICS

Now the customer's needs and information gathered from the literature study and functional analysis are translated into precise targets for the remaining design process. Operational and functional requirements must first be defined. The first step is to rate the user requirements according to their relative importance (Table 3.1).

Table 3.1: The user requirements and their relative importance.

No.	Need	Importance
1	is capable of nitriding large workpieces	5
2	nitrides the inner surface of a pressure vessel	4
3	is transportable	2
4	is easy to manufacture	2
5	is easy to operate	4
6	is safe to operate	4
7	provides a furnace capable of reaching a desired nitriding temperature	4
8	provides a furnace capable of maintaining a desired temperature	3
9	provides temperature measurement of the vessel interior surfaces	4
10	provides the necessary gases at the right flow rates	4
11	provides adequate control of the nitriding process	4
12	enables the user to nitride to a desired case depth and hardness	4
13	provides a means to measure the nitrided case thickness and hardness	3
14	is economical to construct and operate	3
15	requires little maintenance	1

Note: importance rated from low @1 to high @5

The user requirements are now translated into a list of metrics by which the design can be measured, see Table 3.2

Table 3.2: List of Metrics

Metric No.	Need Nos.	Metric	Importance	Units
1	1,2	Max. workpiece mass	5	kg
2	1,2	Max. workpiece dimensions	5	mxmxm
3	5,6,11	No. of operator hours per workpiece	4	hrs
4	7	Furnace max. sustained temperature	4	°C
5	8	Furnace variance	3	°C
6	12	Nitrided case depth	4	µm
7	12	Nitided case surface hardness	4	HV
8	5	Min Process time	4	hrs
9	14	Estimated Plant Cost	4	R
10	14	Operating cost per tonne	3	R

The metrics are then given values to arrive at the target specifications for the system.

3.4.2 TECHNICAL SPECIFICATION (OPERATIONAL DESIGN REQUIREMENTS)

The following target specifications are valid for any final concept for the NP, see Table 3.3.

Table 3.3: Target Specification

Metric No.	Need Nos.	Metric	Impor-tance	Units	Min value	Ideal value
1	1,2	Max. workpiece mass	5	ton	14	20
2	1,2	Max. workpiece dimensions	5	mxmxm	3x2x2	3x3x3
3	5,6	No. of operator hours per workpiece	4	hrs	40	30
4	7	Furnace max. sustained temperature	4	°C	700	800
5	8	Furnace variance	3	°C	20	5
6	12,11	Nitrided case depth	4	µm	200	400
7	12,11	Nitided case surface hardness	4	HV	500	1000
8	5	Min Process time for 14 ton piece	4	hrs	40	30
9	14	Estimated Plant Cost	4	R	500000	100000
10	14	Operating cost per tonne	3	R	40000	20000

3.4.3 FINAL DESIGN REQUIREMENTS

The final design requirements are the target specifications combined with the functional requirements. Here follows a summary of the final design requirements:

1. is capable of nitriding large workpieces of 3 m x 3 m x 2 m, weighing 14 tonnes
2. nitrides the inner surface of a pressure vessel
3. is transportable
4. is easy to manufacture
5. is safe and easy to operate and requires 40 hrs operator time
6. provides a heating furnace capable of 700 °C
7. furnace has a temperature variation of 20 °C
8. provides temperature measurement up to 700 °C
9. provides the necessary gases at the right flow rates
10. provides adequate control of the nitriding process
11. enables the user to nitride to a desired case depth of 200 µm and surface hardness of 500 HV
12. provides a means to measure the nitriding layer thickness and hardness
13. the plant costs R 500 000 to construct
14. operating costs are R 40 000 to nitride one CUD
15. requires little maintenance

3.5. CONCEPT GENERATION

Various concepts were generated to approach the problem for a CUD nitriding plant. Although selection would only be done much later some concepts could already be seen as unfeasible. A

concept screening process was then followed. This process served as a first round of elimination to reduce the amount of concepts from ten to five. Concepts were evaluated based on the selection criteria (section 6.1) and given a + or – rating. As a rule any concept that required a new furnace to be built was given a – rating for manufacturing cost. The scores were added and the top five scoring concepts were selected for further evaluation. These concepts are:

A. Custom made Bulk gas nitriding process chamber, gas furnace
B. Custom made Bulk gas nitriding process chamber, electric furnace
C. Modified Plasma Nitriding furnace
D. Vessel interior process chamber, electric furnace
E. Vessel interior process chamber, gas fired furnace

3.6. CONCEPT EVALUATION AND FINAL CONCEPT

3.6.1 SELECTION CRITERIA

To summarize the user requirements the following selection criteria were established on which to base the final concept selection. The criteria were selected very carefully, so that the final concept would easily accommodate a CUD while being economical and easy to manufacture.

1. Constructability
2. Stirring fan effectiveness
3. Stirring fan design complexity
4. Nitriding quality
5. Ease of assembly
6. Manufacturing cost
7. Safety

3.6.2 WEIGHTING OF CRITERIA

In order to perform final concept evaluation each criterium was weighted according to importance for the success of this research project, see Table 3.4.

Table 3.4: Weighting of concept selection criteria for the NP.

No.	Criterium	Weight
1	Constructability	20.00%
2	Stirring fan effectiveness	10.00%
3	Stirring fan design complexity	10.00%
4	Nitriding quality	20.00%
5	Ease of assembly for process	5.00%
6	Manufacturing cost	15.00%
7	Safety	20.00%

3.6.3 CONCEPT SCORING

Now a single final concept needs to be chosen for further development. The concept scoring method explained in [35] will be used.

3.6.3.1 CONCEPT A

Description: Custom made Bulk gas nitriding process chamber, gas furnace. The CUD housing is rolled into the large nitriding process chamber ready to be nitrided.

Constructability

Modifying an existing gas fired furnace would require the construction of a separate heat resistant process chamber within the gas fired furnace. Since a mixture of methane propane gases are normally burned inside such a furnace the nitriding gases cannot be released directly inside the furnace to nitride the CUD exterior and interior. It will also be very hazardous and the furnace would have to be built leak tight. It will be a challenge to build.

Stirring fan effectiveness

The stirring fan would be required to mix for a significant volume of gas (the entire furnace interior). More than one fan disk will probably be necessary.

Stirring fan design complexity

The fan shaft will not be too long; it just needs to be inside the furnace wall. The shaft will have a small diameter and will be inexpensive.

Nitriding quality

All round nitriding i.e. the exterior and interior of the CUD will be nitrided. The quality might be questionable due to the unpredictable flow on the outside of the process chamber and the inside of the CUD. The process will also require a large amount of unnecessary gas since the exterior of the CUD and the extra process chamber wall do not need to be nitrided.

Ease of assembly

CUD housing is rolled into the large nitriding process chamber ready to be nitrided, little pre-nitriding preparations are required on the CUD.

Manufacturing cost

The CUD will need no modifications (or accessories) since the interior volume does not need to be sealed. The extra process chamber design can be expensive since it will need to be leak tight and heat resistant.

Safety

If the large process chamber leaks gas outside of the furnace it could cause an explosion. The burners inside the furnace should burn off nitriding gases along with the methane and propane.

3.6.3.2 CONCEPT B

Description: Custom made Bulk gas nitriding process chamber, electric furnace

Constructability

An existing electric furnace would require the construction of a separate heat resistant process chamber within the furnace. Because the mixture of nitriding gases are explosive and might be ignited by an electrical spark the gases cannot be released directly inside the furnace to nitride the CUD exterior and interior. Therefore the furnace would have to be built leak tight. Normally electric furnaces are too small to accommodate the CUD and a new electric furnace would need to be built. These furnaces will also be inefficient at this size and will be a challenge to build.

Stirring fan effectiveness

The stirring fan would need to mix the gas for a significant volume (the entire furnace interior). More than one fan disk will probably be necessary.

Stirring fan design complexity

The fan shaft will be short; it only needs to be inside the wall. The shaft will be inexpensive.

Nitriding quality

All round nitriding i.e. the exterior and interior of the CUD will be nitrided. The quality might be questionable due to the unpredictable flow on the outside of the process chamber and the inside of the CUD. The process will also require a large amount of unnecessary gas since the exterior of the CUD and the extra process chamber wall does not need to be nitrided.

Ease of assembly

CUD housing is rolled into the large nitriding process chamber ready to be nitrided, little pre-nitriding preparations need to be done on the CUD.

Manufacturing cost

No modification to the CUD because its interior volume does not need to be sealed. The extra leak tight process chamber can be expensive. A large electrical furnace will need to be built.

Safety

If the large process chamber leaks explosive ammonia and hydrogen gas into the furnace it might ignited by a spark and cause an explosion.

3.6.3.3 CONCEPT C

Description: Plasma Nitriding furnace. This concept is in contradiction with the design guidelines in section 2.7.2 which is for gas nitriding. The functional analysis was also performed for typical gas nitriding functions. This concept will still be evaluated to give it a fair chance.

Constructability

As stated in section 2.5 the only available plasma nitriding facility in South Africa (Bohler Uddeholm) can not accommodate the CUD's size and weight and would cost millions to modify. Building a new plasma nitriding plant for the CUD will cost even more. The construction of such a plant will be complex since it involves a vacuum chamber and other vacuum equipment.

Stirring fan effectiveness

This concept does not need a stirring fan, however components that serve the same purpose as a stirring fan i.e. distribute nitriding gases evenly, are the terminals that apply a uniform DC voltage charge. Since the CUD is such a large block with complex geometry it will be more difficult to apply the voltage evenly throughout.

Stirring fan design complexity

The uniform application of the DC voltage to charge the CUD as the cathode will be complex. That is because of its complex geometry and varying thickness. Threaded bolt holes need to be plugged with steel bolts etc.

Nitriding quality

The quality of the nitriding in the CUD insert holes (that need to be nitrided) will be questionable because of hollow cathode or hole discharge (see section 2.5.2) and extra case thickness around corners.

Ease of assembly

CUD housing is rolled into the large nitriding process chamber ready to be nitrided, little pre-nitriding preparations need to be done i.e. DC voltage electrical contacts applied and threaded bolt holes plugged to prevent hollow cathode discharge etc.

Manufacturing cost

As previously stated it will be the most expensive design to build.

Safety

Since no explosive ammonia or hydrogen gases are present, except for nitrogen in the vacuum chamber, this design will be the safest.

3.6.3.4 CONCEPT D

Description: Vessel interior process chamber, electric furnace

Constructability

The CUD holes need to be sealed off to use the interior volume of the CUD housing as a process chamber. The mixture of nitriding gases are explosive and might be ignited by an electrical spark, therefore the process chamber must be leak tight. The furnace would also need to be built leak tight. Normally electric furnaces are too small to accommodate the CUD and a new electric furnace would need to be built. It will be a challenge to build.

Stirring fan effectiveness

The stirring fan can be positioned inside the CUD barrel and it will mix the gases for a smaller volume and would therefore be effective. A single fan can provide enough turbulence.

Stirring fan design complexity

The fan design is complex because the shaft will need to extend through the furnace wall and then also through the CUD barrel. A shaft of extended length is more expensive and requires extra bearings.

Nitriding quality

The nitriding quality would be the best because of the good stirring fan effectiveness and the reliability of gas nitriding in a complex geometry.

Ease of assembly

CUD housing needs to be sealed off with various accessories and gas piping penetrations.

Manufacturing cost

The accessories to make the CUD interior volume a process chamber could be expensive, however the biggest cost would be to get or build a large enough electric furnace.

Safety

The mixture of nitriding gases are explosive and can be ignited by an electrical spark. If the process chamber leaks, releasing gases directly in the furnace, it could ignite and explode.

3.6.3.5 CONCEPT E

Description: Vessel interior process chamber, gas fired furnace

Constructability

This concept is possibly the easiest to construct. A large number of gas fired furnaces are available and especially in the top hat gas fired furnace configuration (DCD Dorbyl). The CUD insert holes are sealed off to make a process chamber with the interior volume of the CUD housing. Because the nitriding gases are explosive it can not be released directly inside the furnace. However it is not as dangerous as an electric furnace since the burners are already firing and would merely burn off the escaping ammonia before it exits the furnace wall. The top hat furnace would also be easy to modify by installing gas flow pipes beneath the wall through the sand on which it is placed. It is usually lowered with a crane on top of the workpiece.

Stirring fan effectiveness

Since the stirring fan can be positioned inside the CUD barrel it will need to mix the gases for a smaller volume (smaller column diameter) and would be very effective. A single fan can provide enough turbulence for even distribution and mixing of nitriding gases.

Stirring fan design complexity

The stirring fan design can be complex because the shaft will need to extend an appreciable distance first through the furnace wall and then through the CUD barrel. An extended length shaft will be more expensive and will require extra bearings.

Nitriding quality

The nitriding quality would be the best because of the good stirring fan effectiveness and the reliability of gas nitriding in a complex geometry.

Ease of assembly

The CUD housing needs to be sealed off with various accessories and gas piping penetrations.

Manufacturing cost

The accessories to construct the CUD interior volume as a process chamber can be expensive. However, the availability of an existing top hat furnace at DCD Dorbyl will save costs.

Safety

If the process chamber leaks explosive ammonia and hydrogen gas outside of the furnace the furnace burners' flames will just burn off the nitriding gases along with the methane and propane inside the furnace. If some gases do escape through the fan shaft seal it can be dangerous.

3.6.4 CONCEPT SCORING MATRIX

The concept scoring matrix in Table 3.5 shows that concept E must be developed further.

Relative Performance	Rating
much worse than reference	1
worse than reference	2
same as reference	3
better than reference	4
much better than reference	5

		Concept									
		A Bulk gas nitriding process chamber, gas furnace		B Bulk gas nitriding process chamber, electric furnace		C Plasma Nitriding furnace		D Vessel interior process chamber, electric furnace		E Vessel interior process chamber, gas fired furnace	
Selection Criteria	**Weight**	**Rating**	**Weighted score**	**Rating**	**Weighted score**	**Rating**	**Weighted score**	**Rating**	**Weighted score**	**Rating**	**Weighted score**
Constructability	20%	4	0.8	2	0.4	1	0.2	3	0.6	5	1
Stirring fan effectiveness	10%	2	0.2	2	0.2	3	0.3	5	0.5	5	0.5
Stirring fan design complexity	10%	5	0.5	5	0.5	3	0.3	2	0.2	2	0.2
Nitriding quality	20%	3	0.6	3	0.6	2	0.4	5	1	5	1
Ease of assembly	5%	5	0.25	4	0.2	3	0.15	1	0.05	1	0.05
Manufacturing cost	15%	4	0.6	3	0.45	2	0.3	3	0.45	5	0.75
Safety	20%	4	0.8	2	0.4	5	1	3	0.6	4	0.8
Total Score		**3.75**		**2.75**		**2.65**		**3.4**		**4.3**	
Rank		**2**		**4**		**5**		**3**		**1**	
Continue?		**No**		**No**		**No**		**No**		**Develop**	

Table 3.5: Concept Scoring Matrix

3.7. FINAL CONCEPT AND CONCLUSION

3.7.1 FINAL CONCEPT SPECIFIC DESIGN REQUIREMENTS

The final concept that was selected is concept E i.e. using the vessel interior process chamber, with the existing suitable size gas fired top hat furnace at DCD Dorbyl where the CUD was manufactured. The detail design of the NP and its components can now be started. The final design requirements given in section 3.4.3 had been adjusted for using the existing top hat gas fired furnace of DCD Dorbyl and had been defined as performance and physical characteristics.

3.7.2 PROCEEDING WITH THE DETAIL DESIGN OF A PROCESS PLANT SYSTEM

In the process engineering field, for the design of a process plant system, a functional specification[11] is set up using performance and physical requirements (to aid in describing the operation of the plant). In practice the system engineering process for the development of process plants typically requires a development specification document[12], (includes the user needs and target specifications) followed by a functional specification and then the basic and detail design is carried out with an operating description (or operating manual) and design report as output.

In the pure mechanical engineering machine design environment (product development process as described by [35]) the final design requirements (see section 3.4.3) are usually sufficient to proceed with the detail design. Since this is a multidisciplinary design project a functional specification was set up and the plant system was also subdivided into process functional modules (PFMs) for the detail design.

The performance requirements for the functions are listed in Table 3.6 and the physical requirements are listed in Table 3.7. Parameters from the design instructions i.e. section 2.7.2 were used.

[11] The name Functional Specification is given for this type of document within Westinghouse Electric South Africa (Pty) Ltd.

[12] A Development Specification is the name given for this type of document within PBMR (Pty) Ltd.

Table 3.6: Main Performance requirements of the plant.

Function no.	Description	Performance parameter	Value	Unit
1	Oxygen gas cylinder and regulator			
		Oxygen supply duration	4	hrs
		Max Oxygen flow rate	200	ℓ/hr
		Capacity of one cylinder (supplier info)	14	Kg
2	Nitrogen gas cylinder and regulator			
		Nitrogen supply duration	6	hrs
		Max Nitrogen flow rate	2000	ℓ/hr
		Capacity of one cylinder (supplier info)	11	kg
3	Ammonia gas cylinder and regulator			
		Ammonia supply duration	40	hrs
		Max Ammonia flow rate	3000	ℓ/hr
		Capacity of one cylinder (supplier info)	68	kg
4	Fan shaft minimum operating life			
		Total operating time	48	hrs
		Shaft maximum operating temperature	555	°C
5	Furnace			
		maximum temperature	800	°C
		heating rate	50-100	°C/hr
		temperature variance	5	°C
6	CUD Handling			
		maximum handling capacity	20	ton
7	Support for the CUD during furnace operation (CUD cradle)			
		Support CUD weight, load capacity	20	ton
8	Thermocouple and logging equipment supply (for furnace temperature and workpiece temperature only)			
		temperature measurement range	25 – 700	°C
9	Nitriding process chamber (sealed CUD housing including flanges and seals)			
		Leak rate into furnace	ALARA	ℓ/hr
		Seal maximum operating temperature	555	°C
		Vessel maximum operating temperature	555	°C
		Vessel maximum operating pressure	20	kPa
10	Clean 200l oil drum (filled with water)			
		Amount of water	190	l
11	Witness samples of similar material for measuring heat cycle effects on steel yield strength			
		Amount of witness samples	5	
12	Nitriding thickness test samples to measure the thickness and hardness of the nitride layer that is created during nitriding			
		Amount of test samples	10	

Table 3.7: Main Physical Characteristics of the plant.

Service no.	Description	Physical Characteristic	Value	Unit
3.2.1.1	Oxygen gas cylinder and regulator			
		Max size (height X diameter)	2X1	m
3.2.1.2	Nitrogen gas cylinder and regulator			
		Max size (height X diameter)	2X1	m
3.2.1.3	Ammonia gas cylinder and regulator			
		Max size (height X diameter)	2X1	m
3.2.1.4	Fan shaft assembly welded to defuel chute flange			
		Maximum fan diameter	520	mm
3.2.1.5	Furnace			
		required furnace interior dimensions (min required by CUD) (lengthXwidthXheight)	4X2.1X2.2	mxmxm
3.2.1.6	Support for the CUD during furnace operation (CUD cradle)			
		Cradle dimensions (lengthXwidthXheight)	3X2.2X2.2	mxmxm
3.2.1.7	Thermocouple and logging equipment supply			
		Inconel probe (sheath) type thermocouples thickness	3	mm
		Minimum probe length	6	m
3.2.1.8	Hole in furnace for fan shaft			
		Minimum hole size (diameter)	250	mm
3.2.1.9	Coverplate for the hole in the furnace with shaft pipe penetration			
		Cover plate OD	>300	mm
		Size of hole in cover plate for shaft (dependent on Fan shaft dimensions)	88.9	mm
3.2.1.10	Supply a clean 200l oil drum (filled with water)			
		drum capacity	200	l
3.2.1.11	Witness samples of similar material for measuring heat effects on steel yield strength			
		size of samples (lengthXwidthXthickness)	50X50X5	mm
3.2.1.12	Nitriding thickness test samples to measure the thickness and hardness of the nitride layer that is created during nitriding			
		size of samples (lengthXwidthXthickness)	50X50X5	mm
		Min thickness of nitriding layer required	100	µm

Chapter 4: Detail Design

4.1. INTRODUCTION

The detail design of the plant is divided into the different plant functional modules (PFM's, a process system engineering term within industry). The PFM's are the Gas Supply System, Nitriding Furnace, and Gas Exit system. Within the Nitriding furnace PFM the nitriding fan shaft assembly, nitriding process chamber and CUD cradle are subsystems.

4.2. NITRIDING FAN SHAFT ASSEMBLY

4.2.1 FAN SHAFT ASSEMBLY CONCEPT

A decision was made to design the stirring fan shaft such that it enters the process chamber through the weld neck flange hole of the CUD housing, see Figure 4.1. The fan in the CUD barrel is positioned so that it is directly underneath the Spindle insert hole. This requires that the shaft extends a distance of 1.5 m from the weld neck flange opening inside the CUD housing. Since the CUD can not be too close to the furnace wall, the shaft is given an extended length of 1 m outside the housing from the weld neck sealing flange to the V-belt pulley. This allows 500 mm distance to the furnace wall and another 500 mm play outside the furnace wall for the shaft to cool down to a temperature low enough for a standard sealed ball bearing to last. The total unsupported length of the shaft will thus be 2.5 m. The bearing closest to the fan would thus see the furnace maximum temperature of 600 °C. This bearing would need to be specially designed for high temperature operation. The fan material must also be capable of temperatures of up to 600 ˚C. This concept is explained by the 3D CAD model in Figure 4.1. A detailed drawing of the CUD housing can be viewed in Appendix D if so required.

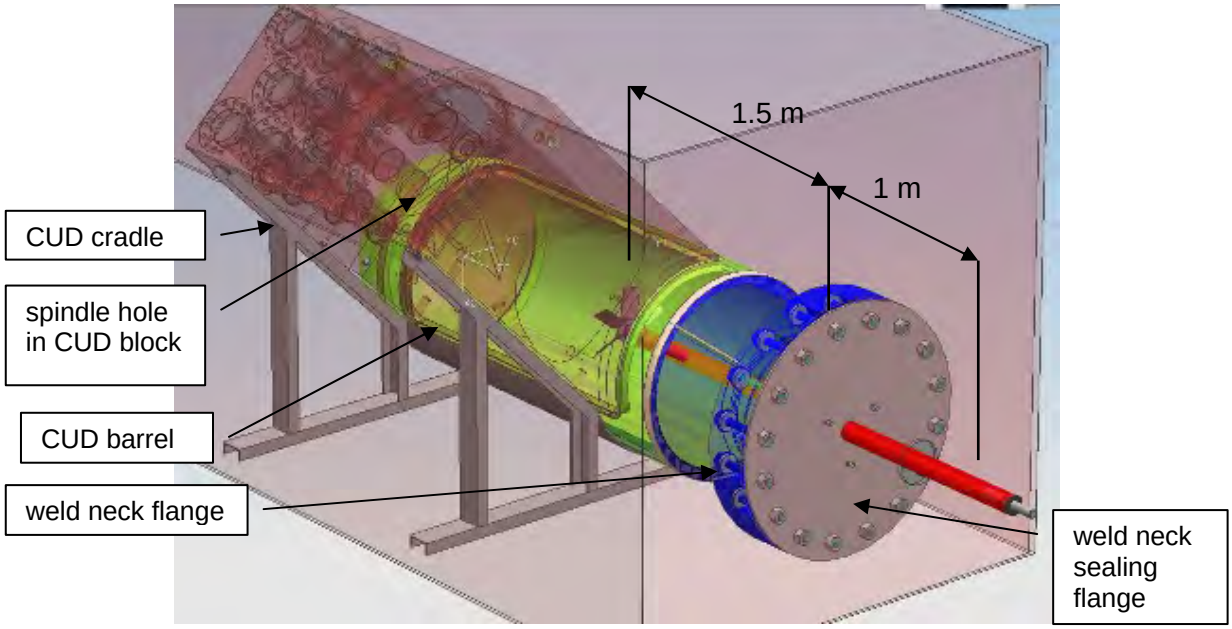

Figure 4.1: CAD model of the CUD housing in the furnace, note the fan position in the CUD barrel.

4.2.2 STIRRING FAN DESIGN AND SIZING

The purpose of the stirring fan is to create sufficient turbulent flow inside the CUD housing/ nitriding process chamber to ensure sufficient mixing of the gases. The best way to ensure turbulent flow throughout the entire CUD housing is to ensure proper circulation throughout the CUD with an axial flow fan. A radial flow fan might only ensure turbulence in its closest surroundings (i.e. the spindle hole).

The purpose of this calculation is to determine the approximate fan power required to ensure turbulent flow inside the CUD barrel during the CUD nitriding process. Turbulent flow of the gases inside the CUD is important to ensure proper stirring of the gases and an equal nitrided layer throughout.

Assumptions:

- Initially assume that the nitriding gases inside the CUD barrel have the properties of air at 550 °C. Later properties for ammonia at 550 °C are used.
- Assume that an ideal propeller would be used, using a fan power coefficient vs. speed ratio curve from White [36] (Figure 11.31 p. 791 in [36]).
- Inside the CUD barrel assume the gas flow pattern depicted in Figure 4.2.

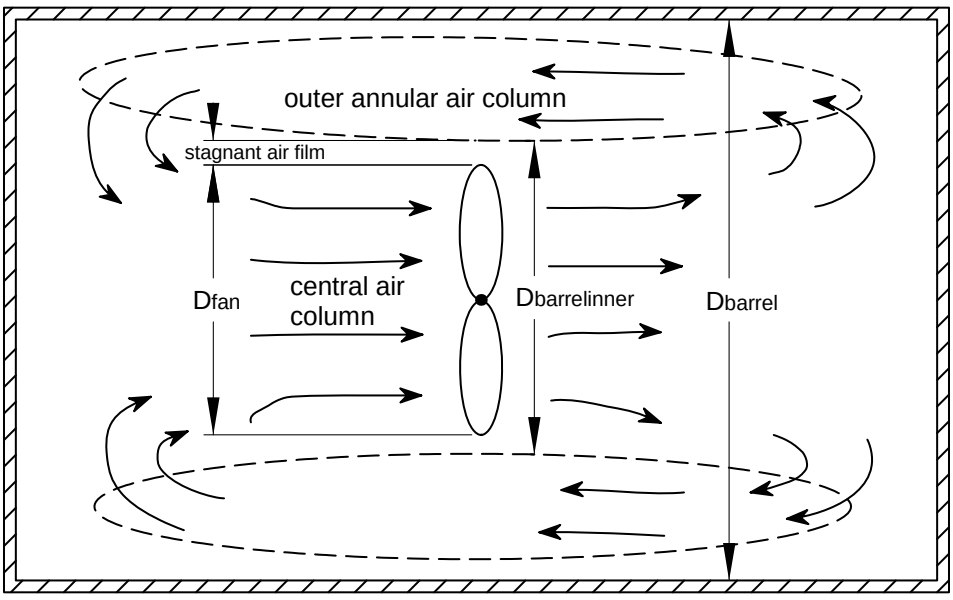

Figure 4.2: Diagrammatic sketch of the flow paths inside the sealed CUD barrel, fan in the centre.

Calculation of the Fan power and diameter for a given Reynolds number

The flow speed required for turbulent flow in the outer annulus is calculated for a given Reynolds number (Re) as follows:

Required velocity, rearrange Re=ρVD/μ [36]

$$V_{required} = \frac{Re \cdot \mu}{\rho \cdot D_h} \qquad (1)$$

where D_h is the hydraulic diameter of the annulus air column flowing through the CUD barrel.

Hydraulic diameter (see [36]) $$D_h = \frac{4 \cdot A_{annulus}}{P} \quad (2)$$

,where P is the wetted perimeter

To calculate the flow speed of the central air column mass conservation is applied:

$$\dot{m}_{annulus} = \dot{m}_{central} \quad (3)$$

where $\dot{m} = \rho A V$, then $$\rho A_{annulus} V_{required} = \rho A_{central} V_1 \quad (4)$$

assume ρ constant and rearrange to get $$V_1 = \frac{A_{annulus} V_{required}}{A_{central}} \quad (5)$$

where V_1 is the central column air speed and $A_{central}$ is the cross sectional area of the central air column (through fan) calculated by guessing the fan diameter.

$$A_{central} = \frac{\pi \cdot D_{fan}^{\ 2}}{4} \quad (6)$$

and $A_{annulus}$ is the outer annulus air column cross sectional area and is calculated as follows:

$$A_{annulus} = \frac{\pi \cdot \left(D_{barrel}^{\ 2} - D_{barrelinner}^{\ 2} \right)}{4} \quad (7)$$

According to the graph in [36] the speed ratio (SR) is read off for an ideal propeller with a given power coefficient (Cp). From the SR and the $V_{required}$ the fan diameter is calculated:

Fan diameter $$D_{fan} = \frac{2 \cdot SpeedRatio \cdot V_1}{\omega} \quad (8)$$

Speed ratio $$SR = \frac{\omega \cdot r}{V_1} \quad (9)$$

where ω is the fan rotational speed in radians per second. Iteration is required until the calculated fan diameter and the guessed central air column diameter are equal (change the fan diameter until they match). Throughout the iterative process it must be ensured that the fan diameter is smaller than the annulus inner diameter (a margin of 20 mm is used for the stagnant air layer thickness). If the fan diameter and annulus inner diameter differ by too much a slightly larger fan diameter can be calculated, by decreasing the annulus inner diameter.

The required electrical power is then calculated as follows (from [36] p. 790):

$$P = \frac{\frac{1}{2} \rho A_{central} V_1^3}{Cp} \quad (10)$$

The electrical power required will then be: $$P_{required} = \frac{P}{\eta} \quad (11)$$

, where η is the electrical efficiency of the motor.

Using this method with Re = 10000 as input, it is calculated that a 400 mm diameter fan with SR = 2, Cp = 0.5 (upper limit for Cp is 0.593), P = 51 W fan power is required in ammonia gas.

Calculation of the Reynolds number for a given fan power and fan diameter

The calculation can also be performed in the opposite direction i.e. the Motor electrical power, $P_{required}$ and the fan diameter is given as an input and the Reynolds number is calculated:

Calculate the central area $A_{central}$ with the given fan diameter

Then calculate the required air speed before the fan, V_1

$$V_1 = \sqrt[3]{\frac{P_{required} \cdot \eta \cdot Cp \cdot 2}{\rho \cdot A_{central}}} \quad (12)$$

Next calculate the speed ratio with eq. (9) using V_1. Iteration is then required until the guessed speed ratio (and corresponding fan power coefficient Cp) matches the calculated speed ratio, Throughout it must once again be ensured that the annulus inner diameter is larger than the fan diameter. To get the annulus flow Reynolds number, first calculate the air speed at the barrel.

Air speed at barrel (using mass conservation)

$$V_b = \frac{A_{central}}{A_{annulus}} V_1 \quad (13)$$

Then calculate the hydraulic diameter with equation (2) and use it to get the Reynolds number.

Reynolds number in annulus (must be turbulent for sufficient mixing)

$$Re = \frac{\rho \cdot V_b \cdot D_h}{\mu} \quad (14)$$

Calculation Inputs:

- P_{motor} = 750W, 4 pole 3 phase @1440rpm, motor efficiency η = 0.85
- Pulley reduction 1.4:1, fan rotation speed 1000 rpm
- rotational speed = 1000 rpm (after V-belt pulley reduction)
- Propeller/Fan power coefficient Cp = 0.34 (p. 791 in [36])
- D_{barrel} = 840mm
- D_{fan} = 400mm (steel tractor engine fan from scrapyard)

The calculation is now done with the motor power and rotational speed given as input and the speed ratio can be varied to iterate until the power coefficient matching that of Figure 11.31 p. 791 in [36] for an ideal propeller is calculated.

Calculation Results:

- Speed ratio, SR=1.1, Cp=0.41. The fan tip speed is thus 1.1 times the axial air flow speed.
- Reynolds number, Re = 34548.4, the Reynolds number is above 10 000 and the annulus flow is thus turbulent with V_1 = 20.1 m/s.

To get properties for ammonia at 550 °C, data in [37] is extrapolated, as shown in Figure 4.3.

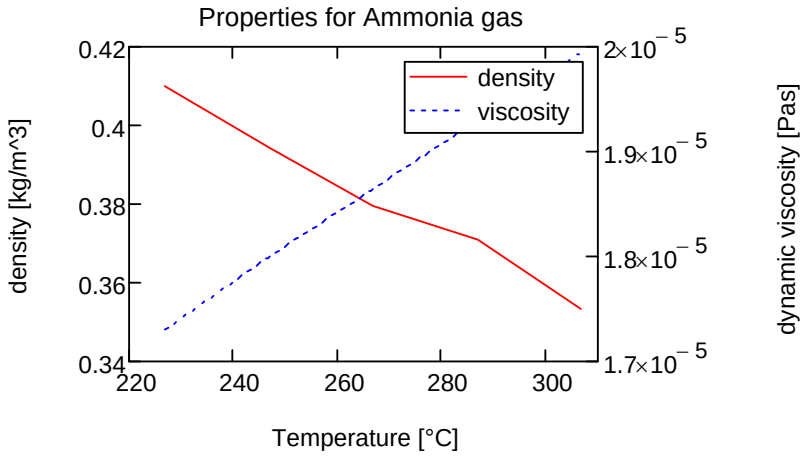

Figure 4.3: Properties for ammonia that are extrapolated to get properties at 550 °C.

Calculation Results for ammonia atmosphere:

With ammonia properties Re = 22000 and SR = 0.8. This is slightly smaller than for the case with air properties, but the Reynolds number is still larger than 10000 and turbulent flow will thus be present. The actual Reynolds number during nitriding should be between these two calculated extremes because for a crack ratio of 40%, only 60% of the volume would consist of ammonia, the rest of the gases will have larger densities. To get an idea of the fan power keep in mind that a normal household appliance cooling fan consumes about 45 W of electricity. As previously calculated a 50 W motor is required for Re = 10 000. Calculations also showed that as fan power is increased the speed ratio and fan power coefficient (Cp) decreases.

For bearing axial location the fan maximum axial force was calculated:

Max Fan axial force in ammonia, see p. 791 in [36]

$$F_{axial} := \rho \cdot A_{central} \cdot V_1 \cdot V_1 = 17.173\,N$$

and it is calculated as 25 N when air properties are used. This axial force is small.

Fan impeller selection:

Most commercially available axial flow fans are constructed of aluminium (CW Fans in South Africa) and have a maximum operating temperature of 350 °C. The melting point of pure aluminium is ± 660 ˚C, [38] Appendix I, (although the aluminium oxide layer melts at more than 1000˚C). Certain automotive aluminium alloys have a melting point of 610 °C (semi-solid between 555 and 610°C [39]). With the nitriding furnace at 600 °C a steel fan is a better choice.

Steel fans are scarce in industry and the possibility was high that this item would need to be specially designed and manufactured. Fortunately a steel fan of 450 mm diameter was acquired from a “Scrap yard” selling old tractor engine parts. Although the fan is not constructed of single crystalline material like gas turbine blades (to prevent creep and stress rupture [38]) it will be adequate. The phase change temperature of commercial mild steel is ± 720 ˚C, which is far

above the design temperature of 600˚C. The fan diameter can not be larger than 500 mm because the inner diameter of the weld neck flange is only 510 mm (refer to the CUD detail drawing in Appendix D). A picture of the fan is shown in Figure 4.4.

Figure 4.4: Photo of the fan assembly before installation onto the CUD housing.

4.2.3 SHAFT WHIRLING SPEED CALCULATION

The minimum unsupported length of the shaft is 2.5 m. With a shaft of such an extended length the loads due to the fan weight, shaft power and shaft weight are usually not the design determining factors. The shaft whirling speed would determine the shaft's diameter etc.The purpose of this calculation is to determine the fundamental (natural) frequency of the CUD Nitriding fan shaft.

Knowledge of this frequency is required to prevent whirling (amplified displacement at the natural frequency) of the shaft during rotation at operating speed. To reduce the whirling speed it was found that the shaft diameter needs to be increased. However a solid shaft has a lower natural frequency than a hollow shaft. Thus the shaft was made hollow with a large diameter.

Assumptions/Inputs:

- Assume that the fan is well balanced
- The fan mass is 2.5 kg
- Shaft length of 2.6 m
- Distance between fan and closest bearing 50 mm
- Distance between bearings 2.5 m

To calculate the shaft's fundamental frequency (whirling speed) Dunkerley's equation may be used:

Dunkerley's equation, [40] p.340

$$n = \frac{1}{2 \cdot \sqrt{\delta_1 + \delta_2 + \ldots + \frac{\Delta}{1.27}}} \cdot Hz \qquad (15)$$

where δ_1 and δ_2 are static deflections due to separate loads at the load application points.

Δ is the static deflection due to the shaft's own weight.

For the static deflection due to the fan load (δ_1) the deflection of a simply supported beam due to an overhanging load needs to be calculated (see [41] p.973):

Deflection due to fan [41]

$$\delta_{fan} = \frac{-F \cdot a^2 \cdot (L + a)}{3 \cdot E \cdot I} \qquad (16)$$

, where F is the fan weight, a is the overhanging distance from the bearing, L the shaft length and I the polar moment of inertia.

Formula for hollow shaft moment of inertia [44]

$$I_s = \frac{\pi \cdot \left(d_o^4 - d_i^4\right)}{64} \qquad (17)$$

For the static deflection due to the shaft's own weight the following equation may be used

Deflection due to shaft weight ([41] p.972)

$$\Delta_{max} = \frac{-5 \cdot w \cdot L^4}{384 \cdot E \cdot I} \qquad (18)$$

,where w is the distributed load in N/m.

Other equations that will be used for calculating bending stresses and shear stresses follow:

Calculation inputs:

The final shaft dimensions and material properties used for calculation are given in Table 4.1.

Table 4.1: Shaft dimensions and material properties.

Description	Symbol	Value	Unit
shaft length	L_s	2.5	m
distance between fan and closest bearing	a	100	mm
shaft outer diameter (schedule 40 pipe)	d_o	60.32	mm
shaft inner diameter (schedule 40 pipe)	d_i	49.44	mm
fan diameter	d_f	0.4	m
mass of fan	m_f	3.5	kg
gravitational acceleration	g	9.807	m/s^2
shaft steel yield stress at 600°C from [16] Table Y	S_y	200	MPa
density of steel	ρ_{steel}	7850	kg/m^3
Steel modulus of elasticity at 600°C from [42]Table TM-1 at 1100°F for EN 8 shaft steel with 0.4% Carbon	E	124	GPa

Mass of shaft

$$m_s = \frac{\pi \cdot \left(d_0^2 - d_i^2\right)}{4} \cdot L_s \cdot \rho_{steel} = 18.407 \cdot kg$$

Distributed weight load in N/m

$$W_s = \frac{m_s \cdot g}{L_s} = 72.203 \cdot \frac{N}{m}$$

Shaft moment of inertia, eq. (17)

$$I_s = 3.566 \cdot 10^5 \cdot mm^4$$

Deflection due to distributed shaft weight, eq. (16)

$$y_s = 0.831 \cdot mm$$

Deflection at shaft overhang for fan, eq. (18)

$$y_{fan} = 6.728 \times 10^{-3} \cdot mm$$

Whirling speed results:

Fundamental frequency eq.(15) (static deflection y_s has the largest influence, fan and pulley deflection negligible)

$$n_f := \frac{1}{2 \cdot \sqrt{\frac{2y_{fan}}{m} + \frac{y_s}{1.27} \cdot \left(\frac{1}{m}\right)}} \cdot Hz = 19.353 \cdot Hz$$

Whirling shaft speed (in rpm) $n_{whirl} := \frac{n_f}{Hz} \cdot 60 \cdot rpm = 1161.206\ rpm$

4.2.4 SHAFT STRENGTH CALCULATIONS

Other equations that will be used for calculating bending stresses and shear stresses follow:

Shaft bending stress [43] $$\sigma_x = \frac{Mr_o}{I_s} \quad (19)$$

, where M is the bending moment, r_o shaft outer radius, and I_s shaft moment of inertia eq.(17)

Shaft shear stress [43] $$\tau = \frac{Tr_o}{I_p} \quad (20)$$

, where T is the applied Torque, and I_p shaft polar moment of inertia

Shaft polar moment of inertia [43] $$I_{ps} = \frac{\pi \cdot \left(d_o^4 - d_i^4\right)}{32} \quad (21)$$

To calculate the peak torque that will be applied to the shaft, ratings of the 750 W induction motor (see par. 4.2.9) are used. For a 4 pole motor the synchronous speed n_s (at 0% slip and zero torque output) is 1500 rpm. The rated speed for full load is 1440 rpm (shaft rotates at 960 rpm after pulley reduction). According to [45] p.621 an induction motor supplies a startup torque 2 times that of rated torque at full load. It supplies its maximum torque, of ± 3 times rated torque at 70% of synchronous speed (30% slip). It is shown by the general induction motor torque vs. shaft speed curve Figure 9.3 b) in [45].

Peak motor torque available at startup $$T_{max} = \frac{3P}{\omega_{rated}} \quad (22)$$

The torque required to accelerate the shaft within a specific time can also be calculated:

Net torque (motor supply minus fan torque) $$T = I\alpha \quad (23)$$

, where P is the nominal motor power in W, ω the rotational speed in rad/s, I the mass moment of inertia and α the rotational acceleration.

Calculate Torque required rotating the shaft:

Shaft mass moment of inertia [44] $I_{sm} := \frac{1}{2} \cdot m_s \cdot \left[\left(\frac{d_o}{2}\right)^2 + \left(\frac{d_i}{2}\right)^2\right] = 0.014\ m^2 \cdot kg$ (24)

Fan mass moment of inertia [44] $I_f := \frac{1}{2} \cdot m_f \cdot d_f^2 = 0.438\ m^2 \cdot kg$ (25)

Total moment of inertia $I := I_{sm} + I_f = 0.451\ m^2 \cdot kg$

Shaft rotational speed $n := 960 \cdot rpm$

Shaft speed in radians per second $\omega = \frac{n \cdot 2 \cdot \pi}{60} = 10.528 \cdot \frac{rad}{s}$

Angular shaft acceleration for 0 to 960 rpm in 0.1s $\alpha = \frac{\omega}{0.1s} = 105.276 \cdot \frac{rad}{s^2}$

Net torque to accelerate the shaft to 960 rpm in 0.1s, eq. (23) $T_{acc} = I\alpha = 47.532 \cdot N \cdot m$

Compare this to the max motor supply torque to predict the shaft's acceleration.

Steady state motor power required to turn fan $P_{fan} = 750 \cdot W$

Full load steady state torque to turn the fan at the rated speed (fan resistance should be lower, this is worst case) $T_{fan} = \frac{P_{fan}}{\omega} = 71.241 \cdot N \cdot m$

Max motor supply torque at 70% of n_s, from eq. (22) $T_{max} = 3 \cdot T_{fan} = 213.724 \cdot N \cdot m$

Shear stress due to maximum applied torque:

Shaft polar area moment of inertia, eq. (21) $I_{ps} = 7.131 \cdot 10^5 \cdot mm^4$

Shaft shear stress due to max motor torque, eq. (20) $\tau = \frac{T_{max} r_o}{I_p} = 9.039 \cdot MPa$

Safety Factor for applied torque $SF1 := \frac{S_y}{\tau} = 22.127$

Stress due to bending moment:

Maximum moment for a beam with simple supports and an overhanging load, (at support next to fan) [41] $M_{end} = -F_f \cdot a = -3.432 \cdot N \cdot m$ (26)

Moment due to distributed load at centre of shaft [41] $M_{cent} = \frac{-W_s \cdot L_s^2}{8} = 56.408 \cdot N \cdot m$ (27)

Maximum bending stress at centre of shaft, eq. (19) $\sigma_x = 4.771 \cdot MPa$

Safety Factor for bending stress $SF2 := \frac{S_y}{\sigma_x} = 41.918$

Both the static bending strength safety factor (SF2) and shear stress safety factor (SF1) are much larger than 1; therefore the shaft will not yield due to bending or torsion.

Total Stress, ($\sigma_1 - \sigma_2$), Shear strain energy yield criteria p.346 in [43] $\sigma_{total} = \sqrt{\sigma_x^2 + 4 \cdot \tau^2} = 18.374 \cdot MPa$ (28)

Safety Factor due to total stress $SF3 := \frac{S_y}{\sigma_{total}} = 10.697$

The safety factor due the total stress intensity (SF3) is much larger than 1; the shaft will thus not yield due to static loads.

The hollow shaft must be rotated either below or above the whirling speed of n_{whirl} = 1161.2 rpm. Resonance (whirling) will be witnessed during start up when the whirling speed is passed if the shaft operating speed is faster than 1162 rpm. The static strength calculations show that the shaft is over designed, with a safety factor of 10. The conclusion is made for the hollow shaft with d_o = 60.32 mm and d_i = 49.44 mm. A standard schedule 80 process pipe is used to manufacture the hollow shaft. The shaft drawings are given in Appendix D.

4.2.5 LOW TEMPERATURE BEARING OUTSIDE FURNACE

The hollow shaft is designed with solid machined ends for the bearings. The shaft detail drawings are given in Appendix D. For the shaft end outside the furnace a standard deep groove ball bearing with seals from the SKF General catalogue[13] was selected. This bearing has reasonable axial load resistance and good radial load resistance. A self aligning ball bearing was considered to account for possible misalignment, but due to its limited axial load resistance it was decided to use a single row deep groove ball bearing.

The solid shaft end is machined down to 40 mm at the bearing surface and fitted into the 60.32 mm hollow shaft with 49.44 mm inner diameter. The bearing housing is a schedule 80 pipe machined to an inner diameter of 80 mm. The selected bearing has an inner race diameter d of 40 mm, outer diameter D of 80 mm and width of 23 mm. Its designation is 62208-2RS1 (international numbering scheme). The solid shaft end is machined to a N6 surface finish and is designed for a H7 g6 fit tolerance (ISO standard). For axial location the solid shaft end and the bearing housing (pipe) were machined with a shoulder and a circlip groove. Note that the rubber seals and bearing have a maximum design temperature of 120 °C. To check whether the temperature of the shaft and shaft housing is below 120 °C a thermal FEA was performed. The verification of this FEA is also done in section 6.2.

4.2.6 HIGH TEMPERATURE BEARING DESIGN

Bearing concept:

As the literature survey in section 2.8 showed there are complex systems used for gas turbine engines [32], [33]. It uses either a different gas at pressure or a pressurised liquid volume with additional seals to isolate the high pressure gas from the low pressure; at the other side of the bearing. Such a system would be extremely expensive and complex to implement for this fan shaft assembly design. Another alternative is using a ceramic ball bearing that could accomodate the high temperature. However, these bearings are not particularly designed for high pressure gas sealing (and a rubber lip seal cannot withstand high temperatures).

The best alternative would be to design a new bearing from first principles. As noted in section 2.8 a few solutions were found in South African industry where graphite journal bearings were used for high temperature conveyors, chain grates at the bottom of coal fired boiler furnaces or synthetic diamond manufacturing machines (by Morgan Carbon SA (Pty) Ltd.[14]). Graphite and carbon can withstand temperatures over 1000 °C and is a self lubricating material.

The design concept is a graphite journal bearing (bush) with a 200 mm long load bearing area (a small PV value). A labyrinth seal is not necessary because the 200 mm length should ensure

[13] SKF General catalogue, Catalogue 4000/IV E, Reg. 47 24000 1994-12

gradual pressure loss to provide an effective seal on the ammonia gas side. A problem with graphite is that its thermal expansion coefficient is more than 3 times smaller than that of steel. It introduces a challenge when designing the bearing for the smallest possible clearance at operating temperature; to ensure minimum leakage.

Design inputs for the graphite bush:

Morgan Carbon SA[15] recommended using a high density isostatically pressed graphite of grade IGS 743. The graphite is also impregnated with phenolic resin to reduce its porosity for ensure optimum sealing. The specifications for material grade selection were a rotation speed of 960 rpm, operating temperature 555 °C, 4kg load and an ammonia gas environment.

Thermal expansion coefficient of Morgan Carbon IGS 743 graphite $\alpha_{graphite} = 3.8 \times 10^{-6} / K$

Thermal expansion coefficient of EN 8 shaft steel (20 °C to 500 °C) $\alpha_{steel} = 12 \times 10^{-6} / K$

The thermal expansion of a cylindrical part is calculated as follows: $\Delta D = \alpha \cdot \Delta T \cdot D$ (29)

, where α is as given above, ΔT is temperature change in K and D is original diameter in mm

It is evident that the steel housing will expand more than the graphite and the fit will loosen at working temperature. In contrast the inner steel shaft will expand more than the bush and the fit will be tighter. The graphite bush thus needs to be shrink fitted into the steel housing by heating the housing to over operating temperature and then slipping the machined bush in. Upon cooling, the inner diameter (ID) of the bush also shrinks by about 1 third of the outer diameter (OD). A graphite bearing should rather be in compression than in tension, because its compressive strength is 3 times its flexural strength (information from Morgan Carbon SA). The required plain bearing ISO fit tolerances at working temperatures are given by Table 4.2.

Table 4.2: Required bearing ISO fit tolerances.

location	ISO fit	Fit tolerance description	Applicable part	Dimension tolerance
ID	H7 g6	almost transition fit to allow slight graphite lubrication	shaft diameter, g6	49.975 mm - 49.991 mm
			bearing ID, H7	50 mm - 50.025 mm
OD	H7 n6	slight interference fit	bearing OD, n6	80.017 mm - 80.033 mm
			housing (pipe) ID, H7	80 mm - 80.035 mm

Graphite bush dimensions at room temperature:

Because the graphite bush is machined to final dimensions before it is fitted into the housing the required dimensions at room temperature must be determined to ensure the right fit at working temperature. Calculations were performed to get the difference in thermal expansion of the steel and graphite using eq. (29) for ΔT = 530 K (555 °C - 25 °C). The results are given in Table 4.3

[14] an international company that supply graphite bearings is Graphite Metalizing Corporation, www.graphalloy.com

[15] Morgan Carbon SA (Pty) Ltd. were the manufacturers of the high temperature bush.

Table 4.3: Thermal expansion calculation results for required room temperature dimensions.

location	Part	D [mm]	ΔD eq. (29) [mm]	Δexpansion [mm]	deviation in ISO machined diameter	machined dimension before shrink fit [mm]
OD	pipe ID	80	0.5088	0.3477	0 mm	80 - 80.035
	bush OD		0.1611		0.35 mm larger	80.367 - 80.383
ID	bush ID	50	0.1007	0.2173	0.3173 mm larger	50.317 - 50.342
	shaft OD		0.318		0 mm	49.975 - 49.991

At temperature the bush OD expands to between 80.528 mm and 80.544 mm; and the steel housing ID expands to between 80.509 mm and 80.544 mm. This ensures an interference fit to prevent the bush from sliding out of the housing.

From Table 4.3 note that the bush ID must be 0.3173 mm larger at room temperature. It is 0.2173 mm for thermal expansion plus 0.1mm to allow for shrink fit compression (one third of the OD shrinkage, 0.347 mm/3 = 0.1 mm). The machined bush ID at room temperature is thus between 50.317 mm and 50.342 mm. After shrink fitting it is between 50.217 mm and 50.242 mm. The shaft is between 49.975 mm and 49.991 mm at room temperature and thus fits loosely. If it is assumed that the bush ID returns to between 50.317 mm and 50.342 mm at temperature, the shaft then expands by 0.318 mm to between 50.29 mm and 50.31 mm at working temperature, ensuring a fit bordering between clearance and transitional.

Manufacturing details:

The shrink fitted bearing bush can be seen in Figure 4.5. To make the shrink fitting exercise easier 4 bushes of 50 mm long each were made and fitted separately. It would be difficult to fit one 200 mm long bush correctly in one movement. The detail drawings of the bush and shaft can be found in Appendix D.

Figure 4.5: Photo of the shrink fitted bearing in the bearing housing pipe.

The design of this shaft end where the fan is fitted also required the design of a hub to which the fan is bolted. Some minor design challenges with spacing for bolts and extra steps were encountered. An explanation is given in Figure 4.6. An important shaft manufacturing note is

that the solid shaft ends need to be welded to the hollow shaft pipe first; before final bearing surface machining is done.

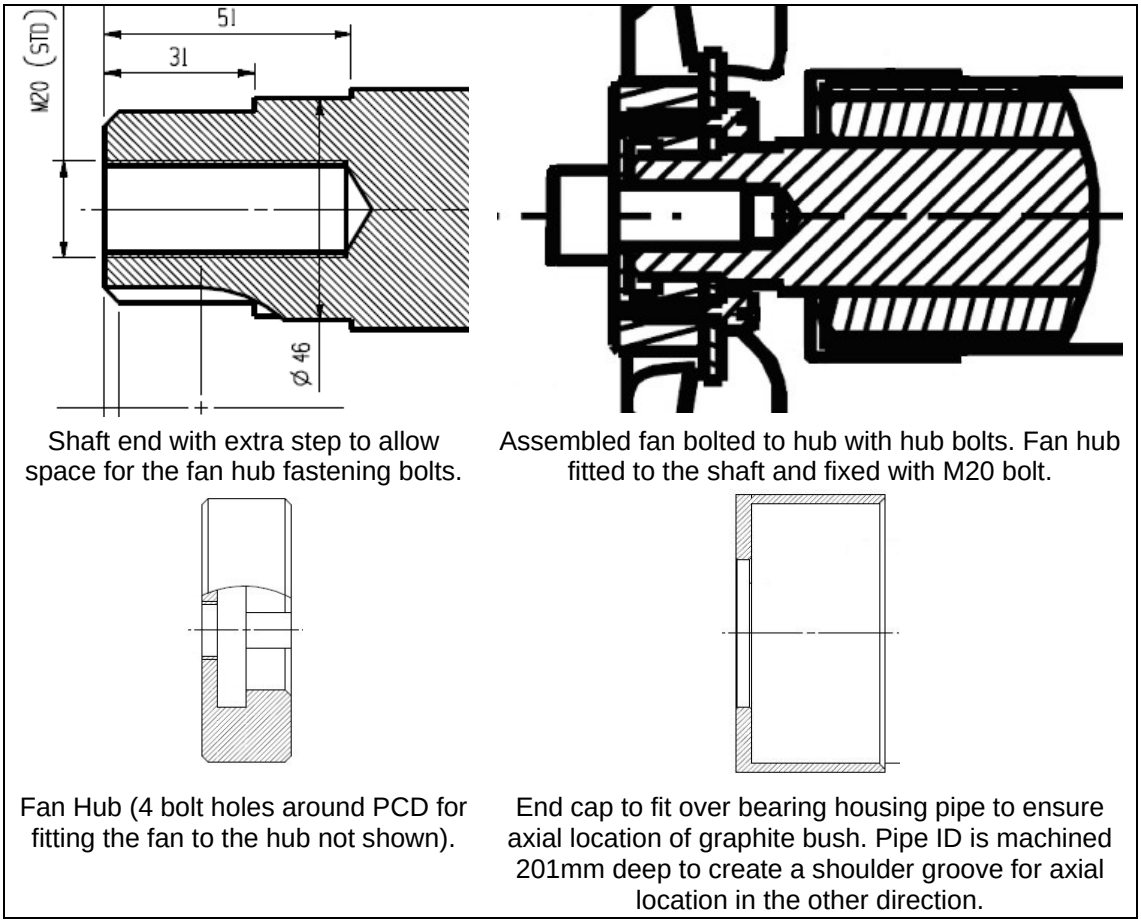

Shaft end with extra step to allow space for the fan hub fastening bolts.

Assembled fan bolted to hub with hub bolts. Fan hub fitted to the shaft and fixed with M20 bolt.

Fan Hub (4 bolt holes around PCD for fitting the fan to the hub not shown).

End cap to fit over bearing housing pipe to ensure axial location of graphite bush. Pipe ID is machined 201mm deep to create a shoulder groove for axial location in the other direction.

Figure 4.6: Sketches from the shaft detail drawings to explain the use of steps and spacing.

4.2.7 BELT DRIVE SYSTEM DESIGN

As calculated in paragraph 4.2.2 a minimum speed reduction ratio of 1.4:1 is required for a driver pulley speed of 1440 rpm. The Fenner Catalogue for Friction Belt Drives[16] was used for the pulley and belt selection. For the 0.75 kW power input a single V-belt design is sufficient with Fenner V-belt profile SPZ (10x8mm cross section dimensions). A driver pulley with pitch diameter of 75 mm is selected and a driven pulley with a pitch diameter of 112 mm; resulting in a speed ratio of 1.49:1. The driver rotational speed is reduced from 1440 rpm to 964.3 rpm, which is well below the shaft whirling speed of 1160 rpm. For the 75 mm driver pulley up to 4 kW can be transferred without excessive loads to bearings and the belt. A pulley centre distance of 393 mm is required for the 1080 mm long SPZ belt. A taper lock bush was specified to fit the driver pulley to the 19 mm motor shaft and another one to fit the driven pulley to the 40 mm fan shaft.

[16] The Fenner belt catalogue (from Fenner SA (Pty) Ltd. can be downloaded from www.fennerdrives.com/catalogs.

4.2.8 FAN SHAFT SUPPORT PIPE STRENGTH CALCULATIONS

The purpose of this calculation is to determine the deflection and maximum stress of the shaft support pipe of the CUD Nitriding fan shaft assembly.

Assumptions/Inputs:

- Assume that the fan is well balanced
- Assume the fan mass is 2.5 kg
- Shaft length of 2.6m, distance between bearings 2.5 m
- Distance between fan and closest bearing 50 mm

The shaft support pipe with the locations of the bearings can be seen in Figure 4.7

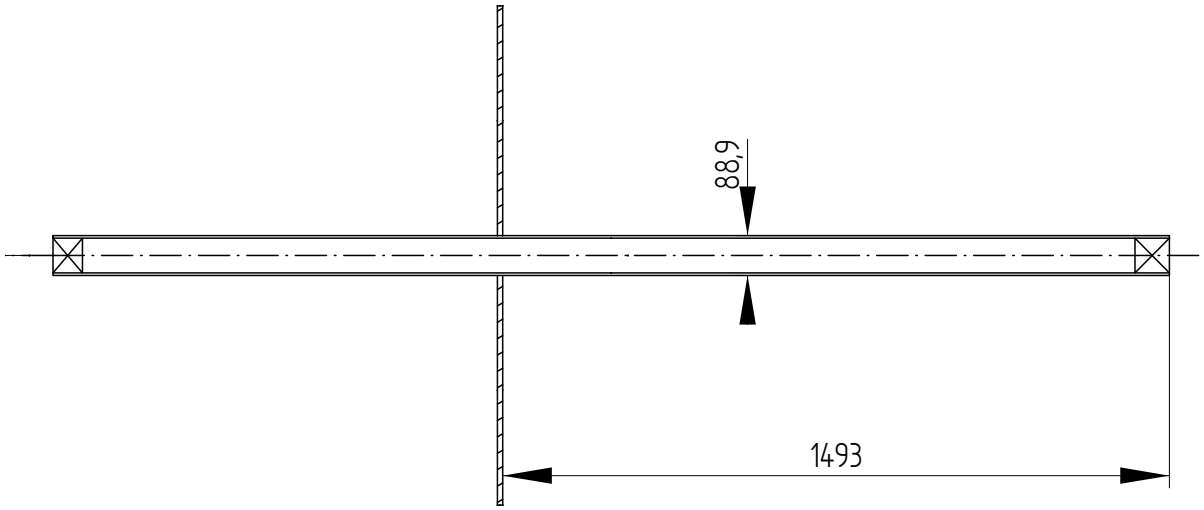

Figure 4.7: Section view of the support shaft with the welded flange.

Input data:

The support pipe dimensions used in the calculation are given in Table 4.4

Table 4.4: Input Data for shaft support pipe calculations

Description	Symbol	Value	Unit
shaft length	L_s	2.5	m
shaft length up to fan	L_{sf}	2.7	m
distance flange to fan (right side overhang length)	$L_{overright}$	1.5	m
pipe outer diameter	d_o	88.9	mm
pipe inner diameter	d_i	77.9	mm
mass of fan	m_f	4	kg
mass of inner shaft	m_{si}	22	kg
gravitational acceleration	g	9.807	m/s^2
fan weight	F_f	39.23	N
inner shaft weight	F_w	215.75	N
shaft steel yield stress at 600°C from [16] Table Y	S_y	200	MPa
density of steel [44]	ρ_{steel}	7850	kg/m^3
Steel modulus of elasticity at 600°C from [42] Table TM-1 at 1100°F for EN 8 shaft steel with 0.4% Carbon	E	124	GPa

To determine the loads on the support pipe the loads on the bearings must first be determined by investigating the fan shaft, see Figure 4.8.

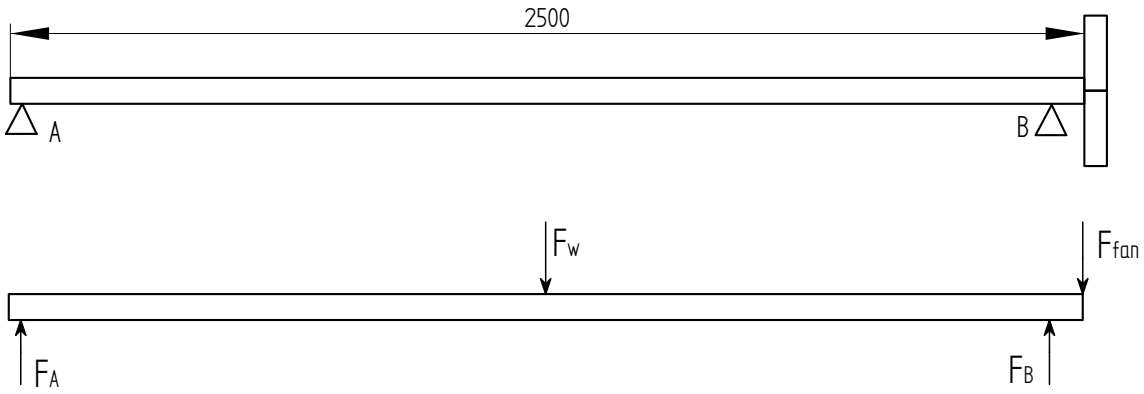

Figure 4.8: Section view and force diagram of the Fan shaft that is inside the support shaft.

As can be seen in Figure 4.8, the shaft can be simplified as a beam with simple supports. The forces F_A and F_B are determined by taking moments about A and then doing a sum of forces.

Moments about A

$$\sum_n M_A = 0 = F_B \cdot L_B - F_{fan} \cdot L_{shaft} - F_w \cdot \frac{L_{shaft}}{2} \quad (30)$$

Force at bearing B, rearrange eq. (30)

$$F_B = \frac{F_f \cdot L_{sf} + \frac{F_w \cdot L_{sf}}{2}}{L_s} = 158.868 \cdot N$$

Sum of vertical forces

$$\sum_n F_{vertical} = 0 = F_{fan} + F_w - F_A - F_B \quad (31)$$

Force at bearing A, rearrange eq. (31)

$$F_A = F_f + F_w - F_B = 96.105 \cdot N$$

The forces are transferred to the support pipe as can be seen in Figure 4.9.

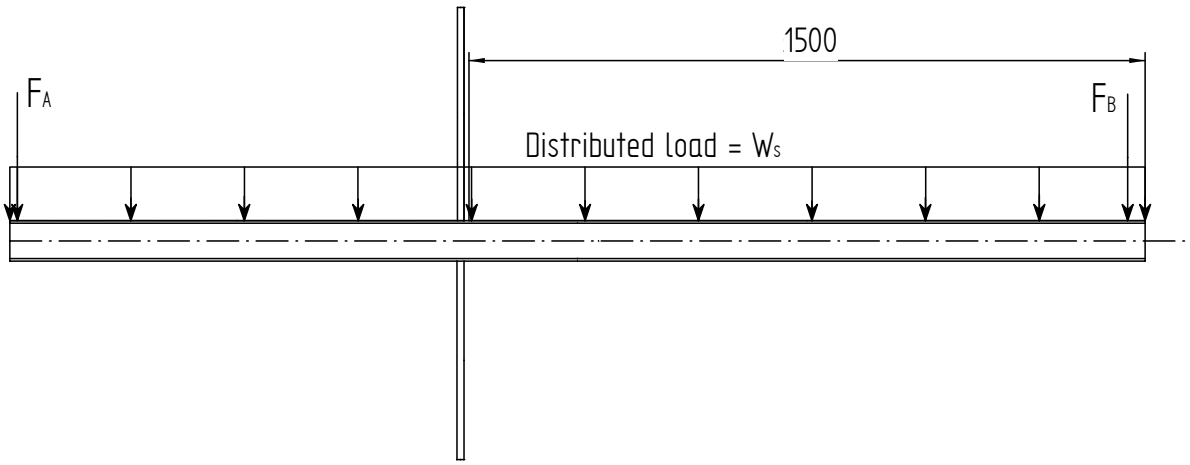

Figure 4.9: Section view and force diagram of the support pipe with the forces of the fan shaft transferred on the pipe.

To analyze the support pipe it can now be simplified as a cantilever beam with both an end load and a distributed load, as shown in Figure 4.10.

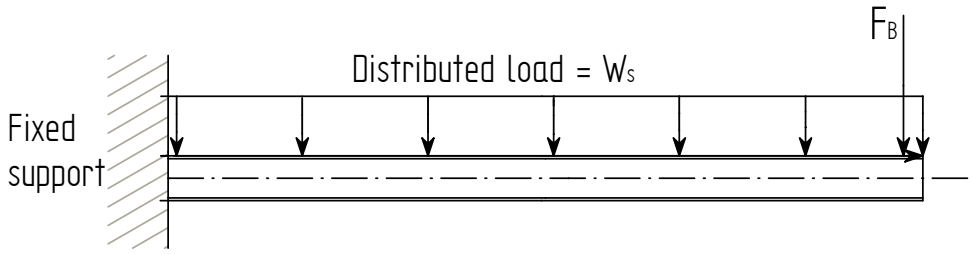

Figure 4.10: Simplification of the long side of the support as a cantilever beam.

According to [41] the maximum moment is at the flange position along the length of the pipe (where the fixed support is located). The moment and deflection are calculated as follows.

Moment due to end load [41] $M_{endload} = F_B \cdot L_{overright} = 238.302 \cdot N \cdot m$ (32)

Support shaft moment of inertia $I_{pipe} = \frac{\pi \cdot \left(d_0^4 - d_i^4\right)}{64} = 1.258 \times 10^{-6} \cdot m^4$

Deflection due to end load at B [41] $y_B = \frac{-F_B \cdot L_{overright}^3}{3 \cdot E \cdot I_{pipe}} = 1.145 \cdot mm$ (33)

Mass of pipe $m_s = \frac{\pi \cdot \left(d_0^2 - d_i^2\right)}{4} \cdot L_s \cdot \rho_{steel} = 28.281 \cdot kg$

Support pipe distributed load in N/m $W_s = \frac{m_s \cdot g}{L_s} = 110.935 \cdot \frac{N}{m}$

Moment due to distributed load [41] $M_{distr} = \frac{W_s \cdot L_{overright}^2}{2} = 124.802 \cdot N \cdot m$ (34)

Deflection due to pipe distributed load [41] $y_d = \frac{-W_s \cdot L_{overright}^4}{8 \cdot E \cdot I_{pipe}} = 0.45 \cdot mm$ (35)

Total deflection at right side of support pipe $y_{total} = y_d + y_B = 1.595 \cdot mm$

The bending stress due to the moments is then calculated as follows:

Bending stress due to load at bearing B $\sigma_{xB} = \frac{M_{endload} \cdot \frac{d_o}{2}}{I_s} = 8.418 \cdot MPa$ (36)

Bending stress due to distributed load $\sigma_{xd} = \frac{M_{distr} \cdot \frac{d_0}{2}}{I_s} = 4.408 \cdot MPa$ (37)

Total bending stress at the weld of the support pipe (superponated) $\sigma_{total} = \sigma_{xB} + \sigma_{xd} = 12.826 \cdot MPa$ (38)

Safety Factor of applied bending stress $SF = \frac{S_y}{\sigma_{total}} = 15.593$

The safety factor is larger than 1 and thus acceptable.

The pipe can withstand large bending moments and has a safety factor of SF = 15.6 at the maximum combined stress (the support pipe has good static strength integrity). It has a small static deflection of y_{total} = 1.595 mm at the right end of the support pipe. The conclusion is made for the hollow pipe with d_o = 88.9 mm and d_i = 77.9 mm (a standard schedule 40 process pipe). Pipe detail drawings are given in Appendix D.

4.2.9 MOTOR DESIGN AND SIZING

As noted by fan sizing calculations in section 4.2.2 a 0.75 kW motor for a 450 mm diameter fan gives a bulk flow Re = 22 000 in ammonia at 555 °C (a normal household cooling fan is 45 W). The motor is to be installed next to the furnace wall with its shaft parallel to the fan shaft. Because of the possibility of ammonia and hydrogen gas leakage the motor has a zone 2 hazardous area safety classification (OHS Act and SANS 10108). Zone 2 areas occasionally represent an explosion hazard. This means that the motor needs to be certified as non-sparking and it requires an IP 65 rating (dust-proof). A standard 4 pole 3 phase induction motor was specified and sent in to a laboratory for spark proofing and IP 65 sealing and testing.

4.3. NITRIDING PROCESS CHAMBER

4.3.1 SEALING FLANGE DESIGN

As previously mentioned what makes this NP unique is the fact that the CUD housing interior volume will be used as the nitriding process chamber. This will be done by closing all the openings of the CUD vessel i.e. all the insert holes in the block where the valve inserts are installed, the large weld neck flange opening etc. First of all sealing flanges need to be designed for the maximum process chamber design pressure of 40 kPa. Note that the CUD housing pressure vessel is designed for a large design pressure of 97 Bar and therefore its permanent flanges and bolts (for use at the HTF) are much larger and heavier. The NP sealing flanges also need penetrations for the stirring fan, thermocouples and the gas inlet and exhaust pipes.

According to the South African OHS Act [49] the nitriding process chamber is not seen as a pressure vessel because its maximum operating pressure of 30 kPa is well below the cut-off value of 40 kPa (pressure vessel definition criteria for any vessel volume). For this reason the chamber pressure boundary does not need to be designed according to ASME VIII [9] or any pressure vessel design code. The least expensive method to seal the process chamber was to manufacture new flanges by laser cutting from thin commercially available steel plate (grade 300W). The bolt holes and holes for gas pipe and thermocouple penetrations (holes NPT threaded later) were also included in the laser cut profile (DXF files were sent to the manufacturer). The bolt hole PCD of each flange matches that of the hole on the CUD housing.

Detail drawings of the flanges can be seen in Appendix D. The sealing flange major specifications are given in Table 4.5.

Table 4.5: Major Dimensions of the laser cut flanges.

Description	Quantity	Bolt size	#bolts/ flange	Outside Diameter [mm]	Bolt PCD [mm]	Plate thickness [mm]
Weld neck flange	1	M36	16	1168 (hole 525)	1100	12
Spindle hole	1	M36	18	815	760	10
Valve insert holes	8	M20	12	275	237	6
Sphere pipe flanges	4	M20	12	195	150	6
bottom dome flange	1	1" UNC	8	245	190	6

As can be seen in Table 4.5 M36 studs are used in the M100 weld neck flange holes (CUD housing designed for 97 Bar). Because the actual expensive M100 studs that would be used for the CUD in operation could not be put through the nitriding furnace, spacer caps were designed (see Appendix D) to allow use of less expensive M36 studs in the M100 holes. On the spindle hole only 18 bolts were used instead of the 36 that will be used in the actual installed CUD.

As an extra safety measure preliminary ASME VIII [9] code calculations for blind flanges were done for the largest flange, the weld neck sealing flange. The check proved that the flange

thickness is acceptable with 12 mm thick 300W steel plate and a low gasket seating stress. The calculations are given in Appendix C section 3. The application of ASME design calculations is not sufficient because 300W is not a pressure vessel steel and no ASME II [16] allowable stresses are listed for it. After an estimate for the required thickness with the code calculations; a Finite Element Analysis (FEA) model of the weld neck sealing flange was created.

4.3.2 WELD NECK SEALING FLANGE STRESS ANALYSIS

4.3.2.1 THE MODEL

Since the weld neck sealing flange has an irregular geometry with the fan shaft pipe and gussets attached (see Figure 4.1); normal blind flange design formulas are not sufficient. A FEA model was created to accurately model the hole in the centre. In Appendix C par. 4 a few preliminary FEA results are given for a 12 mm thick flange with no hole in the centre; using plate elements (only a pressure load was applied and no gasket pressure). To get a more accurate model with gradients through the plate thickness; an axisymmetric model was created as shown in Figure 4.11. Movement along the pressure direction is restricted along the gasket edge to simulate a pressure tight seal. Strand 7 FEA software [51] was used for all the FEA models.

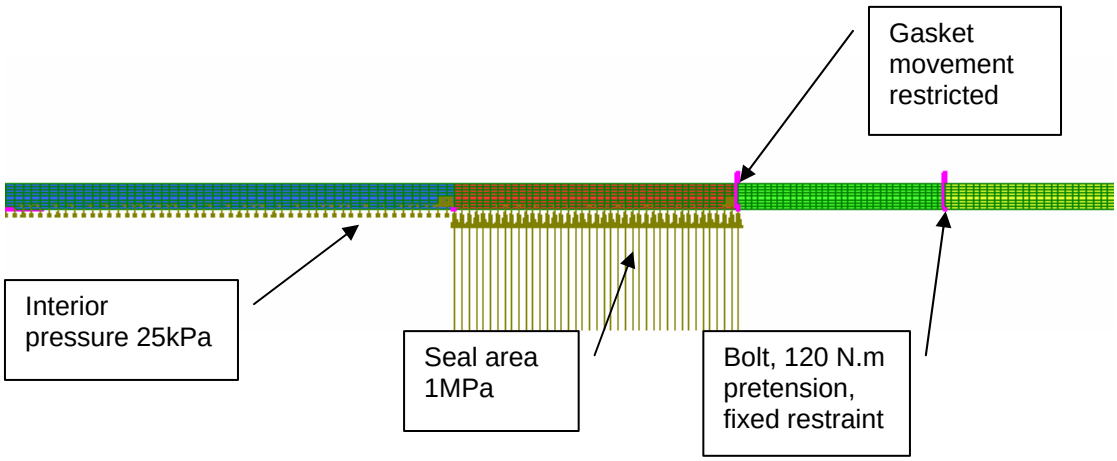

Figure 4.11: Axisymmetric FEA model weld neck sealing flange.

4.3.2.2 LOAD APPLICATION

For the first axisymmetric model only the vessel interior pressure load of 25 kPa and gasket seating stress of 1 MPa is applied, see Figure 4.11. Restraints are applied in such a manner to present the deformation of the flange in an accurate yet conservative manner. Applying fixed restraints at the bolt locations is very conservative (in reality the bolts will deform). Note that the seating stress application is conservative since in reality a much smaller area closer to the edge of the seal surface will apply the 1 MPa seating stress to the flange. The gasket supplier recommended a 60 MPa seating stress. Bolt torque calculations in Appendix C section C.2 show that for human fastening a seating stress of 1 MPa is the limit (for 60 MPa seating stress a

19 m moment arm is required). At the time this was realised the gaskets were already manufactured so reducing the gasket area or using a different material was not an option. Because of the low internal pressure it was decided that the lower seating stress still provides sufficient sealing. This theory would be tested during plant construction.

4.3.2.3 FEA RESULTS

The Von Mises stress results can be seen in Figure 4.12 and for this conservative model the maximum Von Mises stress is found at the gasket edge. It is below the material limit of 300 MPa at ambient temperature. However, this local stress can be discarded because it is a geometric FEA singularity. In practice a soft flat gasket cannot result in a high contact stress. The stresses at the centre of the flange are fairly low, below 70 MPa, as predicted by the preliminary model in Appendix C. At operating temperature it will still be below the material yield strength of 160 MPa at 600 °C (Table Y in [16]). The deformation of the model is given by Figure 4.13.

4.3.2.4 MESH REFINEMENT

No further mesh refinement is necessary since the majority of stresses are fairly low, only the local gasket edge contact stress will increase since it represents a singularity.

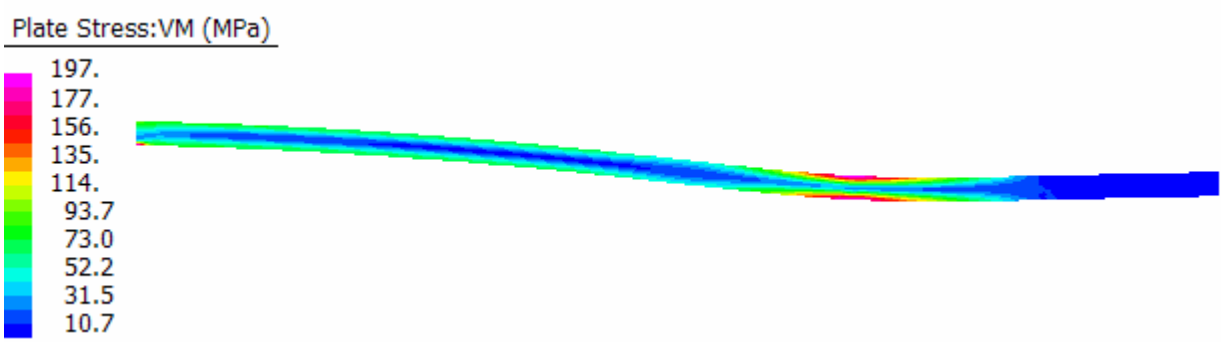

Figure 4.12: Von Mises stress results of the axisymmetric model.

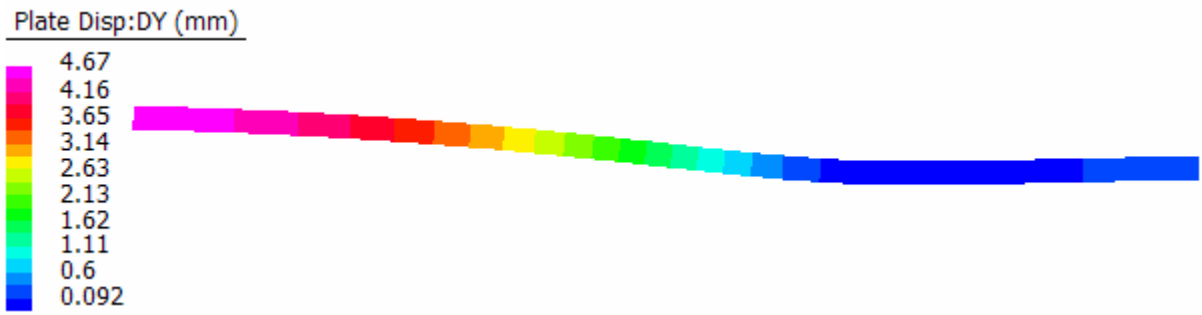

Figure 4.13: Deformed displacement in the pressure direction.

4.3.2.5 DETAILED 3D FEA MODEL

The conservative axisymmetric FEA model has proved that stresses due to only the vessel interior pressure are low and that the flanges are of sufficient thickness. At the time of the detail design no time was available for a detailed 3D FEA analysis and because the axisymmetric

FEA calculations proved that the sealing flange design was sufficient to contain the pressure, construction could commence. After plant operation a more accurate 3D model, of the entire weld neck sealing flange assembly, was created to model the shaft weight, the gussets and the hole in the centre of the sealing flange. The 3D FEA could also be done more accurately since the actual flange deflection after installation could be modelled after it was observed. The detailed 3D FEA model will be described in further detail in section 6.3 once the plant has been constructed and operated, as part of the design validation.

Of importance here is the displacement of the pipe ends, with the loads calculated in par. 4.2.8 applied to the support pipe, see Figure 4.14. The displacements of the FEA model are close to the analytically calculated values in par. 4.2.8, assuming that the support pipe is a cantilever beam (1.5 mm versus 1.31 mm for the FEA model). The smaller deflection of the FEA model can be due to the triangular gussets that effectively reduce the pipe overhanging length.

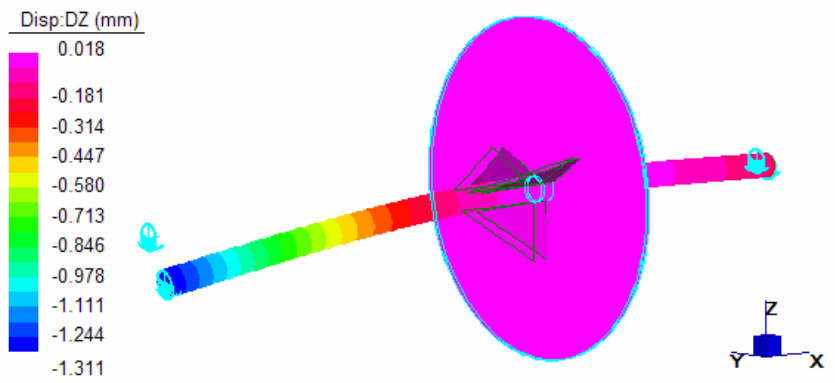

Figure 4.14: Magnified FEA displacement plot of support pipe ends in the vertical direction (z).

4.3.3 HIGH TEMPERATURE GASKET DESIGN

The next step is to design the gaskets of the sealing flanges. The gaskets needed to seal at temperatures as high as 600 °C. Any carbon or ceramic material can withstand temperatures above 600 °C. Klinger seals (Klinger (Pty) Ltd.) suggested a new ceramic fiber seal material called Thermoceram. A deformable flat ring gasket was designed for each hole. The detail drawings of the gaskets can be seen in Appendix D. Note that the gaskets' inner diameter was made larger than the hole to ensure that the machined sealing surface (grammaphone finish) on the edge of the CUD hole was also nitrided. As discussed previously in section 4.3.2.2, the required seating stress is 60 MPa, however a 1 MPa seating stress would be used for design.

4.3.4 GAS PIPE PENETRATIONS DESIGN

For the gas pipe penetrations a [17]Swagelok pipe fitting system will be used with the well known nut and ferrule sealing system (Parker (Pty) Ltd has a similar system). The ferrule system seals

[17] Swagelok is an international trademark and a worldwide supplier, see /www.swagelok.com

the tube onto the fitting body when the nut is tightened see Figure 4.15.a) to c). The male connectors with tapered male NPT thread in particular would be used. The male NPT thread would be screwed into the NPT threaded holes in the sealing flanges.

a) A Swagelok nut and its ferrules, pictures from www.swagelok.com.

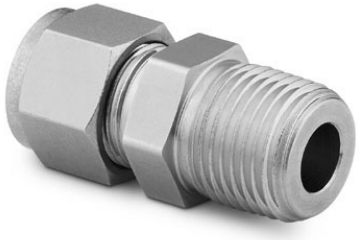

b) A Swagelok tube fitting with tapered NPT thread, pictures from www.swagelok.com.

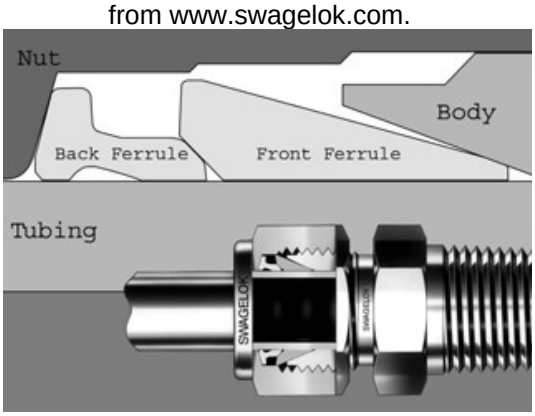

c) A schematic drawing of the Swagelok system, from www.swagelok.com.

d) The 0.5 inch gas supply tubes and Swagelok penetrations fitted to the weld neck sealing flange.

Figure 4.15: Pictures and illustrations of the gas pipe penetrations design.

The seal that is created when the tapered thread is screwed in will ensure minimum leakage under pressure (PTFE tape cannot be used because it disintegrates above 200°C). On the 0.5 inch supply pipes 0.5 NPT fittings were supplied and for the 3/8 inch exit pipes 3/8 inch NPT fittings are screwed into the flanges, see Figure 4.15.d).

4.3.5 THERMOCOUPLE PENETRATIONS DESIGN

For the thermocouple penetrations the same Swagelok system will be used with a ¼ inch male NPT thread, bore through fitting. The difference is that the 3 mm thermocouple sheath penetrates the process chamber and is placed onto the CUD interior wall. Therefore bore through fittings are used. The thermocouples will be enclosed in 3 mm sheath probes, made of inconel or stainless steel alloy, that form the pressure boundary. The actual thermocouples will thus not see the process chamber pressure. Inside the sheaths are type K thermocouples with a measurement range of 0 – 1000 °C. The thermocouples are supplied with calibration certificates, see Appendix H.

4.4. GAS PIPING SYSTEM

4.4.1 GAS PIPING LAYOUT

As mentioned in section 4.1 the NP is divided into three PFMs i.e. the Gas Supply (NP-01), Nitriding Furnace (NP-02) and Gas Exit PFM (NP-03), see Figure 4.16. The piping system design of each PFM will be described individually. For better understanding of the piping system the Process Flow Diagram (PFD) in Appendix B must be studied.

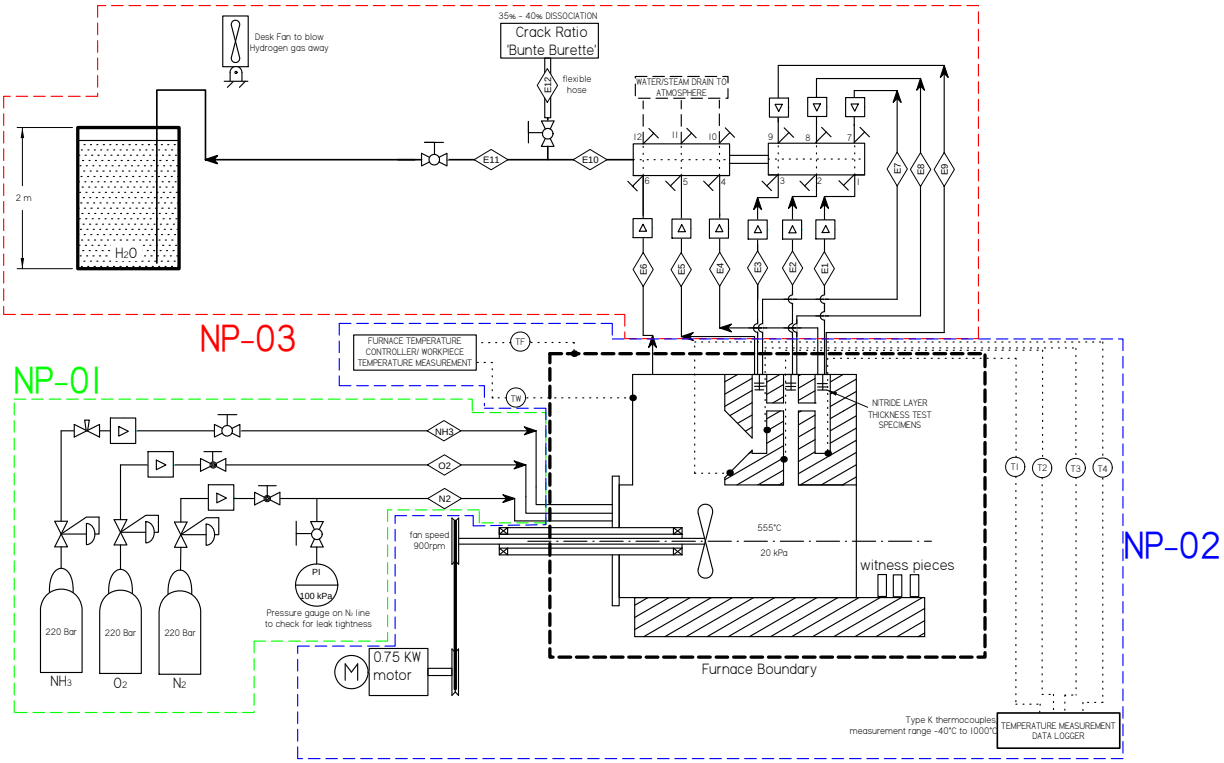

Figure 4.16: Boundaries of the NP with PFM groupings.

4.4.2 GAS SUPPLY PFM

A calculation will now be done to determine the required process flow rates and initial gas masses of each of the gases that will be used during the CUD Nitriding process. The gas cylinder requirements can then be established.

Assumptions:

Assume that the ammonia, oxygen and nitrogen entering the flowmeter is at the operating pressure of 120 kPa (absolute) and at an atmospheric temperature of 25 °C. The specified flow rates in section 2.7.2 are used as a guideline.

Calculation of the required flow rate in the vessel:

Before the flow rate is calculated a guideline for the volume of gas that needs to be circulated, in the housing, in a certain time needs to be defined: According to [10] initially ammonia is

supplied at a flow rate to achieve a minimum of four atmosphere (gas volume) changes in the retort per hour. This initial cycle develops a shallow white layer from which diffusion of nitrogen into the main case structure proceeds.

A good guideline is thus that a minimum of 4 CUD housing volumes must be filled with ammonia per hour at the specified operating temperature and pressure. This would ensure the required initial ammonia dissociation rate of 15 to 35 %. When the dissociation rate starts to get larger than 35 % the ammonia supply flow rate is increased.

Minimum required flow rate in the vessel during the initial nitriding cycle to form the white layer

$$F_{req} = \frac{4 \cdot Volume_{CUD}}{hr} \quad (39)$$

For purging with nitrogen the same philosophy can be followed. However, the amount of CUD volumes (atmospheres) that need to be changed is less. It was decided to replace 2 atmospheres in an hour (this should be sufficient to remove most of the air when purging with nitrogen for two hours).

For cleaning the CUD housing with oxygen during the preparation cycle a different philosophy is followed. It is not necessary to purge the CUD with oxygen (enough oxygen must be delivered to oxidize the entire CUD volume and to act as a catalyst).

Calculation of the required entry flow rate:

Due to temperature differences the volume flow rate at the entrance will differ from the vessel volume flow rate. The calculated vessel volume flow rate needs to be used to determine the entry volume flow rate that is read off manually at the flowmeters. Before this can be done the vessel mass flow rate is calculated from the volume flow rate. The first step is to calculate the gas density in the vessel at the specified vessel operating temperature. The density is calculated with the ideal gas law (equation of state) as follows:

Gas density at the specified vessel operating temperature (ideal gas law) [50] p.65

$$\rho_{oper} = \frac{P_{oper}}{R_{gas} \cdot T_{oper}} \quad (40)$$

The mass flow rate. Mf, through the vessel is then determined as follows, where F_{req} is the required volume flow rate in m^3/hr

$$Mf_{vesselgas} = \rho_{oper} \cdot F_{req} \quad (41)$$

Since $Mf_{in} = Mf_{vesselgas}$, the entry volume flow rate at the flowmeter is calculated as follows:

Entry volume flowrate

$$F_{entr} = \frac{Mf_{vessel\,gas}}{\rho_{in}} \quad (42)$$

where the gas density at the flowmeter is calculated at atmospheric temperature (it is assumed that the gas is at atmospheric temperature) as follows:

Gas density at flowmeter, using the equation of state (ideal gas law) [50] p.65

$$\rho_{in} = \frac{P_{oper}}{R_{gas} \cdot T_{atm}} \tag{43}$$

The required initial gas mass is simply calculated by multiplying the calculated required vessel mass flow rate by the total time that the flow rate needs to be sustained:

Required initial gas mass

$$M_{initial} = Mf_{gas} \cdot t_{min} \tag{44}$$

Input data:

The input data used for flow rate and required gas mass calculations are given in Table 4.6.

Table 4.6: Input data used for calculating the required gas flow rates and initial gas masses.

Description	Symbol	Value	Unit
inner diameter of CUD defuel chute see drawings in Appendix D	D_i	840	mm
length of defuel chute	h_i	2.5	m
spindle hole inner diameter	D_{si}	650	mm
length of spindle hole	h_{is}	1.4	m
inner diameter of valve inserts	D_{ii}	160	mm
length of valve inserts	h_{ii}	600	mm
CUD housing interior volume according to CAD model	V_{CUD}	1960	ℓ
maximum flow rate specified for NH_3 flowmeter, section 2.7.2	F_{spec}	3000	ℓ/hr
maximum flow rate specified for O_2 flowmeter, section 2.7.2	F_{specO2}	200	ℓ/hr
maximum flow rate specified for N_2 flowmeter, section 2.7.2	F_{specN2}	200	ℓ/hr
nitriding absolute operating pressure for the CUD vessel, section 2.7.2	P_{oper}	110	kPa
Ideal gas constant for Ammonia [50]	R_{NH3}	0.4882	kJ/kgK
Ideal gas constant for Nitrogen [50]	R_{N2}	0.2968	kJ/kgK
Ideal gas constant for Oxygen [50]	R_{O2}	0.2598	kJ/kgK
operating temperature	T_{oper}	555	°C
oxygen cleaning/oxidizing temperature	T_{clean}	200	°C
atmospheric temperature	T_{atm}	25	°C
maximum duration of full ammonia flow rate	t_{maxd}	48	hr
duration of initial cycle to form white layer, with 15–35% dissociation	t_{cure}	10	hr

To confirm the CUD volume given by the CAD model in Table 4.6, the CUD internal volume is also calculated as follows:

CUD housing interior volume

$$V_{CUD} = \frac{\pi \cdot h_i \cdot D_i^2}{4} + \frac{\pi \cdot h_{si} \cdot D_{si}^2}{4} + \frac{8 \cdot \pi \cdot h_{ii} \cdot D_{ii}^2}{4} = 1946.515 \cdot \ell$$

This is very close to the 1960 ℓ calculated with the CAD model.

Required ammonia flow rate:

Required volume flow rate, eq. (39) [10] as guideline

$$F_{req} = \frac{V_{CUD} \cdot 4}{hr} = 7840 \cdot \frac{\ell}{hr}$$

Density at furnace operating temperature eq. (40)

$$\rho_{oper} = \frac{P_{oper}}{R_{NH3} \cdot T_{oper}} = 0.272 \cdot \frac{kg}{m^3}$$

Ammonia mass flow rate, eq. (41) $Mf_{operNH3} = \rho_{oper} \cdot F_{req} = 5.925 \times 10^{-4} \cdot \frac{kg}{s}$

Density at flowmeter, atmospheric temperature, eq. (43) $\rho_{in} = \frac{P_{oper}}{R_{NH3} \cdot T_{atm}} = 0.756 \cdot \frac{kg}{m^3}$

Required volume flow rate at entrance, eq. (42) $F_{entr} = \frac{Mf_{operNH3}}{\rho_{in}} = 2822.551 \cdot \frac{\ell}{hr}$

This value is not close to the maximum flow rate specified in section 2.7.2 i.e. F_{spec} = 3000 ℓ/hr.
The margin for the specified flow measurement upper limit is: $F_{spec} - F_{entr}$ = 177.449 ℓ/hr
Initially the flow meter was thus overspecified by 178 ℓ/hr.

Initial ammonia mass required:

The initial ammonia mass required for a 10 hr initial nitriding cycle to provide the white layer is:

initial ammonia mass for a 10 hr cycle, eq. (44) $M_{init} = Mf_{operNH3} \cdot t_{cure} = \cdot 21.331 \cdot kg$

The total mass of ammonia required for a 48 hr nitriding cycle at full ammonia supply flow rate:

Initial ammonia mass for a 48 hr cycle, eq. (44) $M_{init\,max} = Mf_{operNH3} \cdot t_{max\,d} = \cdot 102.387 \cdot kg$

Required Nitrogen flow rate:

Required volume flow rate for N_2 purging, modified eq. (39) $F_{req} = \frac{V_{CUD} \cdot 2}{hr} = 3920 \cdot \frac{\ell}{hr}$

Density at furnace temperature, eq. (40) $\rho_{oper} = \frac{P_{oper}}{R_{N2} \cdot T_{clean}} = 0.783 \cdot \frac{kg}{m^3}$

Nitrogen mass flow rate $Mf_{oper} = \rho_{oper} \cdot F_{req} = 8.529 \times 10^{-4} \cdot \frac{kg}{s}$

Density at flowmeter, atmospheric temperature eq. (43) $\rho_{in} = \frac{P_{oper}}{R_{NH3} \cdot T_{atm}} = 1.243 \cdot \frac{kg}{m^3}$

Required volume flow rate at entrance, eq. (42) $F_{entr} = \frac{Mf_{oper}}{\rho_{in}} = 2470.143 \cdot \frac{\ell}{hr}$

The calculated flow rate is larger than the rate specified in section 2.7.2 i.e. F_{spec} = 200 ℓ/hr.
The margin for the specified flow measurement upper limit is: $F_{spec} - F_{entr}$ = – 2270 ℓ/hr
Initially the flow meter was thus underspecified by 2270 ℓ/hr.

Initial Nitrogen mass required:

The initial nitrogen mass required for a 10 hr purging cycle to prior to nitriding is:

Initial nitrogen mass for a 10 hr cycle, eq. (44) $M_{initN2} = Mf_{oper} \cdot t_{cure} = \cdot 30.705 \cdot kg$

Required oxygen flow rate:

Using eq. (39) for 2 CUD volume changes per hour (3920 ℓ/hr) and equations (40) to (43), the required oxygen flow rate for 2 CUD volume changes per hour is also equal to F_{entr} = 2470.143 ℓ/hr (required oxygen mass flow rate is Mf_{oper} = 9.744 x 10^{-4} kg/s). This volume flow is much larger than the flow rate specified in section 2.7.2 i.e. F_{spec} = 200 ℓ/hr. If 2 CUD

volumes must be replaced per hour the flow meter is underspecified by 2270 ℓ/hr. However, the oxygen supply requirement is not volume flow dependent, but concentration dependent. Just enough oxygen is required to oxidize the metal surface. The flow rate for 2 volume changes per hour will still be used to calculate the initial oxygen mass required in case more oxygen is necessary on site.

Initial oxygen mass required:

Initial oxygen mass for a 10 hr cycle, eq. (44) $M_{initO2} = Mf_{oper} \cdot t_{cure} = \cdot 35.078 \cdot kg$

Summary of results:

The minimum initial amount of oxygen and nitrogen required is strongly dependent on the actual required flow rate. If 4 CUD volumes need to be replaced during purging with nitrogen an initial mass of M_{initN2} = 60 kg (30 kg for 2 CUD volumes), needs to be supplied. If 2 CUD volumes per hour are replaced during oxidation an initial oxygen mass of 35.078 kg needs to be supplied. To maintain the maximum ammonia flow rate for an initial crack ratio of 15 to 35% for 48 hrs, an initial ammonia mass of $M_{initmax}$ = 102.387 kg is required.

According to Afrox (Pty) Ltd. ammonia is supplied in cylinders containing 68 kg. As 102 kg is initially required, 3 cylinders would be more than sufficient. Oxygen is supplied in cylinders containing 14 kg therefore 3 cylinders would be sufficient for the 35 kg required. Afrox supplies nitrogen in cylinders containing 11 kg. Since 25 kg is initially required, 4 cylinders would be more than sufficient.

4.4.3 NITRIDING FURNACE PFM

On the CUD block there are nine insert holes and nine exit penetrations to ensure equal flow and no stagnant areas, in addition to the stirring fan. Nine tubes combine at a common manifold to ensure that the same downstream pressure is seen by all the pipes. This will ensure approximately equal flow rates through each of the nine exit pipes. Equal flow rates should ensure even nitriding on all nine insert holes.

4.4.4 GAS EXIT PFM

A calculation is necessary to ensure that the flow through the nine exit flowmeters don't exceed their design temperature of 120 °C. The exit pipes need to have cooled down sufficiently at the point where the flowmeters are installed. The minimum distance (pipe length) between the furnace and the point where the flowmeters are installed needs to be determined.

Calculation of the exit gas temperature at a specified distance from furnace:

A formula from [48] for laminar flow in a tube using the bulk temperature is used.

Outlet bulk temperature (chapter 4 in [48]) $$T_{bout} = T_s - (T_s - T_{bin}) \cdot e^{\frac{-h_{ci} \cdot 2 \cdot \pi \cdot R_i \cdot L}{Mfe \cdot Cp_{NH3}}} \quad (45)$$

where Mfe is the exiting mass flow, Cp_{NH3} the ammonia specific heat, R_i pipe inner radius and h_{ci} is the heat transfer coefficient to the environment.

The inputs used for this calculation are listed in Table 4.7**.**

Table 4.7: Inputs for the exit tube temperature calculation.

Description	Symbol	Value	Unit
exit pipe outer diameter (OD), 3/8 in Swagelok tube	d_o	9.525	mm
exit pipe inner diameter (ID), 3/8 in Swagelok tube	d_i	7.036	mm
outer radius of tube 3/8 in Swagelok tube, $d_o/2$	R_o	4.762	mm
inner radius of tube 3/8 in Swagelok tube, $d_i/2$	R_i	3.518	mm
viscosity of ammonia at 25°C [50]	μ_{NH3}	1.01E-05	Pa.s
ammonia thermal conductivity at an average temperature of (555+25)/2=290°C, [48])	k	0.0511	W/mK
ammonia specific heat (constant pressure specific heat), [37]	Cp_{NH3}	2420	J/kgK
maximum ammonia mass flow during operation, section 4.4.2	$Mf_{operNH3}$	5.93E-04	kg/s
density of ammonia at exit penetration, ρ_{oper} section 4.4.2	ρ_{pen}	0.272	kg/m^3
density of ammonia outside furnace if at atmospheric temperature ρ_{in} section 4.4.2	ρ_{out}	0.756	kg/m^3

Exiting gas flow calculation:

Mass flow through each exiting pipe $$Mfe = \frac{Mf_{operNH3}}{9} = 6.584 \times 10^{-5} \cdot \frac{kg}{s}$$

Flow Reynolds number [36] at flowmeter @25°C $$Re = \frac{4 \cdot Mfe}{\pi d_i \mu_{NH3}} = 1179.593$$

The exit flow is thus laminar as Re < 2300

Exit tube heat transfer:

Nusselt number for laminar flow in a pipe, [48] $Nu_D = 4.36$

Tube inner surface heat transfer coefficient $$h_{ci} = \frac{Nu_D \cdot k}{d_i} = 31.66 \cdot \frac{W}{m^2 \cdot K}$$

Pipe length from furnace up to flowmeter (1st iteration) $L = 1$ m

Tube surface temperature $T_s = 25$ °C

Bulk gas temperature at exit of furnace $T_{bin} = 555$ °C

Bulk temperature of gas at a distance of 1m, use eq. (45) $T_{bout} = 31.551$ °C

Lower exit mass flow (lower supply) $$Mfel = \frac{Mfe}{4} = 1.646 \times 10^{-5} \cdot \frac{kg}{s}$$

Bulk temperature of gas at a distance of 1m, use eq. (45)

$$T_{bout} := T_s - (T_s - T_{bin}) \cdot e^{\frac{-h_{ci} \cdot 2 \cdot \pi \cdot R_i \cdot L}{Mfel \cdot Cp_{NH3}}} = 25 \cdot °C$$

The calculation above ignores the external heat transfer coefficient; if the external heat transfer coefficient is low the above calculated temperatures are incorrect (and too low).

A low external heat transfer coefficient will now be used i.e. natural convection over a cylinder.

Low external heat transfer coefficient; see section 6.2.2 for a justification $h_{co} = 4 \cdot \frac{W}{m^2 \cdot K}$

Pipe length from furnace up to flowmeter (low h_{co}) L = 3m

More conservative overall heat transfer coefficient [48]

$$UA = \left[\frac{1}{2 \cdot \pi \cdot R_i \cdot L \cdot h_{ci}} + \frac{\ln\left(\frac{R_o}{R_i}\right)}{2 \cdot \pi \cdot k_{steel} \cdot L} + \frac{1}{2 \cdot \pi \cdot Ro \cdot L \cdot h_{co}} \right]^{-1} = 0.307 \cdot \frac{W}{K} \qquad (46)$$

More conservative inner surface heat transfer coefficient $h_c = \frac{UA}{2\pi \cdot R_i L} = 4.623 \cdot \frac{W}{m^2 \cdot K}$ (47)

Bulk temperature of gas at a distance of 3 m from the furnace at a low heat transfer coefficient, eq. (45) design case

$$T_{bout} := T_s - (T_s - T_{bin}) \cdot e^{\frac{-hc \cdot 2 \cdot \pi \cdot R_i \cdot L}{Mfe \cdot Cp_{NH3}}} = 102.386 \cdot °C$$

Summary of results:

Calculations indicate that for lower exit mass flows the exit gas temperature is lower and for lower heat transfer coefficients the exit gas temperatures are much higher. The most conservative calculation with a minimum heat transfer coefficient and a high mass flow showed that a minimum pipe length of 3 m is required outside the furnace before the exit flowmeter is mounted (temperature then is 103 °C). The minimum length of pipe that needs to be outside the furnace before the exit flowmeter is mounted is thus 3 m.

4.4.5 FLOWMETER DESIGN

For the gas supply PFM 3 flowmeters are required i.e. one for ammonia, one for nitrogen and one for oxygen. For the gas exit PFM another 9 flowmeters are required (see the PFD in Appendix B). The reason for installing nine flowmeters on the gas exit is to allow the plant operator to monitor that the flow rates through all nine nitrided insert holes are equal. If the flow is not equal the flow can be balanced with the exit manifold valve.

The type of flowmeters that will be used are Rotameters (least expensive), with small balls floating in a glass tube. These flowmeters must be installed upright to measure correctly. All flowmeters need to be stainless steel, because ammonia reacts with copper (brass). The

oxygen and nitrogen lines' flowmeters can be brass but in case ammonia gas leaks to the oxygen or nitrogen lines (past isolation valves) these flowmeters are also made of stainless steel. A slightly larger and more accurate flowmeter is specified for the ammonia line since the ammonia supply flow rate measurement is the most critical of all.

4.4.6 VALVE SELECTION

For isolation of the three gas supply lines stainless steel Swagelok ball valves are specified. The isolation valves prevent oxygen or nitrogen leakage into the ammonia line and vice versa. Oxygen is a very hazardous flammable gas and it must therefore be isolated when not in use.

Globe valves with fairly fine control are specified on the nitrogen and oxygen lines. The needle valve incorporated on the ammonia supply flow meter will be used to fine tune the ammonia supply flow rate.

On the gas exit the nine exit tubes combine at the exit valve manifold with one tube exiting to the 'Bunte Burette' and water drum. The exit valve manifold has needle valves on each port that can be used to balance the exiting flow rates.

One safety relief valve needs to be installed downstream of the isolation valves on the gas supply PFM. Between any two isolation valves in a pressurized system a pressure safety valve (PSV) is required according to the OHS Act. A pressure sensitive check valve was specified with a specified cracking pressure of 35 kPa. This check valve is used because no safety relief valves are available for the small set pressure of 40 kPa (the limit for a pressure vessel according to OHS Act).

4.5. DESIGN OF THE CUD CRADLE AND CUD POSITIONING IN THE FURNACE

Since a Top hat furnace will be used the CUD can not be positioned directly on top of the sand of the furnace. It must be lifted from the sand to ensure even temperature distribution. Because Top Hat 1 at DCD Dorbyl is not wide enough for the CUD to be put flat on the floor, the CUD will be held at a 45° angle. The 45° angle is better than a vertical position since it will reduce possible thermal strain distortion, due to the weight of the CUD block on the barrel. The inserts on the block where the gas exits will also be higher than where the gas enters. This forces the gas to exit at the top as prescribed by the lab tests in section 2.7.2.

A drawing of the CUD installed on the cradle, with the block at a 45° angle with the ground, is shown in Figure 4.1.

Strength calculations were performed on the vertical column of the CUD Nitriding cradle (the cradle and column design is shown in Figure 4.17). The cradle is mainly checked for buckling

failure since it has the most critical consequences. If the columns were to buckle the CUD block would not be held at 45° in the nitriding furnace throughout the entire nitriding process.

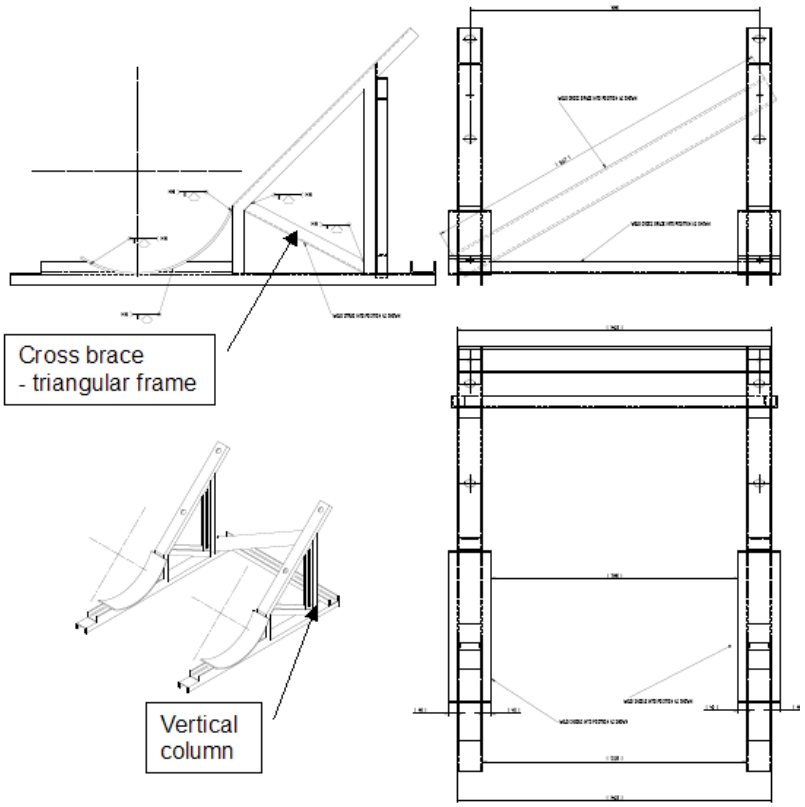

Figure 4.17: CUD cradle showing vertical columns etc.

Loading conditions:

It is assumed that the full weight of the CUD housing rests on the 2 vertical columns. If a less conservative calculation is done, the loads are divided equally between the four contacts. Due to the cross bracing and triangular frame, as shown in Figure 4.17, it would not be necessary to design the column for bending or eccentric loading. Only pure buckling load will be considered.

Calculation technique:

The structural analysis is started by performing calculations based on first principles, by using analytical equations from [43] an elementary strength of materials textbook. Thereafter the SANS 10162 code [46] is applied to check these answers. Note that the code uses a limit state design method as opposed to the allowable stress design method followed with first principles.

Input data:

Beam material properties:

steel modulus of elasticity, from [42] @ 600 °C $E = 140\ GPa$

Poisson's ratio $\upsilon := 0.3$

Shear modulus of steel, from [43] $G := \frac{E}{2 \cdot (1 + \upsilon)} = 53.846 \cdot GPa$

Design for a PFC 120X55 channel beam, with dimensions as given by Table 4.8 (values are from Structural steel tables in [47] refer to Figure 4.18 for a definition of the axis system):

Table 4.8: Beam section dimensions used for buckling structural analysis.

Description	Symbol	Value	Unit
column length, see Figure 4.17	L_{col}	0.9	m
depth of column section	h	129	mm
web thickness	t_w	5.5	mm
flange thickness	t_f	9.1	mm
flange width	b	55	mm
half depth of column section	c_{col}	0.06	m
half depth in yy direction	c_y	0.028	m
monent of inertia about xx	I_x	3.65E+06	mm^4
radius of gyration about x axis	r_x	47.8	mm
moment of inertia about yy	I_y	4.78E+05	mm^4
radius of gyration about y axis	r_y	17.3	mm
polar moment of inertia	J	3.48E+04	mm^4
column cross sectional area	A_{col}	1.60E+03	mm^2
warping torsional constant	C_W	1.06E+09	mm^6
Section Modulus about xx	Z_{pl}	6.09E+04	mm^3
Section Modulus about xx	Z_{ply}	1.31E+04	mm^3
Effective section modulus about xx	Z_e	6.09E+04	mm^3
Material yield strength at 600°C, Table Y in [42]	f_y	160	MPa

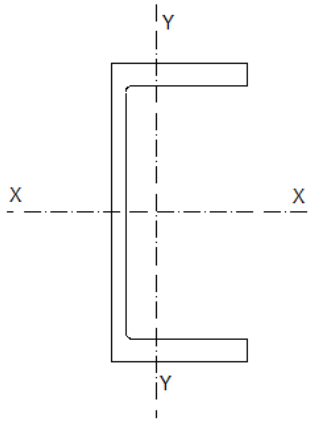

Figure 4.18: axes definition of the lip channel.

Loading Case Definition:

CUD mass $M_{col} = 14000 \cdot kg$

Gravitational acceleration $g = 9.807 \cdot \frac{m}{s^2}$

Vertical column load $P_{col} = M_{col} \cdot g = 137.293 \cdot kN$

Lateral load per column $F_{longit} = P_{col} \cdot \frac{\sin(45°)}{2} = 137.293 \cdot kN$

Longitudinal bending moment per column $M_{longit} = F_{longit} \cdot L_{col} \cdot \cos(45°) = 30.891 \cdot kN \cdot m$

Calculations:

Before starting with the code calculations a first estimate, for the stresses in the column, is obtained with analytical formulas. Buckling stress according to [43], p.273:

Maximum Euler Buckling load $P_c = \frac{4 \cdot \pi^2 \cdot E \cdot I_y}{L_{col}^2} = 3261.6 \cdot kN$ (48)

Compressive stress at the Euler load $\sigma_{c2} = \frac{P_c}{A_{col}} = 2038.5 \cdot MPa$ (49)

Buckling Safety Factor $SF1 = \frac{|\sigma_{c2}|}{f_y} = 12.74$

Check Safety Factor CheckSF1 := if(SF1 > 1, "Acceptable", "Not Acceptable")

CheckSF1 = "Acceptable"

The column thus yields before it buckles.

Maximum compressive stress $\sigma_c = \frac{-P_{col}}{A_{col}} = -85.808 \cdot MPa$

Safety Factor based on yield stress $SF = \frac{f_y}{|\sigma_c|} = 1.87$

Code Calculations:

See Appendix C section 1 for SANS code [46] calculations. It is checked for axial compression, bending, flexural buckling and simultaneous axial compression and bending

Conclusion:

The PFC120X55 beam is adequate. If bending load is considered with the vertical support force divided equally between the four vertical columns, the columns is adequate with K =1 [46]. If K = 2 is assumed for checking pure buckling due to concentric loading, the column is still adequate with a safety factor of 3. The compressive stress in the column if the full weight of the CUD is placed on a single column is σ_c = –85.81 MPa, which is below the yield stress of f_y = 160 MPa at 600 °C.

4.6. MAINTENANCE AND RELIABILITY ANALYSIS

Since this plant will only be used once for 72 hours in total it was not required to do a maintenance analysis at this stage. The component that would be subjected to fatigue is the shaft and the stresses in the shaft are so low that a limited life fatigue analysis will not be necessary. None of the valves etc. would need maintenance for such a short period of use. If problems do occur a shutdown procedure will be included in the plant operating description.

4.7. QUALIFICATION

As the prototype plant is built all the individual components will be tested, qualified and validated. The operation of the high temperature sealing bearing etc. will be tested during plant operation in chapter 5.

4.8. COST ANALYSIS

A cost estimation of the nitriding plant equipment is included in Table 4.9. The operating costs are listed in Table 4.10.

Table 4.9: Approximate Costs of the NP (prices include VAT @14%).

Item no.	Description	Quantity	Supplier	Price/unit [R]	manufacturing process if required	Manufacturing cost/unit [R]	Total Cost
1	Block Insert sealing flanges	8	KARE Sheet Metal	500	laser cut + thread	500	R 8,000.00
2	Block Insert flange gaskets	8	Klinger	100		0	R 800.00
3	Spindle sealing flange	1	KARE Sheet Metal	1000	laser cut + thread	500	R 1,500.00
4	Spindle flange gasket	1	Klinger	600		0	R 600.00
5	Weld Neck sealing flange	1	KARE Sheet Metal	2000	laser cut + thread	500	R 2,500.00
6	Weld neck flange gasket	1	Klinger	800		0	R 800.00
7	sphere pipe sealing flanges	4	KARE Sheet Metal	500	laser cut + thread	500	R 4,000.00
8	sphere pipe flange gaskets	4	Klinger	100		0	R 400.00
9	M36X3 Bolts for spindle flange	18	Studbolt	300		0	R 5,400.00
*10	M20x2.5 studs	150	HTF/Studbolt	0		0	R -
*11	1" X 8 UNC (Unified thread core series) threaded rod	3m	HTF	0		0	R -
*12	nuts for 1" X 8 UNC	8		0		0	R -
13	0.5" BSPP plugs for Gas Tightness lines + aluminium washers on block	5	Media Hydraulics	20		0	R 100.00
14	Stainless steel tubing	20m	Parker/Swagelok	500	extra 7m purchased on site	0	R 3,500.00
*15	connector fittings for flanges	10	Swagelok	0		0	R -
*16	T-pieces	10	Swagelok	0		0	R -
*17	12 to 1 connector valve manifold	3	HTF	0		0	R -
*18	Control valve	3	HTF	0		0	R -
*19	Hand valve (ball valve)	3	Swagelok	0		0	R -
20	Rotameter Flowmeters	11	HM FloConsult	2000		0	R 22,000.00
21	Rotameter ammonia supply	1	HM FloConsult	3000			R 3,000.00
22	0.75kW non-sparking motor	1	Fenner	2000		0	R 2,000.00
23	45cm diameter steel fan	1	scrap yard	450		0	R 450.00
24	Ball bearing for fan shaft	1		500		0	R 500.00
25	graphite bearing for fan shaft	1	Morgan Carbon	500		2200	R 2,700.00

Item no.	Description	Quantity	Supplier	Price/unit [R]	manufacturing process if required	Manufacturing cost/unit [R]	Total Cost
26	1 shaft for fan connection	1	SM Projects	2000	machined by SMP	2000	R 4,000.00
27	1 bearing housing (shaft pipe) for fan fan shaft	1	SM Projects	3000	machined by SMP	3000	R 6,000.00
28	V-belt pulley	1	Fenner	500		0	R 500.00
29	tube and other penetration fittings	20	Swagelok	500		0	R 10,000.00
30	high temperature thermocouples	4	WIKA instruments	700		0	R 2,800.00
31	Stainless steel Pressure gauge	1	WIKA instruments	500		0	R 500.00
						Total Cost	R 82,050.00

Note: Items marked with a * were already available at Westinghouse Electric SA sites and were not purchased

Table 4.10: Costs of services required for operating the plant.

Service #	Description	Quantity	Supplier	Price
1	Oxygen gas cylinder and regulator	2	AFROX	R 2,000.00
2	Nitrogen gas cylinder and regulator	3	AFROX	R 2,000.00
3	Ammonia gas cylinder and regulator	5	AFROX	R 5,000.00
5	Furnace operation and standing time	1	DCD Dorbyl	R 15,000.00
6	CUD Handling	1	DCD Dorbyl	x
7	Make hole in furnace for fan shaft	1	DCD Dorbyl	x
8	2 Clean 200l oil drums (filled with water)	1	DCD Dorbyl	x
9	Bunte Burette for measuring NH_3 dissociation	1	Chris Koch	x
10	test samples for measuring nitriding thickness	4	Chris Koch	x
11	heat treatment witness samples	4	DCD Dorbyl	x
12	CUD cradle manufacturing cost	1	DCD Dorbyl	
			Approximate Total	R 50,000.00

4.9. FINAL DESIGN SPECIFICATIONS

4.9.1 PFM 1: Gas Supply PFM

The major components are the cylinders and the gas pipes.

4.9.1.1 GAS CYLINDERS AND FLOWMETERS

The cylinders shall be supplied with the pressure regulators by Afrox

Table 4.11: Gas Cylinder and flowmeter unit Performance requirements.

Parameter	Value	Comments
Gas capacity margin	100%	Double the required initial mass is supplied
Flow measurement accuracy	±5%	Ammonia flowmeter max 3000ℓ/hr O_2 and N_2 flowmeters also 2000ℓ/hr
Provide reverse flow protection	Pressure regulator	
Provide explosion protection	Pressure regulator	

Table 4.12: Gas Cylinder Physical requirements.

Parameter	Value	Comments
No of cylinders	4 Ammonia 3 Nitrogen 2 Oxygen	Two 68kg ammonia bottles are required (see section 4.4.2) for 100% capacity margin, 4 are supplied)
Flowmeter connections	½ ” line sizes	Standard Swagelok/stainless steel fittings, copper reacts with ammonia
Max temperature of the gas that can flow through the flowmeter	120 °C	The gas supply cylinders are at low temperature

4.9.1.2 GAS SUPPLY PIPING

Table 4.13: Gas Piping Performance requirements.

Parameter	Value	Comments
Max volume flowrate	3000 ℓ/hr	
Max operating temperature	555 °C	
Max design pressure	35 kPa	pressure gauge range of 0-60kPa

Table 4.14: Gas Piping Physical requirements.

Parameter	Value	Comments
Pipe length	3 X 10 m	Three supply lines of 10m each
Pipe line sizes	½ ” line sizes	Standard Swagelok/stainless steel

4.9.2 PFM 2: NITRIDING FURNACE

The major components are the fan shaft assembly and the gas fired furnace.

4.9.2.1 STIRRING FAN SHAFT ASSEMBLY

The stirring fan shaft assembly is subjected to both atmospheric temperature and the furnace max operating temperature of 600°C. The fan shaft assembly also forms part of the pressure boundary.

Table 4.15: Nitriding Fan shaft assembly Performance requirements.

Parameter	Value	Comments
Temperature of fan end	555 °C	Part of the shaft inside the furnace at high temperature
Operating temperature of bearing at fan side	555 °C	High temperature graphite bearing
Temperature of bearing on outside	50 °C	Influenced by environment temperature
Outside Bearing design temperature	120 °C	
Leak flow into bearing shaft pipe at furnace side	0.001 ℓ/hr	A high temperature gas sealing bearing was designed
Max seal Pressure drop	20 kPa (max.)	
Maximum fan rotational speed	1000 rpm	It is limited by the whirling speed of the fan shaft,

Table 4.16: Fan shaft assembly Physical requirements.

Parameter	Value	Comments
Fan diameter	500 mm	Limited by CUD weld-neck flange inner diameter
Shaft length inside CUD vessel	1.5 m	Limited by vessel dimensions,
Minimum length of shaft protruding outside the furnace	0.5 m	Total length of shaft is 2.5m
Fan motor safety classification	zone 2	Safety class zone 0-2, anti-spark etc.

The fan must be balanced and bolts/fasteners must be designed not to come loose during operation.

4.9.2.2 GAS FIRED FURNACE

The gas fired top hat furnace, which will be provided by DCD Dorbyl, is normally used for stress relieving. For nitriding the furnace needs to comply with the following standards.

Table 4.17: Top hat furnace Performance requirements.

Parameter	Value	Comments
Maximum temperature	800 °C	Part of the shaft inside the furnace at high temperature
Operating temperature	555 °C	
Maximum heating rate	100 °C/hr	Note that the actual heating rate will be dependent on the size of the workpiece and its thermal capacity
Normal heating rate	50 °C/hr	The actual heating rate will be dependent on the size of the workpiece
Temperature variance	5 °C	The variance throughout the furnace (furnace map can be provided)
Difference between furnace and workpiece temperature	50 °C	If this is the case the furnace will be at 605°C if the workpiece is at 555°C.

Table 4.18: Top hat furnace Physical requirements.

Parameter	Value	Comments
Furnace dimensions (length X width X height)	4 m X 2 m X 2.2 m	Limited by CUD dimensions

The stirring fan shaft assembly is subjected to both atmospheric temperature and the furnace operating temperature of 600°C. The fan shaft assembly also forms part of the pressure boundary. A hole will be made in the furnace for the stirring fan to fit through and it must be

ensured that there are no heat or gas leaks through this hole by sealing it with a steel plate made to fit over the hole.

Table 4.19: Process chamber Sealing system Performance requirements.

Parameter	Value	Comments
Max operating pressure	30 kPa	Includes water head of water drum and piping flow pressure losses
Max operating temperature	555 °C	
Max leak rate	1 kPa/hr	

Table 4.20: Process chamber Sealing system Physical requirements.

Parameter	Value	Comments
Penetrations/gas pipe connections sizes	½ “supply ¼ “ exit	Swagelok pressure seal fittings.

The flange gaskets must be compatible with ammonia gas and it must withstand the operating temperature of 555°C.

4.9.3 PFM 3: GAS EXIT ASSEMBLY

Table 4.21: Exit piping flowmeters Performance requirements.

Parameter	Value	Comments
Max flowrate	0 – 350 ℓ/hr	an indication that flow is going through all 8 CUD block insert holes and the spindle hole.
Piping operating temperature	555 °C	
Piping operating pressure	20 kPa	

Table 4.22: Exit Gas Piping Physical requirements.

Parameter	Value	Comments
Pipe length	9 X 5 m	Nine 9m pipes and one long pipe to the water drum
Pipe line sizes	¼ ” line from CUD ½ ” to drum	Standard Swagelok/stainless steel fittings, copper reacts with ammonia

A water filled drum with a total water height of 2 m needs to be supplied for the single gas exit pipe to drain in (bubble through); after the gas has passed through the ‘Bunte Burette’.

4.9.4 OTHER SPECIFICATIONS

The plant has a total construction cost of R 100 000 and combined with operating costs it amounts to R 150 000. It has no maintenance requirements since it will only be used once for 72 hours continuously.

The plant can now be constructed from the piping and instrumentation diagram (see Appendix F) and isometric drawings.

Chapter 5: Experimental Study

5.1. INTRODUCTION

The second major objective of this research is to construct and test a prototype plant which will physically demonstrate whether the design is a success. Because this research is essentially a comprehensive design project an experimental model is not necessary to verify a single mathematical model or analysis. The plant operation data and product results will however be used as a number of experiments to validate the theory used in the design.

This chapter starts with a discussion of all the decisions made during the design of the experimental setup. It is important to design the experiment in such a way that the performance of the plant can be monitored. Experimental parameters (operation data) must be recorded in order to correlate it to the quality of the product (the product is a nitrided vessel). The construction of the plant according to the detail design will then be discussed. A description of the experimental procedure followed, to obtain the results, is also given. To conclude the experimental data will be plotted.

5.2. EXPERIMENTAL DESIGN

5.2.1 DESIGN REQUIREMENTS

The major part of the experiment had already been designed i.e. the entire CUD NP. The next step is to ensure that the plant is set up and operated in a manner to generate adequate experimental results to validate the design.

The prototype of the plant needs the following in order to test and qualify the design.

1. Flowmeter instruments to record, monitor and control gas supply flow rates
2. Flowmeter instruments to record exit gas flow rates
3. Process chamber pressure measurement
4. Ammonia dissociation rate measurement
5. Furnace interior temperature measurement and control
6. Nitrided workpiece exterior temperature measurement
7. CUD vessel interior wall temperature measurement
8. Measurement of fan shaft pipe temperature at ball bearing
9. Nitriding fan rotation speed measurement
10. Nitriding samples placed in the CUD vessel to measure the nitride layer
11. Experimental data acquisition

Most of the equipment mentioned above had been designed and specified in chapter 4. The design and implementation of the nitriding samples and temperature measurements will be discussed next. Before the plant is constructed and the operation can commence; a detailed operating description must also be created. A HAZOP meeting (a process engineering term, p. xiii) needs to be held before construction because of the dangerous gases used in the plant.

5.2.2 DESIGN OF NITRIDING SAMPLES ASSEMBLY

The most important part of the experimental model is the nitriding samples used to measure nitride layer thickness and hardness. These need to be installed inside the process chamber in such a way that it does not affect the nitriding. The samples must also be subjected to the same temperature, pressure and gas flow as the rest of the CUD interior. This ensures that the nitriding of the samples is similar to that of the CUD.

A methodology was designed to place the samples inside the nine exit holes of the CUD block. The samples must not touch the vessel interior walls or affect the nitriding quality of the vessel interior. It was decided to place the samples in the centre of the insert holes using a rod attached to the sealing flanges. The sealing flanges are made of commercial carbon steel and do not need to be nitrided (these flanges form part of the pressure boundary).

The specimens were cut from the same material as the CUD block. Specimens were also made from two other materials, to use as a control experiment to test the nitriding on other materials. The specimen plate dimensions are more or less 5 cm X 5 cm X 0.5 cm thick. A 12 mm hole is made in each specimen to allow a 12 mm threaded rod to fit through it. The three specimens are then fastened to the rod with a number of nuts. Each rod is then fitted to the M12 threaded hole in its flange and fastened to the flange with another nut. The threaded hole in the sealing flange is then seal welded in order to prevent any gas leakage through the M12 threads. The assembled design can be seen in Figure 5.1.

Figure 5.1: The nitrided layer samples before nitriding, fitted to the valve insert flanges.

5.2.3 TEMPERATURE MEASUREMENT

The 4 thermocouple probes, that need to measure the CUD interior wall temperature, are fitted through 4 of the insert hole sealing flanges with a Swagelok pressure sealing fitting. These thermocouples are connected to a separate datalogger that records the vessel interior temperatures. The furnace and workpiece thermocouples are mineral insulated wire thermocouples, supplied by the furnace operator, and their ends are welded (fused) to the CUD exterior, on site.

One workpiece thermocouple is placed on the thickest part of the CUD (the block) and one on the thinnest part (the barrel). The difference indicates the maximum temperature variance through the heated workpiece. According to ASME VIII [9] the maximum allowed temperature variance throughout a vessel during heat treatment is 50 °C.

Another thermocouple needs to be placed on the fan shaft support pipe close to the V-belt pulley to measure the pipe temperature close to the ball bearing. The placement of this thermocouple can be seen in Figure 5.2.

Figure 5.2: The external thermocouple fused on the wall of the fan shaft support pipe protruding outside the furnace wall.

The furnace thermocouples are regularly calibrated by DCD Dorbyl. Calibration certificates for the vessel interior thermocouples were supplied by the vendor, see Appendix H.

5.2.4 EXPERIMENTAL DATA ACQUISITION

The internal temperatures are logged automatically with a digital datalogger. The furnace control and exterior workpiece thermocouples are scribed on an analogue recorder. The analogue recorder is regularly calibrated to comply with heat treatment standards. The rest of the data (the flow rates, fan speed, chamber pressure etc.) will need to be manually written down on a prepared template (see Appendix I) by the plant operators.

5.2.5 OPERATING DESCRIPTION DEVELOPMENT

As mentioned in section 3.7.2 the functional specification of a typical process plant is followed by the detail design and an operating description document[18]. The plant is constructed using piping and instrumentation drawings (see Appendix F) and isometric drawings. The end result of an operating description is a list of sequential activities that need to be followed by the plant operator or a computer in the case of automatic control.

The first step of writing the operating description is defining all the plant major functions and then the operating parameters that need to be controlled and monitored. The operating parameters are given high and low control limits to keep the process within operating limits. The alarms and interlocks are also identified. An operating description is a typical process engineering deliverable and is part of the design of any process (chemical) plant. The full operating description document is given in Appendix E. The sequential activities output of the operating description are used as the experimental procedure for this research.

An example of operating parameters and actions for plant equipment, as given in the operating description in Appendix E, is given in Table 5.1.

Table 5.1: The Gas Supply PFM Operating Parameters and Actions.

Description	Type	High/ Low	Value	Action
Pressure				
Indicating process chamber pressures	Pressure gauge PI001 (see P&ID Appendix F for tag numbers)	H	25 kPa	Operator to investigate. Check Exit Gas valve position and water level in water filled barrel
		HH	30 kPa	Stop gas supply. Investigate for overpressure and rectify
Flow rate				
Preparation mode				
Indicating ammonia flow rate through ammonia entrance pipe	Rotameter FI001	H	3200ℓ/hr	The flow rate of the supply gas line must be limited to this maximum rate during preparation to ensure a start-up crack ratio of 15 – 35%. See section 4.4.2 for flow rate calculations. Flow must be reduced to maintain 3000ℓ/hr
		L	2800ℓ/hr	Operator to increase flow rate to maintain 3000ℓ/hr
Indicating oxygen flow rate through ammonia entrance pipe	Rotameter FI002	H	220ℓ/hr	Reduce flow rate. The oxygen flow rate must be controlled at 200ℓ/hr for 2 hours during the preparation mode to ensure sufficient oxygen to start the ammonia cracking.

[18] Operating Description is typically the name given for this type of document within industry.

Description	Type	High/ Low	Value	Action
		L	180ℓ/hr	Increase flow rate to maintain 200ℓ/hr
Indicating nitrogen flow rate through ammonia entrance pipe	Rotameter FI003	H	2200ℓ/hr	Reduce flow rate. The nitrogen flow rate must be controlled at 2000ℓ/hr to ensure sufficient purging of the CUD vessel
		L	1800ℓ/hr	Increase flow rate to maintain 2000ℓ/hr
Heating mode				
Indicating ammonia flow rate through ammonia entrance pipe	Rotameter FI001	H	3200ℓ/hr	The flow rate of the supply gas line must be limited to this maximum rate during heating to ensure a start-up crack ratio of 15 – 35%. See section 4.4.2 for flow rate calculations. Flow must be reduced to maintain 3000ℓ/hr
		L	2800ℓ/hr	Operator to increase flow rate to maintain 3000ℓ/hr
Indicating oxygen flow rate through ammonia entrance pipe	Rotameter FI002	H	220ℓ/hr	Reduce flow rate. The oxygen flow rate must be controlled at 200ℓ/hr for 2 hours during the heating mode to ensure sufficient oxygen to start-up the ammonia cracking reaction
		L	180ℓ/hr	Increase flow rate to maintain 200ℓ/hr
Nitriding cycle mode				
Indicating ammonia flow rate through ammonia entrance pipe	Rotameter FI001	H	55ℓ/hr	The flow rate of the supply gas line must be limited to this rate at the start of the nitriding cycle. See section section 4.4.2. Flow must be reduced to maintain 50ℓ/hr .
		L	45ℓ/hr	Operator to increase flow rate to maintain 50ℓ/hr
Indicating ammonia flow rate through ammonia entrance pipe	Rotameter FI001	H	125ℓ/hr	The flow rate of the supply gas line must be limited to this rate once the furnace has reached 555°C. See section 2.7.2. Flow must be reduced to maintain 120ℓ/hr .
		L	115ℓ/hr	Operator to increase flow rate to maintain 120ℓ/hr .
Indicating ammonia flow rate through ammonia entrance pipe	Rotameter FI001	Interlock	* ± 5 ℓ/hr	The flow rate of the supply gas line must be controlled at this * rate during the 40 hr long nitriding cycle mode to ensure a crack ratio of 35-40%.
Crack ratio				
Indicating low ammonia dissociation rate	'Bunte Burette' AI001	L	10%	Decrease ammonia supply flow rate to increase nascent nitrogen residence time and concentration
Indicating high ammonia dissociation rate	'Bunte Burette' AI001	H	75%	Increase the ammonia supply flow rate to decrease the nascent nitrogen residence time
		HH	80%	Fully open the ammonia supply valve to ensure maximum ammonia supply and to reduce residence time

5.3. PLANT CONSTRUCTION

5.3.1 PROCUREMENT AND MANUFACTURING

The off the shelf equipment such as pipe fittings etc. were obtained from the vendors listed in Table 4.9. The specially manufactured equipment like the shaft and high temperature bearing required more interaction with the contractors. It was necessary to get dimension certificates etc. to ensure the shaft was machined within the required fits and tolerances.

The gas was supplied by Afrox and Afrox personnel installed the pressure regulator and gas cylinder manifold equipment. As listed in Table 4.10 DCD Dorbyl would supply most of the services including the supply and control of the gas fired furnace. Due to the possible dangers of the process DCD Dorbyl management decided to move the sandbank of the furnace outside the fabrication plant, where the top hat furnace is normally used for heat treatment. This would prevent possible disturbance to employees working in the fabrication plant. A general arrangement drawing of the plant layout, as approved for construction, is given in Appendix G.

5.3.2 OVERVIEW OF NP CONSTRUCTION PROCESS

The following activities need to be performed in the given order:

1. The top hat of the furnace is lifted up with the overhead crane and put down outside the fabrication plant next to the new sand bank.
2. All oils are removed from the CUD inner surface. Oils are removed with solvents and then washed out with water. A UV light is used to confirm that all the oil is removed.
3. The insert sealing flanges of the CUD are fitted together with the nitrided layer thickness specimens. The CUD is bolted to the cradle.
4. The CUD is then lifted and moved with the overhead crane and put down on top of the sand. A protective cover is placed over the weld neck flange hole.
5. The CUD is then manoeuvred and positioned with the cradle such that the top hat furnace will fit over the CUD correctly. The cradle is planted in the sand.
6. The weld neck sealing flange with welded fan shaft bearing housing is fitted to the CUD.
7. Make the hole in the wall of the top hat for the fan shaft to protrude through.
8. In parallel with the CUD sealing tasks construction of the gas supply and exit piping systems can already be started.
9. The pipes and cables are then put underneath the sand where the sides of the top hat would be when it is lowered.
10. The thermocouple wires and gas pipes are then connected respectively to the appropriate data loggers, valves and gas cylinder manifolds.
11. If required a plate must be fitted to prevent flame impingement from the furnace burners.
12. After all the thermocouples and gas pipes have been checked for proper functioning, the top hat can be lowered on top of the CUD.
13. The cover plate (insulation wool) for the hole in the side of the top hat, where the fan shaft assembly protrudes through, is fitted to the side of the furnace.
14. The V-belt pulley is fitted to the fan shaft and the V- belt and motor are fitted.

5.3.3 CONSTRUCTION SCHEDULE

Once all the equipment had been purchased the actual plant construction commenced. A detailed schedule had been set up to define the tasks and the resources required to finish the plant in time. The plant construction schedule can be viewed in Appendix K.

5.3.4 REPORT OF THE CONSTRUCTION PROCESS

After final machining the CUD was ready for nitriding. First of all the oils used for machining were removed by degreasing agents (the cleaning agent can't be flammable). The degreasing would also aid in giving the surface layer a thin rust layer that would be beneficial for nitriding [10]. The CUD preparation was done inside the machining shop at DCD Dorbyl to prevent unnecessary dust from entering the cleaned vessel interior while fitting the sealing flanges. Photos of the CUD preparation process can be seen in Figure 5.3.a) to d). Note that copper compound was used on the bolts to ensure the bolts could be easily removed afterwards.

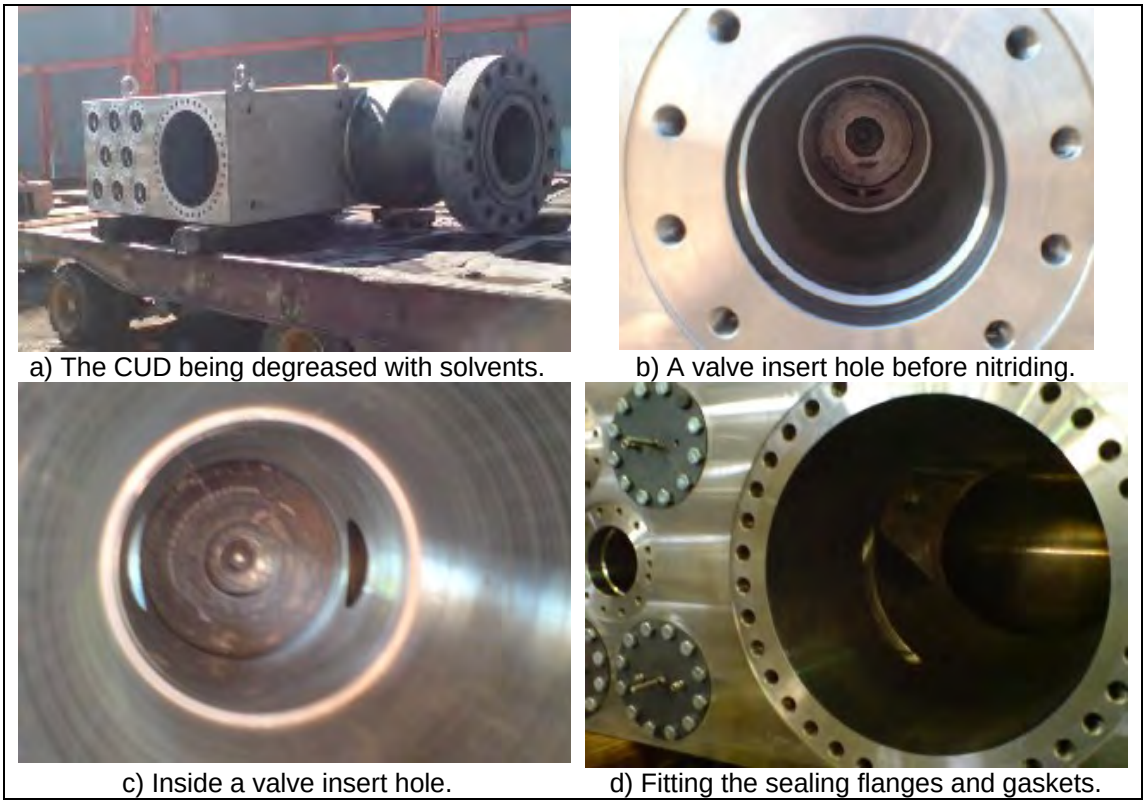

a) The CUD being degreased with solvents.
b) A valve insert hole before nitriding.
c) Inside a valve insert hole.
d) Fitting the sealing flanges and gaskets.

Figure 5.3: Pictures of preparing the CUD for nitriding.

In parallel with the CUD preparation process the plant site was prepared. The furnace was brought out of the fabrication shop and put next to the new sand bank for outdoor use. The SASOL gas line that supplies the gas fired burners of the furnace, as well as the electrical and control equipment, were moved and reconnected. Pictures of the furnace preparation are given shown by Figure 5.4.

a) Moving the furnace outside the fabrication plant.

b) Photo of the inside of the furnace taken from underneath.

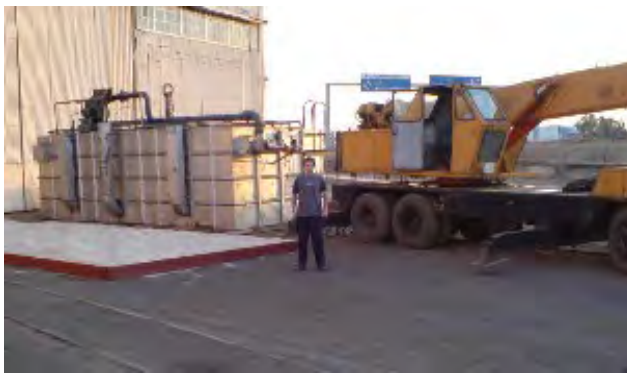

c) The furnace and mobile crane next to the new sandbank.

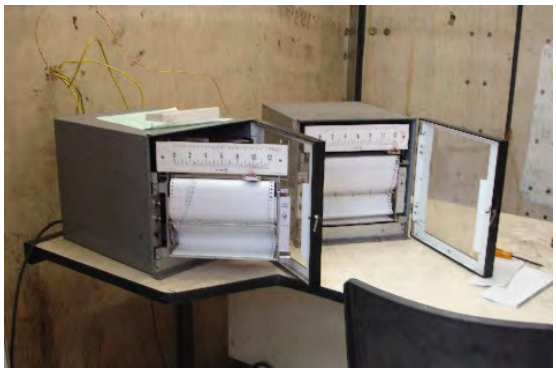

d) Furnace control booth and external thermocouple measurement logger.

Figure 5.4: Preparing the furnace for the nitriding plant.

While the CUD was being prepared in the machining shop construction of the main plant piping could already be started. The gas cylinders were installed on a manifold and tested for safety by Afrox personnel. Next the Gas Exit water drum was prepared by welding two empty standard 200 l oil drums together and burying it in the ground. Constructing the gas piping system with the stainless steel Swagelok tubing required use of tools like a pipe bender and pipe cutter. Piping could only be done up to a certain point until the CUD had been placed in its final position in the sand. Piping was started from the gas cylinders and the water drum respectively.

During preparation of the CUD a few problems were experienced with the fan shaft assembly as it did not rotate smoothly at the graphite bearing side, at room temperature. It was anticipated that the manufacturing tolerance of parallel bearing surfaces was not met. The machinist might have welded the solid shaft ends to the hollow shaft after final machining; despite the instruction on the detail drawing that final machining must be done after welding. The shaft was thus out of straight (“banana” shape). After the shaft was remachined in the machining shop at DCD Dorbyl the assembly was locked by fixing the circlips and fan hub end bolt for axial location. The lesson learned is that the shaft machining must be double checked before acceptance. Pictures of the plant piping and nitriding furnace PFM construction can be seen in Figure 5.5 a) to f).

a) Gas piping being installed underneath the sand to enter the furnace.

b) Heat treatment witness pieces next to the CUD. Note the furnace thermocouples fused onto the exterior of the CUD and witness pieces.

c) The weld neck flange gasket prepared before installation of the fan shaft assembly sealing flange.

d) The Gas Supply PFM as constructed.

e) The fan shaft support pipe being handled in the machine shop.

f) The ammonia gas cylinders connected with a common manifold and pressure regulator.

Figure 5.5: Construction of the gas piping system and other assemblies.

Due to the extra time used for the fan shaft assembly, the CUD was fitted to the cradle in the machine shop, and put on the sand, without the weld neck sealing flange. The fan shaft assembly was then fitted on the sand afterwards, as shown in Figure 5.5.c). This way there was no need to wait while the fan assembly was repaired. Next the rest of the piping could be finished with the CUD in its final position.

The Gas Exit PFM control station is seen on the right in Figure 5.6. The CUD on the cradle can also be seen in Figure 5.6 with the gas supply PFM in the background.

Figure 5.6: A landscape photo of the plant before the Top Hat was lowered over the CUD.

A photo of the nitriding Furnace PFM with the 9 gas exit pipes and CUD interior thermocouples is given by Figure 5.7.

Figure 5.7: The Nitriding Furnace PFM before the Top Hat is lowered.

Note the CUD block with 9 gas exit pipes and thermocouple penetrations in Figure 5.8. The interior thermocouple probes were bent to touch the vessel interior walls before the Swagelok penetration fittings were tightened to form a gas tight seal. Next the gas pipe penetrations and the sealing flange bolts were torqued. A leak test was performed by opening the nitrogen supply valve and putting the process chamber under pressure.

Figure 5.8: CUD block with nine gas exit penetrations and 4 thermocouple penetrations.

Other checks listed in section 5.4.4.4, including fan shaft rotation, were performed. After all checks were passed the furnace was put over the CUD, as shown by Figure 5.9 a) to d).

a) Top Hat lifted by the mobile crane.

b) Top Hat put in position over the CUD.

c) Top Hat being carefully lowered, note the opening for the fan shaft pipe.

d) Photo of the CUD inside the furnace just before the furnace touches the sand.

Figure 5.9: Photos of the Top Hat furnace being lowered over the Nitriding furnace PFM.

The plant was now ready for operation and nitriding could start the following day. The first step would be purging the vessel with nitrogen, see paragraph 5.4.4. Note the Gas Supply PFM Control station with valves and flowmeters installed in Figure 5.10 below.

Figure 5.10: The Gas Supply PFM Control station.

5.4. EXPERIMENTAL PROCEDURE

5.4.1 INTRODUCTION

As stated in paragraph 5.2.5 the sequential activities are the output of the operating description. The sequential activities (experimental procedure), of all three PFM's of this manually operated plant, are discussed in section 5.4.4. Only the tasks of crack ratio measurement and balancing of the flow rates are discussed separately, since these are performed more than once. For the tag numbers of the instruments and other equipment refer to the piping and instrumentation diagram in Appendix F.

5.4.2 CRACK RATIO MEASUREMENT

The ammonia dissociation (crack ratio) must be frequently measured throughout the nitriding cycle. To measure the crack ratio the following actions must be performed in sequential order:

1. The valve to the 'Bunte Burette', HV-004, must be opened
2. Open the 'Burette' glass exit valve for the gas in the 'Burette' to exit.
3. Close the isolation valve to the water barrel, HV-005.
4. Purge the air through the 'Burette' for 1-2 minutes untill the entire atmosphere of the 'Burette' is replaced with the gas from the process chamber.
5. Open the isolation valve to the water barrel, HV-005.
6. Close the isolation valve to the 'Burette', HV-004.
7. Close the 'Burette' glass exit valve to keep the gas in the 'Burette'.
8. Open the 'Burette' water valve to release the water into the 'Burette' and dissolve the undissociated ammonia.
9. Once the water flow has stopped, measure the water level/ the dissociation rate. (It is read off the water level markings of the 'Burette', water level is from 0% dissociation at

the top to 100% at the bottom).

10. Record the crack ratio measurement.
11. Dispose of the water in the 'Burette' to prepare for the next measurement.
12. The crack ratio measurement is fed back to the Gas Supply PFM to control the ammonia supply gas flow. If the crack ratio is too high the ammonia supply must be reduced and vice versa, see the look-up table i.e. Table 5.2.

Table 5.2: Look-up Table for adjusting the ammonia flow rate from crack ratio.

Crack Ratio	Action (change in ammonia supply flow rate)
10% (L)	Decrease ammonia supply flow rate substantially to increase residence time
10% - 35%	Slightly decrease flow rate
35% - 40%	Maintain existing flow rate
40% - 75%	Slightly increase flow rate
75.00% (H)	Increase flow rate substantially
80.00% (HH)	Fully open the ammonia supply valve to ensure maximum ammonia supply

5.4.3 BALANCING FLOW RATES

Note that the entering NH_3 gas flow rate is 3000 ℓ/hr at the start of the nitriding cycle to start the 'white layer' for nitrogen diffusion. When nitriding is started, little or no ammonia cracking will take place and the exiting gas flow will consist of mainly ammonia gas. If the exit flowmeter temperature is close to the entering gas flow temperature, the balance gas flow rate at the exit pipes will be 3000 ℓ/hr /9 = 333 ℓ/hr . However, when the crack ratio is higher (15-35 %) ammonia dissociation takes place and nitrogen is diffused into the metal surface. Mass will therefore not be conserved and the exit mass flow will be lower. The balancing mass flow will thus not be 333 ℓ/hr . It is thus best to balance the exit gas flow rates at the start of the nitriding cycle when no ammonia dissociation has taken place yet. Balancing is done by adjusting needle valves 01 to 12 on Valve Tree 1 and 2, see P&ID Appendix F.

5.4.4 NITRIDING PLANT SEQUENTIAL ACTIVITIES

A full operating manual of all three PFM's will follow in the paragraphs below. Since this is a manually operated plant the sequential activities of each PFM are not given separately but in a step by step chronological order. For valve and instrument tag numbers refer to the P&ID in Appendix F.

Four people are required to operate the plant at any given time: A Safety Officer, Furnace operator, Gas Supply System operator and Gas Exit System operator.

5.4.4.1 PLANT PREPARATION PROCESS DESCRIPTION

Before the Top hat furnace is lowered the following is done:

1. Ensure all oils were removed from the CUD inner surface and all parts in the process chamber. A UV light should have been used to check for remaining oil,
2. Check all the thermocouples for proper functioning
3. Check all gas pipes and valves for proper functioning.
4. Ensure that the hand operated flow valves and pressure regulators are working properly.
5. Check the seals for leaks by purging with Nitrogen and monitoring the pressure drop over time at the pressure gauge PI001. Do not pressurize the system over 20 kPa.
6. While the system is under pressure and at room temperature perform a soap test.
7. Test the fan for proper operation by switching it on and off.
8. Check that the nitride layer thickness test specimens and heat treatment witness samples are still in place.
9. The top hat can be lowered on top of the CUD.
10. Check the water level in the water barrel.
11. Proceed with the test for leak tightness at operating temperature

5.4.4.2 TEST FOR LEAK TIGHTNESS AT OPERATING TEMPERATURE

1. All hand valves must be open except HV-001, HV-002 and HV-003 (NH_3, O_2 and N_2 supply line isolation valves), which must be closed.
2. Heat the process chamber to the maximum operating temperature of 555 °C.
3. Set the furnace on coasting.
4. Close the isolation valve to the water barrel, HV-005, and the valve to the 'Bunte Burette', HV-004.
5. Open and set the N_2 pressure regulator, PCV003 to an outlet pressure of 20 kPa
6. Pressurize the process chamber by fully opening HV-003 until the pressure gauge, PI001 gives a reading of 20 kPa.
7. Close HV-003
8. Check for leaks by checking on the pressure gauge PI001 if the pressure falls over a time of 30 minutes.
9. Note the pressure after 30 minutes on PI001 and calculate the pressure decrease over time.
10. Turn off the furnace and allow the process chamber to cool down to 25 °C
11. If the Pressure decrease over time is less than 1 kPa/hr carry on with paragraph 5.4.4.3

5.4.4.3 START OF THE NITRIDING PROCESS

The furnace operator must continuously monitor the furnace and CUD wall temperature readings in order to adjust the furnace temperature accordingly. A furnace operator with the necessary qualifications and training certificates is required. During furnace operation a safety officer must continuously ensure that there is no risk that any personnel will be subjected to

burns or any fire hazards. Personnel (operators) must also be positioned at the Gas Supply PFM and the Gas Exit PFM to perform manual control functions.

Before the Nitriding process is started the following needs to be done:

1. Recheck that all the thermocouples are calibrated and connected properly
2. Test the measurement output on the thermocouple datalogger display before starting the nitriding process.
3. Notify the furnace operator and the Gas Supply and Gas Exit controllers that the nitriding process is about to start.
4. Ensure that enough Ammonia, Nitrogen and Oxygen cylinders are connected to provide for the 40 hour long nitriding process.
5. Recheck that there are no leaks in the piping and that the hand operated flow valves and pressure regulators are working properly.
6. Ensure that there are no fire hazards (also keep a fire extinguisher close by), and that it is safe to start the nitriding process.

5.4.4.4 PREPARATION MODE

Purge with N_2 to ensure removal of air:

1. Give a signal to the Gas Supply operator that the process is about to start.
2. Ensure that the outlet pressure of the N_2 pressure regulator, PCV003 is still set at 20 kPa.
3. Close HV-004 (valve to the Bunte Burette)
4. Slightly open HV-003 (N_2 line isolation valve)
5. Check the flow rate on FI003 (N_2 line flowmeter)
6. If the flow rate is below 2000 ℓ/hr open HV-003 more until 2000 ℓ/hr is reached
7. If it is higher than 2000 ℓ/hr close HV-003 more until 2000 ℓ/hr is reached
8. If the flow rate of 2000 ℓ/hr can not be reached with HV-006 fully open increase the outlet pressure on the regulator PCV003
9. Keep the flow rate at 2000 ℓ/hr for 1 hour to fully replace the air in the vessel.
10. Once the flow rate is stabilised start the nitriding fan using the on/off switch.
11. Set the fan speed at 950 rpm by setting the frequency on the VSD controller, UAC001, at 50 Hz and keep it at this value throughout until the cycle completion mode.
12. During the purging process check whether bubbles are formed inside the water barrel to ensure that the correct overpressure is provided.
13. Close HV-003 before the ammonia flow is started.
14. Close PCV003

Note: If the vessel needs to be purged in 30 minutes, the flow can be set at 4000 ℓ/hr for 30 minutes. The operator of the Gas Exit PFM must frequently check whether the water level in

the water barrel is above the indicated level. If it is below the operator must fill the barrel with more water.

Start ammonia flow:

1. Ensure HV-002 (O_2 isolation valve) to HV-004 are closed, HV-005 must be open
2. Set the NH_3 pressure regulator, PCV001 outlet pressure to 20 kPa
3. Open HV-001 (the isolation valve on the NH_3 line)
4. Slightly open HV-006 (needle valve on the NH_3 line)
5. Check the flow rate on FI001 (flowmeter on the NH_3 line
6. If the flow rate is below 3000 ℓ/hr open HV-006 more until 3000 ℓ/hr is reached
7. If it is higher than 3000 ℓ/hr close HV-006 more until 3000 ℓ/hr is reached
8. If the flow rate of 3000 ℓ/hr can not be reached with HV-006 fully open increase the outlet pressure on the regulator PCV001
9. Keep the flow rate at 3000 ℓ/hr as described until the nitriding mode is entered.
10. Balance the flow rates on the 9 exit pipes as described in par. 5.4.3. Balancing is done by adjusting needle valves 01 to 12 on Valve Tree1 and Valve Tree 2, and checking the flow rates on FI004 to FI012 (exit flowmeters).
11. Heat the furnace to ±200 °C, the furnace can now be put on hold.
12. Ensure that TE 001 to TE004 (CUD interior thermocouples) measure an average of 200°C. If not adjust the burners accordingly.
13. Monitor and record the temperature readings of TE001 to TE007.

Start oxygen flow:

1. Ensure HV-003 and HV-004 are closed,
2. Set the O_2 pressure regulator, PCV002 outlet pressure to 20 kPa
3. Slightly open HV-002 (the O_2 isolation valve)
4. Check the flow rate on FI002
5. If the flow rate is below 200 ℓ/hr open HV-002 more until 200 ℓ/hr is reached
6. If it is higher than 200 ℓ/hr close HV-002 more until 200 ℓ/hr is reached
7. If the flow rate of 200 ℓ/hr can not be reached with HV-002 fully open increase the outlet pressure on the regulator PCV002
8. Keep the flow rate at 200 ℓ/hr until the heating mode, par. 5.4.4.5, is entered.
9. Purge the mixture through while entering the heating mode.

5.4.4.5 HEATING TO 500 °C

6. Heat from 200 °C to 450 °C @ 56 °C/hr if possible while continuously monitoring all temperature readings on TE001 to TE007 (TE005 to TE007 are furnace thermocouples)

7. Soak the furnace at 450 °C for 1 hour
8. While soaking ensure that TE 001 to TE004 measure an average of 450 °C. If not adjust the temperature accordingly by adjusting the burners.
9. Monitor and record the temperature readings of TE001 to TE007 over time
10. After soaking close the O_2 - flow by closing HV-002
11. Close PCV002 (the CUD internal surface is now activated by the oxidisation and ready for nitriding)
12. Heat the process chamber to 500 °C @ 56 °C/hr if possible, while continuously monitoring all temperature readings on TE001 to TE007
13. Hold the furnace at 500 °C for 2 hours
14. While holding ensure that TE 001 to TE004 measure an average of 500 °C. If not adjust the temperature accordingly by adjusting the burners.
15. Monitor and record the temperature readings of TE001 to TE007 over time
16. Enter Nitriding mode

Note: The operator of the Gas Exit PFM must frequently check whether the water level in the water barrel is above the indicated level. If it is below that, the operator must fill the barrel with more water.

5.4.4.6 NITRIDING CYCLE MODE

Throughout the nitriding cycle continuously monitor the readings for furnace temperature and all the CUD exterior and interior wall temperatures.

1. Reduce NH3 flow to ±50 ℓ/hr by closing/adjusting HV-006 and checking on FI001
2. Measure the crack ratio using the 'Bunte Burette', AI001, according to the procedure explained in par. 5.4.2. Record the crack ratio measurements.
3. If the measured dissociation rate is not between 35% and 40% adjust the flow rate according to par. 5.4.2
4. Heat to 555 °C from 500 °C, @ 50 °C/hr if possible, while continuously monitoring all temperature readings on TE001 to TE007.
5. Increase NH_3 flow to ± 120 ℓ/hr by closing/adjusting HV-006 and checking on FI001
6. Measure the crack ratio using the 'Bunte Burette' according to the procedure explained in par. 5.4.2. Record the crack ratio measurements.
7. If the measured dissociation rate is not between 35 % and 40 % adjust the flow rate according to par. 5.4.2
8. Soak the furnace @ 555 °C for 40 hours.
9. As soon as soaking is started, measure and record the NH_3 dissociation on the outlet gas.
10. If the measured dissociation rate is not between 35% and 40% adjust the flow rate according to par. 5.4.2. It is expected that the NH_3 flow would need to be reduced to ± 20

ℓ/hr by closing/adjusting HV-006 and checking on FI001.

11. Measure and record NH_3 dissociation on outlet gas every 30 minutes.
12. If the measured dissociation rate is not between 35 % and 40 % adjust the flow rate according to par. 5.4.2
13. Frequently adjust the NH_3 flow until the right crack ratio is reached.
14. While soaking ensure that TE 001 to TE004 measure an average of 555 °C. If not adjust the temperature accordingly by adjusting the burners, see par. 5.4.2.
15. Monitor and record the temperature readings of TE001 to TE007 over time while soaking.
16. After 40 hours enter the Cycle Completion mode.

For completeness the procedure for measurement with the 'Burette' explained in par. 5.4.2 is summarised here:

1. Open the valve to the 'Bunte Burette' HV-004
2. Close valve HV-005 to the water barrel
3. Measure with the 'Burette' and note the crack ratio
4. The crack ratio measurement is fed back to the Gas Supply PFM to control the ammonia supply gas flow according to the look-up table, see Table 5.2.
5. Open HV-005
6. Close HV-004

Note: The operator of the Gas Exit PFM must frequently check whether the water level in the water barrel is above the indicated level. If it is below that, the operator must fill the barrel with more water.

5.4.4.7 CYCLE COMPLETION MODE

1. Reduce temperature down to 450 °C @ 20°C/hr if possible, while continuously monitoring all temperature readings.
2. Shut off the nitriding fan with the on/off switch.
3. Increase NH_3 gas flow to 600 ℓ/hr by opening/adjusting HV-006
4. Switch off furnace and allow to cool to 80ºC while maintaining NH_3 flow @ 600 ℓ//hr by continuously adjusting HV-006
5. Confirm that the furnace has cooled down to 80°C by reading TE005
6. Switch off NH_3 flow by closing PCV001
7. Fully close HV-006
8. Close HV-001

Purge with N_2 before opening:

1. Give a signal to the Gas Supply operator

2. Ensure that the outlet pressure of the N_2 pressure regulator, PCV003 is set at 20 kPa.
3. Ensure that HV-004, HV-002 and HV-001 are closed. HV-005 should be open.
4. Start to slightly open HV-003
5. Check the flow rate on FI003
6. If the flow rate is below 2000 ℓ/hr open HV-003 more until 2000 ℓ/hr is reached
7. If it is higher than 2000 ℓ/hr close HV-003 more until 2000 ℓ/hr is reached
8. If the flow rate of 2000 ℓ/hr can not be reached with HV-006 fully open increase the outlet pressure on the regulator PCV003
9. Keep the flow rate at 2000 ℓ/hr for 1 hour to fully replace the NH_3 in the vessel.
10. During the purging process check whether bubbles are formed inside the water barrel to ensure that the correct overpressure is provided.
11. Close HV-003 once the vessel has cooled down to 25 °C
12. Close PCV003
13. Immediately proceed to the Post Nitriding operation.

5.4.4.8 SHUT- DOWN PROCEDURE

A shutdown procedure must be followed in any of the following cases:

- The furnace needs to be shut down, as is the case when the furnace reaches a high high (HH control terminology see Table 5.1) temperature of 650°C.
- A power failure has occurred
- a Pressure regulator or any component malfunctions
- An uncontrolled overpressure was reached (HH of 30kPa)
- ammonia flow has stopped and can not be recovered

The shutdown procedure is not included in this report as it is unnecessary.

5.4.4.9 POST NITRIDING

After the nitriding process is completed and the furnace has cooled down to room temperature the following needs to be done:

1. The fan V- belt pulley assembly is removed and the motor and all electrical connections is disconnected and removed.
2. The top hat is lifted up and removed.
3. Valves 10 – 12 on Valve tree 2 of the Gas Exit system are opened to release any resident pressure (vapour/steam) that formed inside the process chamber to atmosphere.
4. Remove the insert sealing flanges to retrieve the nitride layer thickness test samples.
5. Operators/personnel must not put their heads inside the process chamber/insert holes of the CUD. There is a possibility of inhaling pure nitrogen.

6. Purge the CUD insert holes with compressed air to ensure enough atmospheric air has entered the process chamber/insert holes of the CUD.
7. Purge the CUD interior with compressed air before any person puts his head inside.
8. The water, containing the dissolved undissociated NH_3, must be disposed off. Care must be taken since the water may be corrosive.
9. The thermocouples can be calibrated again if necessary.
10. Print out and document the furnace and wall temperature readings.
11. Measure the Nitrided thickness optically and micro hardness.

5.5. PLANT OPERATION RESULTS

5.5.1 OBSERVATIONS DURING PLANT OPERATION

The plant was operated according to the experimental procedure previously discussed. Early in operation deviation from the expected operation was observed.

The first deviation from ideal behaviour is the actual heating rate that was observed. To prevent excessive thermal stresses/thermal shocks in the metal workpiece ASME VIII [9], recommends a maximum heating rate of 56 °C/hr[19]. The experimental procedure instructed the furnace operator to maintain this heating rate.

In practice a much smaller heating rate was obtained above 200 °C. This can be seen in Figure 5.16. The furnace workpiece thermocouples measure the temperature of the thickest and thinnest part respectively. Because the thicker metal has a larger thermal inertia and heats up much slower; the burners must be kept on hold frequently to allow the temperatures to catch up. If this is not done thermal distortion due to an excessive temperature difference will occur. The temperature difference limit set for operation is 20 °C. This graph and the furnace hold points will be discussed in more detail in section 5.5.2.

Once the furnace reached 450 °C oxygen flow was started and kept at 200 ℓ/hr for 2 hours. This ensured proper oxidation of the surface to be nitrided and to act as a catalyst for the nitriding process [30]. Note the oxygen and simultaneous ammonia supply flow readings in Figure 5.11.

Figure 5.11: Ammonia and oxygen flow during the heating mode of operation.

[19] This is stated in par. UCS-56 of the ASME code Section VIII Div.1 [9]

The second significant observation was that the ammonia dissociation rate is temperature dependent as stated in section 2.6.3. At a temperature of 500 °C, in preparation for the nitriding cycle, dissociation rates of 45 % were already measured. For an unchanged flow rate the dissociation rate increased (to more than 60 % which is too high) as the temperature was brought up to 555 °C. A problem was then encountered with the ammonia supply.

The cylinders were frozen in the early morning winter temperatures and could not provide the required flow rate of 3000 ℓ/hr. It was then decided to reduce the temperature to allow a smaller ammonia flowrate to be supplied and to reduce the crack ratio (dissociation rate). This proved to be successful although it might have had an effect on the nitriding depth. A photo of the frozen ammonia supply cylinders can be seen in Figure 5.12. The anhydrous ammonia cylinders supplied liquid ammonia at the low temperatures and it is believed that the diaphragm of the pressure regulator was also faulty and caused the problem.

Figure 5.12: The frozen gas cylinders that resulted in reduced ammonia supply flow.

The liquid ammonia could be seen at the gas exit flowmeters during operation in the cold early morning hours. From the start of the nitriding process it was noted that the flowrates of the nine gas exit flowmeters were fairly equal, see photos in Figure 5.13 d) and e).

Especially during stable temperature conditions during midday exit flow required little balancing. Only at random instances the flowrate through hole 9 of the CUD block (the spindle hole, see Table 5.3 for numbering scheme) seemed to drop and it might have been due to the nitriding fan turbulence.

a) Balancing flow rates on the Gas Exit control station valve manifold. Little adjustment was necessary.

b) A crack ratio measurement being made on the Bunte Burette.

c) The water filled drum (2 welded together) of the Gas Exit PFM, note the bubbles as the gases exit under the overpressure provided by 2m water depth.

d) Balanced flow rates on the gas exit flow meters.

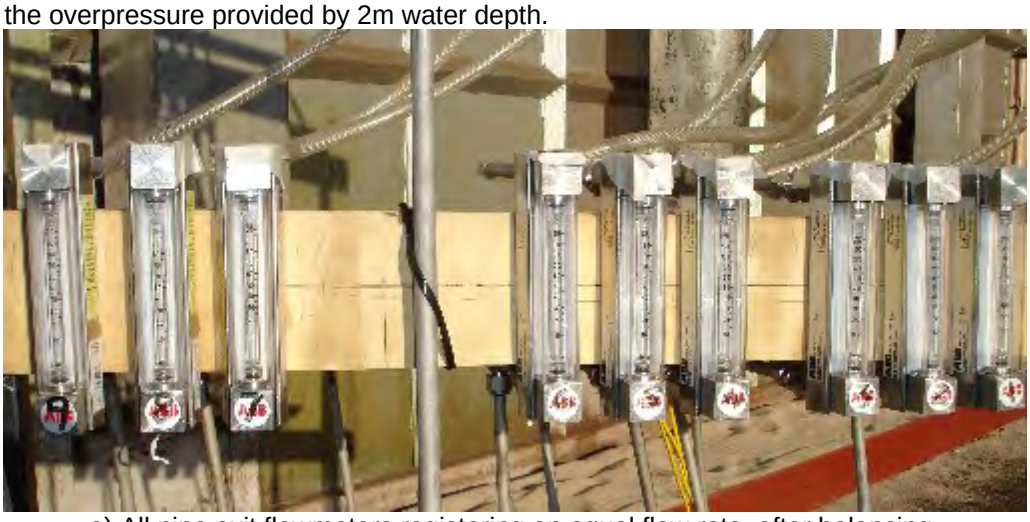

e) All nine exit flowmeters registering an equal flow rate, after balancing.

Figure 5.13: Operation of the Gas Exit PFM.

The nitriding fan was mostly kept rotating at about 800 rpm (corresponds to an electrical supply of 40 Hz with the VSD controller). It was noted that at larger rotation speeds of 1000 rpm the

high temperature bearing started leaking ammonia gas outside the furnace. The fan shaft protruding outside the furnace is shown in Figure 5.14.

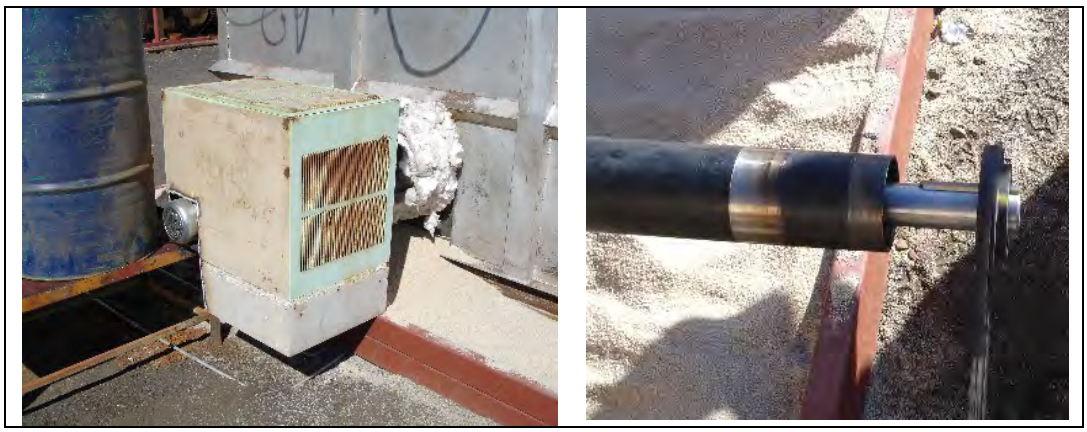

Figure 5.14: The motor and V-belt pulley safety cover to the left, see the uncovered driven pulley and ball bearing side of the shaft on the right.

The internal thermocouple datalogger was kept at the Gas Exit control station; note the yellow wires in Figure 5.15. Continuous monitoring of these temperatures took place in addition to taking frequent ammonia dissociation measurements. Also in Figure 5.15 note the funnel that was used at the top of the Gas Exit control station for pouring water into the 'Bunte Burette' during crack ratio measurement.

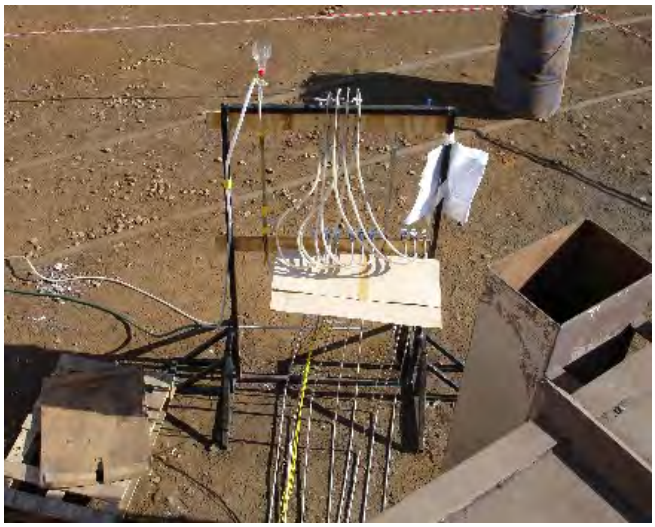

Figure 5.15: View of the Gas Exit PFM from the top of the furnace. Note the pipe leading to the water drum on the left.

During stable conditions (20 hours into nitriding cycle) the flexible hose tubes of the 9 individual exit tubes were removed and fitted to the 'Bunte Burette' one at a time in order to measure the crack ratio of each individual hole. It was done in such a manner as to not disturb the flow that would exist when all 9 tubes combine at the valve manifold to the same downstream pressure. For each tube's measurement it was fitted directly from the flowmeter to the 'Burette' inlet skipping the exit valve manifold. It was found that these measurements were more or less equal

to the measurement of all 9 tubes' flow combined, which was measured the majority of the time. It was thus proven that the stirring fan functioned efficiently and that all 9 insert holes of the CUD would be nitrided equally.

5.5.2 PLANT OPERATING DATA AND RESULTS

5.5.2.1 TEMPERATURE DATA

After plant operation the manually acquired data was captured in digital format and plotted.

The first graph of interest, Figure 5.16, shows the actual heating rate observed versus the ideal planned heating rate (the scrolls in Figure 5.4.d) were manually typed into a spreadsheet). From the graph it is clear that the CUD block temperature always lags that of the barrel and the weld neck flange. It is expected because the CUD block is much thicker than the barrel and has a larger local heat capacitance. At approximately 9 hours and 15 hours into operation it is clear that the burners were put on hold to allow the CUD block and barrel temperature to equalize.

It is also shown in Figure 5.16 that for the first operation mode the CUD block temperature followed the ideal control heating rate of 56 °C/hr closely. After about 6 hours of operation the heating rate reduced significantly (to below 25 °C/hr) since the burners were kept on hold to allow the barrel and block temperatures to catch up.

The actual nitriding cycle, with the furnace at 555 °C was performed for 40 hrs as planned. However, the temperature was reduced to 520 °C after 8 hrs of nitriding in order to reduce ammonia dissociation with the reduced ammonia supply capability in the cold winter morning. The temperature reduction can be seen on the graph at approximately 30 hours of operation and this allowed a smaller ammonia supply flow rate.

In Figure 5.17 the CUD interior temperatures are plotted along with the CUD block and furnace ambient temperatures. It can be noted that the CUD hole temperatures closely followed the externally measured CUD block temperature, however the inner surface also lags the temperature of the block. The reason for this is probably that the CUD is heated from the outside in-wards and thus the interior surface temperatures of the block lag that of the exterior. It is also possible that these thermocouples do not have good thermal contact with the block surface. It then measures the gas temperature that might initially be colder than that of the metal.

The shaft pipe surface temperature is low throughout the process. The highest temperature it reaches is 46 °C. The accuracy of this measurement will be discussed later.

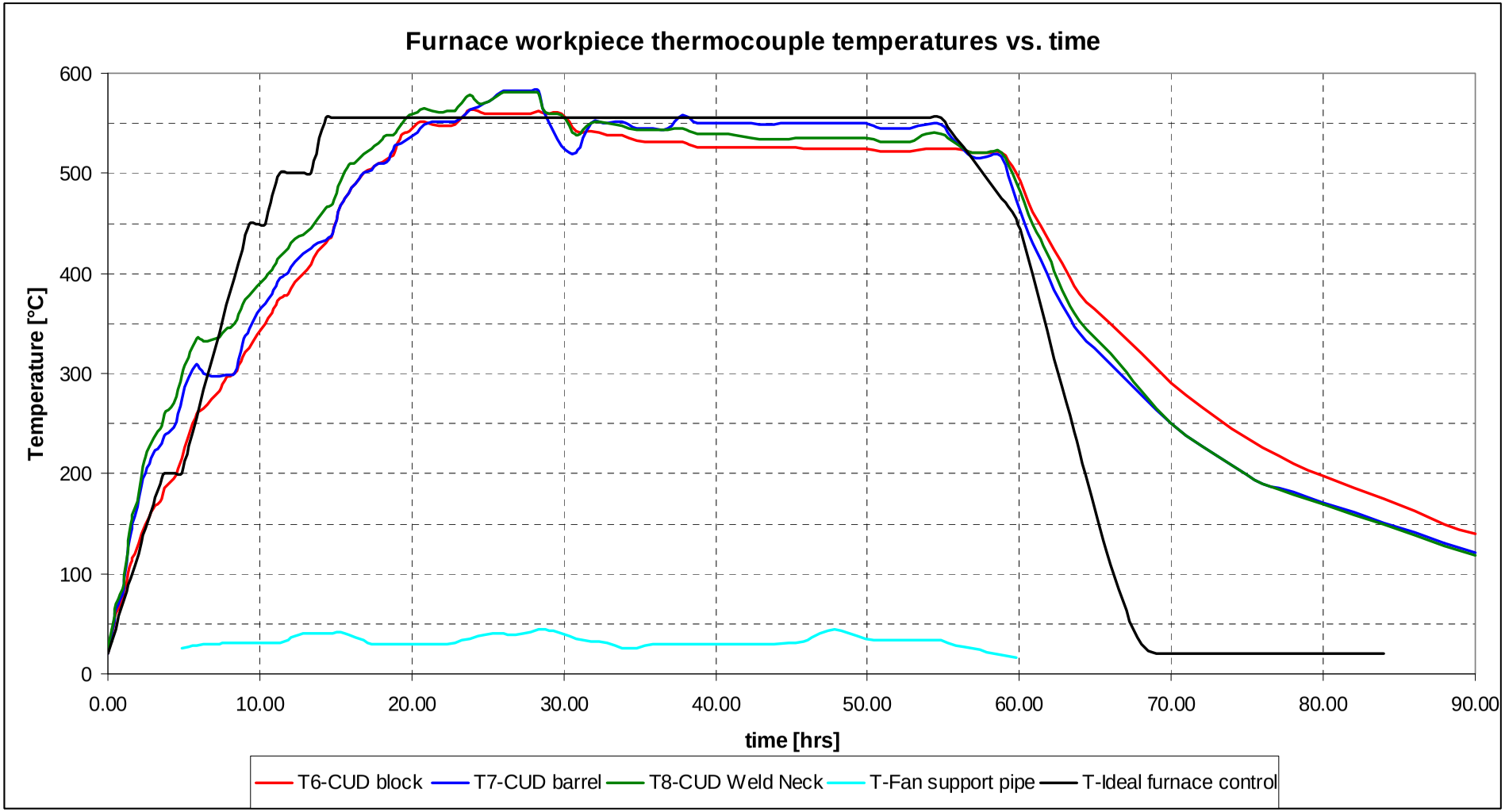

Figure 5.16: Temperature vs. time graph from the furnace control thermocouple readings.

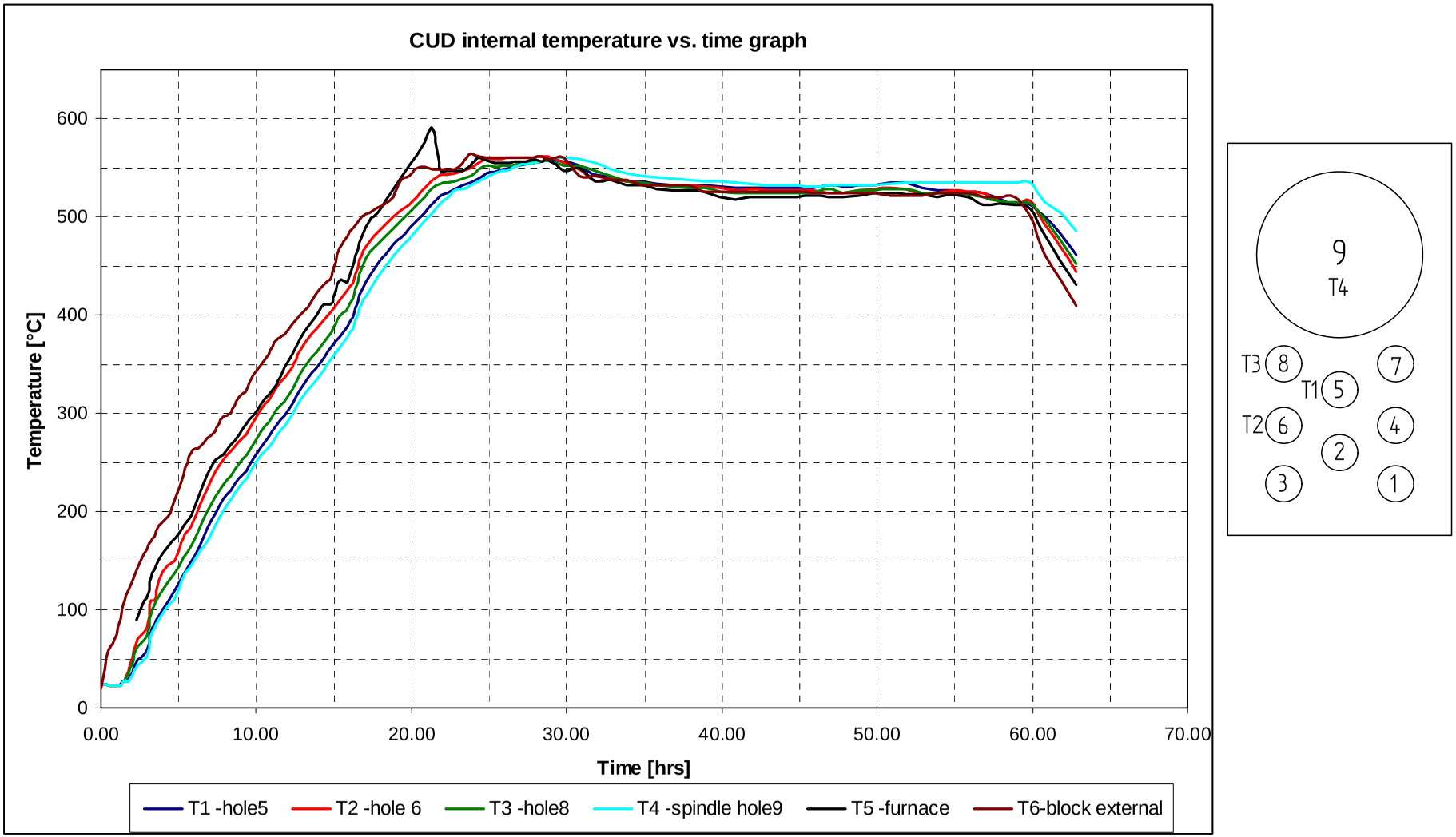

Figure 5.17: CUD internal temperatures vs. time, note the legend for the hole numbers to the right.

5.5.2.2 MEASURED FLOW AND CRACK RATIO

A graph of the measured flow rates over time and the process chamber pressure is given in Figure 5.18. It is shown that the chamber pressure increased proportionally with the ammonia supply flow rate. During operation there were times when the water drum level was lowered to accomodate smaller supply flow rates; pressure is pre-dominantly dependent on water level. However it is clear that at larger supply flow rates; the chamber inlet pressure is higher and flow losses in the process chamber are larger for the same back pressure provided by the water. At 40 – 50 hrs the water level was decreased and a lower inlet pressure resulted.

At instances of increased flow the chamber pressure was above 25 kPa. This means that flow losses of about 5 kPa (subtracting the 20 kPa back pressure) are in order. Just to confirm the back pressure for a standard water density of 998 kg/m^3 [50] and a 2 m water level is:

$$dP = \rho gh = (998)(9.81)(2) = 19.6 \text{ kPa (gauge)} \qquad [36]$$

From Figure 5.18 it can be seen that at 35 hours and at an ammonia supply flow rate of 3200 ℓ/hr the pressure reached a peak of 27 kPa. Keeping in mind that the pressure gauge is installed after the flowmeter on the nitrogen line it is clear that the flow losses from the CUD interior to the water drum are 27 – 19.6 = 7.4 kPa. Nonetheless the process chamber was always kept at an overpressure to ensure that no air could enter the chamber during operation.

It is shown in Figure 5.18 that the exiting flow rates are close to the supply flow rate divided by 9 and that the flow rate through each of the 9 insert holes are more or less equal. Between 8 and 15 hours, during oxygen supply, the exit gas flow through all 9 insert holes was 350 ℓ/hr. At 34 hours, during the nitriding cycle, a peak of 333 ℓ/hr through all 9 insert holes was observed, a small drop in the flow of F010 (hole 3 according to Table 5.3) was observed. A reduced balanced exit flow of 100 ℓ/hr was observed for the reduced NH_3 supply flow of 1050 ℓ/hr.

Table 5.3: CUD block hole numbering scheme used for flowmeters and thermocouples.

Flowmeter #	CUD block hole#	CUD Block Drawing
FI004	9	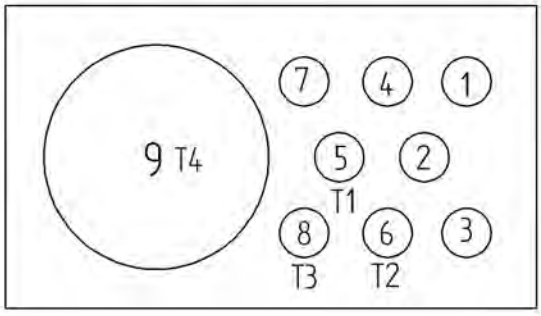
FI005	8	
FI006	7	
FI007	6	
FI008	5	
FI009	4	
FI010	3	
FI011	2	
FI012	1	

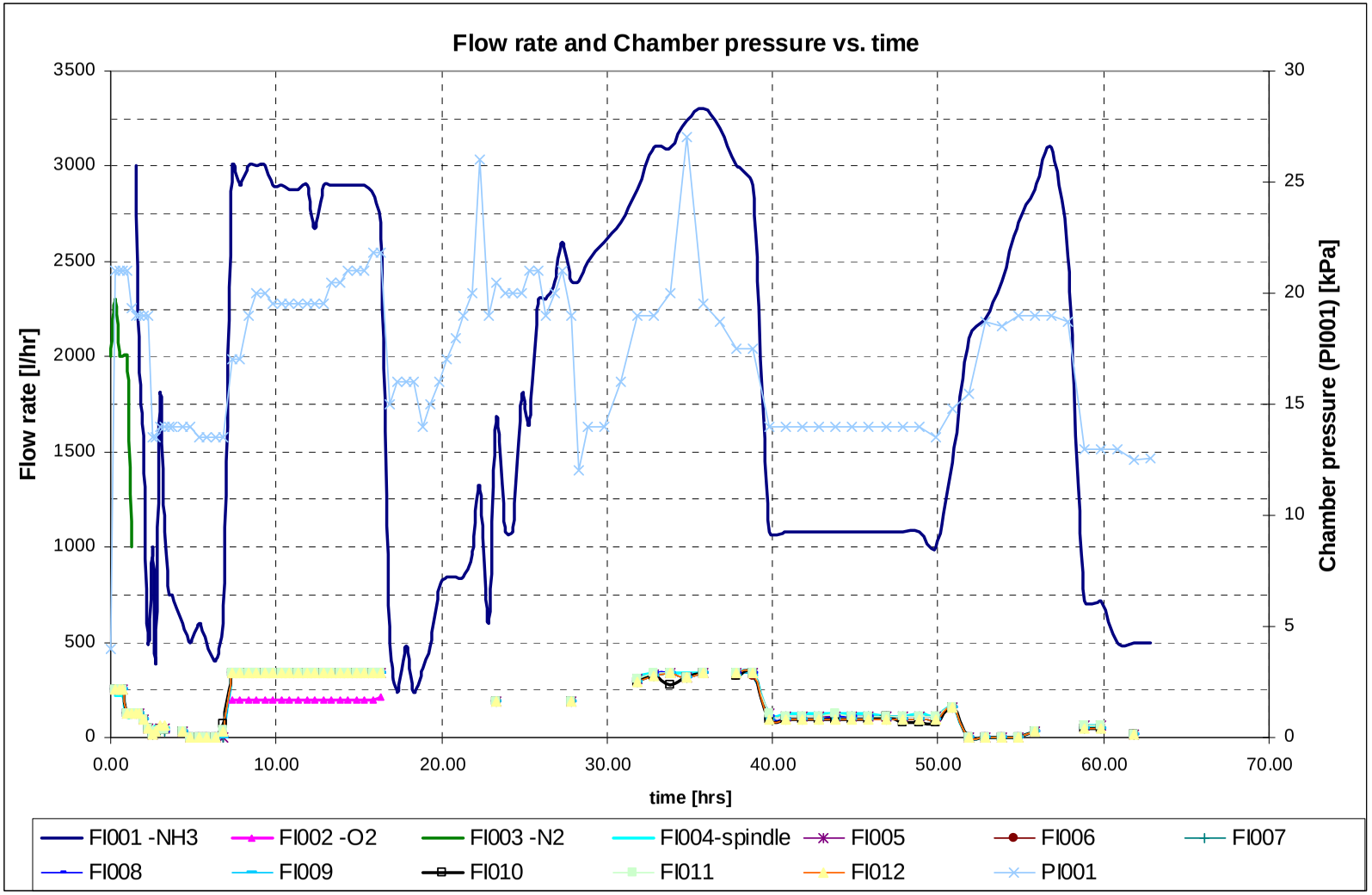

Figure 5.18: Measured flow rates vs. Pressure.

The crack ratio was measured at least every 30 minutes to continuously adjust the flow rate in accordance with Table 5.2. A graph of the crack ratio and flow rates over time is given by Figure 5.19. This graph shows that the crack ratio and ammonia supply flow rates are inversely proportional [10]. The graph of crack ratio and internal surface temperatures over time, given by Figure 5.20, shows an overall trend of a lower crack ratio at the lower surface temperatures.

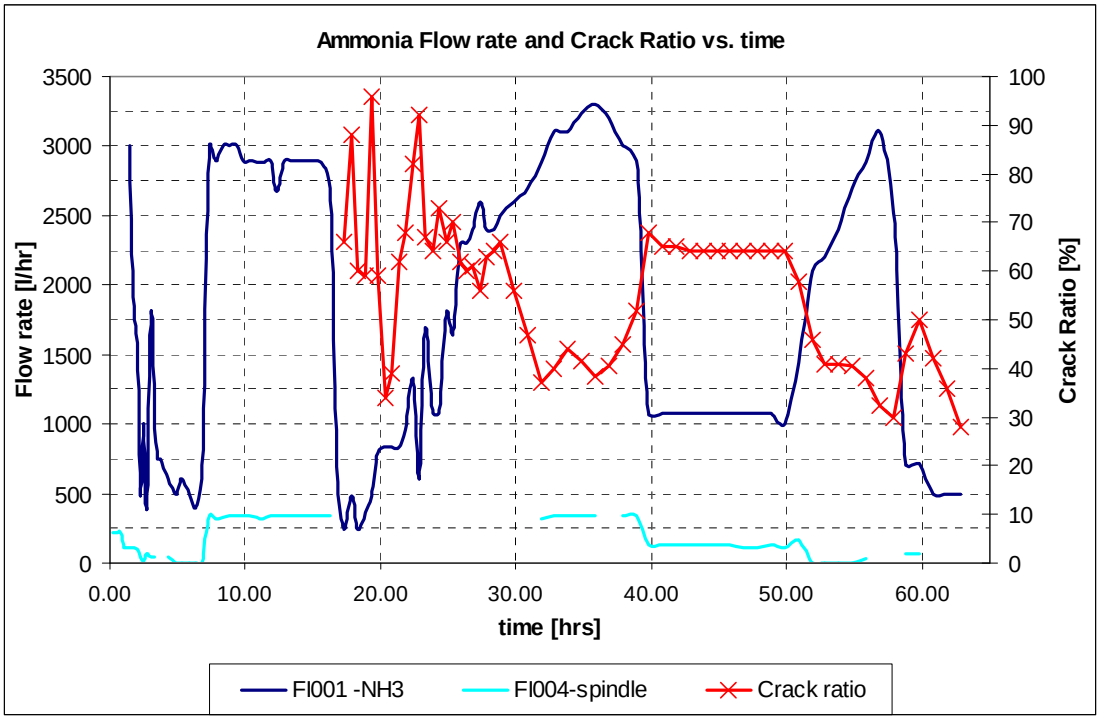

Figure 5.19: Graph of Ammonia flow rate and Crack ratio vs. time.

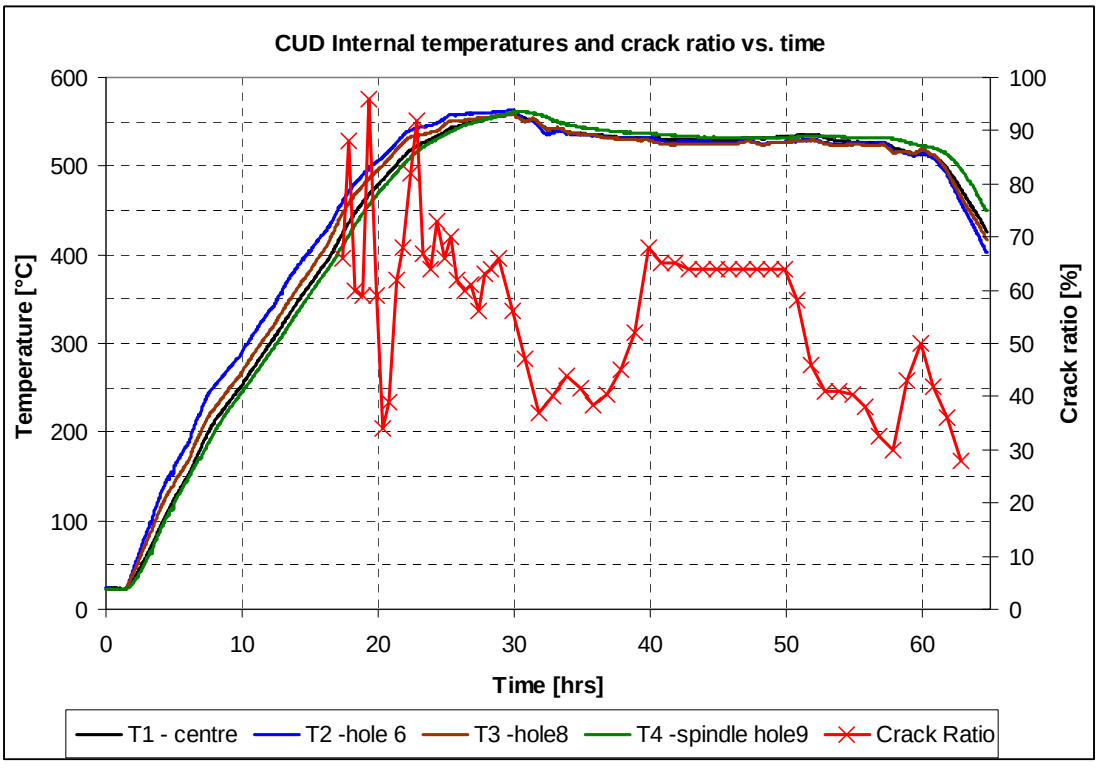

Figure 5.20: Graph of CUD interior temperature and crack ratio vs time.

The graphs of Figure 5.19 and Figure 5.20 combined shows that, for the stable supply flow rate and inetrnal temperature of 520 °C, between 40 and 50 hours the measured crack ratio was also constant. Even though the interior only reached the right temperature at 23 hrs, crack ratios of 64% were already measured before that. The graphs of Figure 5.19 and Figure 5.20 will be further interpreted in chapter 6.

5.5.3 POST NITRIDING TASKS

Two days after the furnace had cooled down the Top Hat was removed. After removal it could be seen that the CUD exterior surface had been severely oxidized and rusted in the furnace, see pictures in Figure 5.21.a) and b). After the plant had been decommissioned and disassembled the CUD surface was first sandblasted before the sealing flanges were removed. Photos of the interior surfaces of the CUD after nitriding can be seen in Figure 5.21.c) and d). It is clear that the surface now has a silver coloured matt sheen as opposed to the shiney metal surface that was evident before nitriding (see Figure 5.3).

a) The rusted CUD exterior surface with the furnace removed 2 days after cooldown.

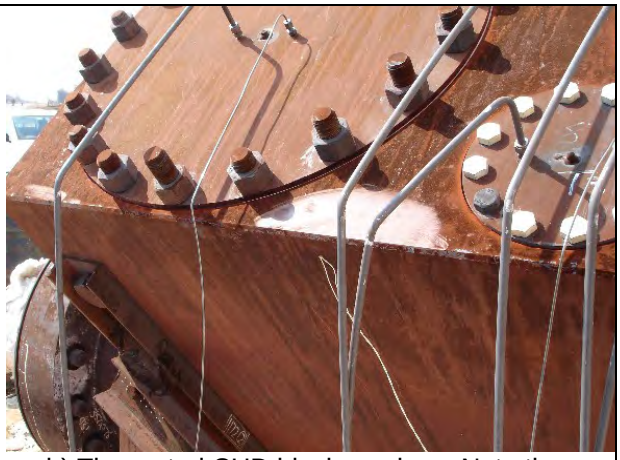

b) The rusted CUD block up close. Note the whitened workpiece thermocouple on the side.

c) The interior surface of the CUD barrel after nitriding.

d) Interior surface of the spindle hole after nitriding.

Figure 5.21: Pictures of the CUD after nitriding and after sandblasting.

When removing the flange seals of the valve insert holes from the CUD block it was noted that the ceramic paper gaskets lost its structural stability and completely disintegrated. The gasket

material that was used is called Thermoceram (Klinger), a ceramic fibre paper. The material certificate of conformance states that the melting temperature of the gaskets is 1760 °C at 3% gasket shrinkage. It was found that although these seals do not melt at 600 °C it loses its structure. Graphite gaskets would definitely work better for future nitriding exercises, although it might be difficult to remove from sealing surfaces afterwards. The sealing surfaces and nitrided valve insert holes can be seen in Figure 5.22.

Figure 5.22: The CUD block face after nitriding with the Klinger seals removed.

It was also observed that various other parts that were not intended for nitriding were indeed nitrided. These include the inner surfaces of the sealing flanges as well as the fan and fan shaft, see Figure 5.23.

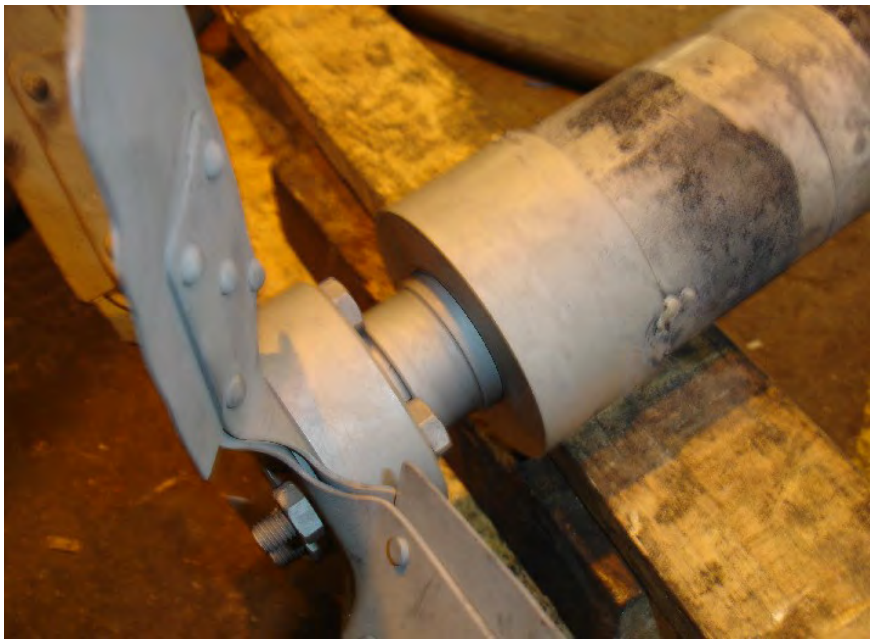

Figure 5.23: The stirring fan after nitriding, although commercial mild steel is not a nitridable steel it is clear that the fan had been nitrided to an extent.

5.6. CONCLUSION

The objective of this chapter was to design and build an experimental setup to demonstrate the nitriding plant design. A list of design requirements were set up and the plant design was used as an experimental model with minor modifications for the experimental setup.

Construction of the plant introduced some challenges. Fan shaft assembly problems had to be addressed on site. The ammonia supply flow was also too low due to low winter ambient temperatures. Gas cylinder heating blankets can be used in future to ensure a constant furnace temperature of 555 °C instead of 520 °C.

Nitriding was performed according to plan and the nitriding cycle was performed for a full 40 hours. The manual data acquisition proved to be cumbersome although effective. However, the advantages of an expensive automatic nitriding control system were easily identified during operation. Still human control was essential to solve problems caused by the low ambient and gas cylinder temperatures. During stable conditions and higher ambient temperatures the predicted required ammonia flow rate of 3000 ℓ/hr was sufficient for maintaining a crack ratio of below 40%. The theory of increasing flow rate to reduce reaction residence time (and crack ratio) [10] was clearly illustrated with this plant.

Nonetheless the nitriding operation still proved to be a success (provided nitriding sample test results are acceptable) and the lessons learned through the prototype plant can be put to good use for future nitriding operations.

Now the experimental results can be compared to the modelled expected results to validate the developed design.

Chapter 6: Verification and Validation

6.1. INTRODUCTION

The purpose of Chapter 5 is to prove that the developed plant design is valid and verified. The NP validation will determine whether the correct physical models were considered for design analyses, and to prove the concept. Furhermore, design assumptions are validated by testing the experimental model. The verification process is done to determine if the correct design input parameters were used and whether the resulting nitrided layer is deep and hard enough.

In Computational Fluid Dynamics (CFD) the term validation refers to whether the correct physics were modelled to simulate reality i.e. whether the correct turbulence model was used [54]. The term verification in CFD refers to how accurately the problem was solved [54] with regard to aspects such as whether the solution converged, and if the mesh was fine enough.

The validity of the plant design as a whole and of detail components will be proven. The fan shaft design concept is investigated first. For example, it is determined whether the high temperature bearing functions properly, and if the shaft protruding out of the furnace is cold enough. To verify the design, the measured temperature at the ball bearing side is compared to the predicted temperature. The structural strength of the fan shaft assembly is also validated, as there was not enough time for detailed structural analyses before plant construction.

To verify and validate the plant design as a whole, the measured and predicted ammonia dissociation rates for certain flow rates are compared. The measured furnace temperature results are also validated. The most important verification of the plant will be the nitriding specimen hardness and layer thickness tests. These tests are the end product of this research and are part of the metallurgical engineering discipline.

6.2. MEASURED AND PREDICTED FAN SHAFT TEMPERATURE

6.2.1 INITIAL FEA MODEL

The Nitriding fan shaft assembly was exposed to temperatures up to 560 °C inside the nitriding furnace. Before plant construction the temperature of the 500 mm long end that protrudes outside of the furnace was determined. The rolling element bearing on this side (the protruding end) cannot be exposed to temperatures above 120 °C. During the detail design a scoping FEA model was created to predict the surface temperature at this location. The exterior pipe surface temperature was also physically measured, during plant operation, to confirm this analysis.

Assumptions:

- Assume the entire fan shaft assembly temperature inside the furnace is at 555 °C.
- Assume an environmental temperature of 25 °C.
- Assume a constant heat transfer coefficient of 5 W/m^{2}K on the external and internal pipe surface of the 500 mm long end protruding outside the furnace.

The fan shaft was modelled with Strand 7 FEA software [51]. Its steady state heat solver was used. The initial model was built with 3D brick elements (see Figure 6.1). For the first analysis only the fan shaft support pipe (bearing housing) was modelled. This analysis was done during the detail design of the shaft and the results are repeated here to compare them to experimental measurements.

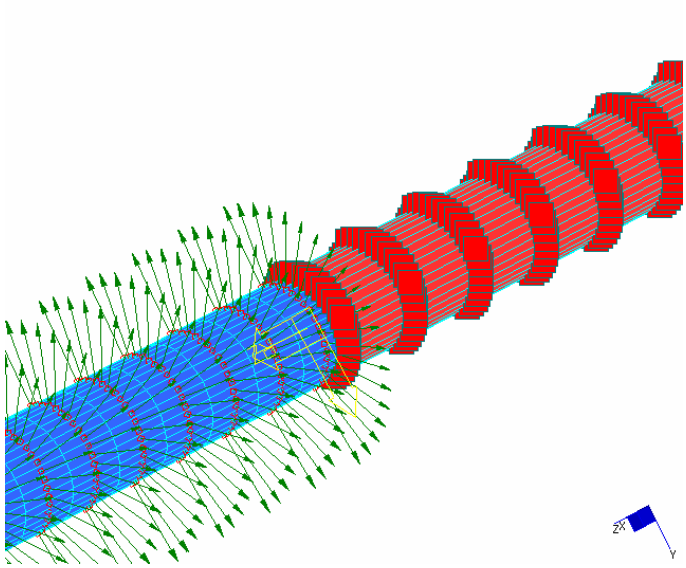

Figure 6.1: FEA model of the exterior fan shaft pipe; arrows to the left indicate the heat transfer coefficient and a constant temperature of 555 °C is applied to the right.

The heat transfer properties that were used for the fan shaft steel are listed in Table 6.1.

Table 6.1: List of properties for the shaft steel that was used in the FEA model.

Property	Value
density [48]	7850 kg/m^3
thermal conductivity [48]	15 W/mK
specific heat capacity [48]	500 J/kgK
modulus of elasticity [43]	200 GPa

Initial model Results:

The results of the first analysis are given in Figure 6.2. For this analysis it was assumed that convection, to 25 °C, takes place on the inside and outside of the pipe. The heat from the inner shaft is neglected because of a high heat transfer coefficient inside the support pipe during shaft

rotation. As shown by Figure 6.2 the pipe cools down quickly and temperatures at the bearing location are below 70 °C.

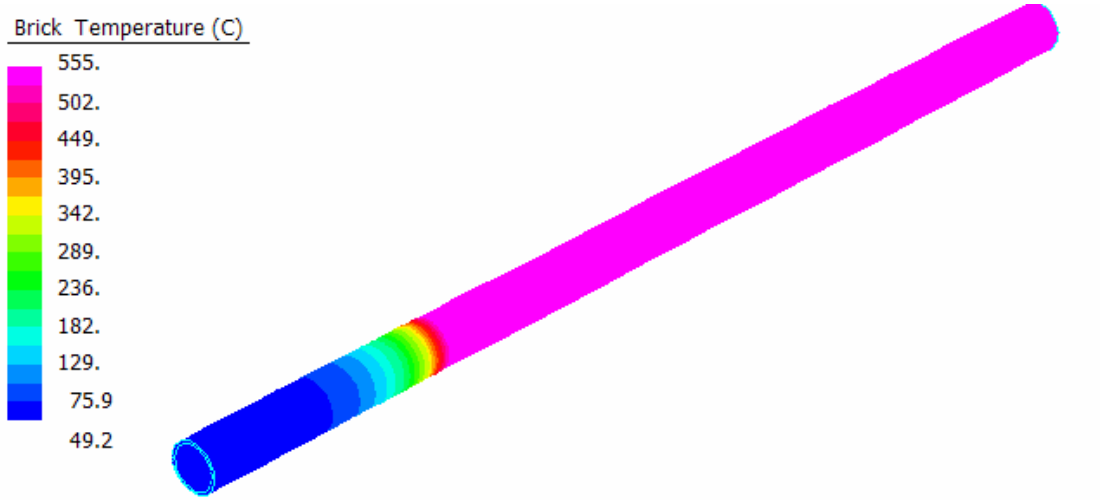

Figure 6.2: Temperature contour results for the exterior fan shaft pipe.

6.2.2 A MORE CONSERVATIVE MODEL

After plant operation a more accurate and conservative model was created in which the inner shaft and stagnant air inside the fan shaft was modelled. This is an axisymmetric FEA model with the same material properties for steel as given in Table 6.1. The conduction through stagnant air inside the shaft was modelled with plate elements with the properties in Table 6.2.

Table 6.2: List of properties for the air elements that were used in the FEA model.

Property	Value
density [48]	1.25 kg/m^3
thermal conductivity [48]	0.027 W/mK
specific heat capacity [48]	1005 J/kgK

The axisymmetric model with a convection heat transfer coefficient on the outside of the fan support pipe is given in Figure 6.3. Note that air elements are modelled inside the hollow inner shaft and between the inner shaft and the support pipe The solid shaft end and bearing are also modelled (see the cyan colored block in Figure 6.3.b), the green section is where the solid shaft end is welded to the hollow pipe of the shaft). The steel ball bearing density was modelled as half that of steel since it is a porous component. The shaft detail drawings are given in Appendix D for a better understanding of the model geometry.

The results of this model should be much more conservative. In practice the air inside the pipe will be moving during shaft rotation and a large heat transfer coefficient will exist. This model will show temperature profiles for the state when the shaft is not rotating. Initially an average natural convection heat transfer coefficient of 10 W/m^{2}K was applied.

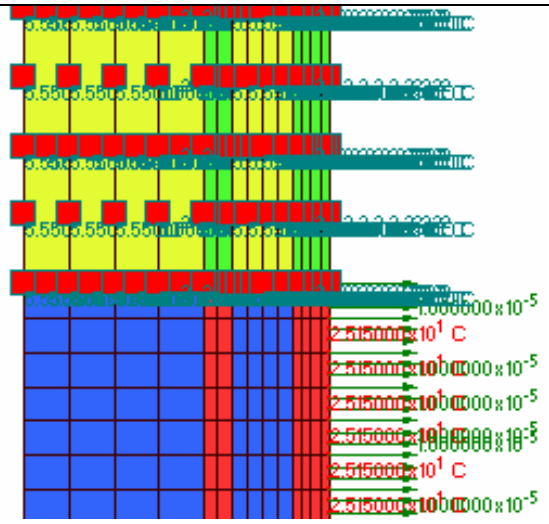

a) close-up view model with the inner shaft, outer pipe (green) and air (yellow) modelled

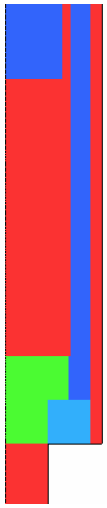

b) the solid shaft end, bearing is cyan coloured

c) a zoomed out view of the FEA model

Figure 6.3: Pictures of the axisymmetric FEA model.

The elements on the 2m long end of the shaft inside the furnace were all given a fixed temperature of 555 °C.

An estimate for the heat transfer coefficient is calculated below using empirical relations from [52]. The empirical relations are for natural convection over an isothermal horizontal cylinder. It is proven below that the average heat transfer coefficient is 10 W/m^{2}K (12 W/m^{2}K at the hot end and 5 W/m^{2}K at the cool end). This justifies the average heat transfer coefficient of 10 W/m^{2}K used in the model.

Heat transfer coefficient calculations:

Environmental temperature	$T_e := 25\ °C$
Maximum surface temperature (shaft reaches a maximum of 555 °C)	$T_s := 555\ °C$
Surface to air temperature difference with average shaft temperature	$\Delta Ta := \frac{(T_s + T_e)}{2} - T_e = 265 \cdot K$
Surface to air temperature difference at max shaft temperature	$\Delta Th := T_s - T_e = 530 \cdot K$
Surface to air temperature difference at min shaft temperature	$\Delta Tc := 55\ °C - T_e = 30 \cdot K$
Air density, properties from [48]	$\rho := \rho_{air}(T_e, 1atm) = 1.184 \frac{kg}{m^3}$
Outer diameter of fan shaft pipe	$D := 89mm$
Volumetric coefficient of expansion	$\beta := \frac{1}{T_e}$

Air kinematic viscosity

$$\nu := \nu_{air}(T_e, 1atm) = 1.55 \times 10^{-5} \frac{m^2}{s}$$

Air Prandtl number

$$Pr := Pr_{air}(T_e) = 0.706$$

Air thermal conductivity

$$k := k_{air}(T_e) = 0.026 \cdot \frac{W}{m \cdot K}$$

Rayleigh number, see [52]

$$Ra_D(\Delta T) := \frac{(\beta \cdot \Delta T) \cdot g \cdot D^3}{\nu^2} \cdot Pr$$

Nusselt number for heat transfer over an isothermal horizontal cylinder, see p.416 in [52]

$$Nu_D(\Delta T) := \left[0.6 + 0.387 \left[\frac{Ra_D(\Delta T)}{\left[1 + \left(\frac{0.559}{Pr} \right)^{\frac{9}{16}} \right]^{\frac{16}{9}}} \right]^{\frac{1}{6}} \right]^2$$

Average heat transfer coefficient

$$h_c := Nu_D(\Delta Ta) \cdot \frac{k}{D} = 9.895 \cdot \frac{W}{m^2 \cdot K}$$

Maximum heat transfer coefficient

$$h_c := Nu_D(\Delta Th) \cdot \frac{k}{D} = 12.188 \cdot \frac{W}{m^2 \cdot K}$$

Heat transfer coefficient

$$h_c := Nu_D(\Delta Tc) \cdot \frac{k}{D} = 5.23 \cdot \frac{W}{m^2 \cdot K}$$

Natural convection on a vertical wall heat transfer coefficient, p. 21 in [48]

$$h_c := 1.3 \cdot \left(\frac{\Delta Ta}{K} \right)^{\frac{1}{3}} \cdot \frac{W}{m^2 K} = 8.35 \cdot \frac{W}{m^2 K}$$

The calculations above indicate that an average heat transfer coefficient of 9.9 W/m^{2}K rounded to 10 W/m^{2}K is acceptable. Temperature contour plots of the axisymmetric model analysis, with average h_c = 10 W/m^{2}K, are given in Figure 6.4.a) and b). However, from the above calculations it is clear that the heat transfer coefficient is larger at the hot side and smaller at the cold end. A more accurate model was also created in which the heat transfer coefficient was applied such that it linearly decreases from the hot side to the cold end. These results are included in Figure 6.4.c) and d).

The contour plots show that the shaft is hottest at its centre and the largest heat flux is radially outwards. Further along the radius the gradient increases significantly, in the air between the inner shaft and outer pipe, as it cools down on the pipe outer surface. The temperature gradient is smaller at the solid end of the shaft and the temperature stabilizes. In all cases the temperature at the bearing location is clearly below 120 °C and within design limits.

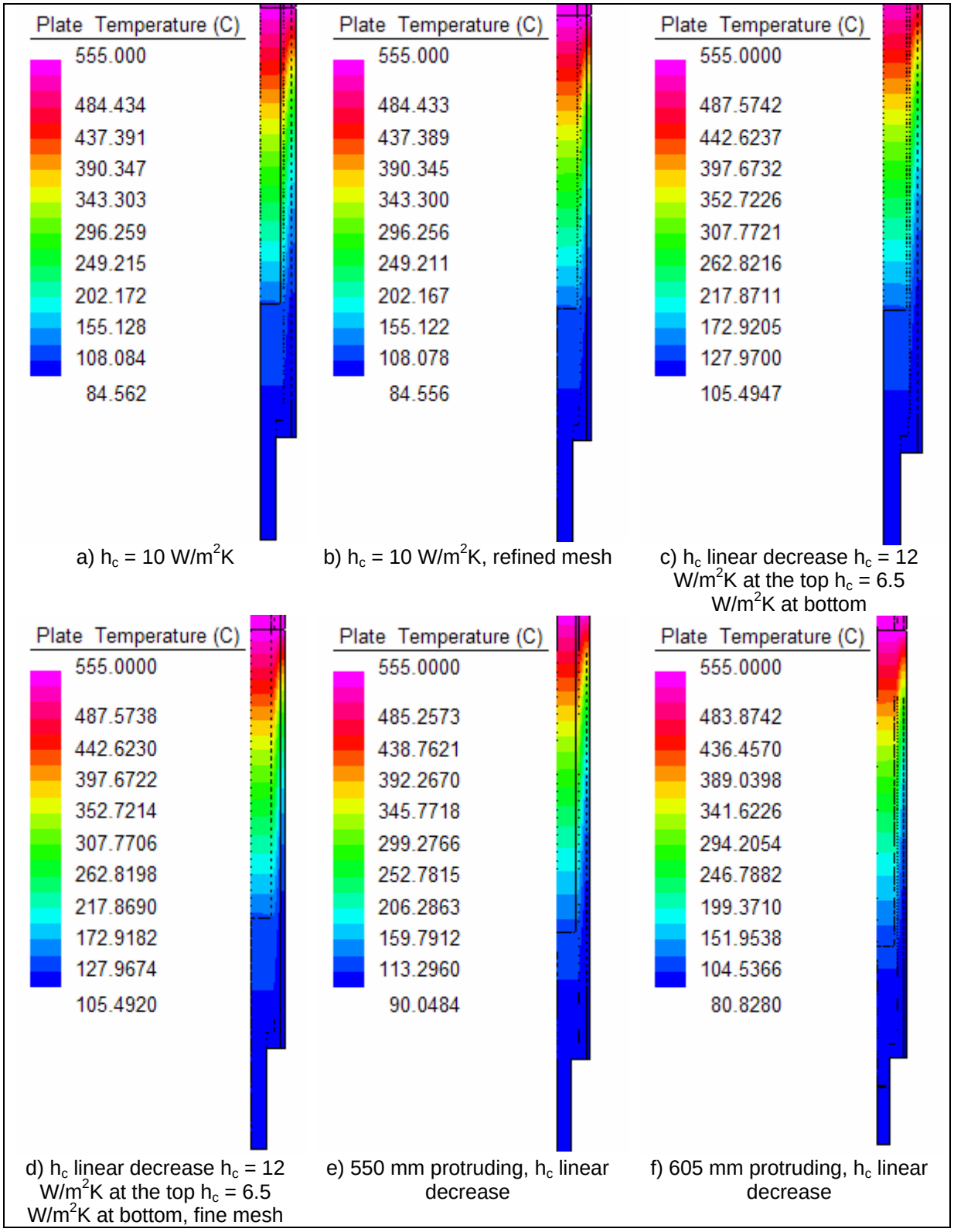

a) h_c = 10 W/m^{2}K

b) h_c = 10 W/m^{2}K, refined mesh

c) h_c linear decrease h_c = 12 W/m^{2}K at the top h_c = 6.5 W/m^{2}K at bottom

d) h_c linear decrease h_c = 12 W/m^{2}K at the top h_c = 6.5 W/m^{2}K at bottom, fine mesh

e) 550 mm protruding, h_c linear decrease

f) 605 mm protruding, h_c linear decrease

Figure 6.4: Steady state temperature contour plots for the conservative model.

The results for a constant heat transfer coefficient of 10 W/m^{2}K are clearly the coldest. However, the linear distribution is more accurate. If the protruding end is made longer the surface temperature at the end drops by 15 °C for every 50 mm extra length. This is shown by Figure 6.4.e) and f); and the support pipe surface temperature plot Figure 6.5. The exact length

of the shaft that protrudes out of the furnace is therefore very important. In Figure 6.5 it is also shown that the temperature stabilizes on the last 15 cm of the shaft.

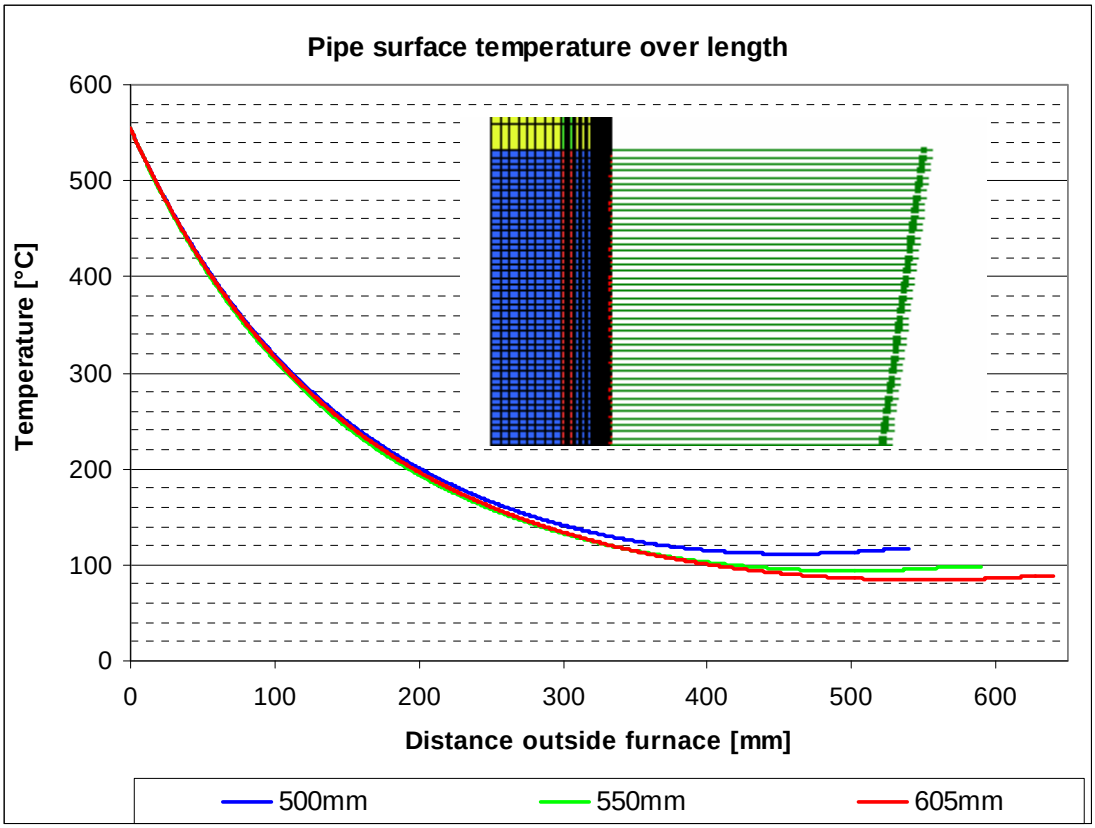

Figure 6.5: Plot of fan shaft support pipe surface temperature vs. protruding length for a linear reduction in heat transfer coefficient (see the FEA model on the plot).

As seen in Figure 6.5 the temperature distribution for a linear reduction in heat transfer coefficient is polynomial and not linear. If a more accurate analysis needs to be done the heat transfer correlation can be programmed into the FEA software to continuously update it with the temperature solution. The ideal would be to create a CFD model that also models the rotation of the shaft that creates forced convection from the air to the shaft. Such a detail analysis is seen as beyond the scope of this research. Of importance here is that this analysis represents a worst case i.e. low convection on the pipe outer surface. The design is therefore within limits.

6.2.3 COMPARISON BETWEEN FEA RESULTS AND THE MEASURED TEMPERATURE

As previously stated the fan shaft pipe surface temperature would be measured for comparison to the FEA analyses that were performed. The placement of the thermocouple on the shaft protruding out of the furnace can be seen Figure 5.2. The temperature measurement graph in Figure 5.16 shows the fan shaft pipe surface temperature over time. The thermocouple measured a maximum temperature of 46 °C over the entire 70 hours. It was placed about 15 cm from the deep groove ball bearing and V- belt pulley. However, the accuracy and dependability of this measurement must be questioned. The correct placement of a thermocouple on a

surface exposed to atmospheric air is extremely difficult. The actual measuring end (fused end) could be in the air and placed halfway in the moving air stream. It was confirmed that the thermocouple was fused directly on the pipe surface and it should therefore be a fairly good representation of the surface temperature.

A more accurate method would be pointing a laser or infrared thermometer at the pipe surface. Such an instrument was not available. Another good indication would be a human hand touch. At temperatures below 100°C it is a very reliable indication (bathroom water temperature is rarely above 65 °C and a human's reflex system kicks in at this temperature). During plant operation the operators frequently felt the pipe surface temperature with their fingertips and it was not hot enough for the reflexes to kick in. It can thus be assumed that the pipe surface temperature never exceeded 65 °C at the particular location. This result can now be compared to the FEA results.

It seems that the initial scoping model, see Figure 6.5, was sufficiently close as it predicted a temperature below 70 °C at the thermocouple location. The more conservative model, with the inside of the shaft also modelled, seems to over estimate the temperature. The closest model is either the one with 605 mm protruding outside the furnace or the model with a constant heat transfer coefficient of 10 W/m^2K applied over the entire surface. However, one should bear in mind that the actual temperature inside the furnace was below 555 °C for most of the time and that the insulation wool was applied more than 500 mm from the V-belt pulley end. This also effectively increases the length of the protruding end. Since the actual length that protrudes outside the furnace was never measured it is difficult to tell which FEA model is more accurate.

At times when it seemed as if the surface temperature increased a wet cloth was wound around the shaft support pipe to enhance cooling. The temperature seemed to increase when the bearing leaked more ammonia gas from the process chamber. The gas flow inside the shaft thus has a large influence and therefore a CFD model would be the most accurate to predict the temperature. The measured pipe surface temperature and all the FEA analyses prove that the ball bearing was not exposed to temperatures above 120 °C and that the design was thus valid.

6.3. COMPARISON OF FAN SHAFT ASSEMBLY 3D FEA TO INSTALLED PROTOTYPE

6.3.1 OBSERVATIONS DURING PLANT CONSTRUCTION

It is not always possible to design all components in detail before construction. Due to time constraints an engineer has to stop calculations as soon as a design is safe enough for construction. After the first prototype has been built and tested a design can be further analysed and validated when time is available. As described in section 4.3.2 the effect of shaft weight and

gravity was initially neglected for the weld neck sealing flange analysis. Pressure containment was the only load considered. After plant operation a detailed 3D FEA was performed, incorporating the observations made during prototype installation, to validate the design. During installation it was observed that the sealing flange deflects by almost 0.5 mm toward the weld neck flange as it is fastened. An exaggerated sketch of this deflection is given in Figure 6.6.

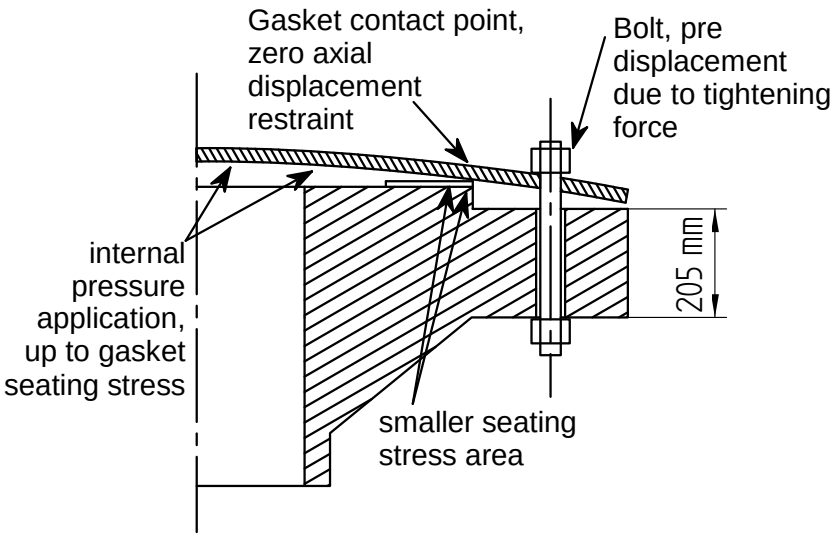

Figure 6.6: Sketch of the exaggerated deformation of the weld neck sealing flange assembly.

6.3.2 THE MODEL

The FEA was performed with Strand 7 [51]. The largest part of the model was built with 2nd order 3D brick elements in order to capture gradients through the thickness of the sealing flange and shaft pipe. For the triangular gussets 2D plate elements were used. To fix these plates to the 3D elements and to represent the welds, master slave links (with dx, dy and dz fixed) were applied to the 3D brick elements. The meshed model with load application is shown in Figure 6.7. To simulate the temperature of 555 °C inside the furnace the standard steel properties were used, but with a reduced Young's Modulus E = 140 GPa from [42] similar to section 4.2.8.

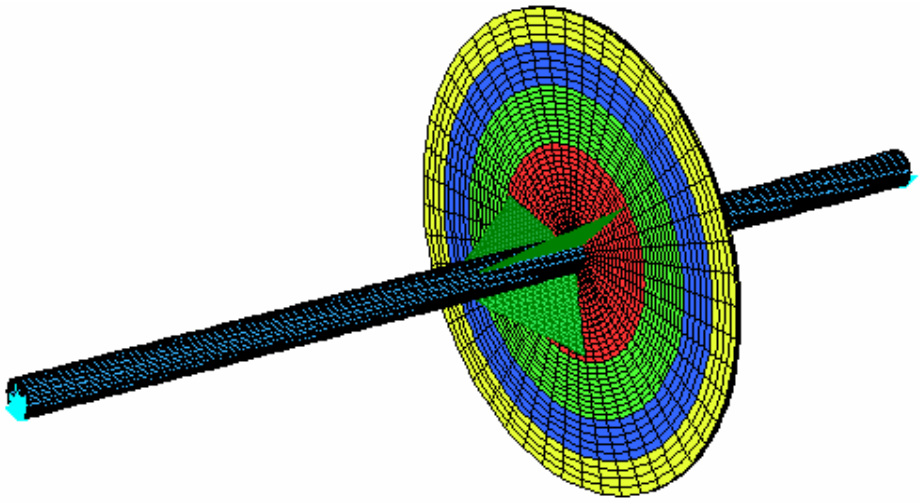

Figure 6.7: The 3D FEA model mesh of the fan shaft assembly (11240 3D elements).

6.3.3 LOAD APPLICATION

The loads that were applied are internal pressure, gravity, gasket seating stress and then the displacement restraints. The load and restraint application to the FEA model can be seen in Figure 6.8.a) to d).

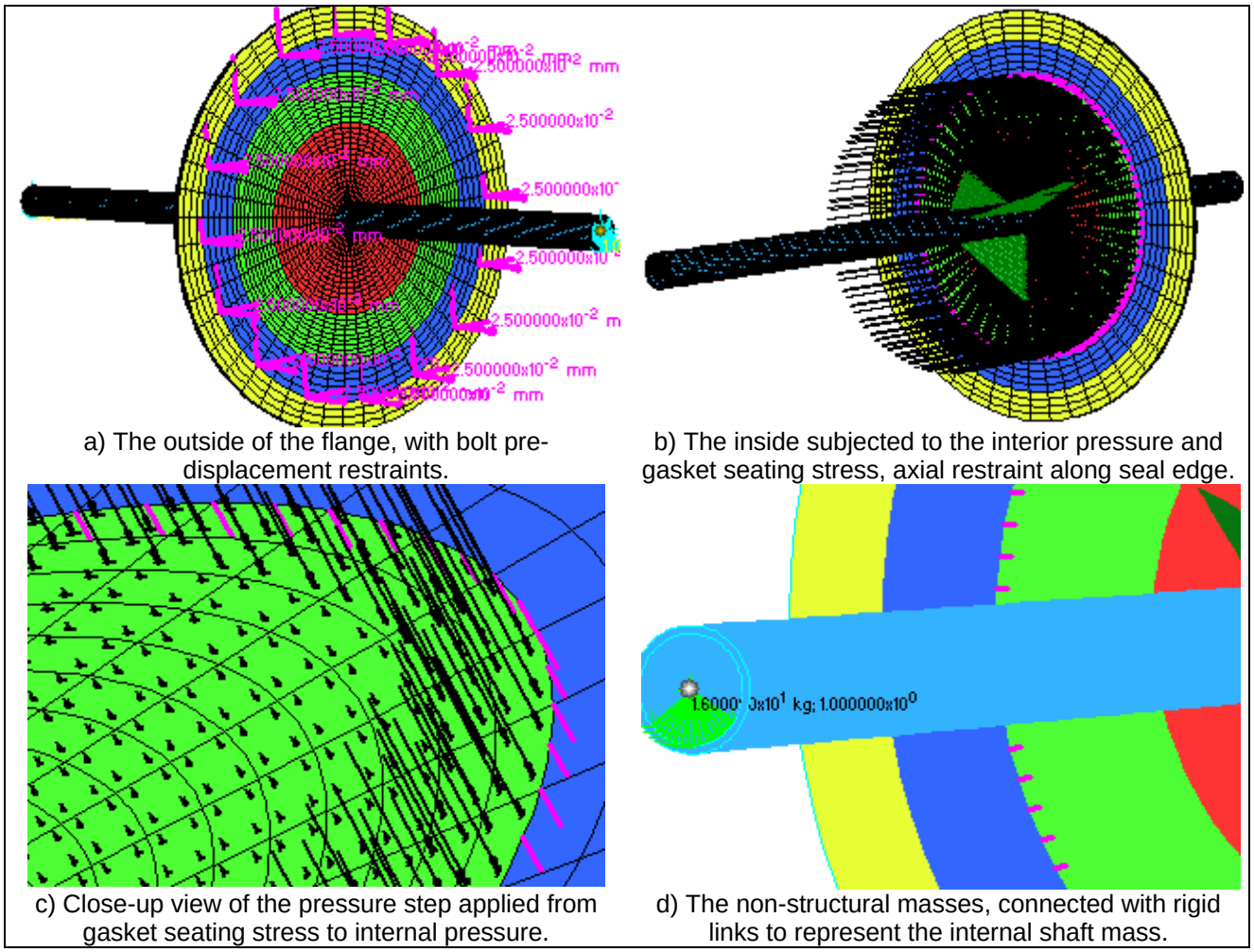

a) The outside of the flange, with bolt pre-displacement restraints.

b) The inside subjected to the interior pressure and gasket seating stress, axial restraint along seal edge.

c) Close-up view of the pressure step applied from gasket seating stress to internal pressure.

d) The non-structural masses, connected with rigid links to represent the internal shaft mass.

Figure 6.8: The boundary conditions and loads that were applied.

The same restraints that were applied to the axisymmetric model in section 4.3.2.2 were applied here i.e. an axial restraint at the gasket sealing edge (gasket contact edge see Figure 6.6). In this model the seating stress was applied over a much smaller area than for the axisymmetric model in Figure 4.11. This was done because of the actual deflection observed as seen in Figure 6.6 (less contact with the gasket due to deflection). The biggest difference is that at each of the 16 bolt locations a pre displacement of 0.025 mm towards the weld neck (negative x direction) was defined to simulate the deflection of the flange upon installation, as described by Figure 6.6. The value of 0.025 mm is the bolt deflection for a seating stress of 1 MPa and it is calculated in Appendix C section C.2 (if the seating stress area is reduced during deflection the seating stress increases and the bolt deflection stays constant).

The most accurate way to model the bolts would be to model its stiffness with beam elements. This would require a non-linear FEA, which is a very comprehensive task and is beyond the scope of this research. The pre-displacement method would still give much more accurate results than just a fixed restraint at bolt locations.

6.3.4 RESULTS

The displacement plots of the linear static analysis in Strand 7 [51] are given in Figure 6.9.

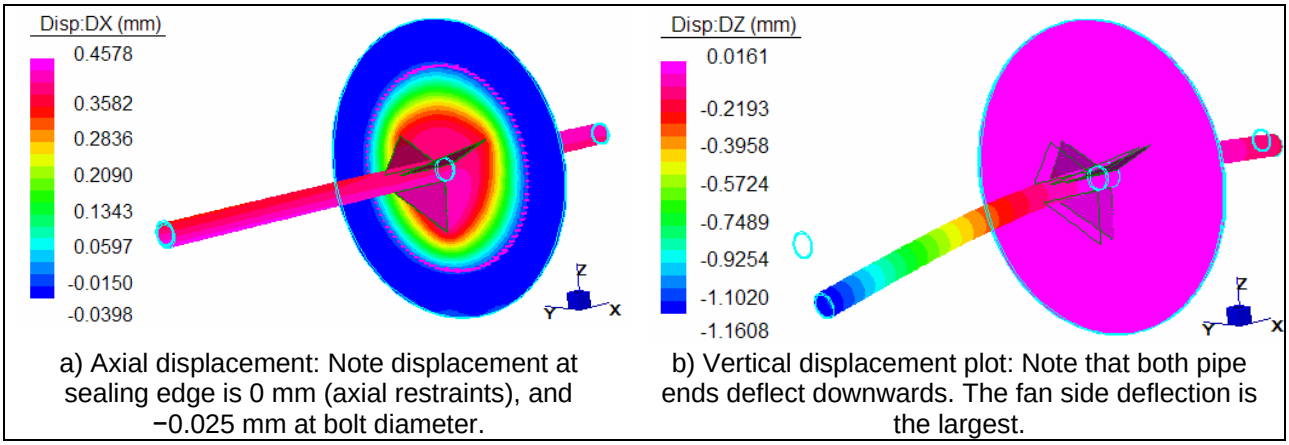

a) Axial displacement: Note displacement at sealing edge is 0 mm (axial restraints), and −0.025 mm at bolt diameter.

b) Vertical displacement plot: Note that both pipe ends deflect downwards. The fan side deflection is the largest.

Figure 6.9: Linear static analysis displacement results for the fan shaft assembly as installed.

The deflection in the axial direction, x-direction see Figure 6.9.a), indicates that the pre-displacement of −0.025 mm in the x-direction, at the bolt locations, is applied correctly. The fan side deflection of 1.161 mm is close to the analytically calculated value of 1.595 mm for a cantilever beam in section 4.2.8. Note that this analysis was done for a modulus E = 140GPa. If the same modulus of E = 124 GPa is used in the FEA model a vertical deflection of 1.31 mm is calculated with the FEA model at the fan end. The deflection calculated with the FEA model is close to the analytically calculated values. The main reason for the difference (1.595 mm vs. 1.31 mm) is the triangular gussets that effectively increase the overhanging length of the pipe. The analytical calculation ignores the gussets.

The Tresca stress contour plots are given in Figure 6.10.a) to c). Tresca stress intensity (the maximum shear-stress criterion [43]) was selected as it is the most conservative of the yield failure criteria. The largest stress exists at the contact point of the bottom triangular gusset, see Figure 6.10.c). Extra analyses were done to account for the larger seating stress that may exist due to the flange deflection seen in Figure 6.6. The same bolt displacement (bolt force) with a larger seating stress of 2 MPa is applied (the same force is applied over a smaller area). The maximum stress for this model is only 10 MPa larger, from 132.8 MPa to 141.1 MPa, see Figure 6.10.d). For a 3 MPa seating stress the maximum stress increases to 149.4 MPa, see Figure 6.10.e). A histogram distribution of the stresses, shown in Figure 6.10.d) to f), shows that the major part of the structure is still at a stress of below 10 MPa. Mesh refinement was done on the model with a 3 MPa seating stress, shown in Figure 6.10.f) and g).

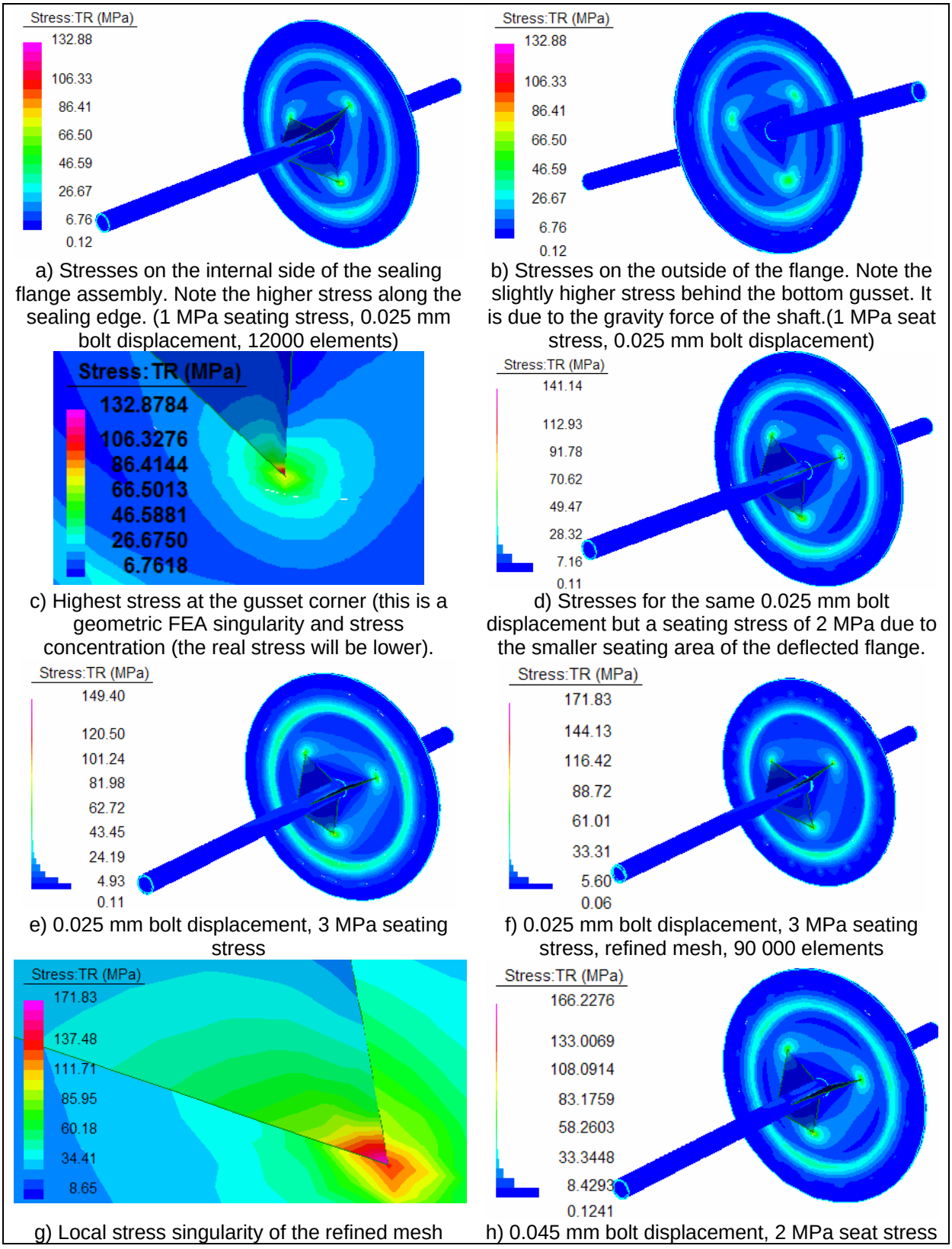

a) Stresses on the internal side of the sealing flange assembly. Note the higher stress along the sealing edge. (1 MPa seating stress, 0.025 mm bolt displacement, 12000 elements)

b) Stresses on the outside of the flange. Note the slightly higher stress behind the bottom gusset. It is due to the gravity force of the shaft.(1 MPa seat stress, 0.025 mm bolt displacement)

c) Highest stress at the gusset corner (this is a geometric FEA singularity and stress concentration (the real stress will be lower).

d) Stresses for the same 0.025 mm bolt displacement but a seating stress of 2 MPa due to the smaller seating area of the deflected flange.

e) 0.025 mm bolt displacement, 3 MPa seating stress

f) 0.025 mm bolt displacement, 3 MPa seating stress, refined mesh, 90 000 elements

g) Local stress singularity of the refined mesh

h) 0.045 mm bolt displacement, 2 MPa seat stress

Figure 6.10: Tresca Stress Contour Plots of the fan shaft assembly as installed in the NP.

The refined mesh shows that the major part of the structure is still at a stress of below 10 MPa. A further analysis with a larger bolt pre displacement of 0.045 mm was performed and is shown in Figure 6.10.h). The major part of the structure is at a low stress of below 20 MPa. In all the stress plots the stresses are below the yield stress of 160 MPa for the 300W steel at 600 °C

(the singularity in Figure 6.10.g) is ignored). It can be concluded that the fan shaft sealing flange assembly is a low-stressed structure even when it is in the furnace at 555 °C. Further analyses that were performed to arrive at the correct FEA model are given in Appendix C section C.5.

6.3.5 NATURAL FREQUENCY ANALYSIS

A natural frequency analysis of the same FEA model was also performed. The results are given in Table C.3 of Appendix C. The analysis was done to ensure that the fan shaft assembly structure does not have any natural frequencies close to the shaft rotation frequency. The lowest natural frequency is at 14.1 Hz and the next at 26.3 Hz (the support pipe is rotated at these lower frequencies). Then there are no modes up to 93.6 Hz. The shaft can thus be safely rotated between 26.3 Hz and 93.6 Hz without exciting the support pipe of the fan shaft assembly. During plant operation the shaft was rotated (excited) between 12.8 Hz (770rpm) and 14.5 Hz (870 rpm) at a VSD electrical supply of 40–45 Hz. However, the first mode shapes are only excited by vertical movement. If the shaft or fan had an imbalance, the first vibration mode (at 14.1 Hz) could have been excited inside the furnace. Further investigation is recommended.

6.4. VALIDATION OF HIGH-TEMPERATURE BEARING DESIGN

The bearing started to leak at high rotational speeds. Because of the machining that was done after manufacturing, the bearing was no longer a slight transition fit at temperature but a full clearance fit. The clearance might also have been larger than the design value because the furnace was operated at a lower temperature than planned. Still, the leakage was minimal and the bearing effectively reduced the danger of an explosion from gas leaking outside the furnace. The shaft did run smoothly after its eccentricity (“banana” shape) was eliminated with extra machining. No damage was observed on the graphite after the plant was decommissioned.

6.5. MEASURED AND PREDICTED AMMONIA CRACK RATIOS AND EXIT FLOWS

Generally, the double-stage nitriding process (Floe process; see section 2.1.2 and [10]) requires a low dissociation rate at the start of the nitriding cycle (the first 4-10 hrs). This produces a shallow white layer from which diffusion into the main case structure occurs. In the second stage a higher dissociation rate of 75 to 85 % is required.

According to instructions from [10], ammonia initially needs to be supplied at such a flow rate that four atmosphere changes per hour occur in the process chamber. This would ensure a dissociation rate of between 15% and 35 %. According to calculations in section 4.4.2 this equates to an ammonia supply flow rate of 3000 ℓ/hr. It is shown by Figure 6.11 that at a supply flow rate of 3000 ℓ/hr (and stable temperature conditions) at 31–37 hours, a crack ratio of 35% to 37 % is measured. The instructions from [10] and [5] are thus valid. Later between 40 and 50 hours when a supply rate of only 1000 ℓ/hr could be reached a higher crack ratio of 65–70 %

was measured. It is thus clear that an external ammonia dissociator was not necessary to obtain the higher second stage dissociation rate. This research clearly demonstrated the inverse proportionality between crack ratio and ammonia flow rate, as stated in section 5.5.2.2.
In the experiment the first crack ratios of 64% were measured at 2 am in the morning and at 18 hours, before the interior reached the right nitriding temperature at 23 hours. At 2 am the ammonia cylinders had already cooled down considerably due to high flow and low ambient temperature (2 °C in the winter time at Vereeniging). Due to the low flow available at this time high crack ratios were measured at the start. The low measurements at 20 hours might be due to human error (operators were not yet familiar with the 'Bunte Burette'). The high crack ratios at the start of the nitriding cycle might have caused a white layer on the nitrided surface. The significance of this will be discussed in section 6.6.4.

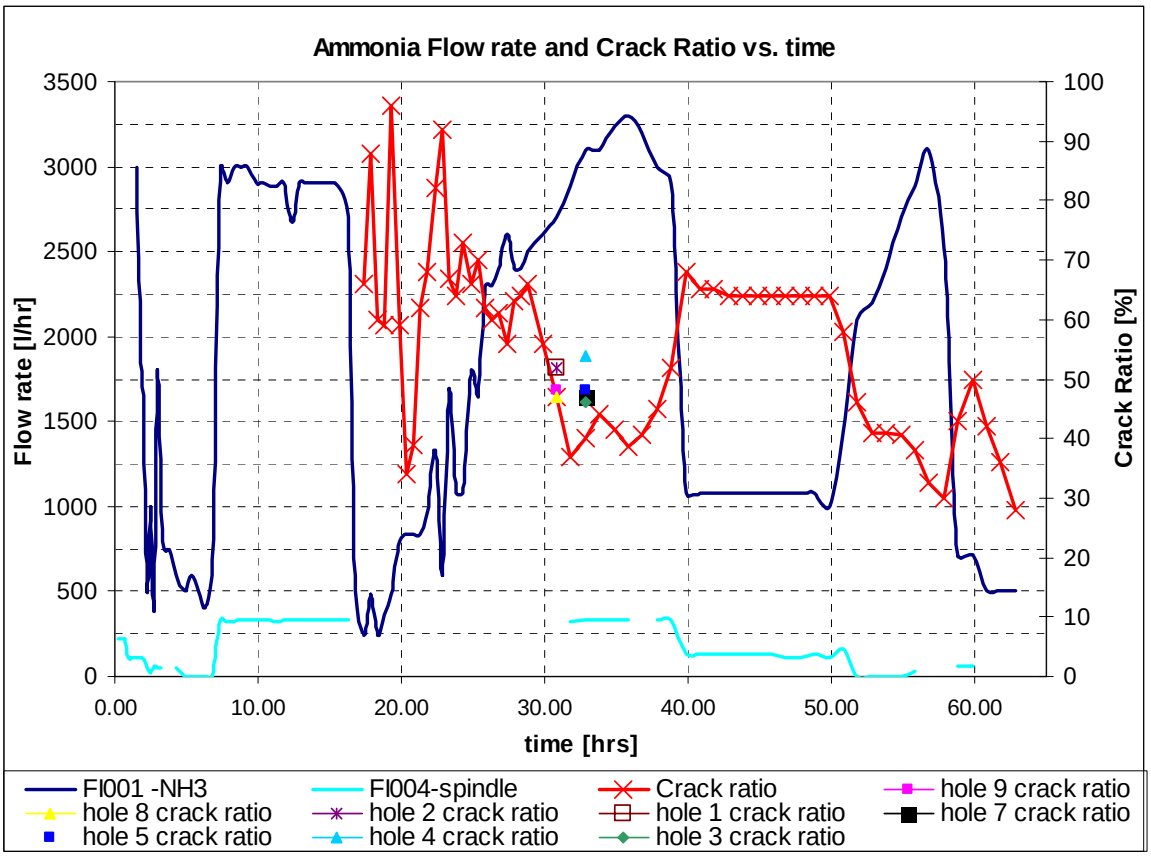

Figure 6.11: Graph of the supplied ammonia flow rate and the resulting crack ratio.

Another observation from Figure 6.11 is the crack ratios measured from flow of the individual insert holes at 31–34 hrs. The measurements are more or less equal to the measurement of all 9 tubes' flow combined. The crack ratios of insert holes 5, 4, 3 and 7 are close to 48% at 33 hrs and those of insert holes 9, 8, 2, and 1 are close to the combined flow measurement of 47% at 31 hrs. It was thus proven that the stirring fan functioned efficiently and that all 9 insert holes of the CUD would be nitrided equally. It can also be attributed to the fact that all 9 exit tubes see the same back pressure (the common valve exit manifold).

During operation it could be sensed with a human touch that the temperature of the exit tubes was lower than 25 °C (ambient). At 3000 ℓ/hr ammonia supply and a tube surface temperature of 25 °C; the calculation done in section 4.4.4 predicted a worst case of 101 °C for fluid bulk temperature at a pipe length of 3 m outside the furnace. The calculation thus seems to be valid.

6.6. NITRIDING SPECIMEN TESTS

6.6.1 PREPARATION OF SPECIMENS

After the plant was decommissioned and the sealing flanges were removed the nitriding specimens were collected. The specimens were marked according to the insert holes in which they were placed.

The specimens were then prepared for microhardness and layer thickness tests. The results of these tests would be the main indication of the success of the NP. The first step was to cut the specimens at a perpendicular angle to the nitrided surface. This specimen was then moulded into a cold setting resin in such a way that the cross section was flush with the surface and the specimen was upright (see Figure 6.12). The resin was cast in a cylindrical mould and once hard it formed a rigid base for hardness tests. The cross section was also polished with specialized equipment until it shone. The polish process involves a very fine sandpaper and polish. The specimens could then be used for hardness and layer thickness tests.

Figure 6.12: A prepared polished specimen placed under the microscope with the Vickers indenter placed on the measured edge.

6.6.2 SPECIMEN MICROSCOPE PHOTOS

The next step was to take photographs of each prepared nitrided specimen’s cross section under a light microscope. First the polished surface is etched with a specific acid that is

specially prepared for the particular grade of steel. For the F22 steel grade of the CUD the prescribed etching agent is called Nutal. The etching acid makes the steel surface structure more visible. It transforms the shiny and glossy polished surface to a matt finish that is visible to the human eye. The microscope photos of the specimens are given in Figure 6.13. The enlargement used for these images ranges from 15 to 16 times.

Figure 6.13: Micrograph images of the etched and polished specimen cross sections.

A distinctly darker ridge can be seen on all nitrided specimens. This ridge represents the nitrided layer. The photos clearly indicate that all 9 insert holes were nitrided to an equal depth. The thickness of the specimens (width of the cross sections) is in the range of 6 to 9 mm.

6.6.3 SPECIMEN MICRO HARDNESS PROFILE

The specimens were then prepared for microhardness profile tests. It is important that the surface must not be etched before hardness testing. The cross section surface must be polished before an accurate microhardness profile can be extracted.

Figure 6.14: A polishing machine used for metallurgical specimen preparation.

Before the microhardness profile is generated the selected hardness scale is justified. The first reason why the Vickers hardness scale was selected is that it is an industry standard for nitriding layer tests (in [4], [5] and [12] most hardness results are given in the Vickers scale; in rare cases Rockwell C is used). The second reason is that it has a fine scale compared to the other hardness test scales. For example when compared to the Rockwell C scale: A Rockwell C hardness of 58–59 HRC is equal to 655–675 HV on the Vickers scale (a difference of 1 HRC is equal to 20 HV). Higher up the Vickers scale is even finer. A Rockwell C hardness of 67–68 HRC is equal to 900–940 HV (a difference of 1 HRC is equal to 20 HV). In addition to this the Rockwell C scale only goes up to 68 HRC (equal to 940 HV) whereas the Vickers scale goes up to more than 1300 HV. The Brinell Hardness scale stops at 622 HB (655 HV on the Vickers scale) and the Rockwell B scale ends at 575 HV. The hardness scale information was obtained from an in industrial Bohler Special Steel Manual (booklet) [55].

The formula for Vickers hardness is as follows, (p.277 in [38]): $$VHN = \frac{1.72P}{d_1^2}$$

where d_1 is the length of the diagonal of the square shaped indentation of the Vickers diamond indenter and P is the applied load of 0.1 kg. The microhardness profile is then generated.

A microhardness profile is generated by making indentations with a Vickers indenter from the specimen surface (edge of the cross section that touches the resin) up to a certain depth. Preferrably measurements need to be made beyond the nitrided ridge, as seen in the photos in Figure 6.13, so that the core hardness can also be tested. The size of each indentation at each

depth is then carefully measured to get a Vickers hardness value, see the setup in Figure 6.12 and Figure 6.15.

Figure 6.15: A light microscope with a Vickers indenter for measuring microhardness profiles.

This procedure was followed for three of the nitrided specimens (insert holes 2, 8 and 9). The results are given in Figure 6.16.

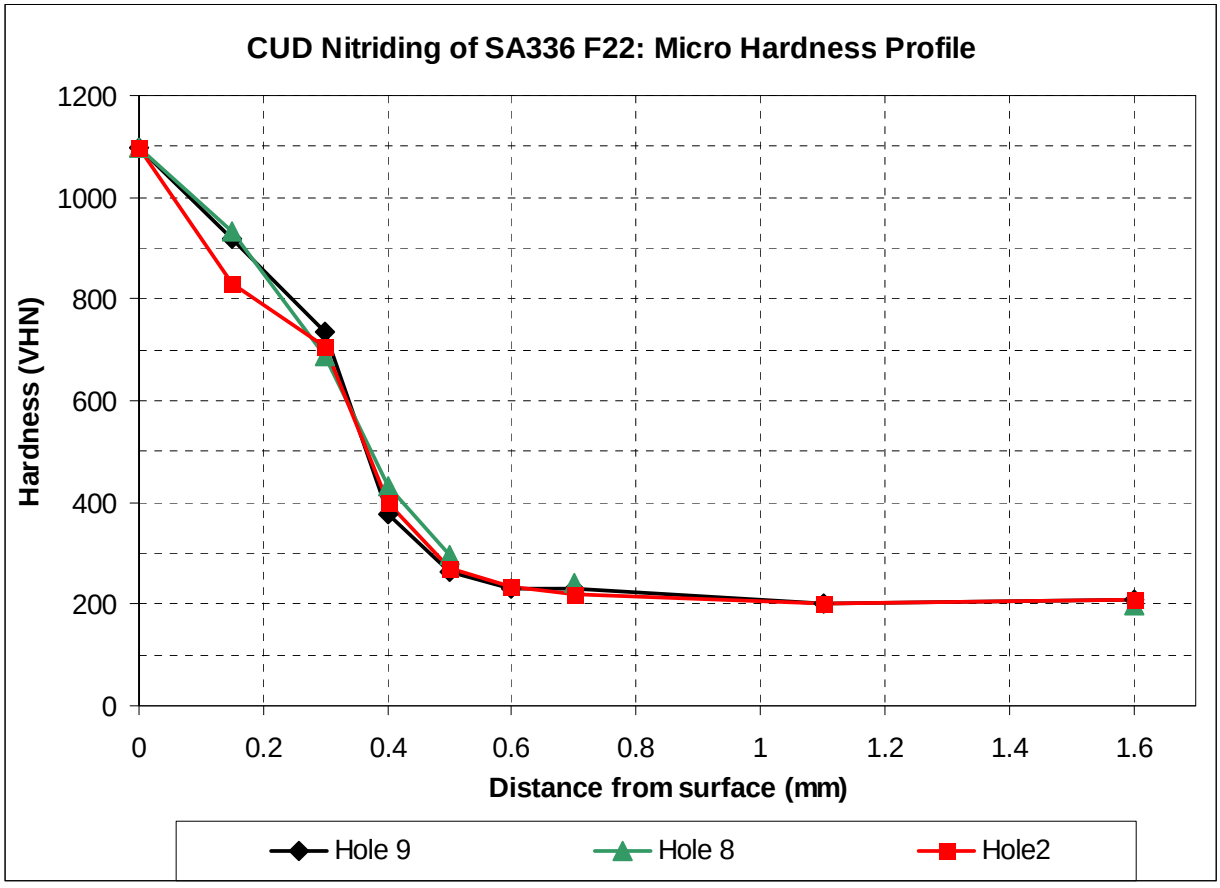

Figure 6.16: Graph of nitride specimen hardness tests i.e. Vickers Hardness vs. depth.

Since similar results were found for all three it was not necessary to get a microhardness profile for the rest of the insert holes. The photos in Figure 6.13 also indicate that similar nitriding depth was achieved for all nine specimens. Hole 9 is the spindle hole, hole 8 a valve insert hole on the side and hole 2 a deep centre valve insert hole, see Table 5.3. This is a good representation of the different insert hole geometries. One can thus extrapolate that the microhardness profiles for the rest of the specimens would look similar to those of insert holes 2, 8 and 9.

In the graph of Figure 6.16 it is shown that a surface hardness of 1100 HV is obtained (1100 VHN at a distance of 0 mm from the surface). The hardness then gradually decreases to 740 HV at a depth of 300 μm at a rate of 1.2 HV/μm. At a depth of 300 μm the hardness has a sharper decrease down to 376 HV at the end of the effective case depth (0.4 mm). The hardness curve then slowly smoothes out up to a depth of 700 μm. From 700 μm to 1mm depth the hardness reduces at a very small rate to the material core hardness of 200 VHN. The total nitride layer thickness can also be deduced from the microhardness profile. In [6] the nitrided case depth is defined as the depth where the hardness is 10% above the core hardness. From Figure 6.16 it can thus be seen that the nitrided case depth is 0.5 mm.

When compared to other microhardness profiles, specifically the one given in Figure 2.11.b), a few similarities can be seen. The surface hardness in the microhardness profile of Figure 2.11 is also 1100 HV. However, it stays constant up to a depth of 0.07 mm and then reduces rapidly; the case depth is much smaller. Since the measurement resolution for this test was only every 0.15 mm a constant hardness up to a certain depth could not be identified, if it existed.

When the profile in Figure 6.16 is compared to hardness profiles of different steels, such as those of [6], it is shown that it is rare to have both a surface hardness above 800 HV and a case depth more than 0.2 mm. A hardness profile for plasma nitrided En 40B steel (a nitridable steel), given by Figure 6.17.b), has a surface hardness of 900 HV and a case depth of only 0.22 mm.

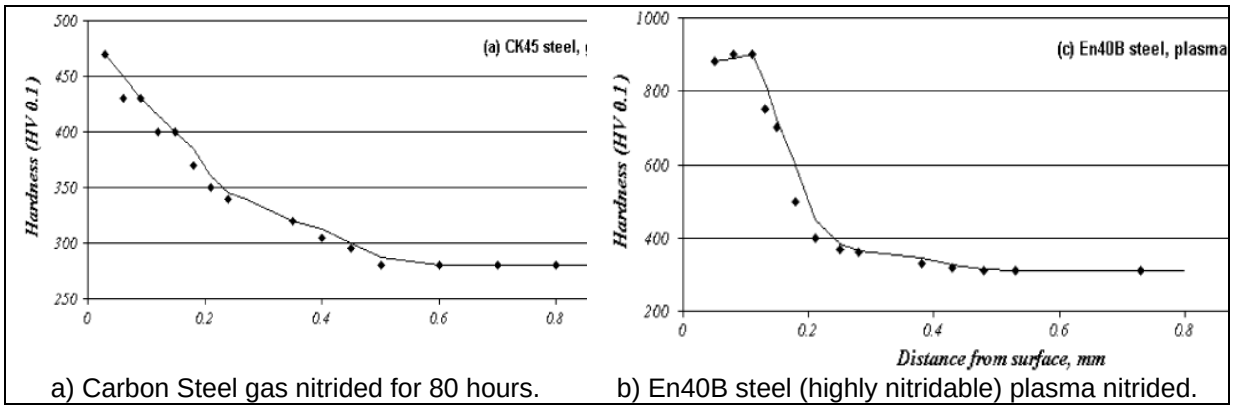

a) Carbon Steel gas nitrided for 80 hours. b) En40B steel (highly nitridable) plasma nitrided.

Figure 6.17: Microhardness profiles of different nitrided steels, from [6].

It can thus be concluded that the CUD nitriding process was significantly successful since both a high hardness and a deep case was achieved. This can be attributed to the high nitridability of the SA 336 F22 CUD steel and the long duration of the nitriding cycle (48 hours).

6.6.4 LINK BETWEEN PLANT OPERATING DATA AND SPECIMEN RESULTS

The parameters that influence the quality of the nitrided case were listed in section 2.6.3 and it will be discussed here to prove their validity.

An increased furnace temperature results in an increased case depth. The high nitriding temperature of 555 °C was maintained for only 10 of the 48 hours of the nitriding cycle (see Figure 5.20); however, it still would have contributed to the 0.4 mm effective case depth that was achieved. If the high nitriding temperature of 555 °C could have been maintained longer, an even larger case depth would have been achieved.

The second important parameter is the process time. The long nitriding cycle time of 48 hours is the main reason for the large nitrided case depth.

The low initial ammonia supply flow rate resulted in an increased crack ratio. The high initial crack ratio could have caused a white layer and also the high surface hardness. If ammonia flow had been controlled better during the first five hours of the nitriding cycle, a shallow white layer could have been guaranteed. It is possible that a hard, brittle white layer had formed on the surface (hardness is 1100 HV); however this cannot be derived from a microhardness profile. The actual hardness of the compound (white) layer cannot be measured because it is too thin [6]. According to [5] the white layer can be reduced to less than 0.025 mm with double-stage nitriding (Floe process). The existence of a white layer can only be confirmed with Scanning Electron Microscope (SEM) analysis or X-Ray diffraction whereby a (ε+γ') phase needs to be identified (graph of intensity on the y axis and theta on the x axis to identify phase concentration). This strictly belongs to the metallurgical field and is beyond the scope of this research.

The nitriding tests on all 9 insert holes' specimens are similar. This can be attributed to the equal flow rates and the equal crack ratios that were measured (see Figure 6.11).

The correct surface pre-treatment also results in increased case depth. The initial oxygen supply lasted seven hours, much longer than the intended two hours. This might also have caused the high dissociation rate at the start.

The maximum attainable hardness is mostly limited by the material composition. According to Table 2.3 the SA 336 F22 material has a chromium concentration of 2 % to 2.5 % and molybdenum concentration of 0.9 % to 1.1 %. The large concentration of Cr forms chromium nitrides (CrN) that result in a hardness of more than 800 HV [5]. The large surface hardness of 1100 HV that was obtained is attributed to the chromium content of the F22 material.

6.7. CONCLUSION

Thermal analyses of the fan shaft support pipe, protruding 500mm outside the furnace wall, confirmed that the ball bearing temperature will be low enough. The support pipe surface temperature measurement confirmed the FEA results.

Structural FEM analyses of the fan shaft assembly were also done. The observed displacement of the installed prototype was modelled. It was proven that the majority of the structure is subjected to low stresses and that deflections compare well with analytical calculations.

The flow rate graph of Figure 6.11 validates the theory that ammonia should be supplied at four atmosphere changes per hour to ensure a crack ratio of 15% to 40%.

Overall, the plant design is a valid solution to the problem. A good nitrided case was obtained for the interior of the CUD. The case is thick and it has a high surface hardness. The case is also similar in all 9 insert holes of the CUD block. The only problem is the possibility that a thick white layer had formed due to the high initial crack ratio. This is only a problem if the layer peels off on a bearing surface. The existence of a white layer can be proved with further SEM tests. The possibility is large since gas nitriding always has a thicker white layer than controlled plasma nitriding [5].

Chapter 7: Conclusion and Recommendation

7.1. PREAMBLE

Briefly, this dissertation has pointed out the importance of designing a novel nitriding plant to successfully nitride a large vessel such as the CUD. Consequently the design of high temperature equipment and sufficient control instrumentation has been illustrated successfully. Off course the validation of the design using an experimental plant is a necessity. Only if the plant operation produced a nitrided layer of adequate quality, the designed process plant can be used for nitriding CUD vessels in the future.

7.2. OVERVIEW OF THE DESIGN RESEARCH PROJECT

A main objective of this dissertation was to design, build and test a nitriding facility to nitride the interior of the PBMR Core Unloading Device. Because the nitriding facility is a small scale plant it would be an integrated design. It was designed by following the entire system engineering process and the integration of mechanical machine design, process engineering and metallurgical engineering disciplines. A summary of the work done to achieve this objective now follows.

A literature study of the history of nitriding was started. It was found that the first patent for the nitriding process was awarded to an American named Machlet in 1913. The early developments gave good insight into the fundamental control parameters of the process. The focus of the literature study was on the metallurgical aspects of nitriding and how to get a desirable nitrided case structure. Different nitriding techniques including plasma and gas nitriding were studied to aid in the concept design at a later stage. Limited literature on the design of a nitriding plant was available especially because this particular design would be so unique. Most gas nitriding plants are commercialized. The design of these expensive mass produced units are company intellectual property. To aid in the design of the nitriding fan the literature was searched for high temperature gas sealing bearings. Existing bearing designs are too complex and would be expensive to implement for the CUD NP.

To start the concept design the user requirements were set up and a functional analysis was performed in line with the product development process [35]. The user requirements were converted into measurable design requirements before various concepts were generated. Among the concepts were building a special bulk nitriding process chamber inside a large nitriding furnace that would nitride both the interior and exterior of the CUD. Plasma nitriding was also considered. To evaluate the five concepts a set of selection criteria were defined

among which constructability, nitriding quality, cost and safety were the most important. The selected concept is a gas nitriding plant using the sealed interior of the CUD as a process chamber and a purposefully modified existing heat treatment furnace at DCD Dorbyl.

The first challenge for the detail design, was determining the stirring fan power input that would result in sufficient turbulence. The result was a large diameter, 2.5 m long hollow shaft with a whirling speed of 1150 rpm. A high temperature graphite gas sealing bearing was then designed for the shaft end inside the furnace. Next the process chamber was designed. To seal the various insert holes blind sealing flanges, with gas pipe and thermocouple penetrations, were designed and analysed for stresses. The process chamber would be subjected to an internal pressure below 40 kPa and is therefore not classified as a pressure vessel according to the OHS Act [49]. For the gas piping system, calculations were performed to determine the minimum required gas flow rates and the amount of gas required for the process. An ammonia supply flow rate of 3000 ℓ/hr would ensure a low enough ammonia dissociation rate. The flowmeters were sized accordingly. To conclude the detail design a cradle was designed to hold the CUD upright in the nitriding furnace. It was analysed for buckling loads. The cost of the plant hardware is R 82, 000.00

The design could then be implemented by constructing and operating a prototype plant. The plant operation data can be used as a number of experiments to validate the theory used in the design. Because the designed plant was used little experimental design was necessary. Only a few extra thermocouples and measurement instruments were specified and an experimental procedure was defined. The plant was constructed within schedule and few problems were experienced. During plant operation a few obstacles were encountered including the effect of low ambient temperature on the ammonia gas supply capacity. The nitriding furnace and CUD internal temperature was lowered from 555 °C to 520 °C to allow a reduced ammonia supply flow rate. After nitriding the CUD was opened and the nitriding specimens were removed to test its nitride layer thickness and hardness.

Finally the experimental data and nitriding specimens could be used to verify and validate the design. A detailed thermal FEA of the installed fan shaft assembly was compared to the measured shaft support pipe surface temperature. The maximum measured temperature of 45 °C is below the values calculated by both a conservative and less conservative FEA model. A structural FEA was also performed of the fan shaft assembly incorporating observations made during site installation. It was proven that stresses are low even inside the furnace at a temperature of 555 °C. To verify the nitriding capability of the plant the nitrided specimens were examined under a microscope and a microhardness profile was generated. The tests confirmed

a nitride layer thickness of 400 µm and a surface hardness of 1100 HV. These results meet and exceed the target values for the nitride layer and the nitriding was therefore succesful.

7.3. REVIEW OF RESEARCH OBJECTIVES

The main research objective was the design of a nitriding plant to nitride the inner surface of the CUD housing pressure vessel. A safe working plant had been designed, built and operated to successfully nitride the CUD. To achieve the main objective the following sub objectives were in the way.

The entire engineering project cycle from a literature survey of nitriding processes and facilities to concept design, detail design, construction, testing and finally verification and validation was executed. The work performed during each step is explained in section 2 above. Each step was successfully executed before moving on to the next step. This is essential for the entire project to succeed. Without a workable concept; the detail design, experiment and validation would not have been succesful.

Different engineering disciplines were combined to design a safe and effective nitriding plant that facilitates testing the nitrided surface afterwards. Understanding the nitriding process required an insight of the metallurgical engineering discipline. It includes an understanding of the desired nitrided case properties. The mechanical components such as the shaft, bearing and flange design and manufacturing form part of the mechanical engineering discipline. The specification of the process control and instrumentation forms part of the chemical engineering discipline. Thermohydraulic analysis of the gas piping system is part of both the mechanical and the chemical engineering disciplines. Various disciplines were successfully combined to design and construct the plant.

A suitable plant and process design has been established that can be used for nitriding future CUD vessels for the PBMR DPP. A solution for future CUD vessels has thus been found.

The literature survey showed that no existing nitriding plants could nitride a vessel as large as the CUD. This research filled this gap in the literature, with the design of a novel nitriding plant using the workpiece interior as the nitriding process chamber as shown in Figure 1.7.

Moreover, the main objective of the research was successfully met. All the defined functional requirements were adhered to (see section 7.4 below) and the nitrided case requirements were exceeded. In addition to this the plant is cost effective and it turned out to be easy to assemble at any site. The plant was built outside the fabrication shop at DCD Dorbyl. The existing furnace

was moved and a new sandbank was created. Other than that the components could easily be disassembled and transported. This makes it portable to an extent (semi-portable).

Although the process control was not ideal and various other mistakes were made on the first prototype plant the nitriding was still a success. The next time such a plant will be constructed it will be much easier and the same mistakes will not be repeated. With better process control and other minor adjustments the design can compete with commercial gas nitriding furnaces and at a fraction of the cost.

As a final proof of the success of the nitriding process the CUD was successfully commissioned at the Helium Test Facility (HTF), see Figure 7.1. After nitriding the CUD passed a hydrostatic pressure test at 114 Bar and it was installed in the fuel handling test set-up at the HTF in Pelindaba. The CUD spindle and other valve inserts were installed into the nitrided insert holes in the CUD block and to date no problems were found with the nitrided surface. Cold welding between CUD metal surfaces will be prevented.

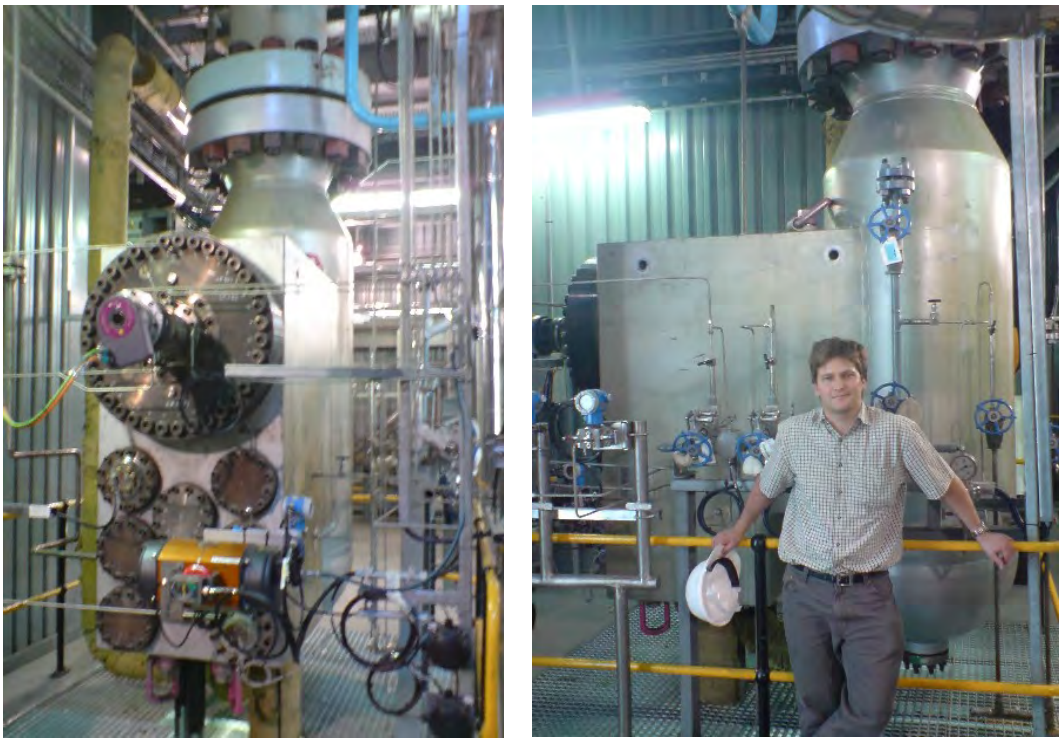

Figure 7.1: The successfully installed CUD at the HTF.

7.4. FUNCTIONAL PERFORMANCE

With a design research project the extent to which the research objectives were achieved can be measured with the conformance to functional and design requirements. The nitriding plant conforms to all the design and functional requirements that were defined during the concept design phase in section 3.4.3.

1. The CUD NP is capable is capable of nitriding large workpieces like the CUD that weighs 14 tonnes
2. It nitrides the inner surface of a pressure vessel
3. It is easy to construct
4. It provides a heating furnace capable of 700°C and provides temperature measurement of various parts
5. It provides the necessary gases at the correct flow rates for nitriding
6. It provides a means to measure nitride layer thickness and hardness
7. It is capable of a case depth of 200 µm and 500 HV hardness with nitridable steels
8. The plant costs less than R 500 000 to construct

7.5. LESSONS LEARNED

Throughout this research various technical and project related lessons were learned. If a second CUD NP is built these lessons prevent the same mistakes from being made twice. All the technical lessons are outlined in Appendix J. The most important ones are listed here.

- Shaft manufacturing – Considerable quality control needs to be applied to ensure that the solid shaft ends are machined after it was welded to the hollow shaft, to ensure the parallel bearing surface tolerances are met. The resulting minimum bearing clearances will reduce ammonia leakage.
- The low winter temperatures in Vereeniging resulted in a lower ammonia supply flow rate capability which in turn resulted in a high crack ratio. This can be prevented by using cylinder heating blankets to ensure the cylinder is kept at high pressure (max 10 Bar).
- The ceramic paper gaskets disintegrated at high temperature and required a very large seating stress to seal (although the CUD seal surfaces were undamaged). In future graphite gaskets should be used in spite of possible problems with its removal afterwards.

An important design lesson is that FEA should be used as a design tool only. If the design does not adhere to fundamental engineering principles a FEA model will not solve the problem.

7.6. RECOMMENDATIONS FOR FUTURE WORK

A number of areas were identified for further investigation in order to improve the design. The possibilities for further work that are beyond the scope of this dissertation are as follows:

1. **CFD modelling of the nitriding process chamber**
   By modelling the flow and the fan inside the process chamber the pressure contours and velocity fields can be identified. This could serve as a further confirmation that all 9 insert

holes in the CUD block are nitrided to an equal thickness and hardness. The effect of increasing the flow in the spindle hole can be investigated. Its effect on the spindle hole nitride layer thickness can be tested with further nitriding and detailed CFD analyses.

2. **Improve the fan shaft assembly**

   The fan can be tested outside the process chamber to test its flow performance, to quantify the graphite bearing friction and to complement the CFD model. The shaft and high temperature bearing design can be improved to ensure a more leak tight high-temperature seal. Further vibration analysis can also be done to determine other possible reasons for the ammonia gas leakage. The fan shaft assembly can also be analysed for thermal creep.

3. **Further metallurgical investigation**

   Due to the low initial crack ratio a white layer could have formed. Its existence can be confirmed with further work. A SEM photo can be taken or X-ray diffraction analysis can be done on the nitrided specimens; to determine the thickness of the formed white layer. The disadvantage of a brittle thick white layer is the possibility of nitride layer peel on bearing surfaces. The nitrided specimens can also be put through accelerated corrosion tests to quantify the corrosion resistance of nitrided F22 steel.

4. **Plant and process modifications**

   The cost of implementing computer controlled nitriding [17] must be investigated. Computer control would substantially improve process quality and reduce operator labour. An investigation can be made to use hydrogen, for process control, instead of alloying elements and ammonia feed. Machlet used hydrogen for this purpose [4]. In addition the plant can be designed to account for low ambient winter temperatures, by adding heating blankets to the ammonia cylinders for example. A plant design requiring a smaller process time would also improve production rate.

5. **Mass production**

   The possibilities of mass production for PBMR demonstration powerplant CUDs must be investigated. Three CUDs will be installed at the bottom of each PBMR core. The sealing flanges and other equipment will need to be designed for repetitive use.

7.7. CONCLUSION

This research proves that a large pressure vessel can successfully be nitrided using the vessel interior as a process chamber. A succesful solution was found to the problem and the end result is a semi-portable plant design. It can compete with commercial facilities at a fraction of the cost.

REFERENCES

[1] Johnson, K.I., Keller, D.V., *Adhesion between atomically pure metallic surfaces; Part IV— the effect of contamination on the adhesion of metallic couples in ultrahigh vacuum*, Rep NASA-CR-71147, Jan 1966, Syracuse Univ, Research Inst, New York, 1996

[2] Moeller, C.E., Noland, M.C., *Cold welding tendencies and frictional studies of clean metals in ultra-high vacuum* : C. E. Moeller and M. C. Noland, ASLE Trans., 10 (1967) 146–157, *Wear*, *Volume 11, Issue 5*, May 1968, Page 386, 1968

[3] Lúcia V., Santos A.B., Vladimir J., Trava-Airoldi A., Evaldo, J., Corat, A., Jadir Nogueira, C., Nélia, F.L., *DLC cold welding prevention films on a Ti6Al4V alloy for space applications*, Surface & Coatings Technology 200 (2006) 2587–2593, Elsevier, 2005

[4] Pye, D., *Practical Nitriding and Ferritic Nitrocarburizing* , ASM International (product no. #06950G), Ohio, USA, ISBN: 0-87170-791-8, 2003

[5] Nisbett, E.G., *Steel forgings: design, production, selection, testing, and application*, ASTM International MNL53-EB, ISBN: 0803133693, 9780803133693, 2005

[6] Ashrafizadeh, F., *Influence of plasma and gas nitriding on fatigue resistance of plain carbon (Ck45) steel*, Elsevier, Surface and Coatings Technology 173-174 (2003) 1196-1200

[7] Kenan, G., Mehmet, D.l, Mehmet, C., *Effect of ion nitriding on fatigue behaviour of AISI 4140 steel*, Materials Science and Engineering A279 (2000) 207-216, Elsevier, 2000

[8] Nathalie, L., Yves, V., Fatigue strength improvement of a 4140 steel by gas nitriding: Influence of notch severity, Materials Science and Engineering A 435–436 (2006) 460–467, Elsevier, 2006

[9] American Society of Mechanical Engineers Boiler and Pressure Vessel Code (ASME), Section VIII Division 1, Edition 2001 with Addenda 2003

[10] *Cast Steel: Gas Nitriding,* Knowledge article from Metals database, Art132 (also available at www.steel.keytometals.com/Articles/Art132.htm, accessed on 28 July 2009)

[11] Floe, C.F., A Study of the Nitriding Process Effect of Ammonia Dissociation on Case Depth and Structure, reprinted from Trans. ASM, Vol.32, 1944, Source Book on Nitriding, P.M. Unterweiser and A.G. Gray, Ed., American Society for Metals, p.144-171, 1977

[12] Darbelly, J., *Gas Nitriding: An Industrial perspective*, presentation for Department of Materials Science and Engineering McMaster University, also available at http://mse.mcmaster.ca/graduate/seminar/2005/ March 22 2006

[13] Du, H., Agren, J.Z., *Gaseous Nitriding Iron – Evaluation of Diffusion of N in and Phases Z.,* Metallkd V.86, 1995

[14] Jack, D.H., Carbides and Nitrides in Steel, Materials Science and Engineering, 1973

[15] Winter, K.M., *Gaseous Nitriding: In Theory and In Real Life*, Technical Paper of United Process Controls, Process-Elcectronic GmbH, A member of United Process Controls, Heiningen, Germany, 2009

[16] American Society of Mechanical Engineers Boiler and Pressure Vessel Code (ASME), Section II Materials ed. 2001 add. 2003

[17] Liliental, W.K., *Controlled Gas Nitriding – The modern surface treatment for the automotive industry*, 1st International Automotive Heat treating Conference 13 July 1998, ISBN-10: 0871706253, ASM International, Elsevier, 2009

[18] Jurci, P., Panjan, P., *PVD Protection enhanced by plasma nitriding-* based on the article *Surface Processing of the PM Vanadis6 Steel with Plasma Nitriding and CrN PVD Coating* for tool steels, Elsevier (0026-0657/06), 2006

[19] Priest, J.M., Baldwin, M.J., et al., *Low pressure r.f. nitriding of austenitic stainless steel in an industrial-style heat-treatment furnace*, Thin Solid Films 345 (1999) 113-118, Elsevier, 1999

[20] Fewell, M.P., Priest, J.M., Baldwin, M.J., Collins G.A., Short, K.T., *Nitriding at low temperature*, Surface and Coatimgs Technology 131 (2000) 284-290, Elsevier, 2000

[21] Nagaea*,* M., Takemoto, Y., Yoshio, T., Takada, J., Hiraoka, Y., *Preparation of structurally controlled dilute molybdenum–titanium alloys through a novel multi-step internal nitriding technique and their mechanical properties*, Materials Science and Engineering A 406 (2005) 50–56, Elsevier, 2005

[22] José, F.d.S., Carlos, M.G., André, P.T., *Improvement of the cavitation erosion resistance of an AISI 304L austenitic stainless steel by high temperature gas nitriding,* Materials Science and Engineering A 382 (2004) 378–386, Elsevier, 2004

[23] Sung, J.H., Kong, J.H., Yoo, D.K., On, H.Y., Lee, D.J., Lee, H.W., *Phase changes of the AISI 430 ferritic stainless steels after high-temperature gas nitriding and tempering heat treatment*, Materials Science and Engineering A 489 (2008) 38–43, Elsevier, 2008

[24] Lee, H.W., Kong, J.H., Lee, D.J., On, J.H., Sung, J.H., *A Study on High Temperature Gas Nitriding and Tempering Heat Treatment in 17Cr-1Ni-0.5C*, Materials and Design 30 (2009) 1691-1696, Elsevier, 2008

[25] Schaaf, P., *Laser nitriding of Metals*, Progress in Materials Science 47 (2002) 1-161, Elsevier, 2002

[26] Ratajski, J., Suszko, T., *Modelling of the nitriding process*, Journal of materials processing technology 195 (2008) 212–217, Elsevier 2007

[27] *Method of nitriding work pieces of steel under pressure*, United States Patent 5211768, Inventors: Preisser, Friedrich (Buedingen, DE), Seif, Rudolf (Bruchkoebel, DE), also available at www.freepatentsonline.com/5211768.html accessed on 28 July 2009

[28] Pinedo, C.E., *The use of selective plasma nitriding on piston rings for performance Improvement*, Materials and Design 24 (2003) 131–135, Elsevier, 2003

[29] Baranowska, J., Wysiecki, M., *Influence of Surface Pretreatment on case formation during gaseous nitriding*, Surface and Coatings Technology 125 (2000) 30-34, Elsevier, 2000

[30] Baranowska, J., Szczecinkski, K., Wysiecki, M., *Increasing of Gas Nitriding Kinetics via surface pre-treatment*, Surface and Coatings Technology 1151-152 (2002) 534-539, Elsevier, 2002

[31] Matin, Ya.I., *Means of Improving Furnaces for gas nitriding*, UDC (047) :621.785.532.662.5:621.783, translated from Metallovedenie I Termicheskaya Obrabotka Metallov, No.3 pp.42-46, consultants Bureau, a division of Plenum Publishing Corporation, New York, 1974

[32] Proctor, M.P., Kumar, A., Delgado, I.R., *High-Speed, High-Temperature Finger Seal Test Results*, NASA/TM—2002-211589, AIAA–2002–3793, 2002

[33] *High Pressure High Temperature Light Gas Drive Shaft Seal*, United States Patent 4123070, Inventors: Peterson, William D, Oct 1978, also available at www.freepatantsonline.com accessed on 2 Oct 2009

[34] *Fluid Bearing Face Seal for Gas Turbine Engines*, United States Patent 5174584, Inventors: Lahrman, Kenneth, A, Dec 1992, also available at www.freepatantsonline.com accessed on 2 Oct 2009

[35] Ulrich, K.T., Eppinger, S, D, *Product Design and Development-Third international edition*, McGraw-Hill, New York, ISBN: 007-123273-7, 2003

[36] White, F.M., Fluid Mechanics fifth edition, McGraw Hill, New York, ISBN: 0-07-121566-2, 2003

[37] Incropera, DeWitt, *Introduction to Heat Transfer*, 4th edition, Wiley, New York, ISBN: 0-471-38649-9, 2002

[38] Smith, W.F., *Principles of Materials Science and Engineering*, third edition, McGraw-Hill, ISBN: 0-07-114717-9, 1996

[39] Shiomi, M., Takano, D., Osakada, K., Otsu, M., *Forming of aluminium alloy at temperatures just below melting point*, International Journal of Machine Tools & Manufacture 43 (2003) 229–235, Pergamon, 2002

[40] Hannah J., Stephens R.C., *Mechanics of Machines* second edition, Edward Arnold Publishers, London, ISBN: 0-7131-3254, 1982

[41] Shigley, J.E., Mischke,C.R., Budynas, R.G., *Mechanical Engineering Design* seventh edition, McGraw-Hill, New York, ISBN: 007-123270-2, 2003

[42] ASME II Part D ed. 2001 add. 2003, Table TM-1

[43] Benham, Crawford, Armstrong, *Mechanics of Engineering Materials* second edition p.273, Prentice Hall, Harlow, England, ISBN: 0-582-25164-8, 1996

[44] Gere, J.M., *Mechanics of Materials* sixth edition p.344, Brooks/Cole, Belmont, ISBN: 0-534-41793-0, 2004

[45] Roadstrum, W.H., Wolaver, D.H., *Electrical Engineering for All Engineers* 2nd edition, John Wiley & Sons, ISBN: 0-471-51043-2, 1994

[46] SANS10162 -1:2005, South African national Standard Part1: Limit State Design of hot-rolled structural steelwork, edition2, 2005

[47] South African Steel Construction Handbook (SAISC), third edition, 1997

[48] Mills, A.F., *Heat Transfer*, second edition, Prentice Hall, New Jersey, ISBN: 0-13-947624-5, 1999

[49] Government Notice. R: 1591, 4 October 1996, Vessels under Pressure Regulations, 1996, Department of Labour (RSA), section 43 of the Occupational Health and Safety Act, 1993 (Act 85 of 1993)

[50] Sonntag, Borgnakke, Van Wylen, *Fundamentals of Thermodynamics* 6th edition, Wiley, ISBN: 0-471-15232-3, 2003

[51] *Strand 7 finite element analysis software system*, G+D Computing, version 2.3.7, www.strand7.com, 2005 Strand7 (Pty) Ltd

[52] Lienhard, J.H. IV., Lienhard, J.H. V., *A Heat Transfer Textbook*, 3rd edition, Phlogiston Press, Cambridge Massachusetts, 2006

[53] MathCAD 14.0 M020, Copyright © 2007 Parametric Technology Corporation. All Rights Reserved, engineering calculation software

[54] *Guide for the Verification and Validation of Computational Fluid Dynamics Simulations*, AIAA G-077-1998, American Institute of Aeronautics and Astronautics (AIAA), Reston, VA 20191-4344 USA, ISBN: 1-56347-285-6, 1998

[55] Bohler Special Steel Manual, AL 005E-10.89-10.000N, Bohler Gesellschaft M.B.H.

[56] Benham, P.P., Warnock, F. V., Mechanics of Solids and Structures, Pitman International, Bath UK, ISBN: 0-273-36191-0, 1978

APPENDIX A: MISSION LEVEL/ FIRST LEVEL FUNCTION DIAGRAMS

A.1 FURNACE PREPARATION

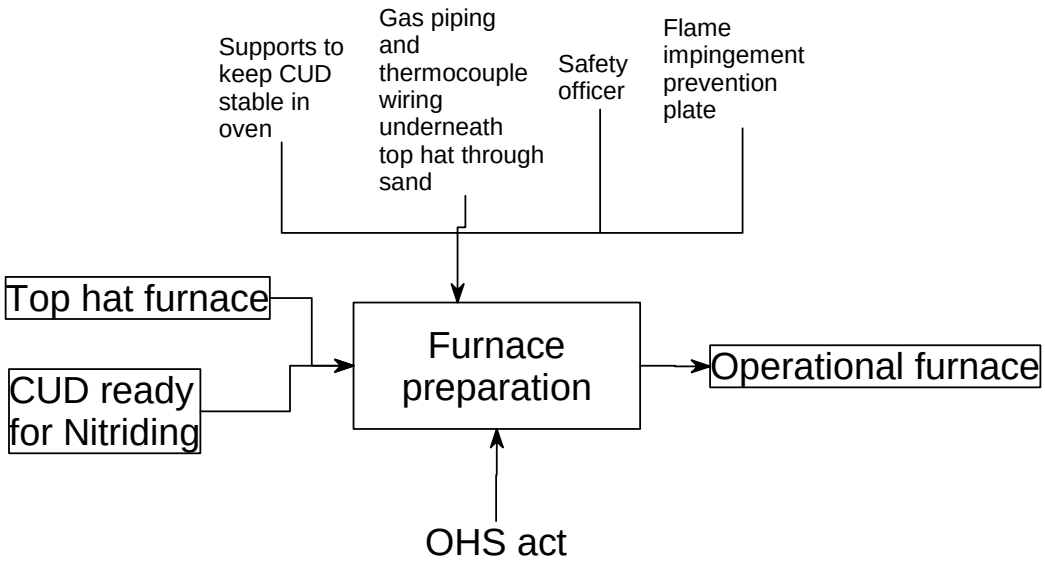

Figure A.1: Flow Diagram of the Furnace preparation process

A.2 FURNACE OPERATION

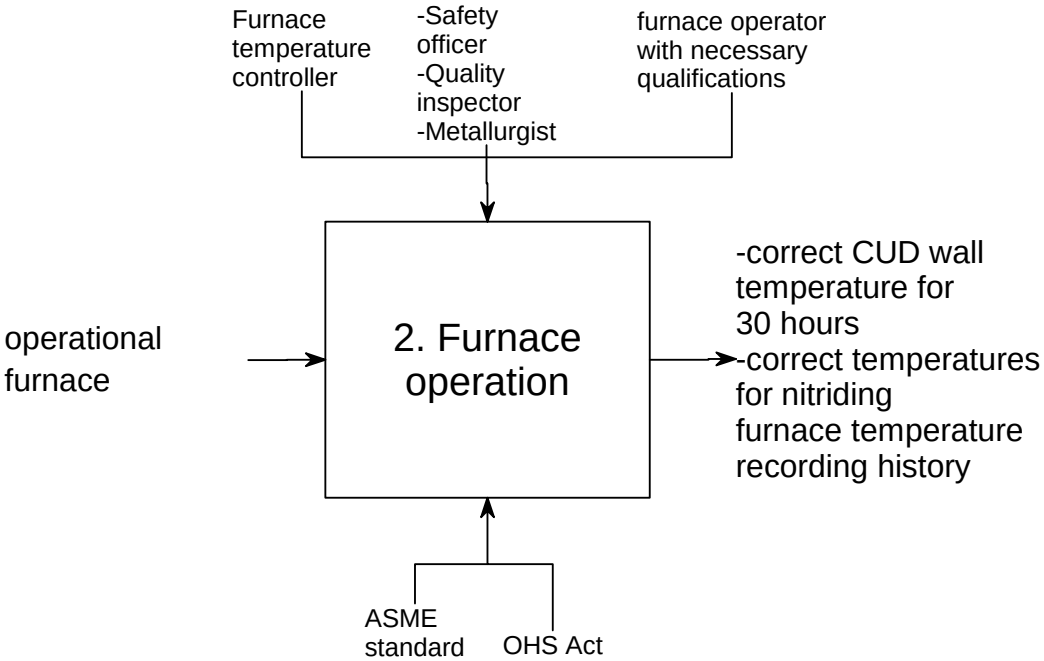

Figure A.2: Flow Diagram of the furnace operation process

A.3 MAKE A HOLE IN THE FURNACE FOR THE FAN SHAFT

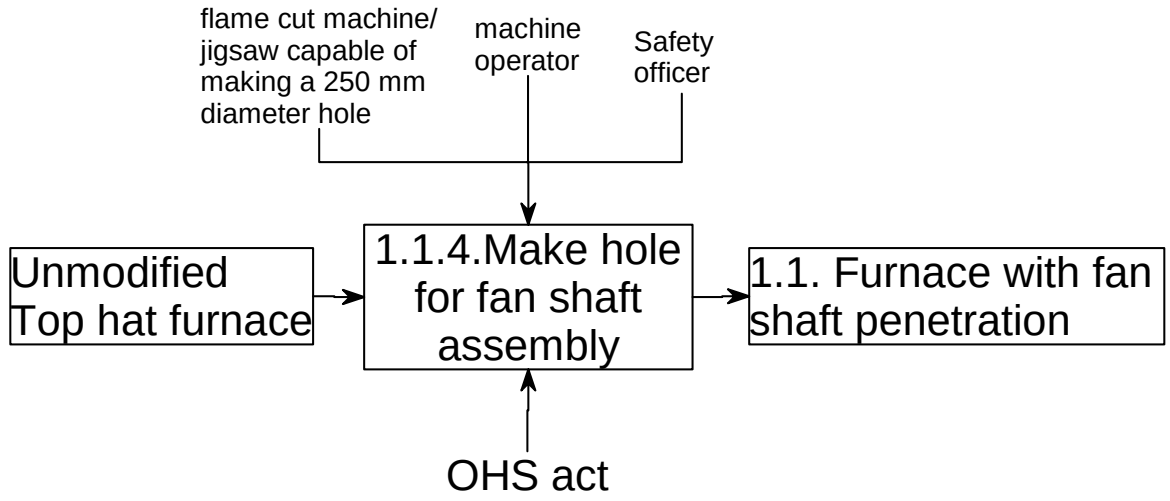

Figure A.3: Flow Diagram of the hole making process

A.4 WELDING THE FAN SHAFT ASSEMBLY TO THE SEALING FLANGE

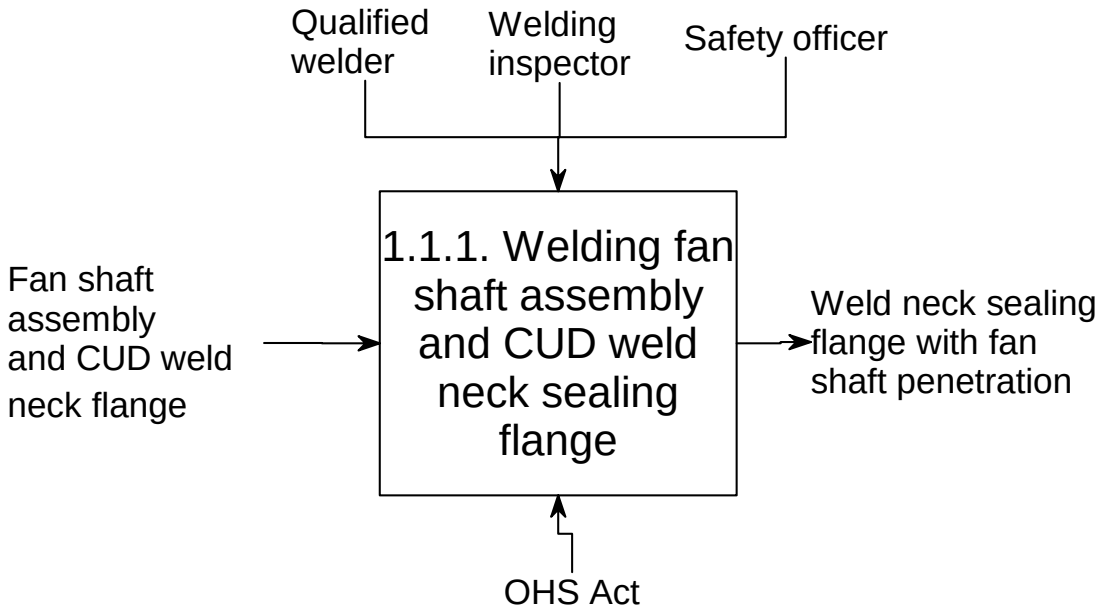

Figure A.4: Flow Diagram of the fan shaft welding process.

A.5 PROVIDE OXYGEN GAS FOR THE NITRIDING PROCESS

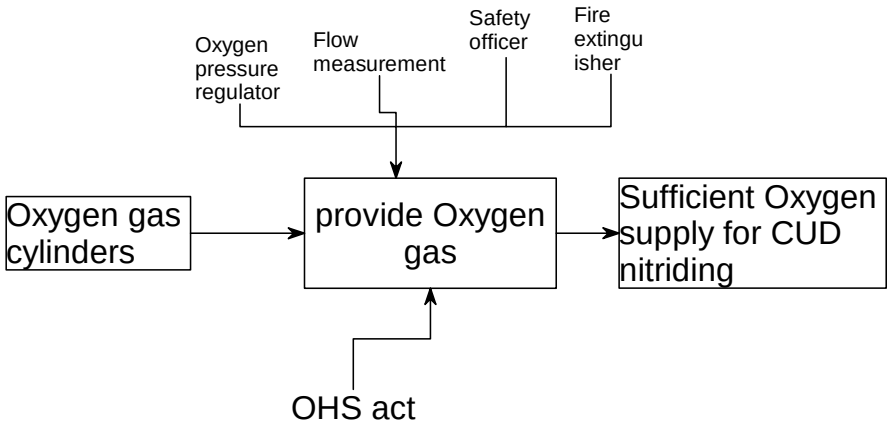

Figure A.5: Flow Diagram of the oxygen provision process

A.6 PROVIDE NITROGEN GAS FOR THE NITRIDING PROCESS

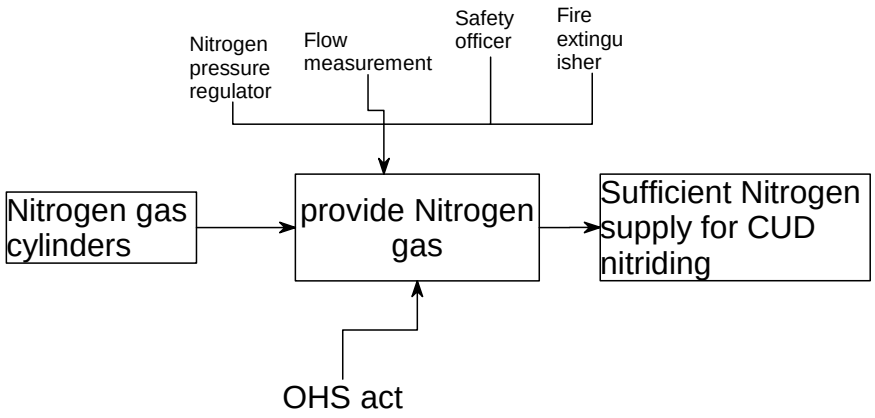

Figure A.6: Flow Diagram of the Nitrogen provision process

A.7 PROVIDE AMMONIA GAS FOR THE NITRIDING PROCESS

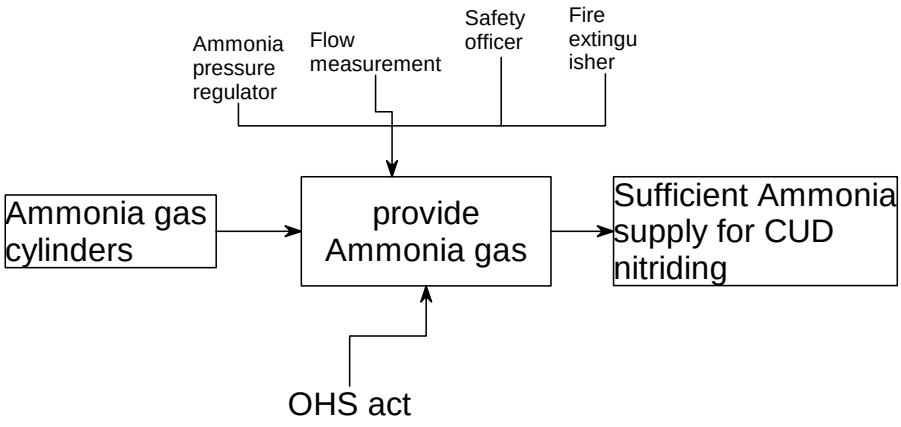

Figure A.7: Flow Diagram of the Ammonia provision process

A.8 MEASURE THE TEMPERATURE DURING FURNACE OPERATION

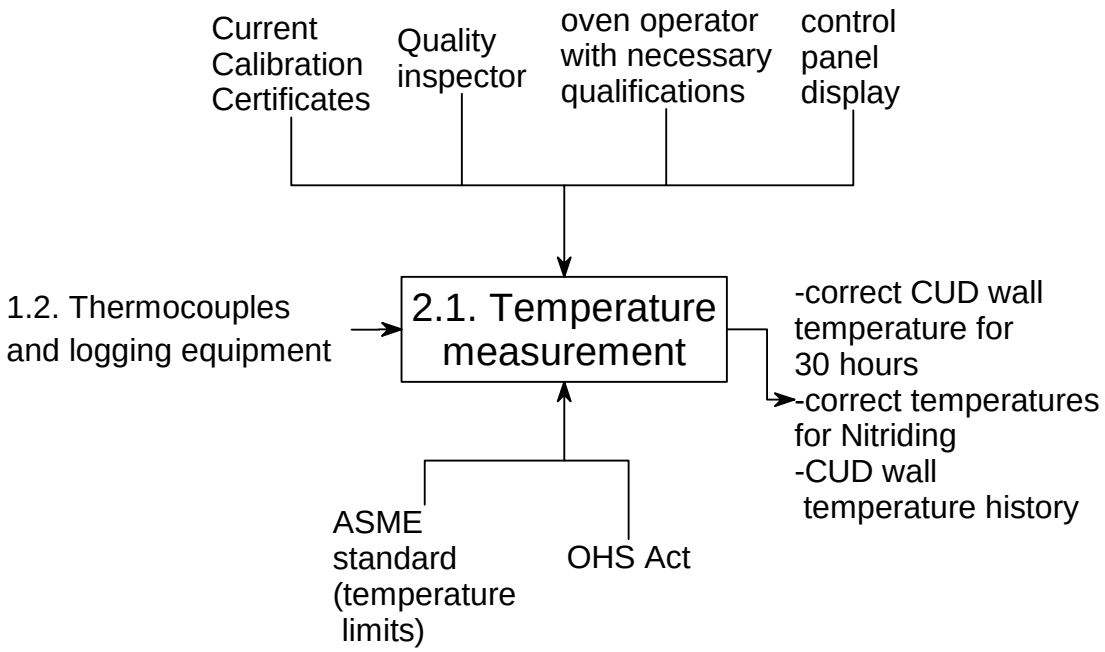

Figure A.8: Flow Diagram of the temperature measurement process

A.9 PROVIDE A CLEAN DRUM FILLED WITH WATER

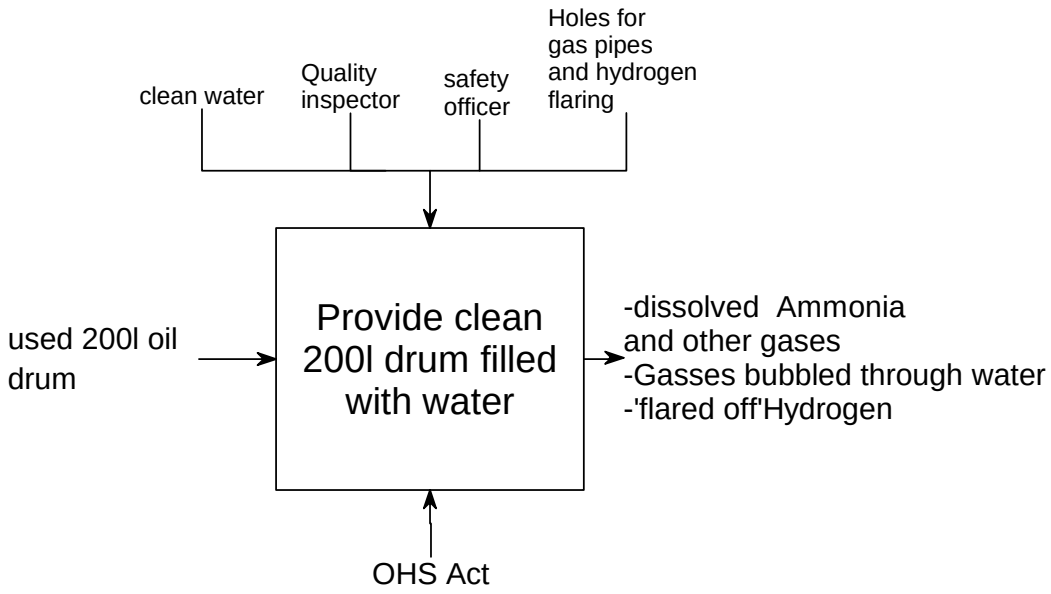

Figure A.9: Flow Diagram of the drum provision task

After the Nitriding process is completed the water, containing the dissolved undissociated NH_3, must be disposed off. Care must be taken since the water may be corrosive and the safety of personnel must be ensured.

APPENDIX B: NP PROCESS FLOW DIAGRAM

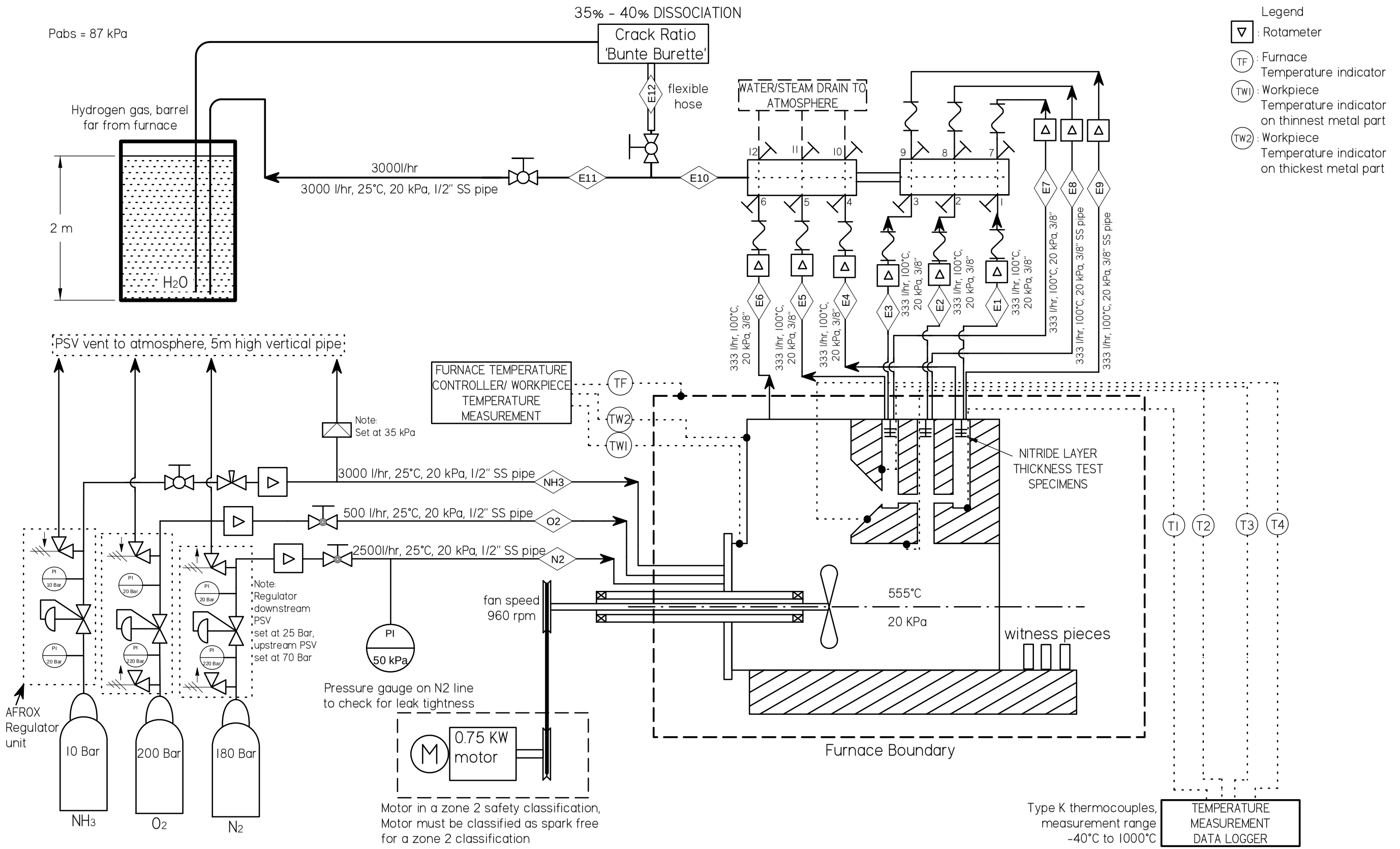

Figure B.1: Process Flow Diagram of the CUD NP as constructed

APPENDIX C: DETAIL CALCULATIONS

All calculations were performed with MathCAD engineering calculation software [53].

C.1 CUD CRADLE COLUMN CODE CALCULATIONS

Code calculation input data (from [46])

width - thickness ratio $\frac{b}{2t_f} = 3.022$

limit for Class 1 section $\frac{145}{\sqrt{350}} = 7.751$

ratio smaller than limit thus Class Section: Class 1

effective length factor (from **[46]** Annex E), column fixed at the bottom and free at the top $K := 1$

resistance factor for structural steel $\varphi := 0.9$

Axial Compression - Flexural Buckling (see clause13.3 in [46])

non-dimensional slenderness parameter $\lambda := \frac{K \cdot L_{col}}{r_x} \cdot \sqrt{\frac{f_y}{\pi^2 \cdot E}} = 0.277$

n exponent $n := 1.34$

Compressive resistance $C_r := \varphi \cdot A_{col} \cdot f_y \cdot \left[1 + \lambda^{(2 \cdot n)}\right]^{\left(\frac{-1}{n}\right)} = 421.907 \cdot kN$

Check compressive resistance $CheckC_r := if\left(C_r > P_{col}, "Acceptable", "Not Acceptable"\right)$

$CheckC_r = "Acceptable"$

Bending - laterally unsupported members (see clause13.5 in [46])

coefficient to account for increased moment resistance of a laterally unsupported beam

$\omega_2 := 1$

about xx direction

Effective length clause 10.4.2.1 in **[46]** $L_{eff} := K \cdot \frac{L_{col}}{r_x} = 18.828 \qquad L_{eff} < 200 = 1$

Plastic Moment resistance $M_p := Z_{pl} \cdot f_y = 18.27 \cdot kN \cdot m$

Factored Moment resistance $M_r := \varphi \cdot M_p$

Critical elastic Moment $M_{crx} := \frac{\omega_2 \cdot \pi}{K \cdot L_{col}} \cdot \sqrt{E \cdot I_y \cdot G \cdot J + \left(\frac{\pi \cdot E}{K \cdot L_{col}}\right)^2 \cdot I_y \cdot C_w} = 54.794 \cdot kN \cdot m$

$0.67 \cdot M_p = 12.241 \cdot kN \cdot m$

Factored moment resistance for laterally unsupported members - Clause 13.6 in Code [2]

$M_{crx} \leq 0.67 M_p = 0$ (true)

Final factored Moment resistance $M_{rx} := \varphi \cdot M_{crx} = 49.314 \cdot kN \cdot m$

Check Moment resistance $CheckM_{rx} := if\left(M_{rx} > M_{longit}, "Acceptable", "Not Acceptable"\right)$

$CheckM_{rx} = "Acceptable"$

This value is larger than the applied lateral moment i.e. $M_{longit} = 30.891 \cdot kN \cdot m$ and it can be concluded that the column is adequate.

about yy direction

Critical elastic Moment $M_{cry} := \frac{\omega_2 \cdot \pi}{K \cdot L_{col}} \cdot \sqrt{E \cdot I_x \cdot G \cdot J + \left(\frac{\pi \cdot E}{K \cdot L_{col}}\right)^2 \cdot I_x \cdot C_w} = 151.413 \cdot kN \cdot m$

Factored moment resistance for laterally unsupported members - Clause 13.6 in Code

$M_{cry} \geq 0.67 M_p = 1$ (true)

Final factored Moment resistance $M_{ry} := \varphi \cdot M_{cry} = 136.272 \cdot kN \cdot m$

Check Moment resistance $CheckM_{ry} := if\left(M_{ry} > M_{longit}, "Acceptable", "Not Acceptable"\right)$

$CheckM_{ry} = "Acceptable"$

This value is larger than the applied lateral moment i.e. $M_{longit} = 30.891 \cdot kN \cdot m$ and it can be concluded that the column is adequate.

Axial Compression and Bending (see clause13.8 in [46])

Ultimate axial load (compressive force) $C_u := P_{col} = 137.293 \cdot kN$

coefficient used to determine equivalent uniform bending effect in beam-columns

$\omega_1 := 0.6$

Euler buckling strength $C_e := \frac{\pi^2 \cdot E \cdot I_x}{L_{col}^2} = 6.226 \times 10^3 \cdot kN$

value of U1 (second order effects) $U_{1x} := \frac{\omega_1}{1 - \frac{C_u}{C_e}} = 0.614$

non-dimensional slenderness parameter about yy $\lambda_y := \frac{K \cdot L_{col}}{r_y} \cdot \sqrt{\frac{f_y}{\pi^2 \cdot E}} = 0.767$

Euler buckling strength about yy $C_{ey} := \frac{\pi^2 \cdot E \cdot I_y}{L_{col}^2} = 815.4 \cdot kN$

value of U1 (second order effects) $U_{1y} := \frac{\omega_1}{1 - \frac{C_u}{C_{ey}}} = 0.721$

Ultimate bending moment in column in x-direction $M_{ux} := \frac{M_{longit}}{2} = 15.445 \cdot kN \cdot m$

Ultimate bending moment in column in y-direction $M_{uy} := \frac{M_{longit}}{2} = 15.445 \cdot kN \cdot m$

a) Overall Member Strength

effective length factor $K_{over} := 1$

non-dimensional slenderness parameter $\lambda_{over} := \frac{K_{over} \cdot L_{col}}{r_y} \cdot \sqrt{\frac{f_y}{\pi^2 \cdot E}} = 0.767$

Compressive resistance for case a) $C_{ra} := \varphi \cdot A_{col} \cdot f_y \cdot \left[1 + \lambda_{over}^{(2 \cdot n)}\right]^{\left(\frac{-1}{n}\right)} = 320.736 \cdot kN$

Moment resistance for lateral torsional buckling $M_{ry} := M_{crx} = 54.794 \cdot kN \cdot m$

overall member strength $Overallmstr := \frac{C_u}{C_{ra}} + \frac{U_{1x} \cdot M_{ux}}{M_{rx}} + \frac{U_{1y} \cdot M_{uy}}{M_{ry}} = 0.824$

Check $CheckOverallmstr := if(Overallmstr < 1, "Acceptable", "Not Acceptable")$

$CheckOverallmstr = "Acceptable"$ see clause 13.8.2. in [2]

b) Lateral Torsional Buckling Strength

effective length factor $K_{lattor} := 1$

factored yield strength, y direction $f_{ey} := \frac{\pi^2 \cdot E}{\left(\frac{K_{lattor} \cdot L_{col}}{r_y}\right)^2} = 510.546 \cdot MPa$

factored yield strength, x direction $f_{ex} := \frac{\pi^2 \cdot E}{\left(\frac{K_{lattor} \cdot L_{col}}{r_x}\right)^2} = 3897.612 \cdot MPa$

polar radius of gyration $r_o := \sqrt{r_x^2 + r_y^2} = 0.051\,m$

factored yield strength, z direction $f_{ez} := \left(\frac{\pi^2 \cdot E \cdot C_w}{K_{lattor}^2 \cdot L_{col}^2} + G \cdot J \right) \cdot \frac{1}{A_{col} \cdot r_o^2} = 890.545 \cdot MPa$

$f_e := f_{ez}$

non-dimensional slenderness parameter $\lambda_{lattor} := \sqrt{\frac{f_y}{f_e}} = 0.58$

Compressive resistance $C_{rb} := \varphi \cdot A_{col} \cdot f_y \cdot \left[1 + \lambda_{lattor}^{(2 \cdot n)} \right]^{\left(\frac{-1}{n} \right)} = 369.555 \cdot kN$

value of U1x (second order effects) $U_{1x} := 1$

value of U1y (second order effects) $U_{1y} := 1$

Moment resistance for lateral torsional buckling $M_{ry} := M_{crx} = 54.794 \cdot kN \cdot m$

lateral torsional member strength $Lattorstr := \frac{C_u}{C_{rb}} + \frac{U_{1x} \cdot M_{ux}}{M_{rx}} + \frac{U_{1y} \cdot M_{uy}}{M_{ry}} = 0.967$

Check Moment resistance $CheckLattorstr := if(Lattorstr < 1, "Acceptable", "Not Acceptable")$

$CheckLattorstr = "Acceptable"$ see clause 13.8.2. in [46]

c) Cross-sectional Strength

effective length factor $K_{lattor} := 1$

non-dimensional slenderness parameter $\lambda_{crossect} := 0$

Compressive resistance $C_{rb} := \varphi \cdot A_{col} \cdot f_y \cdot \left[1 + \lambda_{crossect}^{(2 \cdot n)} \right]^{\left(\frac{-1}{n} \right)} = 432 \cdot kN$

value of U1x (second order effects) $U_{1x} := 1$

value of U1y (second order effects) $U_{1y} := 1$

Moment resistance for lateral torsional buckling $M_{ry} := M_{crx} = 54.794 \cdot kN \cdot m$

lateral torsional member strength $Lattorstr := \frac{C_u}{C_{rb}} + \frac{U_{1x} \cdot M_{ux}}{M_{rx}} + \frac{U_{1y} \cdot M_{uy}}{M_{ry}} = 0.913$

Check Moment resistance $CheckLattorstr := if(Lattorstr < 1, "Acceptable", "Not Acceptable")$

$CheckLattorstr = "Acceptable"$ see clause 13.8.2. **in [46]**

c) Cross-sectional Strength

effective length factor $K_{lattor} := 1$

non-dimensional slenderness parameter $\lambda_{crossect} := 0$

Compressive resistance $C_{rb} := \varphi \cdot A_{col} \cdot f_y \cdot \left[1 + \lambda_{crossect}^{(2 \cdot n)}\right]^{\left(\frac{-1}{n}\right)} = 432 \cdot kN$

value of U1x (second order effects) $U_{1x} := 1$

value of U1y (second order effects) $U_{1y} := 1$

Moment resistance for lateral torsional buckling $M_{ry} := M_{crx} = 54.794 \cdot kN \cdot m$

lateral torsional member strength $Lattorstr := \frac{C_u}{C_{rb}} + \frac{U_{1x} \cdot M_{ux}}{M_{rx}} + \frac{U_{1y} \cdot M_{uy}}{M_{ry}} = 0.913$

Check Moment resistance $CheckLattorstr := if(Lattorstr < 1, "Acceptable", "Not Acceptable")$

$CheckLattorstr = "Acceptable"$ see clause 13.8.2. in [46]

Biaxial Bending (see clause13.6 e) in [46])

Biaxial bending sum $Biaxbending := \frac{M_{ux}}{M_{rx}} + \frac{M_{uy}}{M_{ry}} = 0.595$

Check biaxial bending $CheckBiaxbend := if(Lattorstr < 1, "Acceptable", "Not Acceptable")$

$CheckBiaxbend = "Acceptable"$

Conclusion

The PFC120X55 beam is adequate. If a bending load is considered with the vertical support force divided equally between the four vertical columns, the columns are also adequate with K =1. If K = 2 is assumed for checking pure buckling due to concentric loading, the column still is adequate with a safety factor of 3. The compressive stress in the column if the full weight of the CUD is placed on a single column is $\sigma_c = -85.808 \cdot MPa$, which is well below the yield stress of $f_y = 3 \times 10^8 Pa$.

C.2 FLANGE BOLT LOAD AND TORQUE CALCULATIONS

C.2.1 INPUT DATA

Gasket minimum seating stress	$S_m := 60MPa$
Torque coefficient	$K := 0.2$
Human force application	$F_H := 40kg \cdot g = 392.266\ N$

C.2.2 DETAIL CALCULATIONS

Gasket 1, Weld Neck/Fan shaft flange (800 OD)

outer diameter	$OD := 800mm$
inner diameter	$ID := 535mm$
bolt diameter	$d_b := 36mm$
number of bolts	$n := 16$
Gasket area	$A_g := \frac{\pi \cdot \left(OD^2 - ID^2\right)}{4} = 0.278\ m^2$
Minimum bolt tension force	$F_t := S_m \cdot A_g = 277.854 \cdot kN$
Tension force per bolt	$F_b := \frac{F_t}{n} = 17.366 \cdot kN$
minimum torque per bolt	$T := K \cdot F_b \cdot d_b = 125.034 \cdot N \cdot m$
torque per bolt for a seating stress of 60 MPa	$T := K \cdot F_b \cdot d_b = 7502.064 \cdot N \cdot m$
moment arm for a 40kg human force or seating stress of 2 MPa and 80 kg human force	$x := \frac{T}{F_H} = 318.749 \cdot mm$
moment arm for a seating stress of 60 MPa	$x := \frac{T}{F_H} = 19.125 \cdot m$
weld neck flange thickness	$t := 210mm$
sealing flange and gasket thickness	$t2 := 14mm$
bolt loaded length	$L := t + t2 = 224 \cdot mm$
bolt area	$A_b := \frac{\pi \cdot d_b^{\ 2}}{4}$

Modulus of Elasticity $E := 140GPa$

Bolt deflection as input for FEA model
bolt pre displacement, 1MPa seating stress $\delta := \frac{F_b \cdot L}{E \cdot A_b} = 0.027 \cdot mm$

Gasket2, Spindle hole (815 OD)

outer diameter $OD := 815mm$

inner diameter $ID := 650mm$

bolt diameter $d_b := 36mm$

number of bolts $n := 18$

Gasket area $A_g := \frac{\pi \cdot \left(OD^2 - ID^2\right)}{4} - n \cdot \left(\frac{\pi \cdot {d_b}^2}{4}\right) = 0.172\,m^2$

Minimum bolt tension force $F_t := S_m \cdot A_g = 0.172 \cdot MN$

Tension force per bolt $F_b := \frac{F_t}{n} = 9.529 \cdot kN$

minimum torque per bolt $T := K \cdot F_b \cdot d_b = 68.611 \cdot N \cdot m$

moment arm for a 40kg human force $x := \frac{T}{F_H} = 174.91 \cdot mm$

Gasket 3 (275mm OD, valve insert flanges)

outer diameter $OD := 275mm$

inner diameter $ID := 130mm$

bolt diameter $d_b := 20mm$

number of bolts $n := 12$

Gasket area $A_g := \frac{\pi \cdot \left(OD^2 - ID^2\right)}{4} - n \cdot \left(\frac{\pi \cdot {d_b}^2}{4}\right) = 0.042\,m^2$

Minimum bolt tension force $F_t := S_m \cdot A_g = 0.042 \cdot MN$

Tension force per bolt $F_b := \frac{F_t}{n} = 3.529 \cdot kN$

minimum torque per bolt $T := K \cdot F_b \cdot d_b = 14.118 \cdot N \cdot m$

moment arm for a 40kg human force $x := \frac{T}{F_H} = 35.99 \cdot mm$

Gasket 4 (195mm OD, sphere pipe flanges)

outer diameter $OD := 245mm$

inner diameter $ID := 50mm$

bolt diameter $d_b := 25.4mm$

number of bolts $n := 8$

Gasket area $A_g := \frac{\pi \cdot \left(OD^2 - ID^2\right)}{4} - n \cdot \left(\frac{\pi \cdot {d_b}^2}{4}\right) = 0.041\,m^2$

Minimum bolt tension force $F_t := S_m \cdot A_g = 0.041 \cdot MN$

Tension force per bolt $F_b := \frac{F_t}{n} = 5.141 \cdot kN$

minimum torque per bolt $T := K \cdot F_b \cdot d_b = 26.115 \cdot N \cdot m$

moment arm for a 40kg human force $x := \frac{T}{F_H} = 66.575 \cdot mm$

C.3 ASME VIII DIV. 1 DESIGN BY FORMULA - WELD NECK SEALING FLANGE

Blind Flange Design - ASME VIII Div 1 Edition 2001 With Addenda 2003

Consider Appendix 2 - Rules for flange connections with Ring Type Gaskets.

Nomenclature:

Bolt design stress at ambient temperature	$S_a := 35 \cdot ksi$	$S_a = 241.3 \cdot MPa$
Bolt Design Stress at design temperature	$S_b := 24.5 \cdot ksi$	$S_b = 168.9 \cdot MPa$

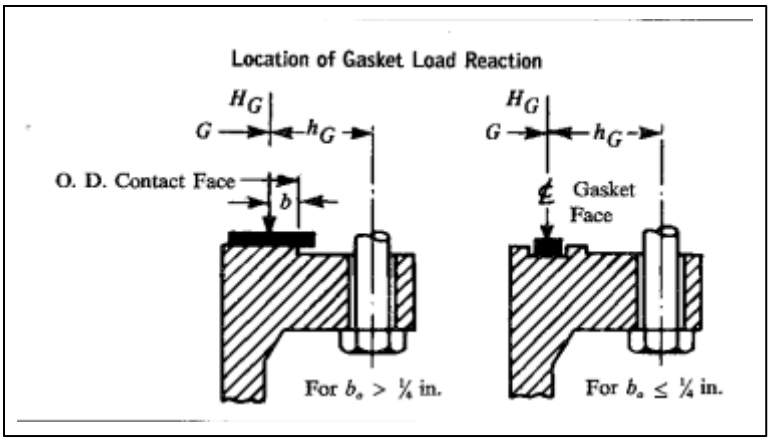

The above figure has been extracted from Table 2-5.2 in [9]

Outside Diameter of Flange: $A := 1165 \cdot mm$

Bolt Circle Diameter: $C := 1100 \cdot mm$

Number of Bolts: $n := 16$

Cross section Area of Bolt 1"UNC 8TPI to ASME B1.1: $A_{bs} := \frac{\pi}{4} \cdot (36 \cdot mm)^2 = 1.018 \times 10^3 \cdot mm^2$

Total bolt area (Actual): $A_b := n \cdot A_{bs} = 0.016\, m^2$

From Table 2-5.1:

Gasket Factor m (from Klinger): $m := 3$

Minimum design seating Stress: $y := 1MPa$

width of gasket: $w := 137.58mm$

Basic Gasket seating width b_0: $b_0 := \frac{w}{4} = 34.395 \cdot mm$

Effective Gasket Seating Width b: $b := b_0 = 34.395 \cdot mm$

Gasket Mean Diameter G_{mean}: $G_{mean} := 662.5mm$

Gasket Outside Diameter G_{od}: $G_{od} := 800mm$

Gasket load reaction diameter:

$$G := if\left(b_0 \le 0.25 \cdot in, G_{mean}, G_{od} - 2 \cdot b\right) = 731.21 \cdot mm$$

Radial Distances: $h_G := \frac{C - G}{2} = 184.395 \cdot mm$

Hydrostatic end Force: $H := \left(0.785 \cdot G^2 \cdot P\right) = 10.493 \cdot kN$

Total joint contact surface compression load:

$$H_P := 2 \cdot b \cdot \pi \cdot G \cdot m \cdot P = 11.852 \cdot kN$$

Minimum Required bolt load for Design Conditions:

$$W_{m1} := H + H_P = 22.345 \cdot kN$$

Minimum required bolt load for Gasket seating:

$$W_{m2} := \pi \cdot b \cdot G \cdot y = 79.011 \cdot kN$$

Required Total Bolt Section Area:

$$A_m := \max\left(\frac{W_{m1}}{S_b}, \frac{W_{m2}}{S_a}\right) = 327.42 \cdot mm^2$$

$Bolt\_Size := if\left(A_b < A_m, "Not\ Acceptable", "Acceptable"\right)$

$Bolt\_Size = "Acceptable"$

$$A_{m2} := \frac{W_{m2}}{S_a} = 327.42 \cdot mm^2$$

Flange Design Bolt load: Internal Pressure

$$W := \max\left[W_{m1}, \frac{(A_m + A_b)\cdot S_a}{2}\right] = 2.005 \times 10^3 \cdot kN$$

Gasket Load: $H_G := W - H = 1.994 \times 10^3 \cdot kN$

Formula for Minimum Thickness of flat head UG-34

diameter, in (mm): $d := 0.75m = 0.75\,m$

a factor depending upon the method of attachment of head, shell dimensions, and other items as listed in UG-34, dimensionless (Fig.UG-34): $C_. := 0.3$

Stress value of Blind Flange @ Design Temperature $S_{DT} := 15 \cdot ksi$ $S_{DT} = 103.4 \cdot MPa$

Stress value of Blind Flange @ atmospheric Temperature $S_{AT} := 38 \cdot ksi$ $S_{AT} = 262 \cdot MPa$

Joint efficiency $E := 1$

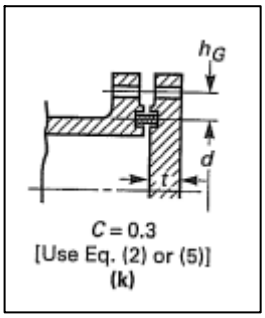

Operating Conditions:

$$t_1 := \left(d \cdot \sqrt{\frac{C_. \cdot P}{S_{DT} \cdot E} + \frac{1.9 \cdot W_{m1} \cdot h_G}{S_{DT} \cdot E\, d^3}}\right) = 11.905 \cdot mm$$

Gasket Seating:

$$t_2 := \left(d \cdot \sqrt{\frac{1.9 \cdot W_{m2} \cdot h_G}{S_{AT} \cdot E \cdot d^3}}\right) = 11.869 \cdot mm$$

minimum required flange thickness $t := \max(t_1, t_2) = 22.208 \cdot mm$

Compare to actual flange thickness $flpass := \text{if}(t < t_f, \text{"Acceptable"}, \text{"Not Acceptable"})$

$flpass = \text{"Acceptable"}$

This is marginal, and because there is a large hole in the centre for the fan shaft pipe a reinforcement thickness calculation is still necessary. The material allowable for gasket seating conditions at atmospheric temperature is stated as 262 MPa (yield is 300 MPa. The large ASME safety factor for allowables stress is thus removed. Further analysis is thus required.

C.4 WELD NECK SEALING FLANGE PRELIMINARY FEA MODELS

A number of preliminary FEA models were created for the weld neck sealing flange stress analysis. The calculation in Table C.1 shows the flange stress state with no gasket seating stress (leaking condition). The FEA results are very close to the analytically calculated stress values (see below) for a diaphragm or circular plate as described in [56] p. 377.

operating pressure	$p := 20kPa$	flange thickness	$h := 12mm$
Poisson's ratio	$\nu := 0.3$	outer radius	$a := \frac{700}{2}mm$

Clamped periphery [56]

$$\sigma := \frac{3 \cdot p \cdot a^2}{4 \cdot h^2} = 12.76 \cdot MPa$$

simply supported periphery [56]

$$M_r := \frac{p \cdot a^2}{16} \cdot (3 + \nu) = 505.313\ N$$

stress [56]

$$\sigma := \frac{6 \cdot M_r}{h^2} = 21.055 \cdot MPa$$

Table C.1: First FEA model of weld neck sealing flange created with Strand 7 FEA software.

First FEA The model, fixed restraints at bolt locations, no sealing edge (incorrect)	Load application, 20kPa Face pressure
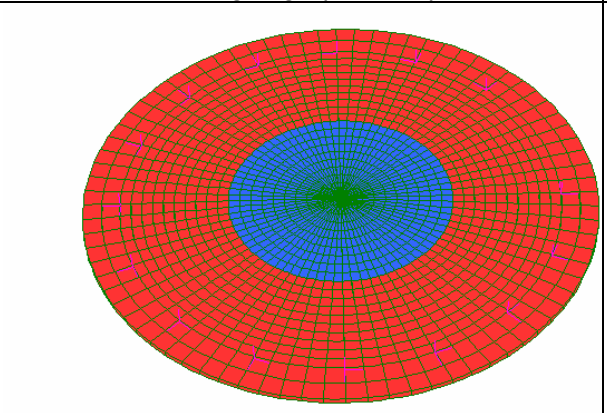	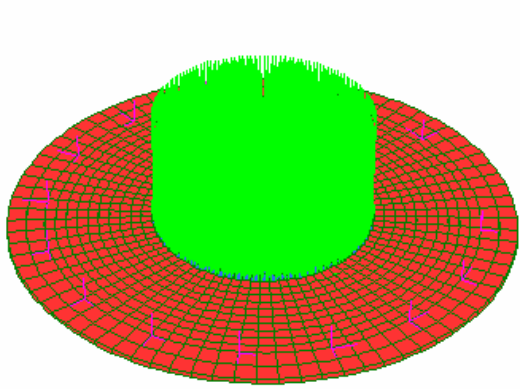
Close-up view	Von Mises Stresses:
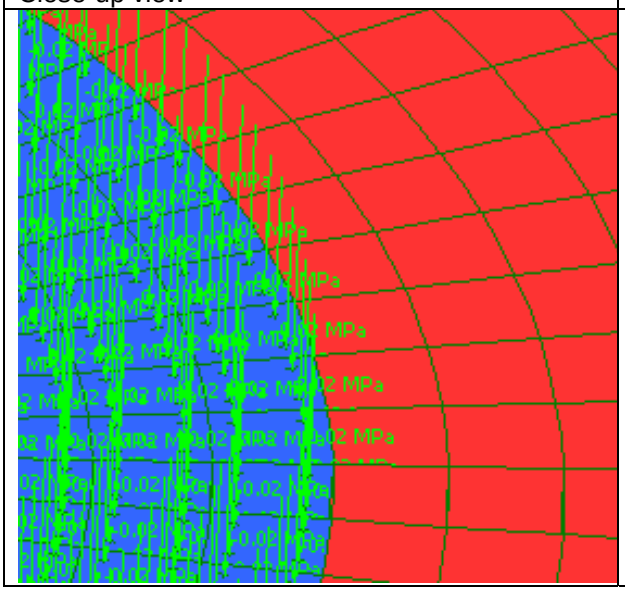	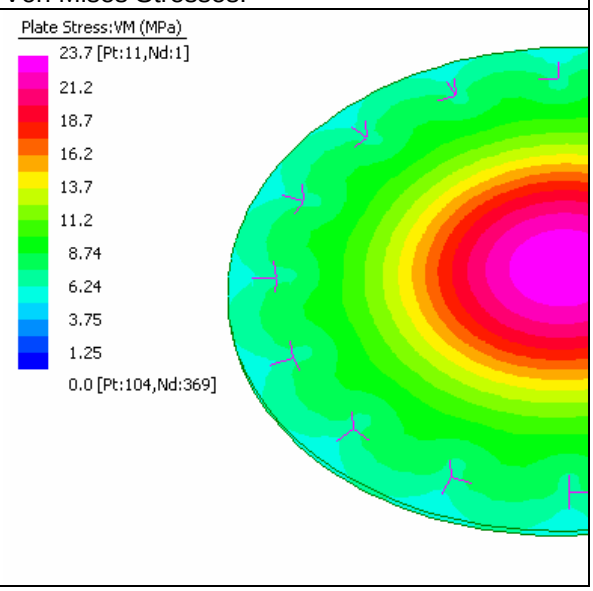

C.5 THREE DIMENSIONAL FEA MODEL OF THE ENTIRE FAN SHAFT ASSEMBLY

Various FEA models, with different boundary conditions, were created and analysed before arriving at the correct model. Results of these different iterations are given in Table C.2. The final model in chapter 6 represents the most accurate deflection and boundary conditions.

Table C.2: Various FEA results with different boundary conditions.

Tresca stress:No end forces, only gravity and internal pressure	Vertical displacement: Only end forces, and gravity no pressure.
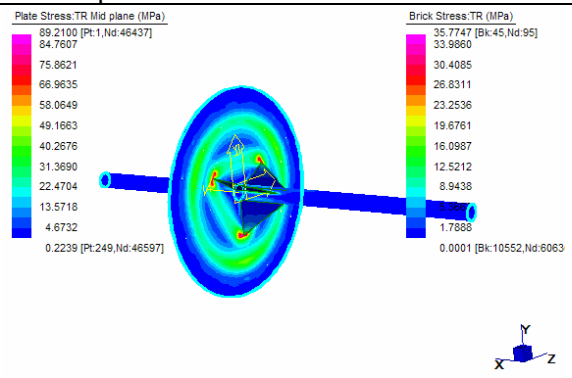	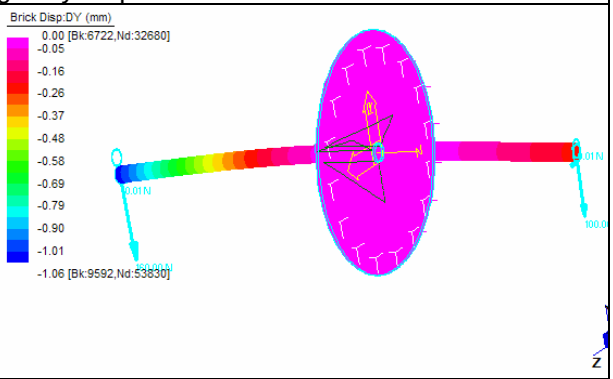
vertical displacement: Only gravity of fan pipe support, no shaft, (calculated in chapter 4 as 0.45mm)	final model, with gradual seating stress, but no pre displacement on bolts only fixed restraints:
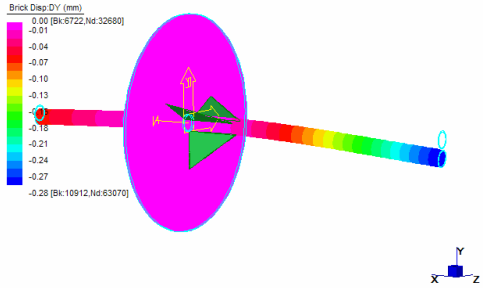	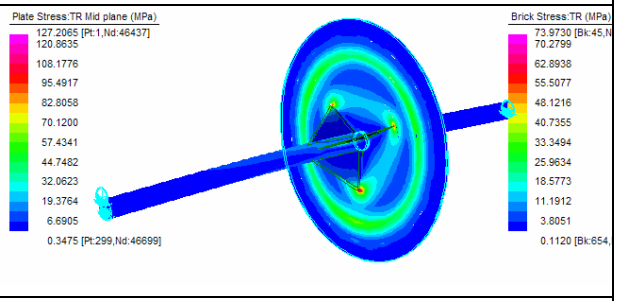
Vertical displacement for 1mm bolt pre-displacement	Axial displacement for 1mm bolt pre-displacement
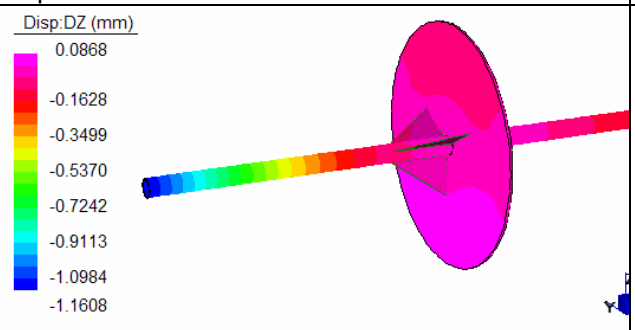	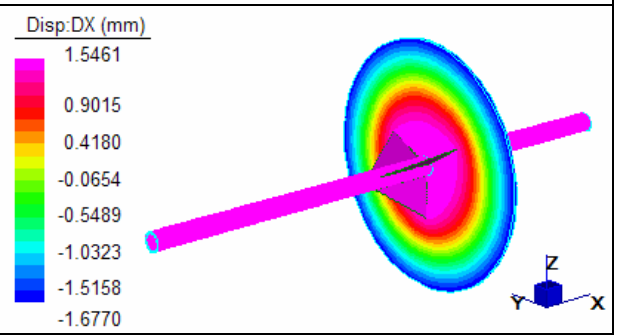
Stresses: bolt pre displacement of 1 mm, 1 MPa seating stress	Stresses: predisplacement of 2mm, 1 MPa seating stress:
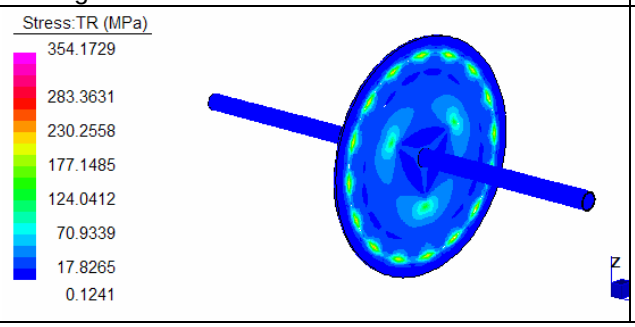	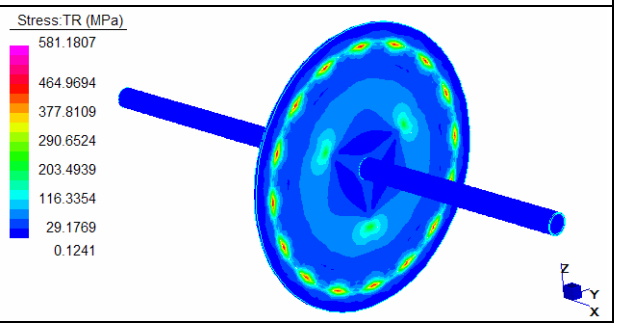

A modal analysis was also performed with Strand 7 using the natural frequency solver. The resulting deflected mode shapes and their frequencies are given in Table C.3.

Table C.3: Natural frequencies and displacement modes for the Fan Shaft Assembly.

1: 14.1 Hz:	2: 14.13 Hz:
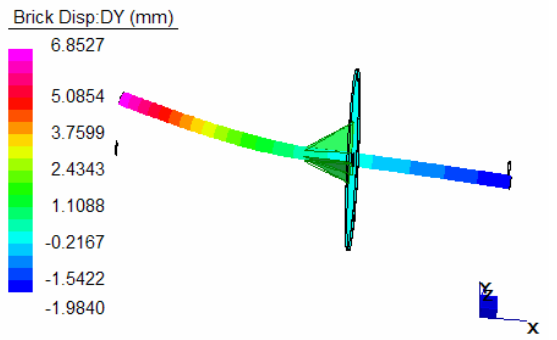	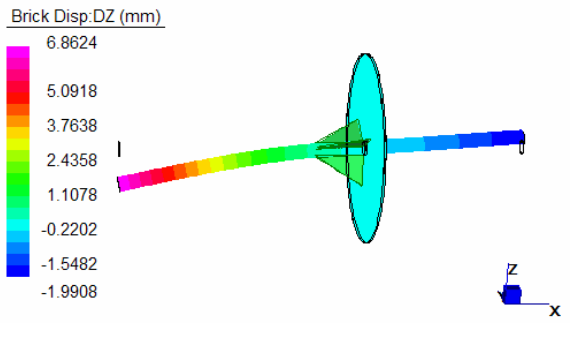
3: 26.23 Hz	4: 26.36 Hz
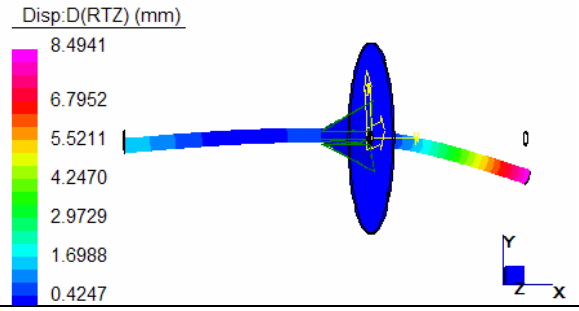	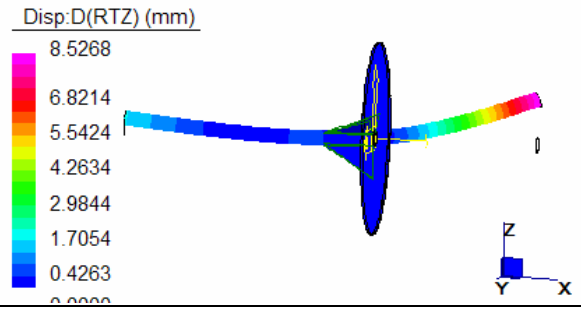
5: 93.572 Hz	6: 132.989 Hz
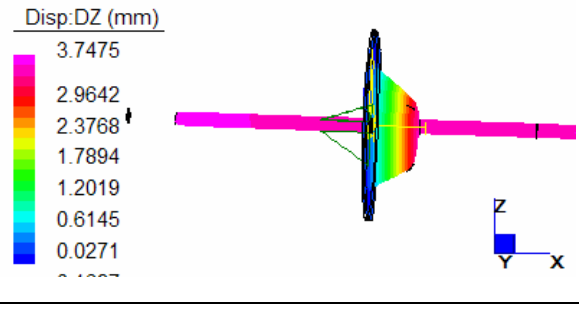	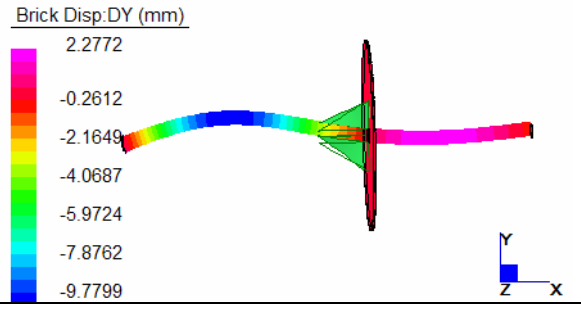
7: 136.382Hz	8: 192.931 Hz
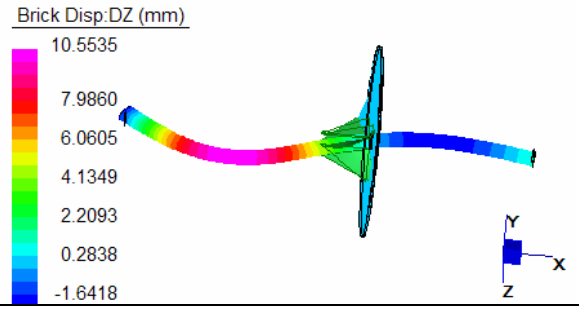	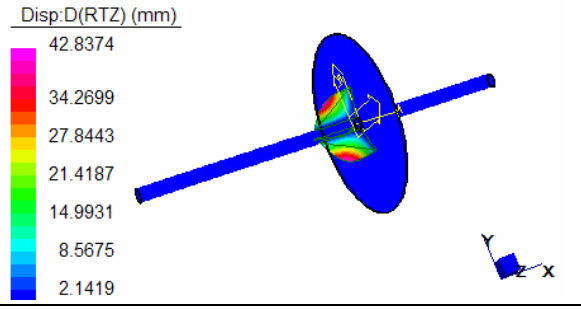

The first 2 mode shapes involve deflection of the extended length shaft support pipe end. During the third and fourth mode shapes the long end of the support pipe deflects. The fifth mode shape involves the axial movement of the sealing flange. The rotation speed of the fan shaft at 45 Hz is not close to any of the natural frequencies and will not cause excitation.

APPENDIX D: DETAIL WORKS DRAWINGS

This appendix contains the detail drawings of the mechanical components that were manufactured for the CUD NP. The drawings included are listed in Table D.1. The full bill of materials including various blots and nuts, valves and flowmeters that were purchased is beyond the scope of this research, however part of it can be seen in the price list of Table 4.9. A detail drawing of the CUD housing, to which the flanges are fastened, is also given (item 12 in Table 4.9) in order to describe the inside of the nitriding process chamber.

Table D.1: Drawing list and part of the Bill of Materials

No.	Description	Drawing number	Quantity	Page
1	Fan shaft flange assembly	IST010769	1	168
2	Internal shaft welded assembly	IST010763	1	169
3	Flange shaft welded assembly, diameter 1105	IST010517	1	170
4	Outer shaft (shaft support pipe)	IST010690	1	171
5	Fan cap (hub)	IST010796	1	172
6	Graphite bearing cap	IST010773	1	173
7	Graphite bearing	IST010768	4	174
8	Flange assembly, diameter 815 (spindle hole)	IST010526	1	175
9	Gaskets	IST011549	N/A	176
10	CUD cradle assembly	N/A	1	177
11	CUD cradle support	N/A	2	178
12	CUD Housing with spindle installed	N/A	1	179

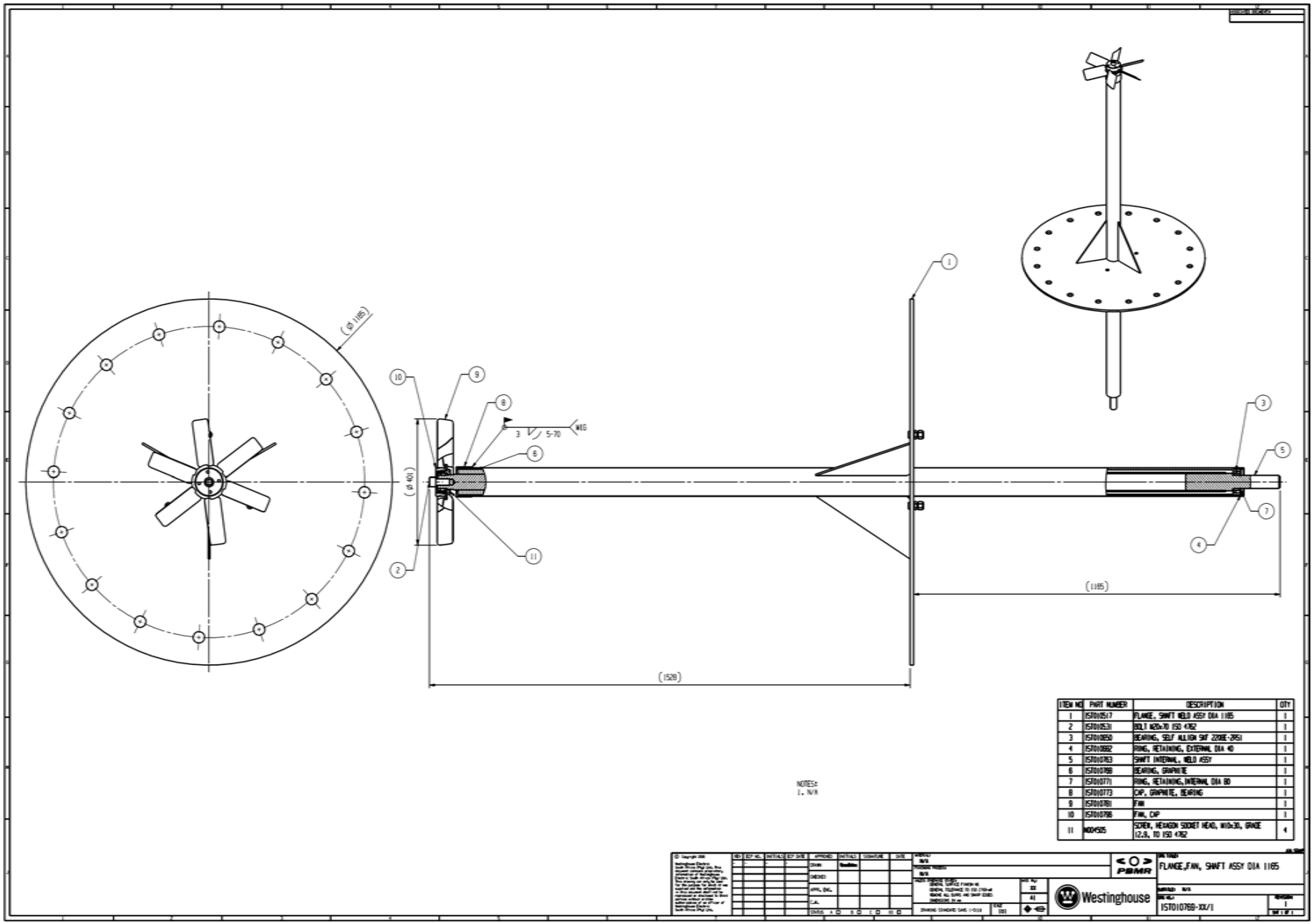

ITEM NO	PART NUMBER	DESCRIPTION	QTY
1	IST010517	FLANGE, SHAFT WELD ASSY DIA 1185	1
2	IST010531	BOLT M20x70 ISO 4762	1
3	IST010850	BEARING, SELF ALLIGN SKF 22208E-2RS1	1
4	IST010882	RING, RETAINING, EXTERNAL DIA 40	1
5	IST010763	SHAFT INTERNAL, WELD ASSY	1
6	IST010788	BEARING, GRAPHITE	1
7	IST010771	RING, RETAINING, INTERNAL DIA 80	1
8	IST010773	CAP, GRAPHITE, BEARING	1
9	IST010781	FAN	1
10	IST010798	FAN, CAP	1
11	M004505	SCREW, HEXAGON SOCKET HEAD, M10x30, GRADE 12.9, TO ISO 4762	4

REV	ECP NO.	INITIALS	ECP DATE	APPROVED	INITIALS	SIGNATURE	DATE	MATERIAL: N/A FINISH: N/A	PBMR	DRAWING TITLE: FLANGE,FAN, SHAFT ASSY DIA 1185
				DRAWN						
				CHECKED						
				APPR. ENG.						
				Q.A.						
				STATUS: A ☐ B ☐ C ☐ D ☐					Westinghouse	IST010769-XX/1

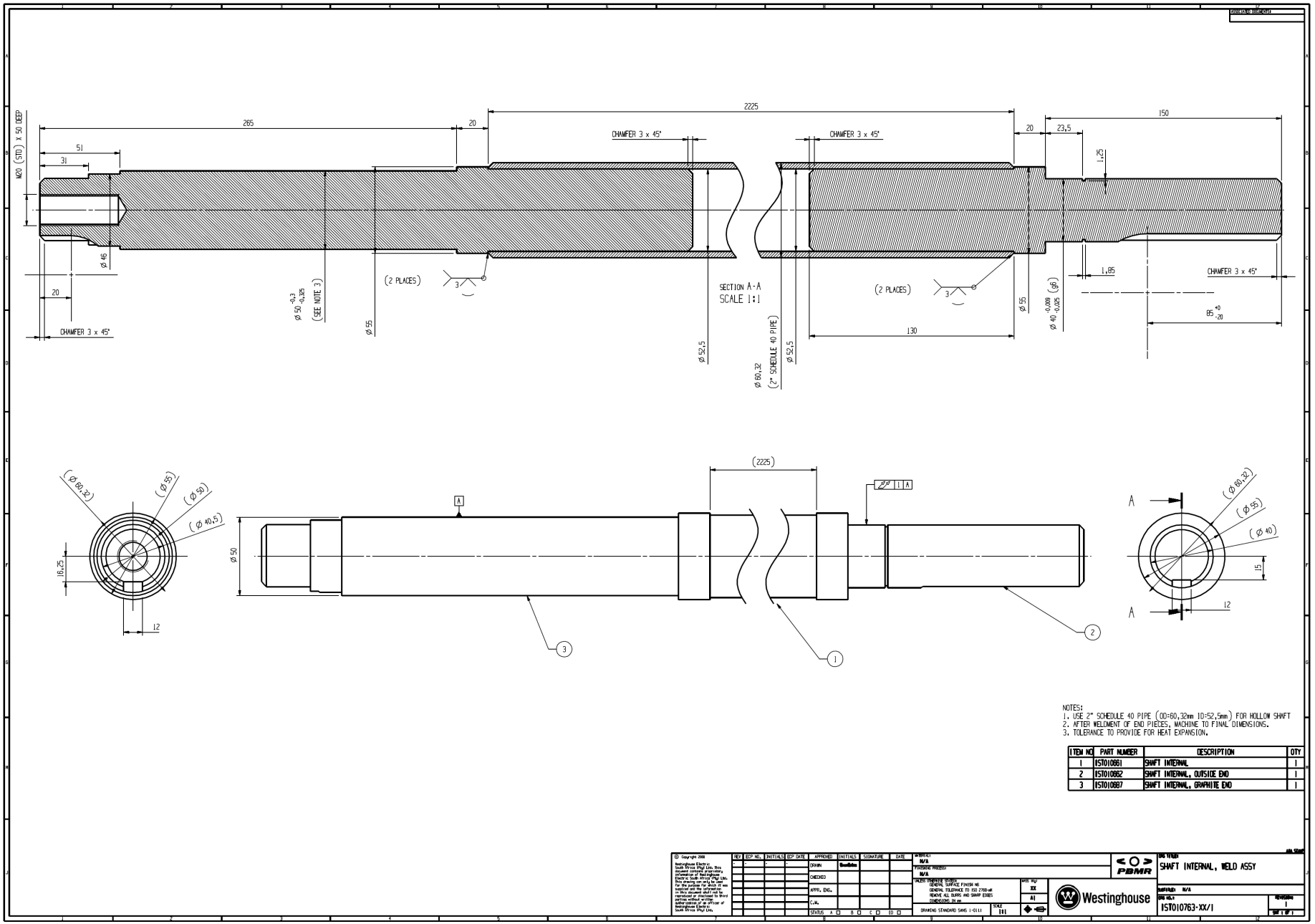

NOTES:
1. USE 2" SCHEDULE 40 PIPE (OD=60,32mm ID=52,5mm) FOR HOLLOW SHAFT
2. AFTER WELDMENT OF END PIECES, MACHINE TO FINAL DIMENSIONS.
3. TOLERANCE TO PROVIDE FOR HEAT EXPANSION.

ITEM NO	PART NUMBER	DESCRIPTION	QTY
1	IST010861	SHAFT INTERNAL	1
2	IST010862	SHAFT INTERNAL, OUTSIDE END	1
3	IST010887	SHAFT INTERNAL, GRAPHITE END	1

REV	ECP NO.	INITIALS	ECP DATE

	APPROVED	INITIALS	SIGNATURE	DATE
DRAWN				
CHECKED				
APPR. ENG.				
C.M.				

STATUS A ☐ B ☐ C ☐ D ☐

MATERIAL: N/A
FINISHING PROCESS: N/A
UNLESS OTHERWISE STATED:
GENERAL SURFACE FINISH N8.
GENERAL TOLERANCE TO ISO 2768-mK
REMOVE ALL BURRS AND SHARP EDGES
DIMENSIONS IN mm
DRAWING STANDARD SANS 1-0111
SCALE 1:1
WEIGHT: XX
SIZE: A1

PBMR

Westinghouse

DESCRIPTION: SHAFT INTERNAL, WELD ASSY
DRAWING NO.: IST010763-XX/1
REVISION: 1
SHT 1 OF 1

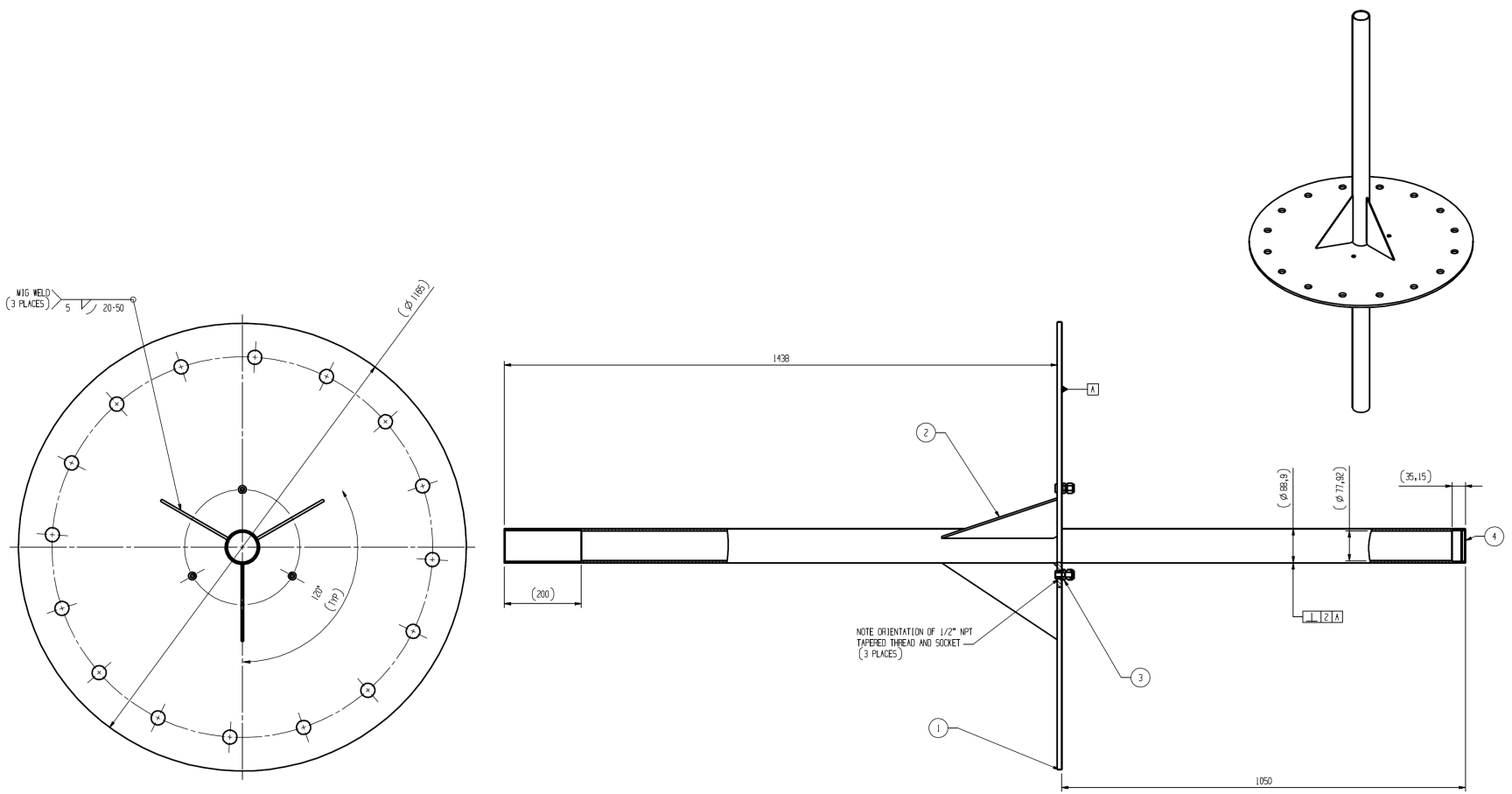

NOTES:
1. N/A

ITEM NO	PART NUMBER	DESCRIPTION	QTY
1	IST010511	FLANGE, DIA 1165	1
2	IST010518	GUSSET	3
3	IST010582	COUPLING, STRAIGHT 1/2"NPT-1/2" TUBE	3
4	IST010690	SHAFT, OUTER	1

REV	ECP NO.	INITIALS	ECP DATE

	APPROVED	INITIALS	SIGNATURE	DATE
DRAWN				
CHECKED				
APPD. ENG.				
C.M.				

STATUS A ☐ B ☐ C ☐ 10 ☐

INTERFACE: N/A
FINISHING PROCESS: N/A
UNLESS OTHERWISE STATED:
GENERAL SURFACE FINISH N9
GENERAL TOLERANCE TO ISO 2768-mK
REMOVE ALL BURRS AND SHARP EDGES
DIMENSIONS IN mm
DRAWING STANDARD SANS 1-0111
SCALE 1:1
MISC. Ref XX
A1

PBMR

Westinghouse

DRG TITLE: FLANGE, SHAFT WELD ASSY DIA 1165
DRG NO.: IST010517-XX/1
REVISION: 1
SHT 1 OF 1

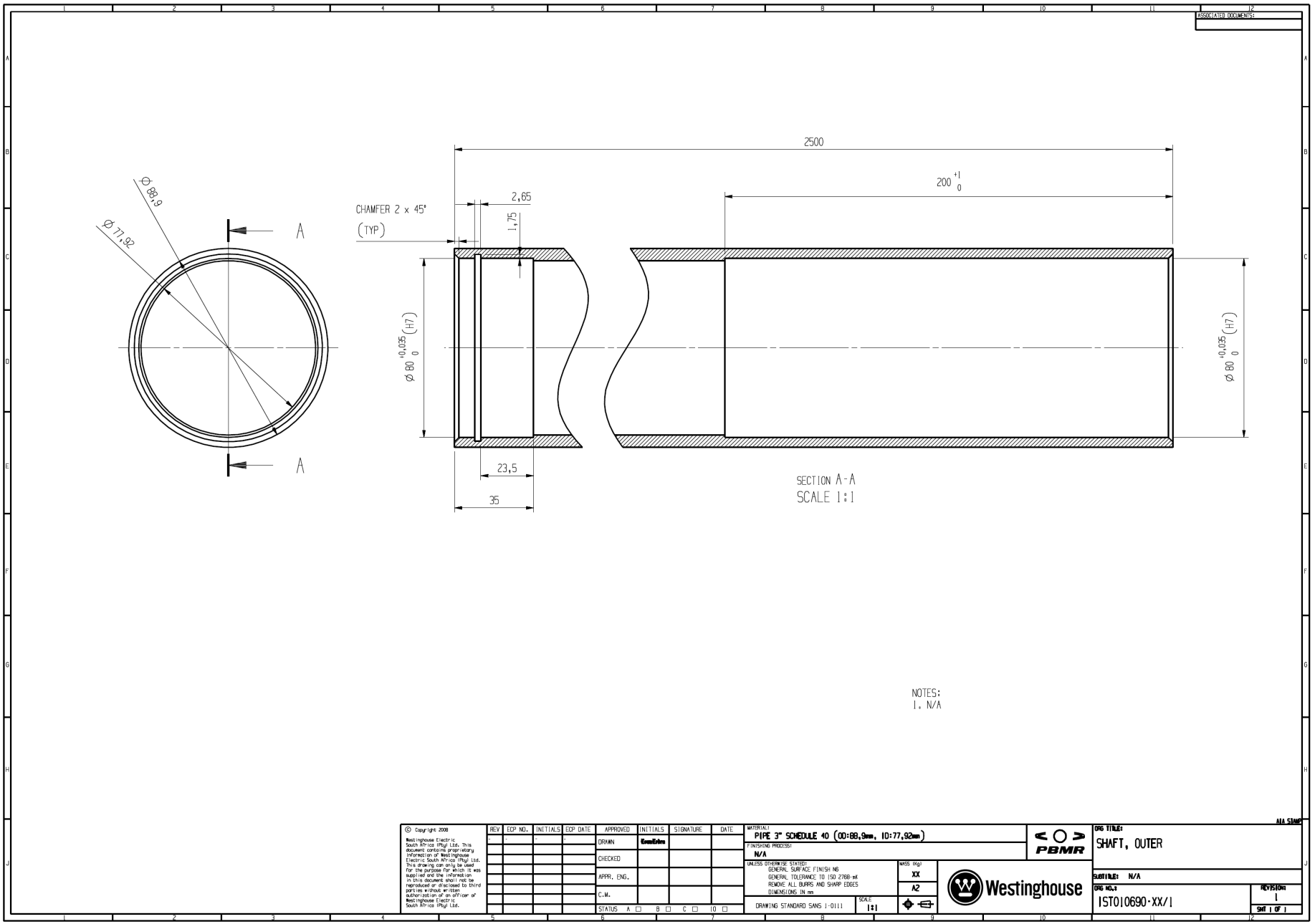
ASSOCIATED DOCUMENTS:
Ø 88,9
Ø 77,92
A
A
CHAMFER 2 x 45°
(TYP)
2,65
1,75
2500
200 +1 0
Ø 80 +0,035 0 (H7)
Ø 80 +0,035 0 (H7)
23,5
35
SECTION A-A
SCALE 1:1
NOTES:
1. N/A
© Copyright 2008
Westinghouse Electric South Africa (Pty) Ltd. This document contains proprietary information of Westinghouse Electric South Africa (Pty) Ltd. This drawing can only be used for the purpose for which it was supplied and the information in this document shall not be reproduced or disclosed to third parties without written authorization of an officer of Westinghouse Electric South Africa (Pty) Ltd.
REV
ECP NO.
INITIALS
ECP DATE
APPROVED
INITIALS
SIGNATURE
DATE
DRAWN
CHECKED
APPR. ENG.
C.M.
STATUS A B C 10
MATERIAL:
PIPE 3" SCHEDULE 40 (OD:88,9mm, ID:77,92mm)
FINISHING PROCESS:
N/A
UNLESS OTHERWISE STATED:
GENERAL SURFACE FINISH N6
GENERAL TOLERANCE TO ISO 2768-mK
REMOVE ALL BURRS AND SHARP EDGES
DIMENSIONS IN mm
DRAWING STANDARD SANS 1-0111
MASS (Kg)
XX
A2
SCALE
1:1
PBMR
Westinghouse
DRG TITLE:
SHAFT, OUTER
SUBTITLE: N/A
DRG NO.:
1ST010690-XX/1
REVISION:
1
SHT 1 OF 1

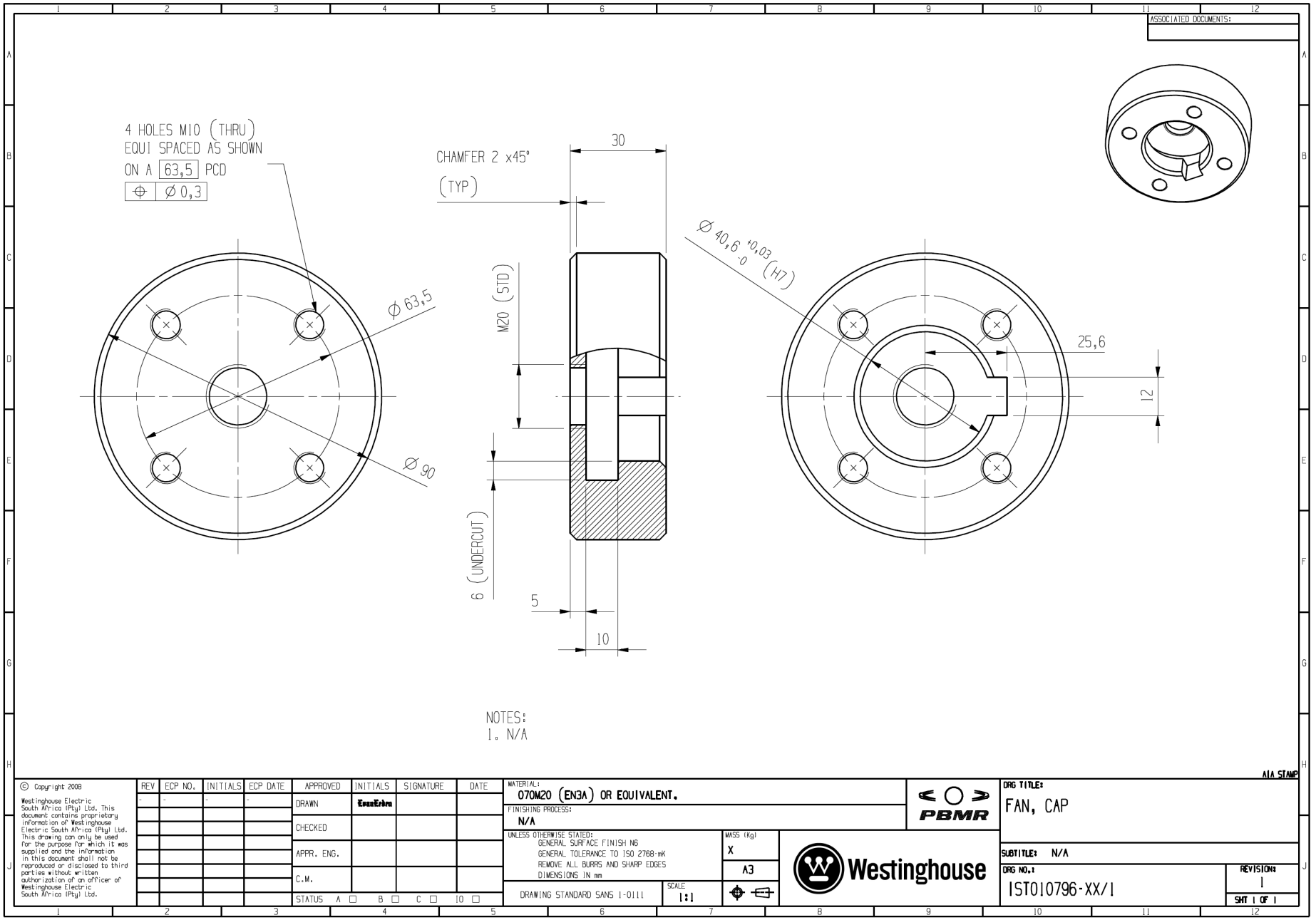
ASSOCIATED DOCUMENTS:
4 HOLES M10 (THRU)
EQUI SPACED AS SHOWN
ON A 63,5 PCD
⌖ Ø 0,3
CHAMFER 2 x45°
(TYP)
30
M20 (STD)
6 (UNDERCUT)
5
10
Ø 63,5
Ø 90
Ø 40,6 +0,03 -0 (H7)
25,6
12
NOTES:
1. N/A
AIA STAMP
© Copyright 2008
Westinghouse Electric South Africa (Pty) Ltd. This document contains proprietary information of Westinghouse Electric South Africa (Pty) Ltd. This drawing can only be used for the purpose for which it was supplied and the information in this document shall not be reproduced or disclosed to third parties without written authorization of an officer of Westinghouse Electric South Africa (Pty) Ltd.
REV | ECP NO. | INITIALS | ECP DATE
APPROVED | INITIALS | SIGNATURE | DATE
DRAWN
CHECKED
APPR. ENG.
C.M.
STATUS A ☐ B ☐ C ☐ 10 ☐
MATERIAL: 070M20 (EN3A) OR EQUIVALENT.
FINISHING PROCESS: N/A
UNLESS OTHERWISE STATED:
GENERAL SURFACE FINISH N6
GENERAL TOLERANCE TO ISO 2768-mK
REMOVE ALL BURRS AND SHARP EDGES
DIMENSIONS IN mm
MASS (Kg) X
A3
DRAWING STANDARD SANS 1-0111
SCALE 1:1
PBMR
Westinghouse
DRG TITLE: FAN, CAP
SUBTITLE: N/A
DRG NO.: 1ST010796-XX/1
REVISION: 1
SHT 1 OF 1

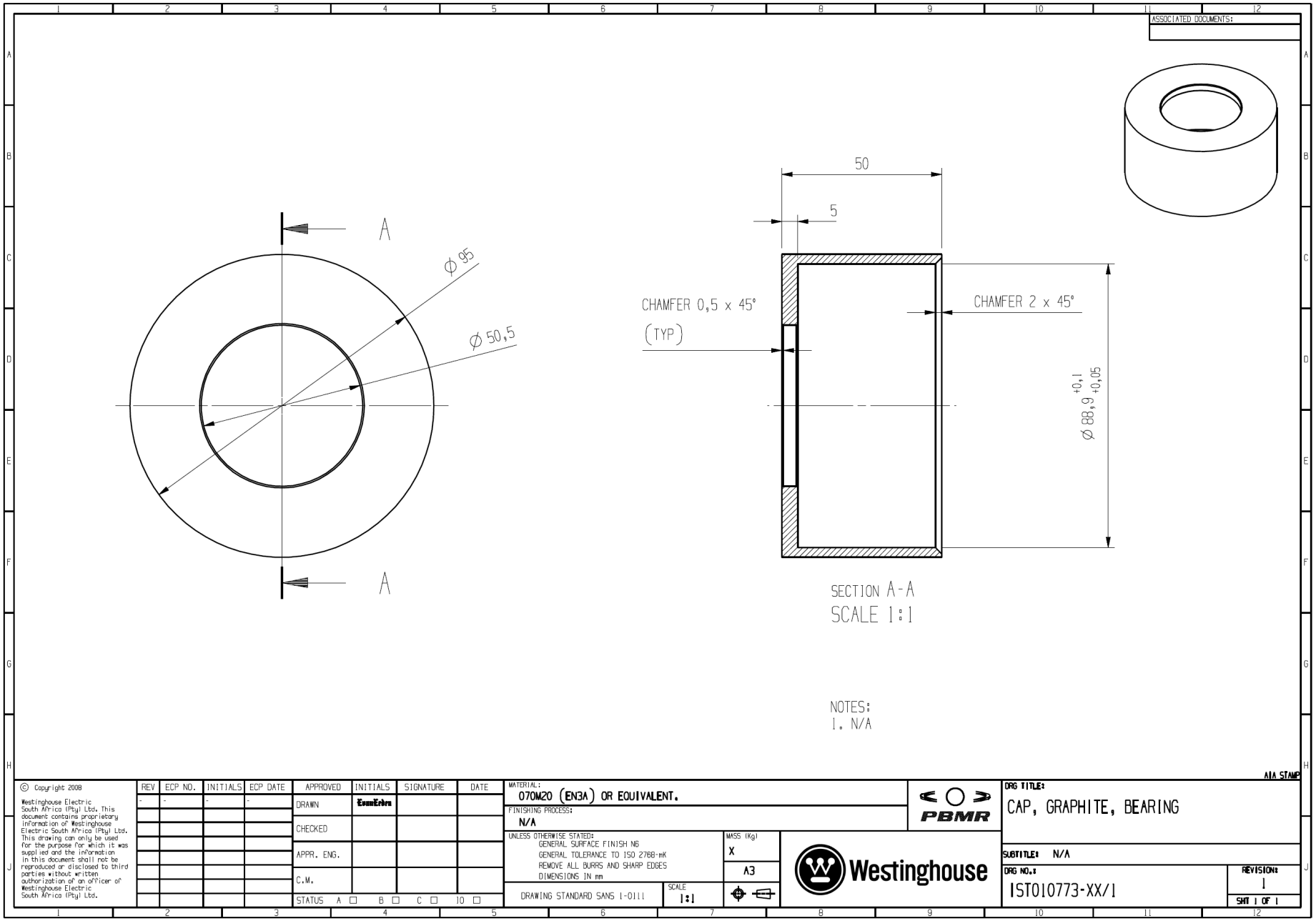
ASSOCIATED DOCUMENTS:
A
ϕ95
ϕ50,5
A
50
5
CHAMFER 0,5 x 45°
(TYP)
CHAMFER 2 x 45°
ϕ88,9 +0,1 +0,05
SECTION A-A
SCALE 1:1
NOTES:
1. N/A
AIA STAMP
© Copyright 2008
Westinghouse Electric South Africa (Pty) Ltd. This document contains proprietary information of Westinghouse Electric South Africa (Pty) Ltd. This drawing can only be used for the purpose for which it was supplied and the information in this document shall not be reproduced or disclosed to third parties without written authorization of an officer of Westinghouse Electric South Africa (Pty) Ltd.
REV | ECP NO. | INITIALS | ECP DATE
APPROVED | INITIALS | SIGNATURE | DATE
DRAWN
CHECKED
APPR. ENG.
C.M.
STATUS A ☐ B ☐ C ☐ 10 ☐
MATERIAL:
070M20 (EN3A) OR EQUIVALENT.
FINISHING PROCESS:
N/A
UNLESS OTHERWISE STATED:
GENERAL SURFACE FINISH N6
GENERAL TOLERANCE TO ISO 2768-mK
REMOVE ALL BURRS AND SHARP EDGES
DIMENSIONS IN mm
MASS (Kg)
X
A3
DRAWING STANDARD SANS 1-0111
SCALE
1:1
PBMR
Westinghouse
DRG TITLE:
CAP, GRAPHITE, BEARING
SUBTITLE: N/A
DRG NO.:
1ST010773-XX/1
REVISION:
1
SHT 1 OF 1

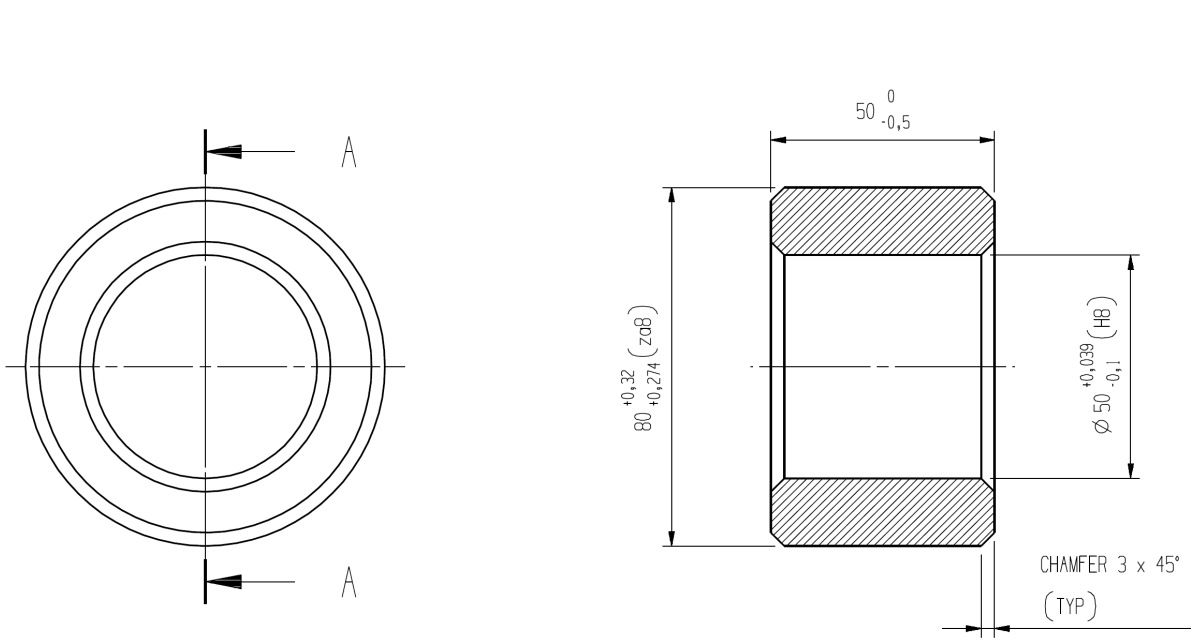

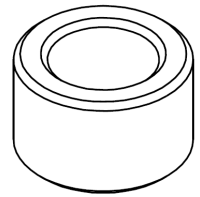

ASSOCIATED DOCUMENTS:

A1A STAMP

REV	ECP NO.	INITIALS	ECP DATE
-	-	-	-

APPROVED	INITIALS	SIGNATURE	DATE
DRAWN	X		
CHECKED			
APPR. ENG.			
C.M.			

STATUS A ☐ B ☐ C ☐ 10 ☐

MATERIAL: GRAPHITE

FINISHING PROCESS: N/A

UNLESS OTHERWISE STATED:
GENERAL SURFACE FINISH N6
GENERAL TOLERANCE TO ISO 2768-mK
REMOVE ALL BURRS AND SHARP EDGES
DIMENSIONS IN mm

DRAWING STANDARD SANS 1-0111

SCALE 1:1

MASS (Kg) X

A3

PBMR

Westinghouse

DRG TITLE: BEARING, GRAPHITE

SUBTITLE: N/A

DRG NO.: IST010768-XX/1

REVISION: X

SHT 1 OF 1

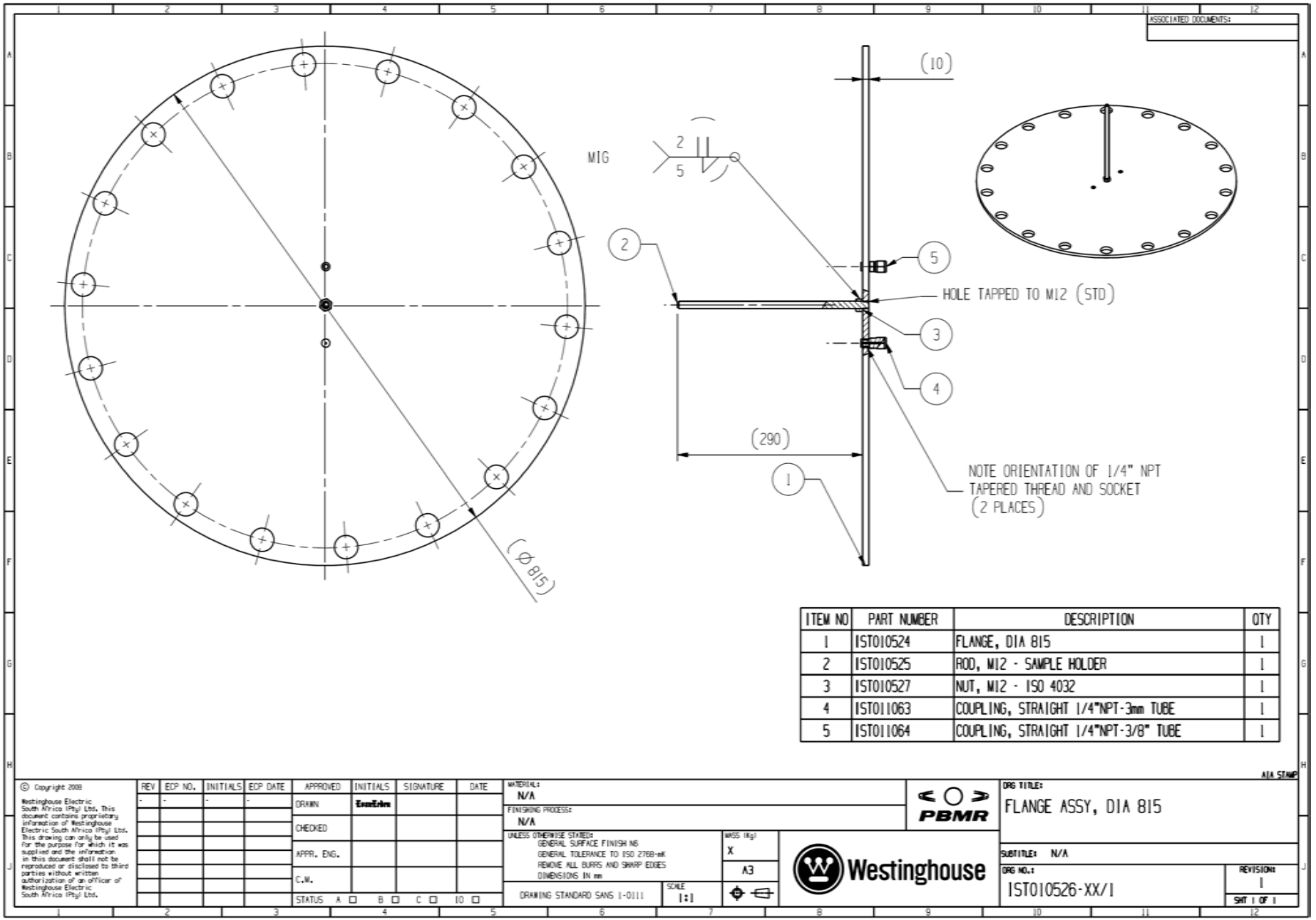

ITEM NO	PART NUMBER	DESCRIPTION	QTY
1	IST010524	FLANGE, DIA 815	1
2	IST010525	ROD, M12 - SAMPLE HOLDER	1
3	IST010527	NUT, M12 - ISO 4032	1
4	IST011063	COUPLING, STRAIGHT 1/4"NPT-3mm TUBE	1
5	IST011064	COUPLING, STRAIGHT 1/4"NPT-3/8" TUBE	1

REV	ECP NO.	INITIALS	ECP DATE
-	-	-	-

	APPROVED	INITIALS	SIGNATURE	DATE
DRAWN				
CHECKED				
APPR. ENG.				
C.W.				

STATUS A ☐ B ☐ C ☐ 10 ☐

MATERIAL: N/A
FINISHING PROCESS: N/A
UNLESS OTHERWISE STATED:
GENERAL SURFACE FINISH N6
GENERAL TOLERANCE TO ISO 2768-mK
REMOVE ALL BURRS AND SHARP EDGES
DIMENSIONS IN mm
DRAWING STANDARD SANS 1-0111
SCALE 1:1
MASS (Kg) X
A3

PBMR
Westinghouse

DRG TITLE: FLANGE ASSY, DIA 815
SUBTITLE: N/A
DRG NO.: IST010526-XX/1
REVISION: 1
SHT 1 OF 1
AIA STAMP

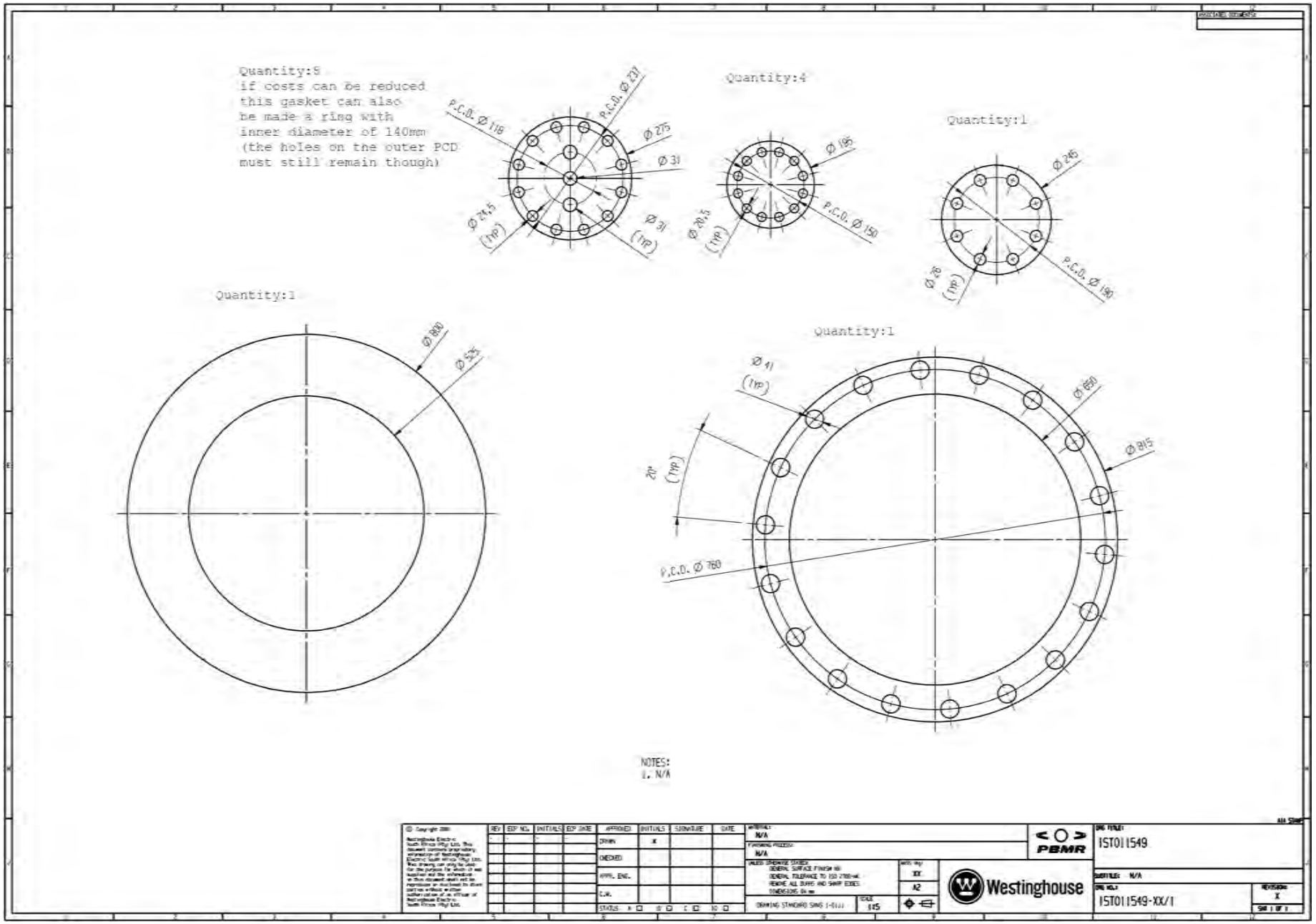
Quantity:8
if costs can be reduced
this gasket can also
be made a ring with
inner diameter of 140mm
(the holes on the outer PCD
must still remain though)
P.C.D. Ø 118
P.C.D. Ø 237
Ø 275
Ø 31
Ø 14,5
(TYP)
Ø 31
(TYP)
Quantity:4
Ø 195
Ø 20,5
(TYP)
P.C.D. Ø 150
Quantity:1
Ø 245
Ø 26
(TYP)
P.C.D. Ø 190
Quantity:1
Ø 800
Ø 525
Quantity:1
Ø 41
(TYP)
Ø 850
Ø 815
20°
(TYP)
P.C.D. Ø 760
NOTES:
1. N/A
PBMR
Westinghouse
1ST011549
1ST011549-XX/1

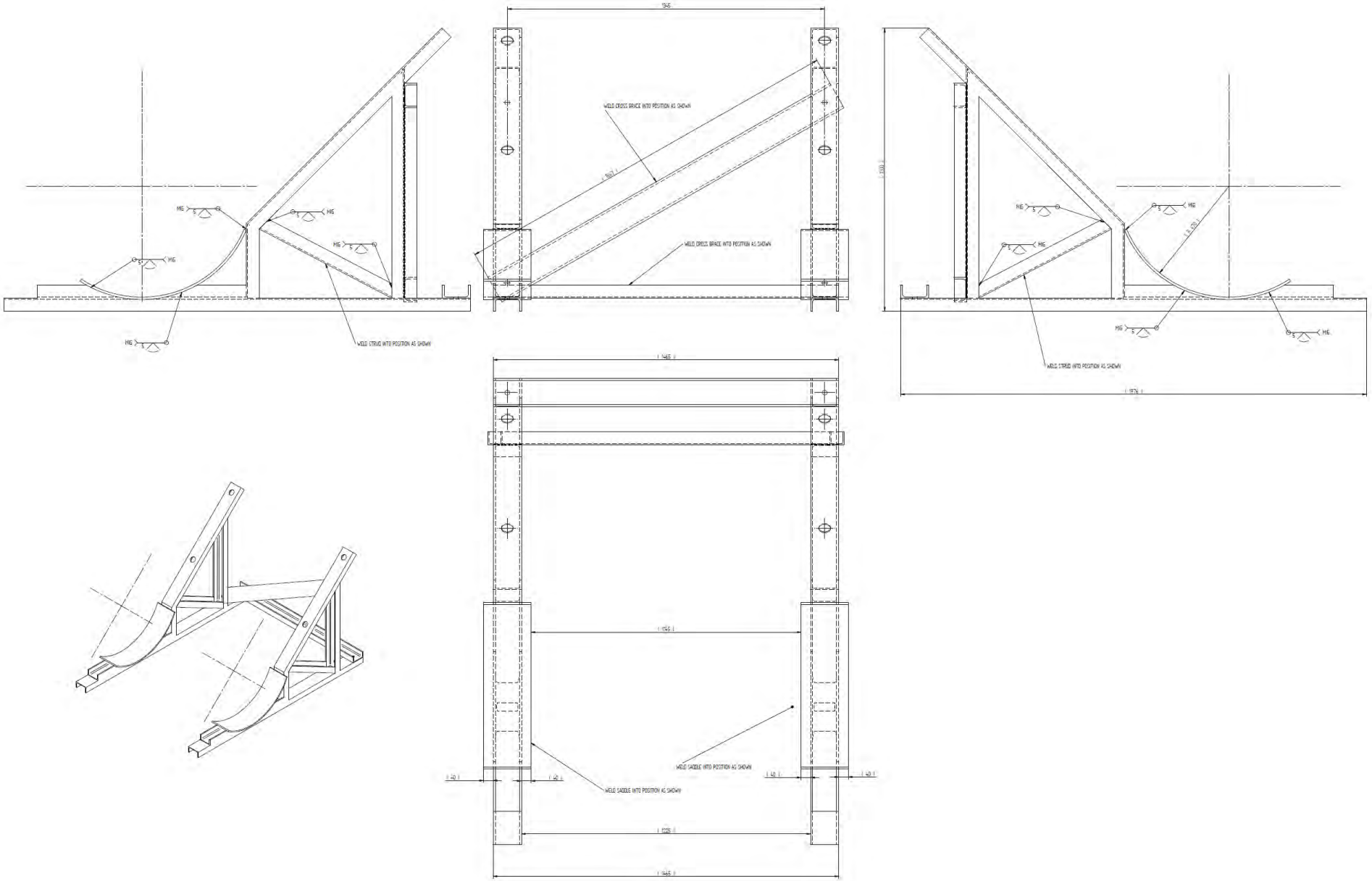
WELD CROSS BRACE INTO POSITION AS SHOWN
WELD CROSS BRACE INTO POSITION AS SHOWN
WELD STRUT INTO POSITION AS SHOWN
WELD STRUT INTO POSITION AS SHOWN
WELD SADDLE INTO POSITION AS SHOWN
WELD SADDLE INTO POSITION AS SHOWN

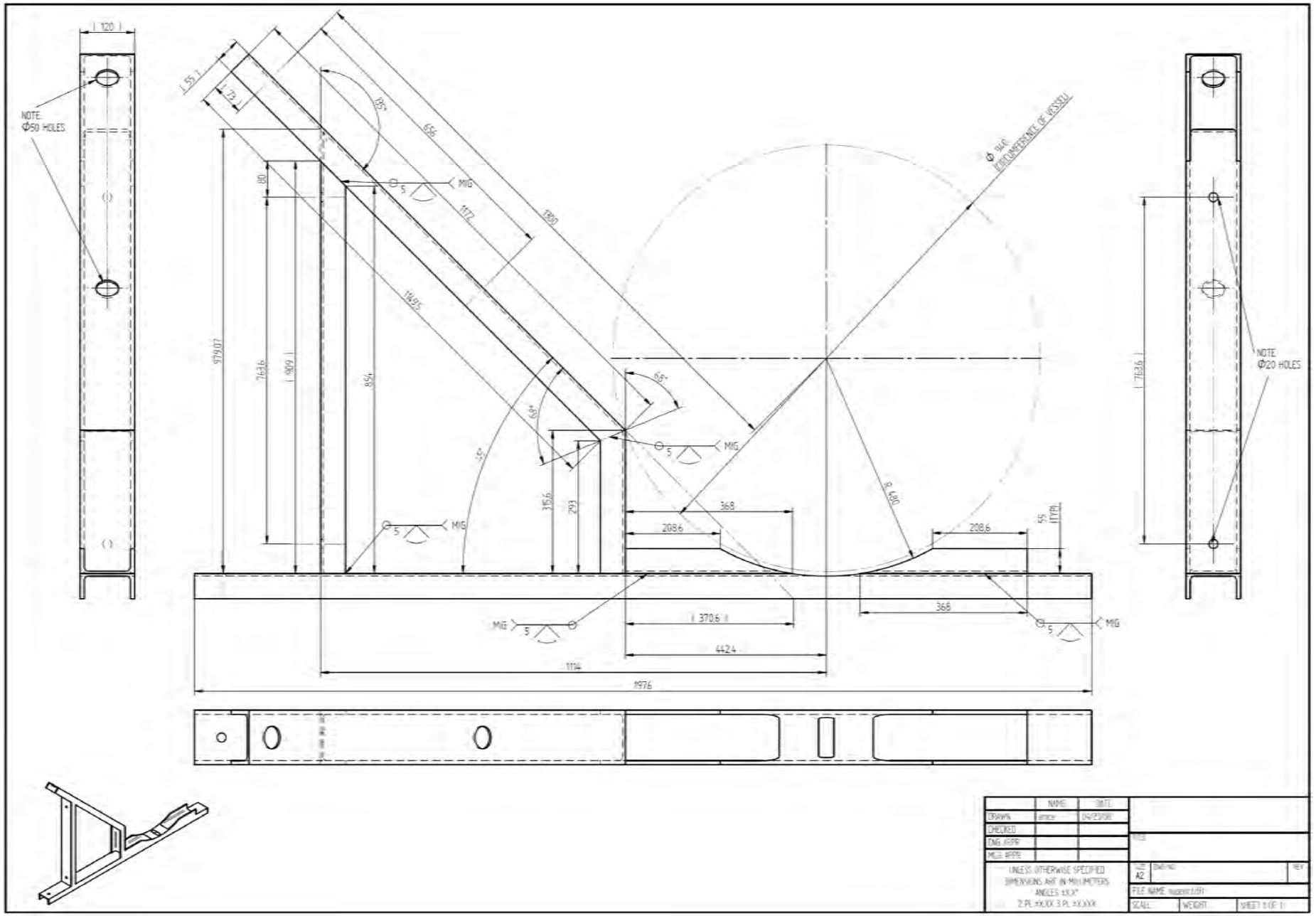
NOTE:
Φ50 HOLES
NOTE:
Φ20 HOLES
MIG
5
45°
68°
125°
Ø TBC
CIRCUMFERENCE OF VESSEL
368
208.6
366
370.6
4424
1976
UNLESS OTHERWISE SPECIFIED
DIMENSIONS ARE IN MILLIMETERS
ANGLES ±X.X°
2 PL ±X.XX 3 PL ±X.XXX
DRAWN
CHECKED
ENG APPR
MFG APPR
NAME
DATE
SIZE
A2
SCALE
WEIGHT
SHEET 1 OF 1

Appendix D: Detail Drawings

CUD Housing with spindle installed

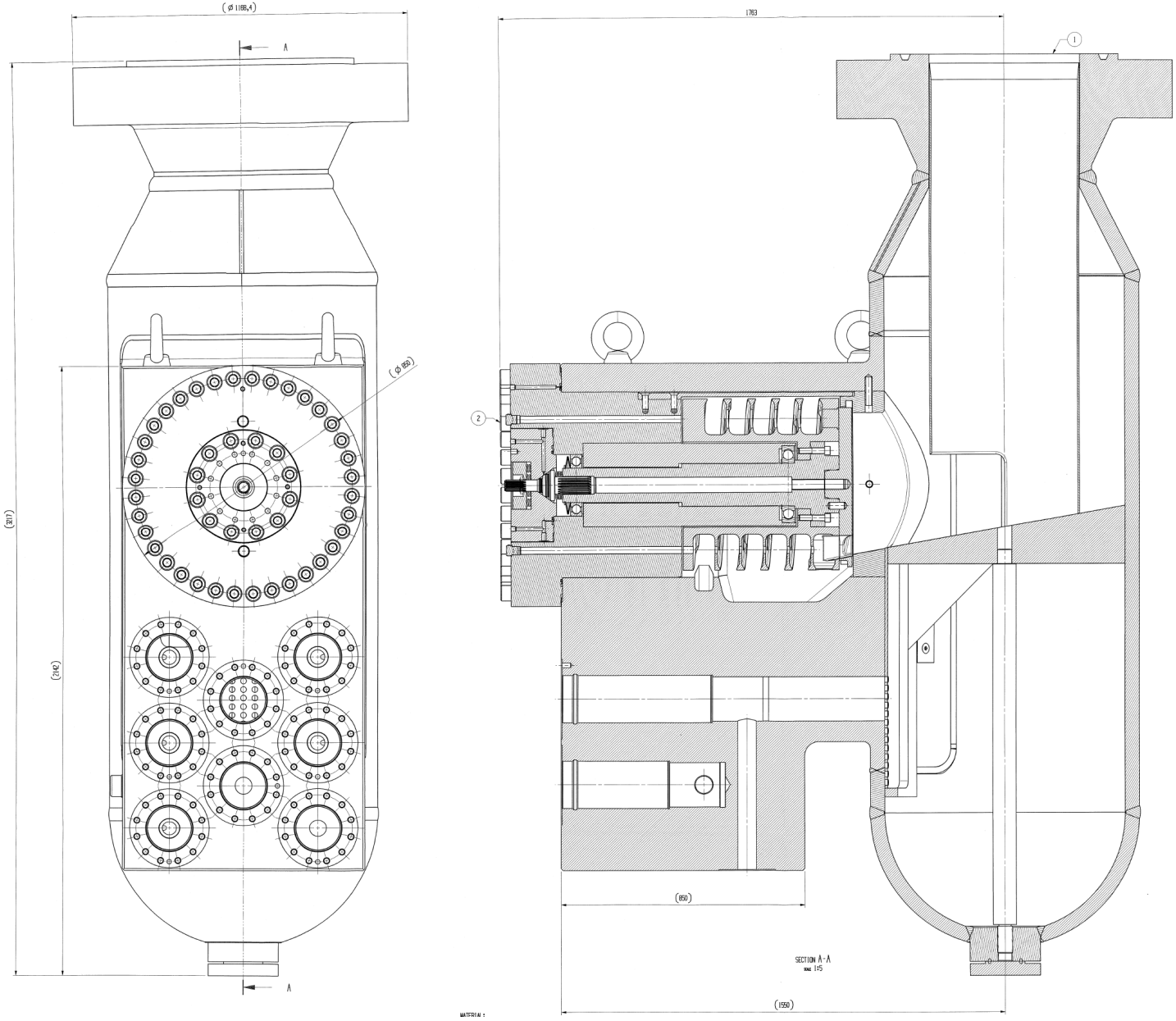

APPENDIX E: SYSTEM OPERATING DESCRIPTION DOCUMENT [20]

E.1 GENERAL OVERVIEW

A single stage Gas Nitriding procedure will be performed by the CUD NP. The main processes involved in the Nitriding task are the plant preparation for nitriding process and the plant operation process.

The NP is required to perform the following functions (see section 3.3.3 chapter 3):

1. The Gas Supply System supplies and controls entering gas flows
2. The furnace heats the gas up to the required temperature
3. Furnace stirring fan assembly, provides the necessary turbulence
4. CUD housing Process chamber provides a closed volume for nitriding
5. Sealing system and gas pipe penetrations prevents gas leakage
6. Nitriding test samples provides a means to qualify the nitriding process
7. The Gas Exit System controls, captures and measures exit gas flows.

Refer to Appendix D for the NP process flow diagram.
Table E.1 gives the specified input operating data required for the design of this system.

Table E.1: Operating Data, see section 2.7.2.

Operation	Inputs
Furnace maximum operating temperature	800°C
Furnace heating rate	50°C/h – 100°C/h
Max operating pressure	25kPa
Maximum ammonia gas flow rate	3000 l/h
Minimum ammonia gas flow rate	20l/h
Process chamber gas flow minimum Reynolds number (turbulent flow)	10 000

The process data for the plant is shown in Table E.2.

Table E.2: Process Data

Item	Property	Value	Reference
ammonia gas supply	Maximum flow rate *	3000 ℓ/hr	section 2.7.2
	Minimum flow rate	20l/h	
	Max duration of continuous supply	48hrs	section 2.7.2

[20] This Appendix consists of excerpts from an internal document of Westinghouse Electric SA, doc no. HTF-A-000417-225 Rev.1

Item	Property	Value	Reference
oxygen gas supply	Maximum flow rate *	200 ℓ/hr	section 2.7.2
	Minimum flow rate	20l/h	
	Max duration of continuous supply	2hrs	section 2.7.2
nitrogen gas supply	Maximum flow rate *	2000 ℓ/hr	section 2.7.2
	Minimum flow rate	20l/h	
	Max duration of continuous supply	2hrs	section 2.7.2

* Values with properties at a temperature of 20°C and a pressure of 20kPa gauge, 87 kPa absolute pressure

Table E.3 shows the NP operating conditions.

Table E.3: Plant Operating Data, see section 4.9.

Parameter	Value	Units
Normal conditions		
Stirring fan maximum speed	1000	rpm
operating gas	NH_3 (O_2, N_2)	-
operating temperature	555	°C
Operating pressure	20	kPa

E.2 FUNCTIONAL GROUP BREAKDOWN

E.2.1 FUNCTIONALITY

The functions of the CUD NP, prescribed in section 3.4 chapter 3 are as follows:

1. **Supply Gas for Nitriding**
   - *1.1. Provide Gas flow (ammonia, oxygen and nitrogen) for:*
   - *1.2. Provide different gases for different stages/modes*

     ammonia for the nitriding cycle
     oxygen for the furnace preparation cycle (oxidising the CUD inner surface)
     nitrogen for purging and for safety purposes
   - *1.3. Provide Gas flow Control*
   - *1.4. Provide Gas flow measurement*
2. **Heat up the process chamber**
   - *2.1. Heat the Nitriding process chamber to the different required temperatures*
   - *2.2. Temperature control*
3. **Stir the gas to ensure turbulent mixing**
   - *3.1. Ensure turbulent gas flow inside the process chamber to ensure sufficient mixing*
   - *3.2. Seal off the ammonia gas from the furnace*
   - *3.3. Penetrate the furnace wall and the weld-neck sealing flange*
4. **Contain the gases using the CUD housing as a process chamber**
   - *4.1. Contain and seal off the ammonia gas within the process chamber to prevent a possible explosion*
   - *4.2. Provide a contained volume and surface area for nitriding*
5. **Seal with gas pipe and other penetrations**
   - *5.1. Gas pipe penetrations prevent ammonia, oxygen and nitrogen gas from entering the furnace, flange seals also provide sealing*
   - *5.2. Thermocouple penetrations ensure thermocouples are placed inside the CUD housing without leakage into furnace*
6. **Provide test samples to test for the quality of nitriding**
   - *6.1. Samples for qualifying the nitriding process*
   - *6.2. Test for nitride layer thickness and hardness*
   - *6.3. Witness pieces to test for the heat treatment cycle effects*
7. **Provide a means for the Gas to Exit**
   - *7.1. Manage Pressure inside the process chamber*
   - *7.2.* Direct the flow to either the ‘Bunte burette’ or the water barrel
   - 7.3. *Control the flow through each exit flow gas pipe*

i. Measure and balance the flowrate through each exit pipe

7.4. Measure the crack ratio

Capture the dissociated ammonia and other gases in water

E.2.2 HARDWARE BREAKDOWN OF THE NP

E.2.2.1 FUNCTIONAL UNITS

The hardware of the NP is grouped together in functioning units. This grouping is done in order to design and manufacture hardware assemblies that can be separately assembled and pre-tested before system integration is performed. The following functional units make up the NP:

1. Gas Supply Cylinder manifolds and pressure regulator;
2. Gas supply flowmeters and control and isolation valves
3. Heating furnace and controls
4. Furnace stirring fan assembly
5. CUD housing Process chamber
6. Sealing system and gas pipe penetrations
7. CUD wall temperature thermocouples and penetrations
8. Nitriding test samples
9. Gas Exit system flowmeters
10. Gas Exit system control manifold
11. Gas Exit system flow measurement station
12. Gas Exit system exit gas removal station

The sizing of the equipment comprising the functional units is described in chapter 3.

E.2.2.2 PROCESS INTERFACES

The NP has an external interface with the warehouse building in which the heating furnace is located. The electrical power for the temperature measurement data logger and the stirring fan motor is provided from the warehouse building's electricity supply.

E.2.3 PROCESS FUNCTIONAL MODULES

In order to perform the specified functions, the NP essentially provides the required gas flow rate at acceptable operating conditions through the integration of several functioning units. These functioning units (physically grouped together main components) are grouped together in a logical way in Process Functional Modules (PFM's) in order to perform common functions in a structured and logical way.
The boundaries of the NP are shown in Figure E.1 also see the PFD Appendix B.

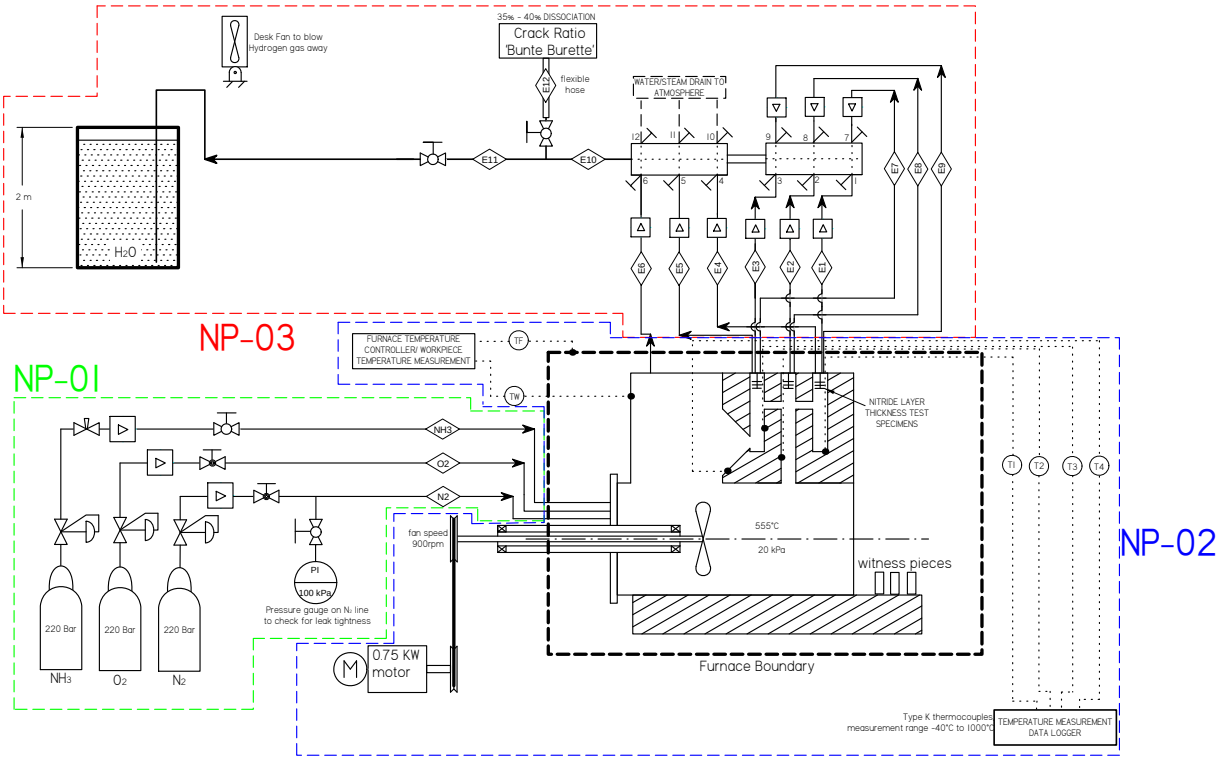

Figure E.1: Boundaries of the NP with PFM groupings

The NP has been divided into three different PFMs as shown in Figure E.1. These PFMS are described in Table E.4.

Table E.4: NP process functional modules.

PFM number	PFM Name	Description	Refer to
NP-01	Gas Supply	The Gas Supply PFM provides the different gases at the specified flow rates as required during the different stages of the nitriding process. The PFM consists of the ammonia, oxygen and nitrogen gas cylinders, and its manifolds and pressure regulators, pressure gauge, the flowmeters and isolation valves.	E.3.1

PFM number	PFM Name	Description	Refer to
NP-02	Nitriding Furnace	This PFM contains everything inside the heating furnace 1. CUD housing and support cradle 2. heating furnace; 3. CUD flanges, seals and penetrations 4. furnace temperature measurement and control 5. CUD interior temperature measurement and control 6. The nitriding test samples 7. The stirring fan assembly	E.3.2
NP-03	Gas Exit	The Gas Exit PFM contains all the gas pipes that exit the furnace, the flowmeters on each of these gas pipes, the manifold with control valves where these pipes come together, the'Bunte Burette' for measuring the ammonia dissociation (crack ratio), and the water filled barrel where the undissociated ammonia is captured.	E.3.3

E.2.4 PFM MODES

Table E.5 provides the states of each NP PFM.

Table E.5: PFM Modes

PFM	Modes	Mode Description
Gas Supply PFM NP-01	preparation	The nitriding process chamber is prepared for nitriding. This includes purging the chamber with nitrogen and oxidising the CUD surface before starting the ammonia supply.
	heating	The vessel is gradually heated up from 200°C to 450°C and then the oxygen supply is stopped.
	nitriding	Only ammonia gas is supplied . The vessel is heated up to the nitriding temperature and the nitriding cycle is started. The crack ratio is continuously monitored and the ammonia supply is adjusted accordingly
	completion	The nitriding cycle is completed. Ammonia supply is stopped and the vessel is purged with nitrogen gas while it is cooling down.
Nitriding furnace PFM NP-02	preparation	While the vessel is prepared the furnace is heated up to 200°C and then oxygen gas is supplied to oxidise the vessel
	heating	The vessel is heated from 200°C to 450°C when the oxygen flow is stopped. It is then heated to 500°C
	nitriding	The nitriding cycle is started and the vessel is heated from 500°C to 555°C. The stirring fan is turned on. Temperature maintained at 555°C during the nitriding cycle.
	completion	The furnace temperature is reduced.
Gas Exit: PFM NP-03	preparation	The exit manifold valves are closed when testing for leaks with nitrogen gas. The valves are opened to prevent the vessel from overpressurizing
	heating	The valves are opened to prevent the vessel from overpressurizing
	nitriding	The manifold valves of each exiting gas pipe are controlled to balance the exiting gas flow rates through the 9 exit pipes during nitriding

PFM	Modes	Mode Description
	completion	The valves are opened to prevent the vessel from overpressurizing

E.2.4.1 MODES AND TRANSITIONS

N/A

E.2.4.2 MAINTENANCE

The plant can be shut down during the nitriding cycle if maintenance is necessary. The nitriding process can be continued where it has stopped after repairs are done.

E.3 PFM DESCRIPTIONS

E.3.1 NP- 01 GAS SUPPLY PFM

E.3.1.1 FUNCTIONALITY

The Gas Supply PFM has the main function of providing ammonia, oxygen and nitrogen at the required flow rates. Oxygen is provided during the furnace preparation cycle i.e. oxidising the CUD inner surface. Nitrogen is used for purging and safety purposes. Ammonia is supplied during the nitriding cycle mode. The gas supply flow rates are continuously measured and controlled manually.

E.3.1.2 PROCESS FLOW AND CONTROL DESCRIPTION

The Gas Supply PFM control consists of manually controlling the ammonia gas flow rate according to the measured ammonia dissociation rate (crack ratio).
The control of oxygen and nitrogen gas flow rates during preparation for the nitriding cycle are also included. The flow rate is controlled by the pressure regulators and flow control valves (globe valves). The control valves and pressure regulator valves to the nitrogen and oxygen need to be closed when the ammonia flow is introduced into the process chamber because it might chemically react with brass components in the nitrogen/oxygen pressure regulators, see Figure E.2.

The required oxygen flow rate was calculated with chemical mass balance formulas for the lab test in section 2.7.2 to ensure that the right concentration of oxygen is present in the vessel to ensure sufficient cracking of ammonia during the nitriding cycle.
Note that the process chamber must be under pressure of 20 kPa when introducing oxygen for the preparation mode. This means that the exit pipes must be connected to the water barrel.

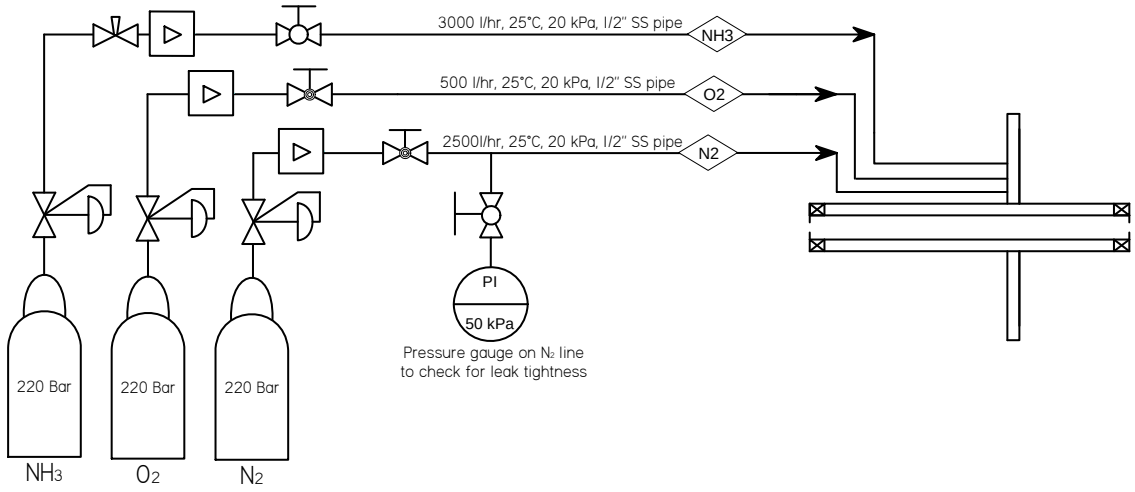

Figure E.2: The main control devices of the Gas Supply PFM

During testing for leakage with nitrogen at the operating temperature, before ammonia is introduced, the nitrogen gas flow is controlled until the vessel reaches its design pressure of 20kPa. The nitrogen control valve is fully closed and the pressure gauge is then monitored to check for leaks at the maximum operating temperature.
The nitrogen flow rate during the first purging exercise should be sufficient to ensure removal of air before introducing ammonia for the first time. Note that the process chamber must be under

pressure of 20 kPa when introducing nitrogen for purging. The overpressure will ensure that no air enters the process chamber.

E.3.1.3 GAS SUPPLY PFM COMPONENTS

The Gas Supply PFM components are listed in Table E.6.

Table E.6: Gas Supply Component List

Component	Description/ Reason
Ammonia line	
Ammonia gas cylinders (X4)	4 Cylinders connected to a manifold. Extra ammonia cylinders are supplied in case the estimated required initial amount is too little.
Ammonia gas cylinder pressure regulator	Open the gas cylinder to supply ammonia at 20 kPa from a source pressure of 220 Bar
Ammonia flow meter	A Rotameter (Variable area flow meter) with a range of 0-3000 ℓ/hr to measure the ammonia supply rate. See section 4.4.2 for flow calculations.
Needle valve on flowmeter	This valve will be used to control the flow rate
Isolation valve	To isolate the ammonia line when oxygen and nitrogen is supplied to the process chamber.
Stainless steel gas pipes	Supply and contain the ammonia to the furnace at a maximum temperature of 555°C
Oxygen line	
Oxygen gas cylinders (X4)	4 Cylinders. Extra cylinders are supplied in case the estimated required initial amount is too little.
Oxygen gas cylinder pressure regulator	Open the gas cylinder to supply oxygen at 20 kPa from a source pressure of 220 Bar
Oxygen flow meter	A Rotameter (Variable area flow meter) with a range of 0 – 1000ℓ/hr to measure the oxygen supply rate. See section 4.4.2 for flow rate calculations. Only 200ℓ/hr required to oxidise the CUD surface according to chemical calculations done in section 4.4.2.
Control valve	A globe valve to control the oxygen flow rate, and to isolate the oxygen line
Stainless steel gas pipes	Supply and contain the oxygen to the furnace at a maximum temperature of 200°C
Isolation valve	Isolate the oxygen pressure regulator from the ammonia gas during furnace preparation
Nitrogen line	
Nitrogen gas cylinders (X4)	4 Cylinders. Extra cylinders are supplied in case the estimated required initial amount is to little.
Nitrogen gas cylinder pressure regulator	Open the gas cylinder to supply nitrogen at 20 kPa from a source pressure of 220 Bar
Nitrogen flow meter	A Rotameter (Variable area flow meter) with a range of 0 – 2000ℓ/hr to measure the nitrogen supply rate. See section 4.4.2 for flow rate calculations.
Stainless steel gas pipes	Supply and contain the nitrogen to the furnace at a maximum temperature of 500°C
Control valve	A globe valve to control the nitrogen flow rate, and to isolate the nitrogen line

Component	Description/ Reason
Leak tightness pressure gauge	Test for leaks by monitoring the pressure gauge after pressurizing the vessel with nitrogen at the operating temperature

E.3.1.4 CONTROL PARAMETERS

Table E.7 lists the parameters of the control instrumentation of the Gas Supply PFM

Table E.7: Control Instrumentation and their parameters of the Gas Supply system

Description	Instrument No. see P & ID	Range
Pressure		
Process chamber pressure	PI 001	0 – 50 kPa
Flow rate		
Ammonia flow rate	FI001	0 – 3600l/h
Oxygen flow rate	FI002	0 – 700 l/h
Nitrogen flow rate	FI003	0 – 2800 l/h
Dissociation rate Feedback for ammonia flow control		
Crack Ratio	AI001	0% – 100%

E.3.1.5 OPERATING PARAMETERS AND ACTIONS

Table E.8 identifies alarms and process interlocks with the appropriate actions.

Table E.8: The Gas Supply PFM Operating Parameters and Actions

Description	Type	High/ Low	Value	Action
Pressure				
Indicating process chamber pressures	Pressure gauge PI001	H	25 kPa	Operator to investigate. Check Exit Gas valve position and water level in water filled barrel
		HH	30 kPa	Stop gas supply. Investigate for overpressure and rectify
Flow rate				
Preparation mode				
Indicating ammonia flow rate through ammonia entrance pipe	Rotameter FI001	H	3200ℓ/hr	The flow rate of the supply gas line must be limited to this maximum rate during preparation to ensure a start-up crack ratio of 15 – 35%. See section 4.4.2 for flow rate calculations. Flow must be reduced to maintain 3000ℓ/hr
		L	2800ℓ/hr	Operator to increase flow rate to maintain 3000ℓ/hr

Description	Type	High/ Low	Value	Action
Indicating oxygen flow rate through ammonia entrance pipe	Rotameter FI002	H	220ℓ/hr	Reduce flow rate. The oxygen flow rate must be controlled at 200ℓ/hr for 2 hours during the preparation mode to ensure sufficient oxygen to start-up the ammonia cracking reaction
		L	180ℓ/hr	Increase flow rate to maintain 200ℓ/hr
Indicating nitrogen flow rate through ammonia entrance pipe	Rotameter FI003	H	2200ℓ/hr	Reduce flow rate. The nitrogen flow rate must be controlled at 2000ℓ/hr to ensure sufficient purging of the CUD vessel
		L	1800ℓ/hr	Increase flow rate to maintain 2000ℓ/hr
Heating mode				
Indicating ammonia flow rate through ammonia entrance pipe	Rotameter FI001	H	3200ℓ/hr	The flow rate of the supply gas line must be limited to this maximum rate during heating to ensure a start-up crack ratio of 15 – 35%. See section 4.4.2 for flow rate calculations. Flow must be reduced to maintain 3000ℓ/hr
		L	2800ℓ/hr	Operator to increase flow rate to maintain 3000ℓ/hr
Indicating oxygen flow rate through ammonia entrance pipe	Rotameter FI002	H	220ℓ/hr	Reduce flow rate. The oxygen flow rate must be controlled at 200ℓ/hr for 2 hours during the heating mode to ensure sufficient oxygen to start-up the ammonia cracking reaction
		L	180ℓ/hr	Increase flow rate to maintain 200ℓ/hr
Nitriding cycle mode				
Indicating ammonia flow rate through ammonia entrance pipe	Rotameter FI001	H	55ℓ/hr	The flow rate of the supply gas line must be limited to this rate at the start of the nitriding cycle. See section 4.4.2. Flow must be reduced to maintain 50ℓ/hr .
		L	45ℓ/hr	Operator to increase flow rate to maintain 50ℓ/hr
Indicating ammonia flow rate through ammonia entrance pipe	Rotameter FI001	H	125ℓ/hr	The flow rate of the supply gas line must be limited to this rate once the furnace has reached 555°C. See section 2.7.2. Flow must be reduced to maintain 120ℓ/hr .
		L	115ℓ/hr	Operator to increase flow rate to maintain 120ℓ/hr .
Indicating ammonia flow rate through ammonia entrance pipe	Rotameter FI001	Interlock	* ± 5 ℓ/hr	The flow rate of the supply gas line must be controlled at this * rate during the 40 hr long nitriding cycle mode to ensure a crack ratio of 35-40%.
Crack ratio				

Description	Type	High/ Low	Value	Action
Indicating low ammonia dissociation rate	'Bunte Burette' AI001	L	10%	Decrease ammonia supply flow rate to increase nascent nitrogen residence time and concentration
Indicating high ammonia dissociation rate	'Bunte Burette' AI001	H	75%	Increase the ammonia supply flow rate to decrease the nascent nitrogen residence time
		HH	80%	Fully open the ammonia supply valve to ensure maximum ammonia supply and to reduce residence time

Note: These values are typical operating points
* This flow rate will be determined during the nitriding cycle and is dependent on the crack ratio, see look-up **Error! Reference source not found.** for how the flow rate is adjusted according to the crack ratio.

E.3.1.6 SEQUENTIAL ACTIVITIES

The sequential activities of all three PFM's are discussed in chapter 5 since this is a manually operated plant.

E.3.2 NP- 02 NITRIDING FURNACE

E.3.2.1 FUNCTIONALITY

The gas fired top hat furnace provides the correct heating rate to heat up the process chamber to 555°C.
The furnace contains the process chamber i.e. the sealed CUD vessel in which the gases are contained and which forms the nitrided surface area.
The sealing flanges and seals, penetrations for the gas pipes and thermocouples ensure that no ammonia gas leaks into the gas fired furnace volume.
The different gases are supplied via gas pipes that penetrate the boundaries (sealing flanges) of the process chamber (the CUD vessel). The CUD wall thermocouples provide feedback on the CUD surface temperature in order for the furnace operator to adjust the furnace temperature accordingly.
The furnace and workpiece thermocouples provide control feedback to the furnace operator.
The stirring fan provides the necessary turbulence to mix the ammonia gas during the nitriding cycle to ensure that nascent nitrogen is always available in the right concentration to ensure successful nascent nitrogen diffusion into the metal surface.
Nitriding thickness test specimens are installed to measure the nitride layer thickness afterwards. Heat treatment witness pieces are also inside the furnace to test for the effects of the heat cycle on the tensile strength.

E.3.2.2 PROCESS FLOW AND CONTROL DESCRIPTION

Before the furnace is heated up it must be ensured that all the test samples are in place and that all the flanges and penetrations are sealed tightly. The gas pipes and thermocouples must enter the top hat structure from underneath the sand. No openings must exist on the bottom for heat loss to occur.

The furnace is heated up to 200°C during the preparation for nitriding stage/mode and the pre-oxidation phase. It is then heated to 450°C, the oxygen flow is stopped and it is heated to 500°C. The nitriding cycle is started and the furnace is heated to 555°C and kept there for the CUD vessel to soak for 40 hrs. The furnace is then cooled down slowly during the cycle completion phase. During the entire heat cycle the furnace, workpiece and CUD wall

temperatures must be continuously monitored. The furnace temperature must be adjusted continuously by the furnace controller/operator if the temperatures deviate from the specified temperature for a specified stage/mode, see Figure E.3.
Another important operating principle is the use of workpiece thermocouples on the thin and thick metal parts of the CUD. When the difference between the thin and thick metal parts' temperature is too large, the furnace is put on hold to allow for the thick part's temperature to catch up with the thin metal part's temperature. To prevent excessive thermal stresses/thermal shocks in the metal workpiece the ASME code, Section VIII Div.1 par. UCS-56 [9], recommends a maximum heating rate of 56°C/hr.

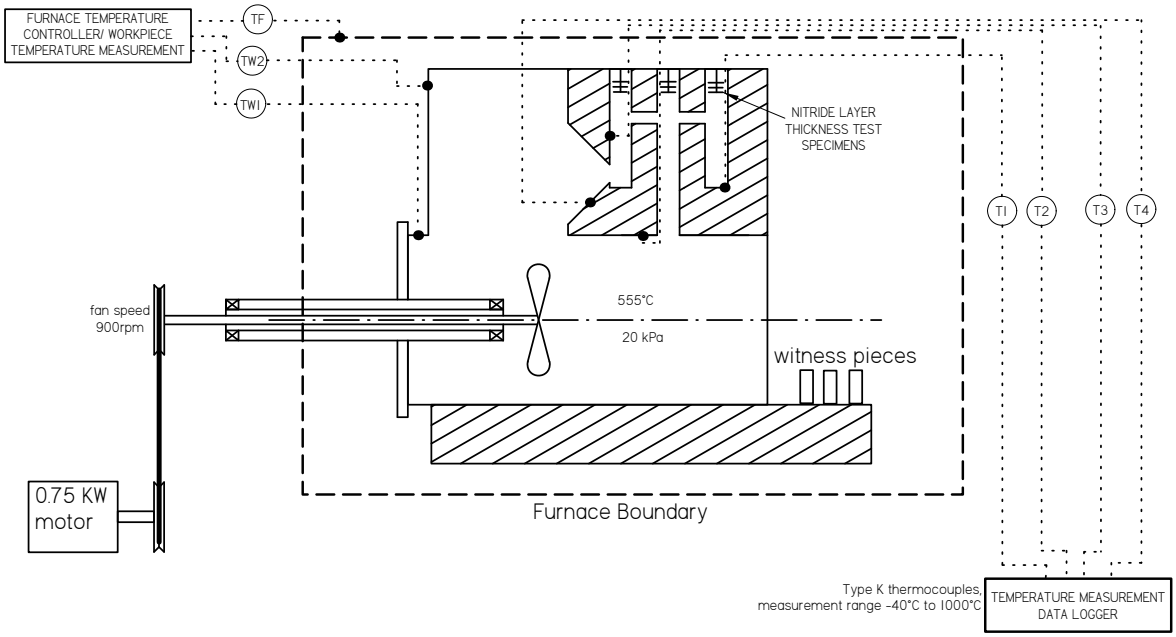

Figure E.3: The main control devices of the Nitriding Furnace PFM

The Stirring fan is started as soon as the nitriding cycle is started. The speed can be adjusted using a VSD. The stirring fan sizing and operating speed were calculated in section 4.2.2. After the nitriding cycle is completed and the furnace has cooled down, the top hat furnace can be lifted and the CUD sealing flanges etc. can be removed. The nitriding test specimens can be removed to test whether nitriding was succesful.

E.3.2.3 NITRIDING FURNACE COMPONENTS

The Nitriding Furnace PFM components are listed in Table E.9.

Table E.9: Nitriding Furnace Component list

Component	Description/ Reason
Top hat furnace	
Top hat structure	A steel structure which is lowered onto the sand on top of the CUD vessel/ nitriding process chamber
Top hat penetration for stirring fan assembly	A hole is made in the side of the top hat for the fan shaft to protrude through. This hole is also sealed to prevent heat loss.
Gas fired burners	Care must be taken to ensure that the burners do not cause flame impingement on the CUD vessel wall.
Furnace and workpiece thermocouples	The furnace has a temperature indicator for both the furnace interior temperature and the workpiece (in this case the CUD vessel exterior) temperature

Component	Description/ Reason
Top hat furnace	
Furnace Controller	The heating rate and furnace temperature is set here
Nitriding process chamber	
CUD vessel	The interior volume of the CUD housing (vessel) forms the nitriding process chamber. It is a sealed volume in which the ammonia and other gases are contained at high temperature.
Sealing flanges and seals	Flanges with seals are fitted to the shaft penetration and other holes of the CUD housing to form the closed volume of the process chamber.
Gas pipe penetrations	Special pressure boundary penetration fittings are screwed into the flanges and the gas pipes are connected to these fittings. The gas supply and gas exit pipes are fitted to the flanges with these pressure boundary penetration fittings to ensure sealing.
Thermocouple penetrations	Special pressure boundary penetration fittings are screwed into the flanges and the CUD vessel wall thermocouples are connected to these fittings.
Nitride layer thickness holders (rods fixed to the inside of the flanges)	The nitride layer test specimens are fitted to rods that are connected to the interior of the flanges on the shaft penetration holes etc.
CUD vessel wall thermocouples	
4 type K thermocouples	The thermocouples are placed at strategic points within the CUD housing to measure the wall temperature.
Stirring fan assembly	
Stirring fan	The fan is turned on during the nitriding cycle to ensure proper mixing of the gas.
Fan assembly electric motor	The shaft is constantly rotated at 950 rpm with a B-belt pulley to reduce the single phase motor constant speed of 1440rpm.

E.3.2.4 CONTROL PARAMETERS

In Table E.10 the parameters of the control instrumentation of the Nitriding Furnace PFM are listed.

Table E.10: Control Instrumentation and their parameters of the Nitriding Furnace PFM

Description	Instrument no. see P&ID Appendix F	Range
Temperature		
Furnace interior temperature	TE005	0°C– 800°C
Workpiece thin metal temperature	TE006	0°C– 800°C
Workpiece thick metal temperature	TE007	0°C– 800°C
4 temperature readings on the CUD interior wall	TE001-TE004	-20°C – 600°C
Fan speed		
Rotation speed (frequency reading), see section 4.2.3	UAC001	((0Hz– 60Hz)/50Hz) X 950rpm

E.3.2.5 OPERATING PARAMETERS AND ACTIONS

Table E.11 identifies alarms and process interlocks with the appropriate actions.

Table E.11: The Nitriding Furnace PFM Operating Parameters

Description	Type	High/ Low	Value	Action
Temperature				
Preparation mode				
Vessel wall temperature (thermocouples 1 to 4)	Temperature transmitters on interior wall of CUD housing (TE001 to TE004)	Interlock	200°C±5°C	Furnace operator must control the furnace temperature at this temperature during the oxidation in the preparation for nitriding mode
		HH	220°C	Set furnace on hold
Heating mode				
Vessel wall temperature (thermocouples 1 to 4)	Temperature transmitters on interior wall of CUD housing (TE001 to TE004)	Interlock	450°C±5°C	Furnace operator must control the furnace temperature at this temperature for 1 hour during the oxidation cycle of the heating mode
		HH	470 °C	Set furnace on hold
		Interlock	500°C±5°C	Furnace operator must control the furnace temperature at this temperature for 2 hours during the heating mode after oxygen flow was stopped
		HH	520°C	Set furnace on hold
Nitriding cycle mode				
Furnace temperature	Temperature transmitter on furnace TE 005	Interlock	555±5°C	Monitor temperature. Furnace operator must keep the furnace temperature at this value for 40 hours
		HH	650°C	Shut down furnace and the nitriding process, stop ammonia supply
Thin part workpiece temperature	Temperature transmitter on thin metal part of workpiece TE006	Interlock	555±5°C	Monitor temperature. Furnace operator must maintain this temperature
		HH	600°C	Shut down furnace and the nitriding process, stop ammonia supply

Description	Type	High/ Low	Value	Action
Thick part workpiece temperature	Temperature transmitter on thick metal part of workpiece TE007	Interlock	555±5°C	Monitor temperature. Furnace operator must maintain this temperature
		HH	600°C	Shut down furnace and the nitriding process, stop ammonia supply
Difference between thin and thick part workpiece temperature	Difference between thin and thick metal temperatures (TE006 – TE007)	H	20°C	A large temperature difference within the workpiece can cause distortion. The furnace burners must be put on 'hold' (small heating rate) to allow for conduction within the workpiece in order for the thick metal part temperature to catch up with the thin metal part.
Vessel wall temperature (thermocouples 1 to 4)	Temperature transmitters on interior wall of CUD housing (TE001 toTE004)	Interlock	555±5°C	Furnace operator must control the furnace temperature at this temperature during the nitriding cycle for 40 hours (Furnace wll be set on 'coasting')
		HH	600°C	Shut down furnace and the nitriding process, stop ammonia supply
Cycle completion mode				
		Interlock	450°C±5°C	Furnace operator must control the furnace temperature at this temperature when starting to introduce ammonia at 600l/h during the cycle completion. It can then be switched off and allowed to cool to 80°C
Heating rate				
Heating mode				
Indicating furnace heating rate	Furnace controller (TE005)	Interlock	56°C/hr	Heating rate must be controlled at this rate when heating from 200°C to 450°C and then to 500°C in the heating mode. Note that the actual heating rate will be dependent on the CUD housing mass and whether the furnace is set on hold.
Nitriding cycle mode				

Description	Type	High/ Low	Value	Action
		Interlock	50°C/hr	Heating rate must be controlled at this rate when heating from 500°C to 555°C in the nitriding cycle.
Cycle completion mode				
		Interlock	-20°C/hr	Furnace cooling rate must be controlled at this rate when cooling from 555°C to 450°C in the completion cycle.
Fan speed				
Indicating fan rotational speed	VSD controller UAC001	H	52Hz	Decrease the speed of the fan on the UAC001
		HH	54Hz	Shut off the electricity supply to the fan to prevent any potential whirling of the fan shaft, see section 4.2.3.

Note: These values are typical operating points

E.3.2.6 SEQUENTIAL ACTIVITIES

The sequential activities of all three PFM's are discussed in chapter 5 since this is a manually operated plant.

E.3.2.7 INTEGRATED FURNACE CONTROL

The temperature readings are used to adjust the furnace temperature and vice versa. If only one of the 4 CUD wall temperature readings deviates from the other 3 it would probably not be necessary to adjust the furnace temperature. The decision to adjust the furnace temperature in such a case will be to the discretion of the engineers and operators present during the nitriding process.

E.3.3 NP- 03 GAS EXIT PFM

E.3.3.1 FUNCTIONALITY

The process chamber pressure is managed by the water height and the isolation valves of the Gas Exit PFM. The flow through each of the 9 exit gas pipes can also be controlled by measuring with the flowmeters and adjusting with the needle valves on the distribution manifold. The exit flow is also directed to either the water barrel or the 'Bunte burette' in order to measure the crack ratio. The dissociated ammonia and other gases are captured in the water of the water filled barrel.

E.3.3.2 PROCESS FLOW AND CONTROL DESCRIPTION

The Gas Exit PFM control consists of controlling the process chamber pressure during the nitriding process. The isolation valve to the water filled barrel must be opened to ensure that the operating pressure supplied by the water level is maintained. If the isolation valve to both the water filled barrel and the 'Bunte Burette' are closed the process chamber will eventually overpressurize and it might exceed the design pressure of 35 kPa.

The control also consists of controlling the flow through each of the 9 exit gas pipes. Flowmeters are installed on each of the exiting gas pipes. If all the control valves are opened fully, on the manifold where these 9 pipes connect, there is still a possibility that the flows are not equal. This is due to the different pressure profiles within the process chamber (CUD

vessel). The control valves can thus be adjusted to make the flow through all 9 pipes more or less equal (balanced exit flow). This would ensure an equal nitride layer thickness through each of the 9 exit gas insert holes of the CUD vessel.

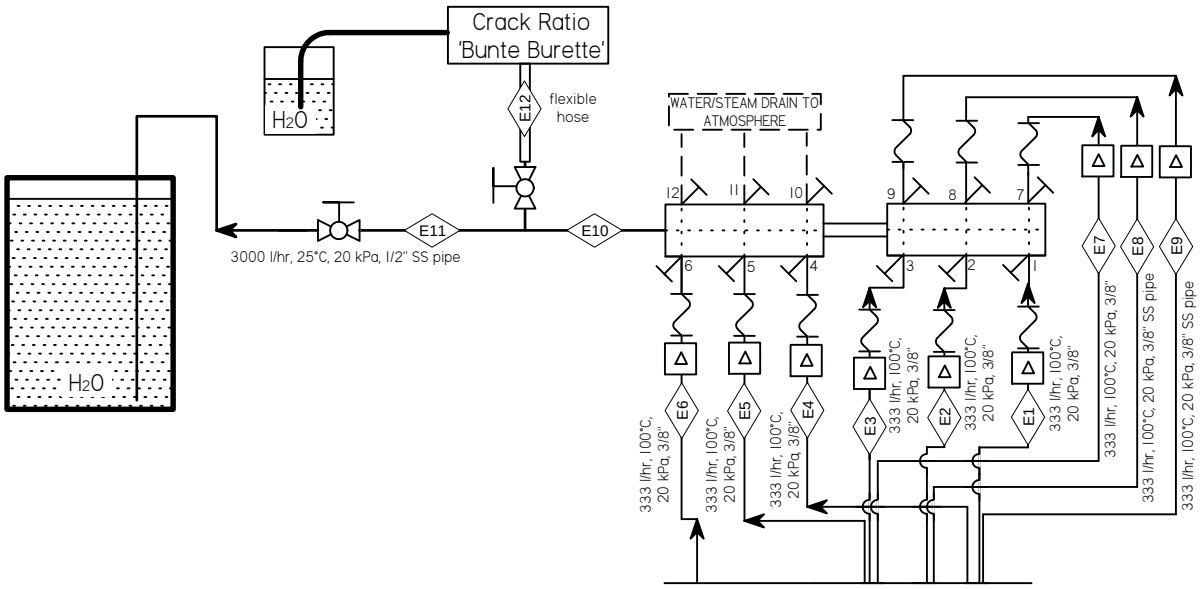

Figure E.4: The main control devices of the Gas Exit PFM

When the crack ratio is not measured all the undissociated ammonia and nitrides are captured in the water in the barrel. The ammonia dissociation (crack ratio) must also be continuously measured throughout the nitriding cycle. To measure the crack ratio the exit flow to the water barrel must be shut off with the isolation valve. The valve to the 'Bunte Burette' must be opened before the isolation valve to the water barrel is closed. The measurement will only take place every half hour and it should not take longer than 2 minutes. To reduce the ammonia emissions to atmosphere the Burette exit pipe must be put through a water filled container/bucket. The crack ratio measurement is fed back to the Gas Supply PFM to control the ammonia supply gas flow. If the crack ratio is too high the ammonia supply must be increased. If the crack ratio is too low the ammonia supply flow rate must be decreased (this will increase reaction residence time). After measurement the water barrel isolation valve must first be opened and then the valve to the Burette must be closed. Note that during measurement with the Burette the pressure inside the process chamber must be controlled at ±20kPa by controlling the valve to the Burette.

At all times during the nitriding cycle the hydrogen gas forming on top of the water of the water filled barrel will be dispersed into the atmosphere as it will be put outside and far from the furnace.

Note that the process chamber must be under an overpressure of 20 kPa when introducing oxygen and nitrogen during the preparation mode. This means that the exit pipes must be connected to the water barrel. This would prevent air from entering the process chamber immediately after purging or oxidising.

E.3.3.3 GAS EXIT COMPONENTS

The Gas Exit PFM components are listed in Table E.12.

Table E.12: Gas Exit PFM component list

Component	Description/ Reason
9 exit gas lines	

Component	Description/ Reason
9 exit gas lines	
Ammonia flow meter	A Rotameter (Variable area flow meter) with a range of 0 – 333ℓ/hr to measure the ammonia exit gas flow rate.
Stainless steel gas pipes	Contain the ammonia from the furnace at a maximum temperature of 555°C
Exit pipe Manifold	
Connections for the 9 exit pipes	The 9 exit pipes connect to the manifold such that each sees the same exit pressure provided by the water height.
Control valves for each of the 9 exit pipes	The flow through each of the 9 exit pipes are controlled by adjusting these needle valves and monitoring the flow on the 9 flowmeters.
3 holes for water/steam drain fitted with valves	If there are any water/ steam inside the process chamber after the nitriding cycle is completed it is released through these holes by opening the valves
Single gas exit line	The combined flow from the 9 exit pipes exit through this single line on the manifold
'Bunte Burette' line	
'Burette' isolation valve	This valve is opened only if the crack ratio needs to be measured.
'Bunte Burette'	This instrument is used to measure the crack ratio as a percentage. The ammonia supply rate must be adjusted accordingly.
Water barrel line	
Isolation valve	This valve can be used to control the pressure inside the nitriding process chamber. It is closed when measuring the crack ratio and when testing for leak tightness with nitrogen gas.
Water barrel	The undissociated ammonia and nitrides are captured in the water. It also supplies the pressure head.

E.3.3.4 CONTROL PARAMETERS

Table E.13 lists the parameters of the control instrumentation of the Gas Exit PFM.

Table E.13: Control Instrumentation and their parameters of the Gas Exit system

Description	Instrument no. see P&ID Appendix	Range
Exit pipe Flow rate (9 values)		
Ammonia flow rate	FI004 – FI012	0 – 350 ℓ/hr see section 4.4.4
Dissociation rate Feedback for ammonia flow control		
Crack Ratio	AI001	0% – 100%

E.3.3.5 OPERATING PARAMETERS AND ACTIONS

Table E.14 identifies alarms and process interlocks with the appropriate actions.

Table E.14: The Gas Exit PFM Operating Parameters and Actions

Description	Type	High/ Low	Value	Action
Pressure				
Indicating high process chamber pressures	Pressure gauge PI001	H	25 kPa	Operator to investigate. Check Exit Gas valve position and water level in water filled barrel
		HH	30 kPa	Shut down furnace and the nitriding process, stop gas supply
Flow rate				
Preparation mode				
Indicating ammonia flow rate through exit pipe 1 - 9	Rotameter (FI004 – FI012)	Interlock	333 ℓ/hr max	The flow rate of each of the 9 exit gas pipes must be controlled at this value if the ammonia supply flow rate is 3000 ℓ/hr . See section 4.4.2 for flow rate calculations.
Nitriding cycle mode				
*Work point	Rotameter (FI004 – FI012)	Interlock	100 ℓ/hr	The flow rate of each of the 9 exit gas pipes must be controlled at this value if the ammonia supply flow rate is 900 ℓ/hr . If ammonia cracking takes place, mass will not be conserved and the exit balance flow rate will not be equal to the entering flow rate divided by 9.
Crack ratio				
Indicating low ammonia dissociation rate	'Bunte Burette' AI001	L	10%	Decrease ammonia supply flow rate to increase nascent nitrogen residence time and concentration, see par. E.3.1.5
Indicating high ammonia dissociation rate	'Bunte Burette' AI001	H	75%	Increase the ammonia supply flow rate to decrease the nascent nitrogen residence time, see par. E.3.1.5
		HH	80%	Fully open the ammonia supply valve to ensure maximum ammonia supply and to reduce residence time, see par. E.3.1.5
Level in water barrel	visual	L	Below indicated level	Fill the barrel with water

Note: These values are typical operating points
* This represents a possible workpoint if the supply flow rate is adjusted such as to ensure a crack ratio of between 35% and 40% as explained in Table 5.2.

E.3.3.6 SEQUENTIAL ACTIVITIES

The sequential activities of all three PFM's for this manually operated plant are discussed in chapter 5 section 5.4 Only the control involved during crack ratio measurement and balancing the flow rates is discussed here since it is repeated a number of times during operation.

APPENDIX F: NP PIPING AND INSTRUMENTATION DIAGRAM

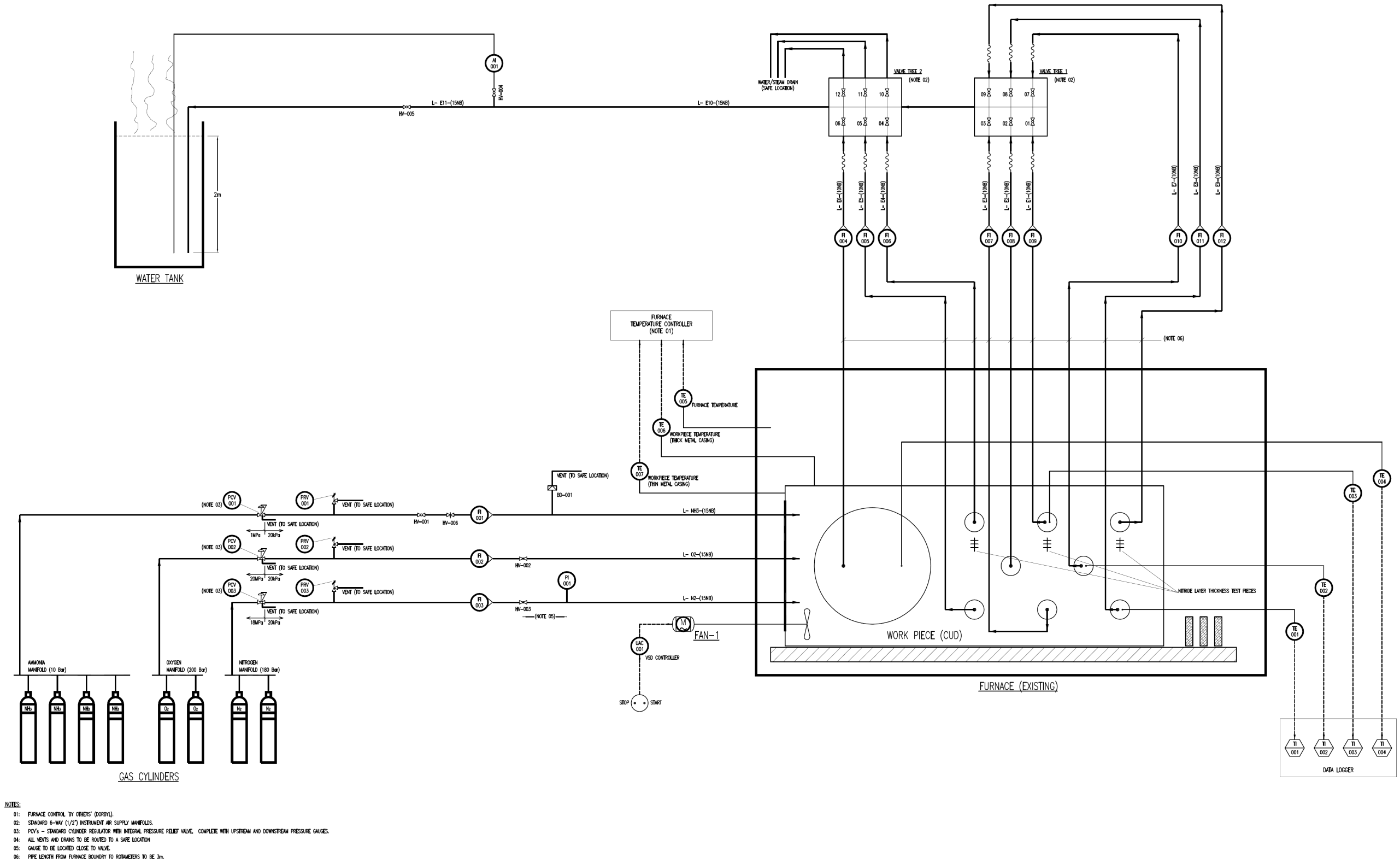

NOTES:

01: FURNACE CONTROL 'BY OTHERS' (DORBYL).
02: STANDARD 6-WAY (1/2") INSTRUMENT AIR SUPPLY MANIFOLDS.
03: PCV's – STANDARD CYLINDER REGULATOR WITH INTEGRAL PRESSURE RELIEF VALVE, COMPLETE WITH UPSTREAM AND DOWNSTREAM PRESSURE GAUGES.
04: ALL VENTS AND DRAINS TO BE ROUTED TO A SAFE LOCATION
05: GAUGE TO BE LOCATED CLOSE TO VALVE.
06: PIPE LENGTH FROM FURNACE BOUNDRY TO ROTAMETERS TO BE 3m.

Figure F.1: Piping and Instrumentation Diagram of the CUD NP used for construction (from drawing of Westinghouse Electric South Africa (Pty) Ltd.).

APPENDIX G: GENERAL ARRANGEMENT DRAWING OF THE NP

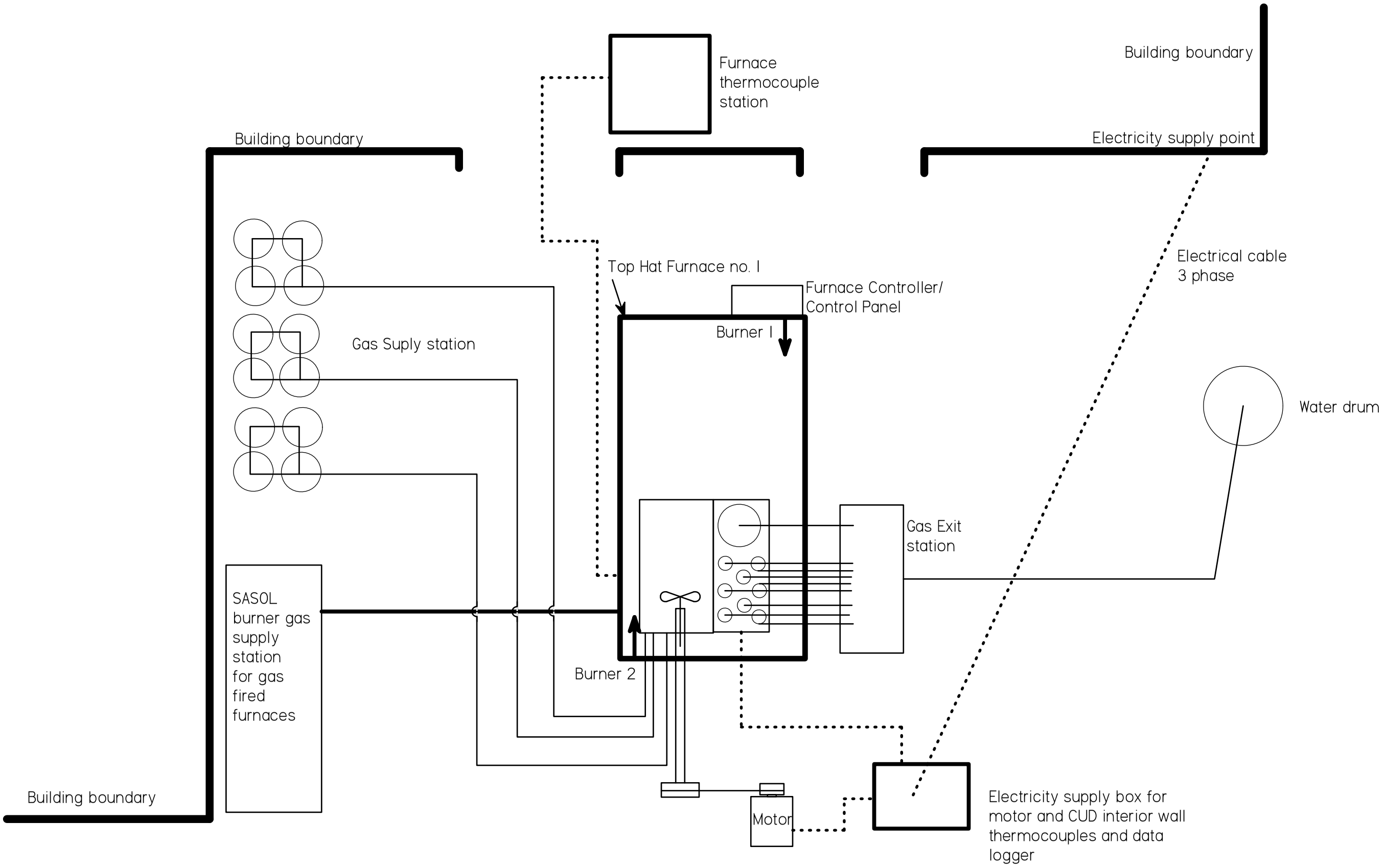

Figure G.1: General Arrangement of the proposed plant layout approved for construction.

APPENDIX H: QUOTATIONS / CALIBRATION CERTIFICATES

Flowmeter quotation:

HM FloConsult cc
Reg.No. CK 98/28970/23

43 Neon Avenue, Ext. 5, LENASIA
PO Box 1795, LENASIA, 1820
JOHANNESBURG, SOUTH AFRICA
Tel: 27 11 854 5115
Fax: 0866 71 76 77
Cell: 083 463 4028
e-mail: hmahomed@global.co.za

Flow Measurement Engineering

FAX MESSAGE

TO	WESTINGHOUSE ELECTRIC SOUTH AFRICA (PTY) LTD	**DATE**	30 JUNE 2008
NAME	RYNO NELL	**FROM**	HANIF MAHOMED
FAX NUMBER	012 621 4010	**OUR REFERENCE**	2886/08/e
TEL NUMBER	012 621 4080 / 082 575 0045	**Page 1 of**	2
e-mail	ryno@ist.co.za		

Subject: **VA METER FOR AMMONIA, NITROGEN AND OXYGEN GAS**
Our Quote 2886/08c dated 26.06.2008

Ryno, Further to your e-mail, we quote as follows:

Ammonia Gas

Type:	**ABB Fischer & Porter Glass Tube VA Meter without Integrally-Mounted Needle Valve**
Accuracy:	+- 4% of maximum flowrate
Scale Length:	3" / 80 mm
Model:	10A6131A/T62 (smallest sized meter)
Connection Size:	1/4" NPTF Horizontal In/Out
Fittings:	316 Stainless Steel
Needle Valve:	Without, Not Required
Shield:	Included in Polycarbonate Plastic
Seals:	Buna N
Scale:	% of maximum flowrate
Flowrange:	32 – 320 Nl/h Ammonia Gas metered at 1 bar (abs) & 20 C (=0.2 bar gauge).
PRICE:	**R1 748.00 each**
Quantity:	9 off

Nitrogen Gas

Type:	**ABB Fischer & Porter Glass Tube VA Meter without Integrally-Mounted Needle Valve**
Accuracy:	+- 4% of maximum flowrate
Scale Length:	3" / 80 mm
Model:	10A6131A/B10 (smallest sized meter)
Connection Size:	1/4" NPTF Horizontal In/Out
Fittings:	Brass
Needle Valve:	Without, Not Required
Shield:	Included in Polycarbonate Plastic
Seals:	Buna N
Scale:	% of maximum flowrate
Flowrange:	230 - 2300 Nl/h Nitrogen Gas metered at 1 bar (abs) & 20 C (=0.2 bar gauge)
PRICE:	**R1 423.00 each**
Quantity:	1 off

Oxygen Gas

Type:	**ABB Fischer & Porter Glass Tube VA Meter without Integrally-Mounted Needle Valve**
Accuracy:	+- 4% of maximum flowrate
Scale Length:	3" / 80 mm
Model:	10A6131A/B10 (smallest sized meter)
Connection Size:	1/4" NPTF Horizontal In/Out
Fittings:	Brass
Needle Valve:	Without, Not Required
Shield:	Included in Polycarbonate Plastic
Seals:	Buna N
Scale:	% of maximum flowrate
Flowrange:	100 - 1000 Nl/h Oxygen Gas metered at 1 bar (abs) & 20 C (=0.2 bar gauge)
PRICE:	**R1 423.00 each**
Quantity:	1 off

interior thermocouple quotation:

Quotation

TO:	WESTINGHOUSE ELECTRIC
ATT:	RYNO NEL
CELL / TEL EMAIL:	082 575 0045 / 012-621 4080 ryno@ist.co.za
FROM:	ERIC BOTES
REF#:	EB08/201
DATE:	15 APRIL 2008
Pages	2 including 1st page

WIKA

Pressure and Temperature Instrumentation

WIKA Instruments (Pty) Ltd.
807 Mansfield Ave, Mayville, Pretoria
P.O. Box 23197, Gezina
Pretoria, 0084

Tel: (012) 335 2481
Fax: (012) 335 5278

Email: ebotes@wika.co.za

Also available from WIKA Instruments ...

Tronic Line

Good day RYNO

As per your emailed RFQ, we thank you for your valued enquiry and have pleasure in quoting as follows:

NP0253352
PBDFH3B 10.35.03
- COC

ITEM 1. 4 OFF WIKA THERMOCOUPLE MODEL TEB

- WIKA **Type K** thermocouple.
- 2-wire simplex.
- Probe **Inconel 600**.
- Mineral insulated.
- Probe diameter **3mm**.
- Probe length **4000mm**.
- Un-grounded.
- Potted seal termination with relief spring.
- **2 meter** PVC fly leads.
- Manufactured in accordance to stringent **IEC** quality standards

Complete with:

- **Ø3mm x 1/4" NPT** stainless steel compression gland fitting.

PRICE: R660-00 each + V.A.T

DELIVERY: + 3 WEEKS

Interior thermocouple probe calibration certificate:

WIKA Instruments (Pty) Ltd
Reg. No. 1979/000475/07

Manufacturers and Distributors of WIKA Pressure and Temperature
Instrumentation and Distributors of Associated Instruments

Head Office: Chilvers St, Denver, 2094
Johannesburg, South Africa

PO Box 75225, Gardenview, 2047
Tel: (011) 621 0000
Fax: (011) 621 0060 (Sales)
(011) 621 0059 (Admin)
email: temperature@wika.co.za
sales@wika.co.za

TEMPERATURE CALIBRATION TEST REPORT

Certificate Number: WCT-CL- 7639

Customer: Westinghouse Electrical
Customer PO Number: NPO253352
WIKA Job Number: W70585
Item Number: 1
Tag / Article Number: N/A

Instrument under Test:
Calibration of: Thermocouple
Description: T1TEBKSX30
Serial Number: TE-5835
Range: -40 to 1000 °C
Manufacturer: WIKA Instruments (Pty) Ltd.

Reference Instrument:
Type: HEWLETT PACKARD
Serial No: 2619A40999.
Probe: PT100 & Thermocouple "S"
Probe Serial No: TE-84636 & TE-84637
Calibration Medium: Dry Block Calib.

Notes:

RESULTS OF CALIBRATION:

Applied Temperature (°C):	IUT* Reading (°C):	Observed Deviation (°C):
200.08	200.23	0.15
500.48	501	0.52
555.99	556.88	0.89

*IUT - Instrument Under Test

1) The measuring standard used for the purpose of this certification was calibrated by or is traceable to an NLA approved (or similar) laboratory.

2) The values in this certificate are correct at the time of calibration/certification. Subsequently the accuracy will depend on such factors as operating temperature, the care exercised in handling, frequency of use and its use under conditions other than specified by the manufacturer and/or conditions of calibration/certification. Recertification should be performed after a period which has been chosen to ensure that the equipment's accuracy remains within the limits required.

3) Testing has been carried out under an ambient temperature of 20 °C.

4) In the event of a mistake being made by WIKA INSTRUMENTS in calibration/certification work performed for the applicant, any legal liability arising therefrom shall be limited to the cost of recalibration and/or certification, but the applicant indemnifies WIKA INSTRUMENTS against any consequential or other loss.

Test Person: P. Wellcome. **Checked by:** R. Uriberger **Date:** 2008/06/17

WIKA quality control

APPENDIX I: NITRIDING PLANT OPERATION DATA ACQUISITION

The data in the following tables were manually recorded during operation of the plant. The graphs in chapter 5 and 6 were generated from this data.

1. Test for leak tightness at operating temperature

Leak rate		kPa/hr

2. Preparation mode NH3 flow

	time [hr]	PCV003 (outlet) [kPa]	FI003 [l/hr] (N2)	PI001 [kPa]	Fan speed [hz]	PCV001 (outlet) [kPa]	FI001 [l/hr]	TE001 [°C]	TE002 [°C]	TE003 [°C]	TE004 [°C]	TE005 [°C]	TE006 [°C]	TE007 [°C]
30-Jul	5:10	40	2000	4			0	23.5	23.5	23.5	23.5			
	5:25	41	2300	21			0	23.5	23.5	23.5	23.5			
	5:40	41	2000	21			0	23	23	23	23			
	5:55	41	2000	21				23	23	23	23			
	6:10	41	2000	21				22.8	22.5	22.5	22.5			
	6:25		1000	19.3										
	6:40		0	19		50	3000	27.5	27.5	27.5	27.5			
	6:55		0	19		40	2000	29.1	36.9	34.8	26.5			
	7:10			19		45	1500	36.7	50.2	45.6	32.9			
	7:25			19		40	500	46.6	66.5	59.4	41.9	90		
	7:40			13.5		35	1000	51	73.2	65	45.6			
	7:55			13.5		40	400							
	8:10			14		45	1800	62.2	88	78.6	58	116		
	8:25			14		45	1080	77	109	95	73	132		
	8:40			14		45	750	85	110	105	81	142		
	8:55			14		45	750	93	129	114	90	151		
	9:10													
	9:25													
	9:40													
	9:55													
	10:10													

	time [hr]	Heating rate [°C/hr]	PCV002 (outlet) [kPa]	FI002 [l/hr]	FI004 [l/hr]	FI005 [l/hr]	FI006 [l/hr]	FI007 [l/hr]	FI008 [l/hr]	FI009 [l/hr]	FI010 [l/hr]	FI011 [l/hr]	FI012 [l/hr]	Average of TE001 to TE004
	5:10													
	5:25				224	256	256	256	256	256	256	256	256	
	5:40				224	256	256	256	256	256	256	256	256	
	5:55				224	256	256	256	256	256	256	256	256	
	6:10				112	128	128	128	128	128	128	128	128	
	6:25				112	128	128	128	128	128	128	128	128	
	6:40				112	128	128	128	128	128	128	128	128	
	6:55				112	128	128	128	128	128	128	128	128	
	7:10				96	96	96	96	96	96	96	96	96	
	7:25				48	48	48	48	48	48	48	48	48	
	7:40				16	16	16	16	16	16	16	16	16	
	7:55				64	32	32	32	32	32	32	32	32	
	8:10				48	48	48	32	32	48	38.4	38.4	64	
	8:25				48	48	48	32	32	48	38.4	38.4	64	
	8:40													
	8:55													
	9:10													

2. Heating mode

	time [hr]	PCV003 (outlet) [kPa]	FI003 [l/hr]	PI001 [kPa]	Fan speed [hz]	PCV001 (outlet) [kPa]	FI001 [l/hr]	TE001 [°C]	TE002 [°C]	TE003 [°C]	TE004 [°C]	TE005 [°C]	TE006 [°C]	TE007 [°C]
30-Jul	9:30			14		45	600	108	145	128	104	164		
	10:00			14		45	500	122	152	139	113	174		
	10:30			13.5		45	600	136	173	154	133	185		
	11:00			13.5		40	500	149	185	166	146	196		
	11:30			13.5		40	400	164	205	183	159	218		
	12:00			13.5	30	40	600	183	223	200	170	237		
	12:30			17	30	98	3000	197	240	215	185	252		
	13:00			17	30	98	2900	212	252	227	200	258		
	13:30			19	30	98	3000	221	261	236	212	268		
	14:00			20	30	100	3000	233	271	248	224	277		
	14:30			20	30	90	3000	242	279	257	234	289		
	15:00			19.5	30	98	2900	253	291	268	245	297		
	15:30			19.5	30	98	2900	266	304	282	257	310		
	16:00			19.5	30	95	2880	276	314	291	266	319		
	16:30			19.5	30	93	2880	288	327	304	278	330		
	17:00			19.5	30	90	2900	298	336	312	287	347		
	17:30			19.5	30	95	2670	310	347	324	299	360		
	18:00			19.5	30	80	2900	325	365	341	313	376		
	18:30			20.5	30	100	2900	337	376	352	325	388		
	19:00			20.5	30	90	2900	346	386	362	334	399		
	19:30			21	30	100	2900	357	395	372	345	411		
	20:00			21	30	90	2900	368	405	383	357	412		
	20:30			21	35.1	90	2900	378	415	399	367	435		
	21:00			21.8	35.1	98	2850	389	426	407	378	434		
	22:00			21.8	30	98	2700	402	437	421	390	454		
	22:30			15	30	90	500	426	462	449	412	481		
	23:00													
	23:30													

	time [hr]	Heating rate [°C/hr]	PCV002 (outlet) [kPa]	FI002 [l/hr]	FI004 [l/hr]	FI005 [l/hr]	FI006 [l/hr]	FI007 [l/hr]	FI008 [l/hr]	FI009 [l/hr]	FI010 [l/hr]	FI011 [l/hr]	FI012 [l/hr]	Average of TE001 to TE004
	9:30				48	32	32	32	32	32	32	32	32	
	10:00				0-48	16-48	16-48	32-48	16-48	0-32	0-32	16-48	16-48	
	10:30				32	32	32	32	32	32	32	32	32	
	11:00				16	16	16	16	16	16	16	16	16	
	11:30				16	32	12	16	16	16	14	16	16	
	12:00				32	32	25.60	32	32	32	70.40	38.40	28.80	
	12:30		90	200	336	336	336	336	336	336	336	336	336	
	13:00		90	200	320	336	336	336	336	336	336	336	336	
	13:30		90	200	326	336	336	336	336	336	336	336	336	
	14:00		90	200	336	336	336	336	336	336	336	336	336	
	14:30		90	200	336	336	336	336	336	336	336	336	336	
	15:00		90	200	336	336	336	336	336	336	336	336	336	
	15:30		90	200	336	336	336	336	336	336	336	336	336	
	16:00		90	200	333	336	336	336	336	336	336	336	336	
	16:30		90	200	320	336	336	336	336	336	336	336	336	
	17:00		90	200	336	336	336	336	336	336	336	336	336	
	17:30		90	200	336	336	336	336	336	336	336	336	336	
	18:00		90	200	336	336	336	336	336	336	336	336	336	
	18:30		100	200	336	336	336	336	336	336	336	336	336	
	19:00		100	200	336	336	336	336	336	336	336	336	336	
	19:30		100	200	336	336	336	336	336	336	336	336	336	
	20:00		100	200	336	336	336	336	336	336	336	336	336	
	20:30		100	200	336	336	336	336	336	336	336	336	336	
	21:00		100	200	336	336	336	336	336	336	336	336	336	
	22:00		100	210	336	336	336	336	336	336	336	336	336	

3. Nitriding Cycle mode

	time [hr]	Crack Ratio	Average of TE001 to TE004	PI001 [kPa]	Fan speed [hz]	PCV001 (outlet) [kPa]	FI001 [l/hr]	TE001 [°C]	TE002 [°C]	TE003 [°C]	TE004 [°C]	TE005 [°C]	TE006 [°C]	TE007 [°C]
	22:30													
	23:00	66		16	30	100	240	441	475	465	426	496		
	23:30	88		16	30	100	480	452	484	472	439	505		
31-Jul	0:00	60		16	30	100	240	462	492	481	450	516		
	0:30	59		14	30	90	360	472	500	489	461	529		
	1:00	96		15	30	90	480	479	507	496	470	540		
	1:30	59		16	30	100	792	488	513	504	478	552		
	2:00	34		17	30	90	840	496	521	513	487	563		
	2:30	39		18	30	90	840	505	530	521	496	576		
	3:00	62		19	30	90	840	514	538	530	505	590		
	3:30	68		20	30	90	960	522	543	534	514	547		
	4:00	82		26	30	90	1320	525	543	535	519	547		
	4:30	92		19	30	90	600	528	545	537	527	547		
	5:00	67		20.5	30	120	1680	532	547	539	528	547		
	5:30	64		20	39	90	1080	535	550	542	532	553		
	6:00	73		20	39	75	1080	539	555	548	536	560		
	6:30	66		20	39	50	1800	544	559	552	540	558		
	7:00	70		21	39	46	1650	546	559	551	544	555		
	7:30	62		21	39	47	2300	548	559	552	547	555		
	8:00	60		19	39	50	2300	550	560	553	549	555		
	8:30	61		20	39	80	2400	552	560	554	552	557		
	9:00	56		21	39	60	2600	554	560	555	554	557		
	9:30	63		19	39	50	2400	555	561	557	555	559		
	10:00	64		12	39	50	2400	557	562	557	557	557		
	10:30	66		14	39	50	2500	558	562	558	559	559		
	11:30	56		14	44.5	60	2600	556	555	553	561	547		
	12:30	47		16	44.5	60	2700	552	549	553	559	550	individual crack	
	13:30	37		19	44.5	58	2880	543	536	547	555	536	ratios measured	
	14:30	40		19	40	65	3100	540	539	542	548	538		
	15:30	44		20	40	100	3100	537	536	537	545	533		
	16:30	41.5		27	40	100	3240	536	535	535	542	532		
	17:30	38.5		19.5	40	98	3300	534	533	533	541	528		
	18:30	40.5		18.7	42	95	3200	533	532	531	539	527		
	19:30			17.5	42	75	3000	532	532	530	538	527		
	20:30	52		17.5	42	75	2900	532	531	530	537	526		
	21:30	68		14	42	50	1080	531	530	526	536	520		
	22:30	65		14	42	50	1080	530	527	524	535	518		
	23:30			14	42	50	1080	530	528	525	534	520		
01-Aug	0:30	64		14	42	50	1080	530	527	525	533	520		
	1:30	64		14	42	50	1080	530	527	525	533	520		
	2:30	64		14	42	50	1080	530	527	525	532	520		
	3:30	64		14	42	50	1080	530	527	525	531	522		
	4:30	64		14	42	50	1080	533	525	528	532	521		
	5:30	64		14	42	50	1080	531	525	524	532	521		
	6:30	64		14	42	50	1080	533	527	527	532	522		
	7:30	64		13.5	42	50	1000	533	528	527	533	524		
	8:30	58		14.8	45	60	1440	535	530	529	534	525		
	9:30	46		15.5	45	55	2100	535	529	528	535	523		
	10:30	41		18.75	45	52	2200	530	525	524	535	523		
	11:30	41		18.5	45	50	2400	527	525	524	535	521		
	12:30	40.5		19	45	51	2700	527	527	525	535	523		
	13:30	38		19	45	55	2880	526	526	523	535	521		
	14:30	32.5		19	45.1	58	3100	525	524	521	535	513		
	15:30	30		18.75	45	52	2520	519	516	517	535	514		
	16:30	43		13	45	100	720	513	512	515	535	512		
	17:30	50		13	45	90	720	512	516	514	535	509		
	18:30	42		13	45	90	500	500	493	498	515	482		
	19:30	36		12.5	40	70	500	483	470	476	504	455		
	20:30	28		12.6	40	100	500	462	444	453	486	431		

Appendix I: Nitriding Plant Operation Data Acquisition

	time [hr]	Heating rate [°C/hr]	PCV002 (outlet) [kPa]	FI002 [l/hr]	FI004 [l/hr]	FI005 [l/hr]	FI006 [l/hr]	FI007 [l/hr]	FI008 [l/hr]	FI009 [l/hr]	FI010 [l/hr]	FI011 [l/hr]	FI012 [l/hr]
	22:30												
	23:00		0	0	0	0	0	0	0	0	0	0	0
	23:30			0	0	F	F	0	F	0	F	0	F
31-Jul	0:00				0	0	0	0	0	F	F	0	0
	0:30				0	F	F	0	0	F	0	F	F
	1:00				0	F	F	0	0	F	F	F	F
	1:30				F	F	F	F	F	F	F	F	F
	2:00				F	F	F	F	F	F	F	F	F
	2:30				F	F	F	F	F	F	F	F	F
	3:00				F	F	F	F	F	F	F	F	F
	3:30				F	F	F	F	F	F	F	F	F
	4:00				F	F	F	F	F	F	F	F	F
	4:30												
	5:00				192	192	192	192	192	192	192	192	192
	5:30												
	6:00												
	6:30												
	7:00												
	7:30												
	8:00												
	8:30												
	9:00												
	9:30				160	192	192	192	192	192	192	192	192
	10:00												
	10:30												
	11:30												
	12:30												
	13:30				320	304	288	288	288	288	288	304	288
	14:30				336	329.6	320	320	336	320	320	336	320
	15:30				336	336	336	336	336	336	278.4	336	336
	16:30				336	313.6	313.6	313.6	313.6	313.6	313.6	313.6	313.6
	17:30				336	336	336	336	336	336	336	336	336
	18:30												
	19:30				336	336	320	336	336	320	320	336	336
	20:30				336	336	320	336	336	320	336	336	336
	21:30				128	128	96	112	112	96	96	128	96
	22:30				128	112	96	96	96	96	96	112	96
	23:30				128	112	96	96	96	96	96	112	96
01-Aug	0:30				128	112	96	96	96	96	96	112	96
	1:30				128	112	96	112	112	96	96	128	96
	2:30				128	112	96	112	112	96	96	112	96
	3:30				128	112	96	112	112	96	96	112	96
	4:30				112	112	96	96	96	96	112	112	96
	5:30				112	112	96	96	96	96	80	112	96
	6:30				128	112	96	96	96	96	80	112	96
	7:30				112	112	96	96	96	96	80	112	96
	8:30				160	160	160	160	160	160	160	160	160
	9:30				256	249.6	208	224	240	224	192	249.6	224
	10:30				256	256	217.6	224	240	224	192	249.6	224
	11:30				320	272	230.4	256	262.4	240	217.6	272	249.6
	12:30				278.4	313.6	272	288	297.6	278.4	249.6	304	278.4
	13:30				32	32	32	32	32	32	32	32	32
	14:30												
	15:30												
	16:30				64	64	48	48	48	48	48	64	48
	17:30				64	64	48	48	48	48	48	64	48
	18:30												
	19:30				16	16	16	16	16	16	16	16	16

Data processing:

All flow meter readings vs. the mean measured crack ratio:

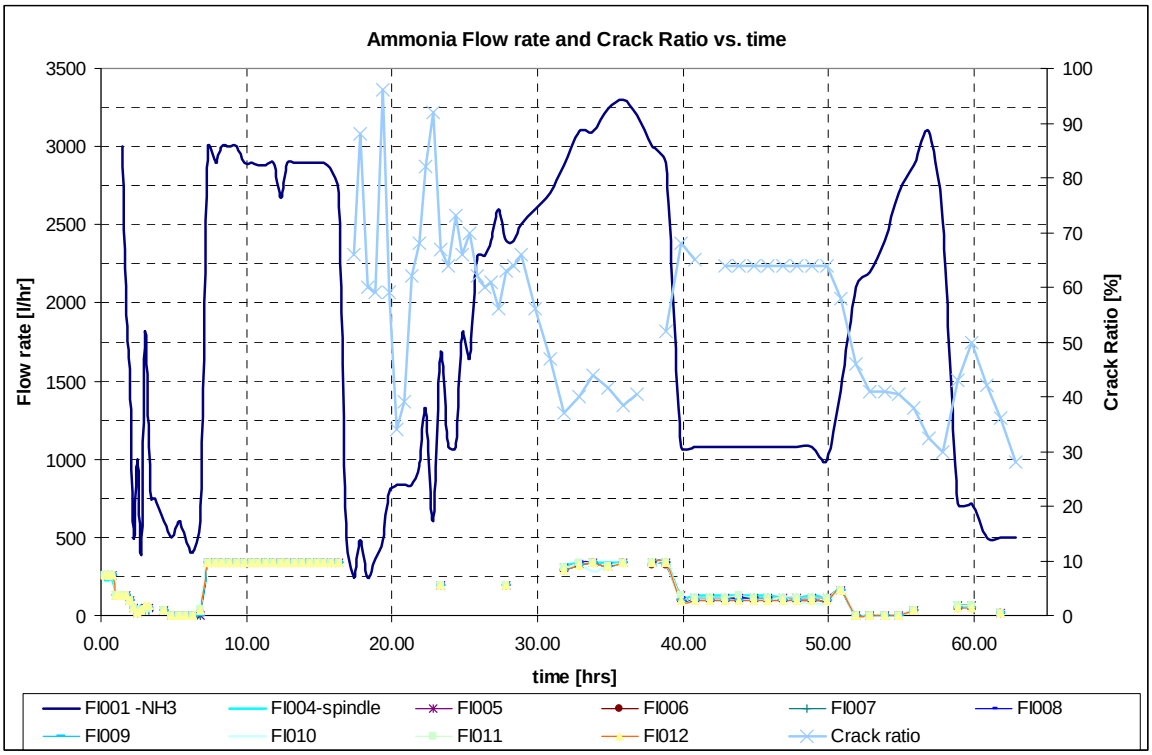

Figure I.1: Ammonia flow rate for all 9 insert holes vs. Crack ratio

APPENDIX J: LESSONS LEARNED

Table J.1: Technical lessons learned

Technical lessons learnt			
Item	**Problem Description/ Observation**	**Root Cause**	**Solution/Action**
1	Upon assembly the shaft proved to have an out of straight form and this caused a sticky point in the rotation. It was fixed by bending with a clock gauge and remachining. It is uncertain whether the shaft's ends were machined after or before welding the solid ends to the tube. 	Detailed notes on a drawing for manufacturing is not sufficient if one needs to ensure that any manufacturing sequential requirements were adhered to. In this case the one dimension governing the shaft roll-out was not included in the dimension certificate and the person who collected the shaft at the manufacturer did not realise this until installation of the shaft.	To ensure that the shaft ends were machined after welding the Quality Inspector needs to witness the shaft being turned on a lathe after welding and it can be balanced as well.
2	Ammonia gas leakage through shaft bearing.	Due to the fact that the shaft's run-out on the bearing surfaces was not within 0.3mm (specified at 1mm) after remachining. The small clearance of 0.45mm at room temperature between the graphite and the steel was not sufficient to seal the gas. The graphite bearing was designed to ensure a tight seal (virtually 0mm clearance at operating temperature and 0.3mm at room temperature due to graphite's smaller thermal expansion properties).	It is proposed that a fibreglass wool (like at the RCS vessel of the HTF) needs to be installed between the shaft and the outer pipe bearing housing along its 2.4m length. This would minimise pressure losses and ensure a tighter seal. It would also require that the shaft be machined along its entire length. 2. The use of labyrinth seals for the shaft can also be investigated.
3	If too much copper slip is used an oily substance is	Too much Copper compund was used on the	High temperature copper slip must be

Technical lessons learnt			
Item	**Problem Description/ Observation**	**Root Cause**	**Solution/Action**
	formed at temperature. The oils creeps from the flange bolt holes into the CUD insert hole faces. It causes oil oxidation during the oxygen provision phase. 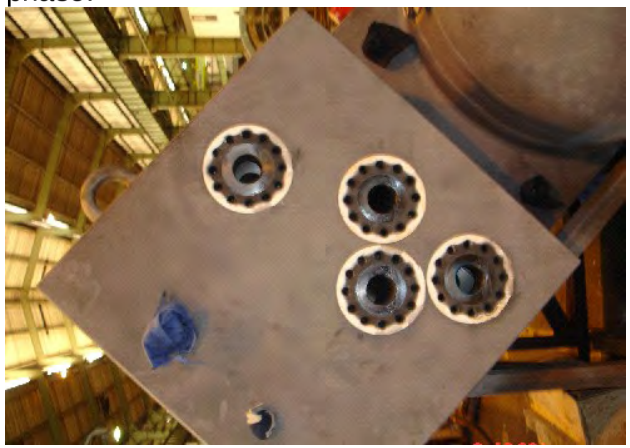	bolts ('high temperature copper slip for bolts') 	used in moderation.  Instead of copper slip; graphite powder or molyslip can be used.
4	A blue flame shaped mark was formed on the surface of the entrance of the CUD weld neck flange hole. The mark is close to where the oxygen line inlet nozzle was located on the flange. 	It is believed that the low oxygen flow rate, along with the higher density of the oxygen gas compared to the ammonia gas, caused the oxygen to drop to the surface and created the mark.	The gases must be mixed before it enters the vessel or the nozzle must be directed upwards.
5	Blue marks on exit holes/ seal surfaces of inserts	At points where gas exits at flanges/or where	Better seals to prevent gas leakage and

Technical lessons learnt			
Item	**Problem Description/ Observation**	**Root Cause**	**Solution/Action**
		thread cutting/tapping fluid fumes/ copper slip oil fumes exist. Oil oxidation during the oxygen provision phase. 	moderate use of copper slip
6	Ammonia smell close to water barrel. 	The ammonia gas is released and can be smelled as soon as the water is saturated.	A larger water volume is required since the water becomes saturated with ammonia too quickly. A better way to dispose of the saturated water must be used.
7	The Klinger ceramic paper gaskets that were used on the sealing flanges did not seal adequately and could not sustain the high temperatures.	The gaskets also required a very high seating stress in order to seal properly. This required excessive and unpractically large torques on the bolts. The gasket material that was used is called Thermoceram (Klinger), a ceramic fibre paper with a product number 731-70-122-006-0. The certificate of	It is recommended that graphite/ stainless steel/copper seals be used in the future. Fire gum paste can also be used. Do not take Klinger sales advice.

Technical lessons learnt			
Item	**Problem Description/ Observation**	**Root Cause**	**Solution/Action**
		conformance of the material states that the melting temperature of the seals is 1760°C and a 3%shrinkage. It was found that although these seals do not melt at 600°C it loses its structural stability completely and disintegrates. Klinger sales people were not correctly informed of their own product.	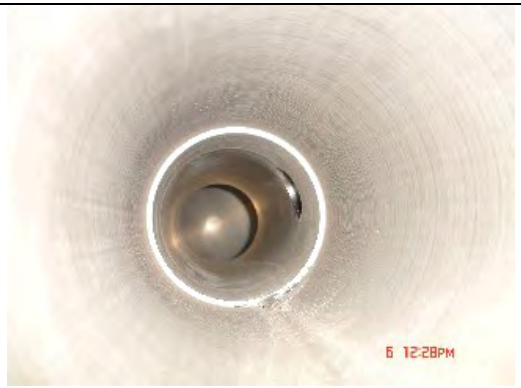
8	Heating rate very slow	The planned maximum heating rate of 56°C /hr was very optimistic. The maximum heating rate that was achieved is closer to 20°C/hr. This is mainly due to the large variety in metal thickness of the CUD housing.	For future heat treatments this should be taken into account.
9	Nuts/bolts that were tightened with PTFE thread tape tends to stick.thread tape can't sustain high temperatures	PTFE thread type must be avoided for any bolts/plugs that need to be screwed into the housing and sees large temperatures. The PTFE melts and burns off at 250°C and could cause metal parts to seize due to temperature.	Use copper slip instead of PTFE thread tape.
10	Galvanized coating on galvanized bolts disintegrates in the furnace and leaves a white coating. As a result of this one of the galvanized plug bolt heads were broken off when trying to remove it.	The galvanize coating forms a type of soldering material that welds threads together. The 0.5" BSP plugs on the Gas Tightness lines were galvanized and screwed in with PTFE thread tape as well.	Galvanized bolts/plugs also need to be avoided.
11	Site housekeeping: tools and swagelock fittings were not always where one expected it to be.	Tools etc. were not replaced at their original positions after use	All workers/personnel must be briefed on site housekeeping before construction starts.

Technical lessons learnt			
Item	**Problem Description/ Observation**	**Root Cause**	**Solution/Action**
12	Manual writing down of measurements can become cumbersome. All measurements must be typed into a computer afterwards.	No laptop on site to record measurements	Use a Laptop on site to insert the instrument readings after each measurement
13	Process control: Very large flows are required at high temperatures to decrease the dissociation rate. Flows in excess of 3000ℓ/hr were required where it was predicted that flows in the order of 200ℓ/hr would be required during soaking at 555°C.	The nitriding process is completely temperature dependent. At the proposed soaking temperature of 555°C a flow of more than 3000ℓ/hr was required to reduce the dissociation rate to 40%.	The soaking temperature was lowered during the nitriding process to reduce the required flow rate.
14	It is believed that the ammonia pressure regulator diaphragm valve was damaged. (upstream pressure reading lower than downstream reading, gauge also broken) 	It is believed the pressure regulator was at a low temperature (freezing) during the night and then the knob was turned quickly to adjust the outlet pressure setting to increase the flow rate.	Pressure regulators must be handled with care and outlet pressure settings must be kept constant.
15	Low ammonia flows was experienced during night time and early in the mornings. The upstream pressure on the regulator showed a very low setting.	It is believed that the liquid ammonia was frozen by the low environmental temperatures. The flow rate was too high to ensure that enough liquid ammonia was converted into gas. Four cylinders were opened at once on the manifold to rectify the problem, but four open cylinders were still not sufficient. The soak temperature of the furnace was thus lowered to decrease the dissociation rate.	Ammonia gas cylinders must be heated at low temperatures (during night time) to ensure sufficient flow.

Technical lessons learnt			
Item	**Problem Description/ Observation**	**Root Cause**	**Solution/Action**
16	Adaptor fittings for one size Swagelok A-lock fitting thread to a different size thread are the same cost as an A-lock fitting of the right thread.	Adaptor fittings were ordered to fit to the A-lock tube fittings that were available. It would have been cheaper to just buy the right size thread A-lock tube fittings.	Check and compare prices for the different solutions to a problem before purchasing.
16	316L stainless steel tubes also show some corrosion after removed from the furnace at these high temperatures. 	The Gas fired furnace which runs on SASOL gas and the high temperatures could be a cause for this	It must be kept in mind when 316L stainless steel is used at these high temperatures
17	Furnace does not allow economic heating/regulating of temperature	Furnace is too large, insulating wool missing	Use a smaller furnace in the future if one is available
18	During night time or early mornings the exiting ammonia gas is in liquid form and the readings on the flowmeters are unstable (fluctuating heavily) because of this.	The environmental temperature is too low, exit gas flow condensates too quickly. The flow on the supply flowmeter also fluctuates in the morning when the ammonia cylinder is at a too low temperature and the gas condenses too quickly.	Implement a trap for liquid/condensed ammonia/water on each gas pipe outlet, upstream of each outlet gas flow meter to improve readings on flow meters./ Only operate the plant in summer when it is hotter outside or make the plant indoors.
19	A future supplier of a large gas nitriding furnace for the DPP CUD blocks will still need a stirrer etc. to ensure the same high quality internal nitriding that was done for the HTF CUD	Commercial gas nitriding furnaces are built to focus more on external nitriding	Ensure the future supplier employs the right techniques for high quality internal nitriding. Specify the internal nitriding requirements for the supplier.
20	Large pressure losses were experienced on the	The system pressure rised from 22 kPa to 30	Take note of this aspect for future use of

Technical lessons learnt			
Item	**Problem Description/ Observation**	**Root Cause**	**Solution/Action**
	exit flow manifolds in the controllable range of the Sustech manifold valves. The system pressure rised from 22 kPa to 30 kPa.	kPa when the controllable range was reached and the valves were almost fully closed.	the Sustech manifolds with high flow rates.
21	Work surfaces were dirty and unsuitable for construction. Tools were dropped in the ground and sand etc.	The dusty surface and the exterior location of the plant is the reason.	Ensure sufficient sand or neat working surfaces for future construction.
22	Westinghouse Employees were not always safety conscious/injury conscious when performing hands-on construction jobs.	Most of the personnel performing the construction were used to an office and design atmosphere.	Anytime Westinghouse personnel perform hands-on jobs they need to be safety/injury conscious.

APPENDIX K: PLANT CONSTRUCTION SCHEDULE

	Name	Duration	Start	Finish	P...	C...	...
1	**Prepare Exterior Nitriding area**	**1.5 days?**	**08/07/21 08:00**	**08/07/22 01:00**	...	...	...
2	I-beams and sand bed	1 day	08/07/21 08:00	08/07/21 05:00	...	...	...
3	Gas cylinder and manifold assembly	1 day	08/07/21 08:00	08/07/21 05:00	...	...	...
4	Water barrel welding and sinking into ground.	1 day	08/07/21 08:00	08/07/21 05:00	...	...	...
5	position exit flowmeter rack and all other large p...	1 day	08/07/21 08:00	08/07/21 05:00	...	...	...
6	Thermocouple station position	1 day	08/07/21 08:00	08/07/21 05:00	...	...	...
7	Prepare 3 phase and 1 phase electricity connection	1.5 days?	08/07/21 08:00	08/07/22 01:00	...	...	...
8	Start pipe layout from gas supply side	3 days	08/07/21 08:00	08/07/23 05:00	...	...	...
9	Start pipe layout from gas exit side	3 days	08/07/21 08:00	08/07/23 05:00	...	...	...
10	**Prepare CUD for nitriding**	**0.25 days**	**08/07/21 08:00**	**08/07/21 10:00**	...	...	...
11	Prepare the CUD for nitriding by removing all oils	0.25 days	08/07/21 08:00	08/07/21 10:00	...	...	...
12	Perform UV light inspection	0.25 days	08/07/21 08:00	08/07/21 10:00	...	...	...
13	**Fit insert and spindle flanges**	**3.25 days**	**08/07/21 08:00**	**08/07/24 10:00**	...	...	...
14	Fit thermocouples in the correct position in CUD	0.15 days	08/07/21 08:00	08/07/21 09:12	...	...	...
15	assemble Nitriding test samples on insert flanges	0.15 days	08/07/21 09:12	08/07/21 10:24	...	...	...
16	Ensure test samples at correct depth	0 days	08/07/24 05:00	08/07/24 08:00	...	...	...
17	tighten flange bolts	0 days	08/07/24 08:00	08/07/24 08:00	...	...	...
18	Position thermocouple ends by manouvering from...	0.1 days	08/07/24 08:00	08/07/24 08:48	...	...	...
19	tighten thermocouple swagelok fittings	0.15 days	08/07/24 08:48	08/07/24 10:00	...	...	...
20	Fit dome and sphere pipe flanges	1 day	08/07/24 01:00	08/07/24 05:00	...	...	...
21	Fit CUD to cradle	0.25 days	08/07/21 08:00	08/07/21 10:00	...	...	...
22	Transport and position CUD and cradle on sand	0.5 days	08/07/23 01:00	08/07/23 01:00	...	...	...
23	**Fit defuel chute flange and fan**	**0.55 days**	**08/07/24 10:00**	**08/07/24 03:24**	...	...	...
24	Assemble the fan shaft assembly on a crane	0.25 days	08/07/24 10:00	08/07/24 01:00	...	...	...
25	Ensure the fan is rotating properly	0.1 days	08/07/24 01:00	08/07/24 01:48	...	...	...
26	Fit the flange	0.1 days	08/07/24 01:48	08/07/24 02:36	...	...	...
27	Tighten the bolts	0.1 days	08/07/24 02:36	08/07/24 03:24	...	...	...
28	**Fit fan drive assembly**	**0.2 days**	**08/07/24 03:24**	**08/07/24 05:00**	...	...	...
29	Fit V-belt and puilleys	0.2 days	08/07/24 03:24	08/07/24 05:00	...	...	...
30	Test the fan at speed	0.2 days	08/07/24 03:24	08/07/24 05:00	...	...	...
31	Finish gas exit pipe layout at CUD	1 day	08/07/24 10:00	08/07/25 10:00	...	...	...
32	Finish Gas supply pipe layout at CUD	1 day	08/07/24 03:24	08/07/25 03:24	...	...	...
33	**Make hole in furnace wall for fan shaft**	**0.3 days**	**08/07/25 03:24**	**08/07/28 08:48**	...	...	...
34	determine best position for hole	0.15 days	08/07/25 03:24	08/07/25 04:36	...	...	...

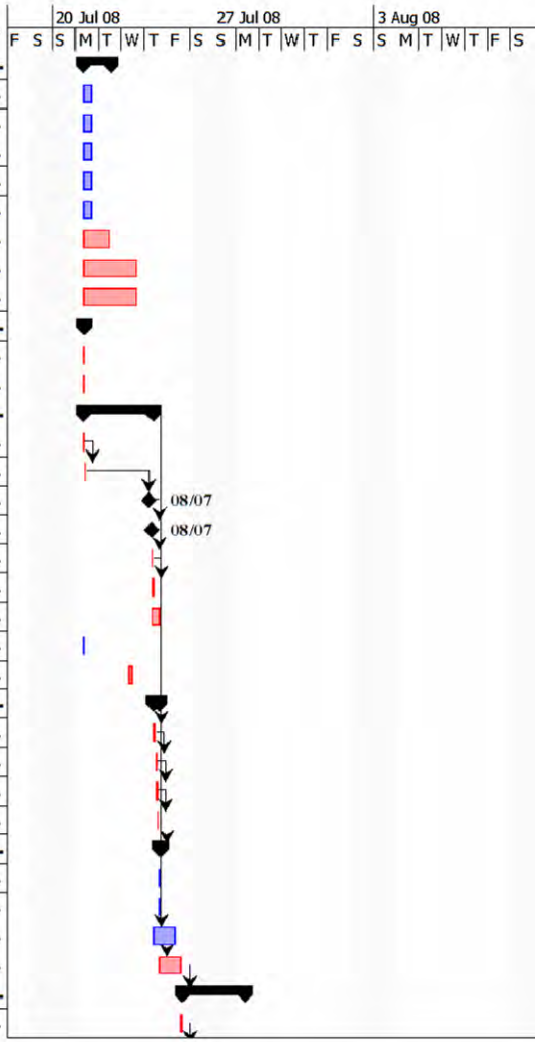

Nitriding plant construction plan - page1

Appendix K: Plant Construction Schedule

	Name	Duration	Start	Finish	P...	C...	...
35	make hole with flame cutter	0.15 days	08/07/25 04:36	08/07/28 08:48	...	...	...
36	Perform pre nitriding leak tests etc.	0.188 days	08/07/28 08:00	08/07/28 09:30	...	...	...
37	Move Top hat furnace outside and place over CUD	0 days	08/07/28 08:48	08/07/28 08:48	...	...	...
38	Perform Nitriding Procedure	4 days	08/07/29 08:00	08/08/01 05:00	...	...	...